

**THE CONTRIBUTION OF DISCOIDIN DOMAIN
RECEPTOR 1 TO THE PATHOGENESIS OF
DIFFUSE LARGE B CELL LYMPHOMA**

BY

SANDRA MARGIELEWSKA



A thesis submitted to
The University of Birmingham
for the degree of
DOCTOR OF PHILOSOPHY

Institute of Cancer and Genomics Sciences

Collage of Medical and Dental Sciences

University of Birmingham

May 2018

UNIVERSITY OF
BIRMINGHAM

University of Birmingham Research Archive

e-theses repository

This unpublished thesis/dissertation is copyright of the author and/or third parties. The intellectual property rights of the author or third parties in respect of this work are as defined by The Copyright Designs and Patents Act 1988 or as modified by any successor legislation.

Any use made of information contained in this thesis/dissertation must be in accordance with that legislation and must be properly acknowledged. Further distribution or reproduction in any format is prohibited without the permission of the copyright holder.

ABSTRACT

Collagen is the ligand for the discoidin domain receptor 1 (DDR1), a receptor tyrosine kinase that is over-expressed in Hodgkin lymphoma. However, the role of DDR1 in diffuse large B cell lymphoma (DLBCL) is not known. I showed that DDR1 is over-expressed in a subset of DLBCL where it positively correlates with expression of its collagen ligands, and negatively correlates with expression of mitotic spindle genes. DDR1 correlated genes also overlapped with three aneuploidy signatures and DDR1 expression correlated significantly with autosomal aneuploidy index. RNAseq analysis revealed that over-expression of DDR1 in primary germinal centre B cells down-regulated expression of CENPE, an essential component of the mitotic spindle checkpoint that when inactivated leads to chromosome mis-segregation and aneuploidy. CENPE expression was also significantly reduced in primary DLBCL. Moreover, I showed that the constitutive activation of DDR1 in an in vitro lymphoma model led to aneuploidy. Finally, I showed that DDR1 can be inhibited by three small molecules and established the basis for in vivo model to test these inhibitors in DLBCL xenograft. My data provide evidence that DDR1 can induce aneuploidy in B cells, and as such identify a mechanism to potentially explain the link between chronic inflammation and lymphomagenesis.

ACKNOWLEDGEMENTS

I would like to thank Professor Paul Murray for his supervision during my PhD; for his guidance during my project, patience, time and expert advice, from whom I have learnt so much over the years. I would also like to acknowledge Professor Ciaran Woodman for his additional support, passion and enthusiasm. I will always be grateful for this opportunity, through which I was able to develop my passion for this work. I have been very fortunate to be able to work amongst such an inspirational people and great scientists.

I would also like to thank all past and present members of the Murray Group for their general help and lovely work atmosphere, who have made this a wonderful journey. I offer my appreciation to Dr Maha Ibrahim, for all her time at the microscope helping me assess my slides and for her fantastic friendship and support; to Dr Robert Hollows, for all his help with statistical analysis; [REDACTED] for her help with the animal experiments; a special thank you to Dr Eszter Nagy, my lab' supervisor, who helped me to develop my lab' skills.

Personal thanks to my friends who supported me during this journey and to my wonderful family for their never-ending support, unconditional love and constant encouragement. Without them I would not be where I am today.

CONTENT

1.	CHAPTER 1: INTRODUCTION	1
1.1	Diffuse large B cell lymphoma	2
1.1.1	Epidemiology and classification	2
1.1.2	Molecular subgroups of DLBCL	5
1.1.2.1	Normal B cell development	5
1.1.2.2	DLBCL GCB and ABC subtypes	10
1.1.2.3	Identification of GCB DLBCL and ABC DLBCL subtypes	14
1.1.3	Prognostic factors and DLBCL survival	16
1.1.3.1	Survival of DLBCL patients	16
1.1.3.2	Prognostic factors in DLBCL	18
1.1.4	Treatment of DLBCL	19
1.1.4.1	Front-line treatment	19
1.1.4.2	Treatment of relapse and refractory disease	20
1.1.4.3	Novel therapies for treatment of DLBCL	21
1.2	Receptor tyrosine kinases (RTKs)	24
1.2.1	RTK structure and general mechanism of action	24
1.3	Discoidin domain receptors (DDR's) family	30
1.3.1	DDR's expression and function	30
1.3.2	Discoidin domain receptor 1 (DDR1) structure and isoforms	32
1.3.3	DDR1 activation by collagen	36

1.3.4	DDR1 mediated signalling	38
1.3.5	DDR1 cooperation with other receptors and growth factors	43
1.4	DDR1 expression in diseases	45
1.4.1	Atherosclerosis	45
1.4.2	Fibrosis	46
1.4.3	Cancer	47
1.5	DDR1 as a therapeutic target in cancer	52
1.5.1	DDR1 inhibitors	54
1.6	Chromosomal instability and cancer	58
1.6.1	Mitosis	58
1.6.2	Mitotic checkpoints	61
1.6.3	Aneuploidy and chromosomal instability (CIN)	65
1.6.4	The roads to whole chromosomal aneuploidy	66
1.6.5	Aneuploidy and CIN in cancer	68
1.6.6	The causes of aneuploidy in tumours	71
1.6.7	Prognosis and treatment	73
1.6.8	CENPE- a mitotic checkpoint gene in cancer	74
1.7	Study aims	76
2	CHAPTER 2: MATERIALS AND METHODS	77
2.1	Cell culture	78
2.1.1	Maintenance of the cell lines	78
2.1.2	Cryopreservation of cells and recovery of frozen cells	81

2.1.3	Cell counting	81
2.2	Isolation and maintenance of primary human GC B cells from tonsils	82
2.2.1	Tonsil specimen	82
2.2.2	Purification of tonsillar mononuclear cells (TMCs)	82
2.2.3	Purification of CD10 positive GC B cells	83
2.3	Plasmid preparation	84
2.3.1	Broth and agar preparation	84
2.3.2	Preparation of plasmid from glycerol stock	84
2.3.3	Transfection of bacteria with plasmid	85
2.4	Transfection of cell lines and primary GC B cells	86
2.4.1	Nucleofection	86
2.4.1.1	DDR1 expression plasmid	86
2.4.1.2	Knock down of gene using siRNA	87
2.4.2	Electroporation	89
2.5	Stimulation with collagen and cell harvest	89
2.6	Cells sorting	91
2.7	Treatment of the cells with inhibitors	92
2.8	Trypan blue viability assay	93
2.9	RNA analysis	94
2.9.1	RNA extraction and purification	94
2.9.2	cDNA preparation	95
2.9.3	Amplification of cDNA for gene expression analysis	95

2.9.4	RNA sequencing (RNAseq)	96
2.9.5	Quantitative real time polymerase chain reaction (qRT-PCR)	96
2.9.6	Fluidigm®48.48 Fast Real Time PCR	97
2.9.6.1	Fluidigm® Gene Expression Specific Target Amplification	97
2.9.6.2	Fluidigm®48.48 real time polymerase chain reaction	97
2.9.7	qRT-PCR and Fluidigm data analysis	100
2.10	Protein analysis	100
2.10.1	Western blotting	100
2.10.1.1	Protein extraction	100
2.10.1.2	Determination of protein concentration	101
2.10.1.3	Sodium dodecyl sulphate polyacrylamide gel electrophoresis (SDS- PAGE)	101
2.10.1.4	Protein transfer	102
2.10.1.5	Immunoblotting	102
2.10.2	Sample preparation for immunohistochemistry (IHC) and immunofluorescence (IF)	105
2.10.2.1	Preparation of cytopins	105
2.10.2.2	Preparation of Poly-Lysine coated slides and Hela cells seeding	105
2.10.2.3	Primary paraffin embedded samples	106
2.10.3	Metaphase spread	106
2.10.4	Van Gieson staining method	107
2.10.5	Immunohistochemistry (IHC)	108

2.10.5.1	Preparation of slides for immunohistochemistry (IHC)	108
2.10.5.2	Antigen retrieval	108
2.10.5.3	Detection and visualisation of antigen by immunohistochemistry (IHC)	109
2.10.5.4	Slides scoring	110
2.10.6	Detection of antigen by single/multiple immunofluorescence (IF) staining using Opal™ kit	110
2.10.6.1	Preparation of slides	111
2.10.6.2	Opal™ fluorophore staining	111
2.10.7	Flow cytometry	113
2.11	Mouse model	114
2.11.1	L591, BJAB, A20 xenograft	114
2.12	Statistical analysis	114
2.12.1	RNAseq data analysis from GC B cells	114
2.12.2	Re-analysis of published datasets	115
2.12.3	Measurement of aneuploidy index	116
2.12.4	Overall survival analysis in DDR1 positive DLBCL	116
3	CHAPTER 3: RESULTS PART I	118
	Investigating the contribution of DDR1 to the pathogenesis of diffuse large B cell lymphoma.	
3.1	Expression of DDR1 receptor and its ligand collagen in DLBCL	119
3.1.1	Over-expression of DDR1 in primary diffuse large B cell lymphoma	119
3.1.2	DDR1-expressing DLBCL are enriched for the expression of collagen	128

	genes	
3.2	Genes negatively correlated with DDR1 expression in DLBCL are enriched for mitotic spindle associated genes	133
3.3	DDR1 expression correlates with aneuploidy in primary DLBCL	137
3.4	Regulation of lymphoma-associated genes by DDR1 in primary and transformed GC B cells	140
3.4.1	Optimization of conditions for the transfection and analysis of DDR1-transfected primary GC B cells	140
3.4.2	Optimization of collagen stimulation of DDR1 transfected GC B cells	143
3.4.3	Identification of DDR1 target genes in primary GC B cells	143
3.4.4	Validation of DDR1 target genes	145
3.4.5	Validation of DDR1 target genes in lymphoma cell lines and establishment of cell line model for in vivo and in vitro studies	156
3.5	CENPE is down-regulated in primary DLBCL and transformed GC B cells	170
3.6	CENPE is down-regulated in DDR1a transfected BJAB and DG75 cell lines, after collagen stimulation	180
3.7	DG75 cell line as a good model to investigate DDR1 impact on development of aneuploidy in tumour cells	182
4	CHAPTER 4: RESULTS PART II	197
	Potential therapeutic reversal of DDR1 activation using DDR1 inhibitors.	
4.1	Blocking the phosphorylation of DDR1 receptor by small molecular	198

	inhibitors	
4.2	Establishing an in vivo model to test DDR1 inhibitors	203
4.2.1	Tumour growth of L591 and BJAB xenografts	203
4.2.2	DDR1 expression in L591 xenograft	203
4.3	Collagen expression in mouse tumours	206
4.4	DDR1 and collagen expression in A20 xenograft	208
5	CHAPTER 5: DISCUSSION AND FUTURE PERSPECTIVES	210
	Discussion and future perspectives	211
	Future plans – summary	220
	APPENDICES	222
	REFERENCES	236

LIST OF FIGURES

CHAPTER 1: INTRODUCTION

1.1	Normal B cell development	9
1.2	Molecular subtypes in DLBCL and their key oncogenic pathways	13
1.3	Hans algorithm for classification of DLBCL subtypes	15
1.4	Structure of receptor tyrosine kinases (RTKs)	26
1.5	Dimerization and activation of receptor tyrosine kinases (RTKs)	29
1.6	Structure of different DDR1 isoforms	35
1.7	Main signalling pathways activated by DDR1	42
1.8	DDRs therapeutic therapy strategy in cancer	53
1.9	Phases of mitosis	60
1.10	Mitotic checkpoint in mammals – activation and deactivation	64

CHAPTER 3: RESULTS PART I

Investigating the contribution of DDR1 to the pathogenesis of diffuse large B cell lymphoma.

3.1	Over-expression of DDR1 in diffuse large B cell lymphoma	121
3.2	Validation of DDR1 antibody	123
3.2D	DDR1 expression in diffuse large B cell lymphoma	126
3.3	Overall survival in DDR1 positive and negative DLBCL patients	127
3.4	DDR1-expressing DLBCL are enriched for the expression of collagen genes	130
3.5	Genes negatively correlated with DDR1 expression in DLBCL are enriched	134

	for mitotic spindle associated genes	
3.6	DDR1 expression correlates with aneuploidy in primary DLBCL	139
3.7	Optimization of the time of post-transfection of GCB cells	141
3.8	Optimization of the method of GC B cells transfection	142
3.9	Summary of data from GC B cells transfected with DDR1 or EV and harvested for RNAseq analysis	144
3.10	Overlap between genes correlated with DDR1 in DLBCL and differentially expressed following collagen stimulation of DDR1-expressing GC B cells	147
3.11	DDR1 expression in primary GC B cells transfected with DDR1a and EV as a control, in 3 separate donors	151
3.12A	Analysis of the expression of genes up-regulated in collagen-treated DDR1 compared with empty vector-transfected primary GC B cells and in primary DLBCL versus normal GC B cells	152
3.12B	Analysis of the expression of genes up-regulated in collagen-treated DDR1 compared with empty vector-transfected primary GC B cells and in primary DLBCL versus normal GC B cells	154
3.13	DDR1 expression in HL and DLBCL cell lines	157
3.14A	Optimisation of the collagen concentration for DDR1 activation	158
3.14B/C	DDR1 expression and phosphorylation after collagen stimulation in HL and DLBCL	159
3.15A	DDR1 expression in cell lines treated with collagen	161
3.15B	Summary of the analysis of the expression of genes up-regulated in	162

	collagen-treated cell lines	
3.15C	Analysis of the expression of genes up-regulated in collagen-treated cell lines	163
3.16A	Summary of the analysis of the expression of genes down-regulated in collagen-treated cell lines	167
3.16B	Analysis of the expression of genes down-regulated in collagen-treated cell lines	168
3.17	DDR1 expression correlates with aneuploidy in primary DDR1-expressing GC B cells	171
3.18	Down-regulation of CENPE in DLBCL	173
3.19	CENPE expression in lymphoma cell lines	175
3.20	CENPE is down-regulated in primary DLBCL	177
3.21A	CENPE and DDR1 expression in DLBCL - multiplex immunofluorescence	178
3.21B	CENPE and DDR1 expression in tonsil - multiplex immunofluorescence	179
3.22	CENPE expression in lymphoma cell lines after activation of DDR1 by collagen	181
3.23A	Analysis of cell size based on metaphases of DG75, BJAB and L591 cells	183
3.23B	Analysis of chromosome number in metaphase spreads of DG75, BJAB and L591 cell lines	184
3.24	Dislocation of CENPE protein in HeLa cells after treatment with GSK923295	186
3.25	Experimental plan for induction of aneuploidy in DG75 cells	187

3.26A	Aneuploidy in DG75 cells after CENPE/MPS1 kinase inhibition, as measured by metaphase cell size	189
3.26B	Aneuploidy in DG75 cells after CENPE/MPS1 kinase inhibition, as measured by chromosome number	190
3.27	Validation of constitutively active DDR1 (DIV) plasmid in BJAB and DG75 cell line	192
3.28A	Increased detection of hyperploidy in DG75 cells expressing a constitutively active DDR1, as measured by cell size	194
3.28B	Increased detection of hyperploidy in DG75 cells expressing a constitutively active DDR1, as measured by chromosome number	196

CHAPTER 4: RESULTS PART II

Potential therapeutic reversal of DDR1 activation using DDR1 inhibitors.

4.1	Inhibition of DDR1 activation by 7rh, 7rj and DDR1-IN-1 in BJAB cells transfected with DDR1a, after collagen stimulation	199
4.2	Toxicity assay with trypan blue on DDR1a transfected BJAB cell line, treated with 7rh DDR1 inhibitor	200
4.3	Toxicity assay with trypan blue on DDR1a transfected BJAB cell line, treated with 7rj DDR1 inhibitor	201
4.4	Toxicity assay with trypan blue on DDR1a transfected BJAB cell line, treated with DDR1-IN-1 DDR1 inhibitor	202
4.5	Tumour growth in L591 and BJAB mice xenograft	204
4.6	Human DDR1 expression in L591 xenograft model	205

4.7	Van Gieson staining showing collagen expression in mouse xenograft models	207
4.8	DDR1 expression in A20 cell line	209
4.9	Van Gieson staining showing collagen expression in A20 xenograft	209

LIST OF TABLES

CHAPTER 1: INTRODUCTION

1.1	WHO classification of DLBCL	4
1.2	Mitotic checkpoint components	63

CHAPTER 2: MATERIALS AND METHODS

2.1	Summary of cell lines and the culture conditions	79
2.2	Details of used plasmids	88
2.3	CENPE siRNA information	88
2.4	List of TaqMan® Gene Expression Assays used for qRT-PCR and Fluidigm®	99
2.5	List of used primary and secondary antibodies	104
2.6	Fluorophores used for multiplex immunofluorescence staining	113

CHAPTER 3: RESULTS PART I

Investigating the contribution of DDR1 to the pathogenesis of diffuse large B cell lymphoma.

3.1	DDR1 target genes selected for validation by Fluidigm® 48.48 Fast Real Time PCR	149
-----	---	-----

LIST OF ABBREVIATIONS

AA- amino acid

AID - activation-induced cytidine deaminase

ALL - acute lymphocytic leukemia

AML - acute myeloid leukaemia

APC - adenomatosis polyposis Coli tumor suppressor

APC/C - anaphase promoting complex/cyclosome

AURA – aurora kinase A

BCL-6 - B cell lymphoma 6 transcription factor

BCR – B cell receptor

BCR-ABL - Breakpoint Cluster Region-Abelson kinase

BCSG1 – breast cancer specific gene 1

Bim-1 - bisindolylmaleimide-based protein 1

BRCA1 – breast cancer 1

BUB - budding uninhibited by benzimidazole

BUBR1 - BUB1-related protein

CDC20 - cell-division-cycle 20 homologue

CDK1 - cyclin-dependent kinase 1

CDKs – cyclin-dependent kinases

CENPE - centromere protein E

CHFR - checkpoint with forkhead and ring finger domains

CHOP - cyclophosphamide, doxorubicin, vincristine and prednisone

CIN – chromosomal instability

CML – chronic myelogenous leukaemia

CRC- colorectal cancer

CSR - class switch recombination

DDR1 – discoidin domain receptor 1

DDRs – discoidin domain receptors

DLBCL – diffuse large B cell lymphoma

DLBCL-NOS - DLBCL, not otherwise specified

DS - discoidin domain

E2F – E2F transcription factors

EBV – Epstein-Barr virus

ECM – extracellular matrix

EMT - epithelial to mesenchymal transition

ERK - extracellular signal-regulated kinase

FBS – Fetal Bovine Serum

FDC – follicular dendritic cell

GC – germinal centre

Grb2 - growth factor receptor-bound protein 2

HCV - hepatitis-C virus

HHV8 - human herpes virus 8

HL – Hodgkin lymphoma

HRS - Hodgkin-Reed-Sternberg cells

HSC - hematopoietic stem cells

IF - immunofluorescence

Ig – immunoglobulin

IgH – immunoglobulin heavy-chain

IgL – immunoglobulin light-chain

IHC- immunohistochemistry

IPF - idiopathic pulmonary fibrosis

JNK – c-jun N-terminal kinase

KRAS - Kirsten rat sarcoma viral proto-oncogene

LATS1 – large tumour suppressor homologue 1

Ldlr - low-density lipoprotein receptor

MAD - mitotic arrest deficient

MAPK - mitogen-activated protein kinase

MAPK - mitogen-activated protein kinase pathway

MEKK2/3 - mitogen-activated protein kinase kinase kinase

MMP – metalloproteinase

MPS1 - monopolar spindle 1

MYCN - neuroblastoma-derived V-myc avian myelocytomatosis viral related oncogene

NEB – nuclear envelope breakdown

NSCLC - non-small cell lung carcinoma

OS - overall survival

p53 – tumour protein p53

PCA1 - prostate cancer antigen 1

PDK-1 - 3-phosphoinositide-dependent protein kinase-1

PI3K – PI-3 kinase

PIP2 - phosphatidylinositol 4,5-bisphosphate

PIP3 - phosphatidylinositol 3,4,5-triphosphate

RAG1,2 - recombination activating genes 1 and 2

RAS - GTPase-activating protein

RB – retinoblastoma associated protein

RT- room temperature

RTKs – receptor tyrosine kinases

SAC - spindle assembly checkpoint

SHM - somatic hypermutation

SMC – smooth muscle cell

SMED-SL - spondylo-meta-epiphyseal dysplasia

SOS - 'son of sevenless' protein

TGF- β - transforming growth factor beta

WHO – World Health Organisation

WNK1 - lysine deficient protein kinase 1

CHAPTER ONE

INTRODUCTION

1. Introduction

1.1 Diffuse large B cell lymphoma

1.1.1 Epidemiology and classification

Diffuse large B cell lymphoma (DLBCL) is an aggressive and heterogeneous group of malignancies derived from normal developing B cells, and is the most common type of non-Hodgkin lymphoma among adults accounting for approximately 30% to 40% of all lymphoid cancers (Team, 1997, Friedberg and Fisher, 2008, Lenz and Staudt, 2010b, Smith et al., 2015). The disease appears to be slightly more frequent in males than females, and most commonly occurring between the age of 60 to 80 (Novelli et al., 2013), although the disease is not restricted to any age group. Patients usually present with enlarged lymph nodes or rapidly growing extra-nodal masses, which are mostly restricted to one area (Gatter et al., 2012). In the majority of cases, the cause of this disease is not clear. However, a few factors which could contribute to the process of tumorigenesis have been suggested; an increased risk of developing DLBCL was connected with immunosuppression (including HIV) (Harris et al., 2008, Doll and Ringenber, 1989), chemical substances such as pesticides and fertilizers (Weisenburger, 1985), but also alkylating agents in combination with exposure to ultraviolet radiation (as used in cancer therapy) were shown to increase the risk of lymphomas as secondary malignancies. Moreover, in a subset of DLBCL, EBV infection is also linked with the development of this cancer and associated with a poorer prognosis (Park et al., 2007,

Hoeller et al., 2010). Also infection with other viruses, such as hepatitis C virus (HCV) and human herpes virus 8 (HHV8), have been linked with DLBCL (Swerdlow et al., 2008).

The diagnosis of DLBCL is generally based on the analysis of histological, immunological and cytogenetic investigations, which demonstrate a high level of diversity between the subtypes. Histology usually shows a diffuse infiltrate of large lymphoid cells, whose size is described as “more than twice the size of a normal lymphocyte” (Harris et al., 2008, Swerdlow et al., 2016, Gatter et al., 2012). The immunophenotype is extremely broad and strictly correlated with a specific subtype of DLBCL. The hallmarks of DLBCL subtypes also include some specific and complex chromosomal alterations. The most common one (in around one third of cases) is connected with changes in the BCL-6 gene, which is crucial for the formation of germinal centers (Spagnolo et al., 2004, Lo Coco et al., 1994).

Because of high clinical and biological heterogeneity, the classification of DLBCL is under constant evaluation. The most commonly accepted classification is by the World Health Organisation (WHO) (Swerdlow et al., 2016). The 2016 WHO revision of a previously published classification of lymphoid neoplasms is based on novel discoveries, which have important implications towards diagnosis, prognosis and therapy for these diseases. This report lists many different subtypes of DLBCL, based on their clinical and molecular features (Table 1). Other types of DLBCL which did not fit into these criteria and therefore could not have been divided into specific subgroups, are referred to as DLBCL, not otherwise specified (NOS). Within this group, based on the origin of malignant cells and diversity in clinical outcome, two molecular subgroups were recognised: germinal center

B cell (GCB) type and activated B cell (ABC) type (Table 1) (Swerdlow et al., 2016). In this thesis DLBCL refers to the DLBCL-NOS group of lymphomas.

Table 1.1 WHO classification of DLBCL (Swerdlow et al., 2016).

Diffuse large B -cell lymphoma (DLBCL), NOS - Germinal centre B-cell type - Activated B-cell type	
DLBCL subtypes	T-cell/histiocyte-rich large B-cell lymphoma
	Primary DLBCL of central nervous system (CNS)
	Primary cutaneous DLBCL, leg type
	EBV DLBCL, NOS
Other lymphomas of large B cells	DLBCL associated with chronic inflammation
	Primary mediastinal (thymic) large B cell lymphoma
	Intravascular large B-cell lymphoma
	ALK large B-cell lymphoma
	Plasmablastic lymphoma
	Primary effusion lymphoma
	HHV8 DLBCL, NOS
	High-grade B-cell lymphoma, with MYC and BCL2 and/or BCL6 rearrangements
	High-grade B-cell lymphoma, NOS
	B-cell lymphoma, unclassified, with features intermediate between DLBCL and classic Hodgkin lymphoma.

1.1.2 Molecular subgroups of DLBCL

Different gene expression profiles and mutational signatures in DLBCL cases led to the identification of two distinct molecular classes of DLBCL. These subtypes are associated with different clinical outcomes, specific genetic alterations and mediate different molecular signalling pathways (Vockerodt et al., 2015, Rosenwald et al., 2002). As they are derived from lymphocytes at different developmental stages, it is important to first understand the process of normal B cell development and signalling.

1.1.2.1 Normal B cell development

B (bone marrow-derived) lymphocytes are highly conserved cells (Cooper and Alder, 2006), which express a variety of immunoglobulin (Ig) receptors able to recognize specific epitopes on antigens, and therefore are the first line of immune response in mammals. In humans, the development of these cells starts in the bone marrow (primary lymphoid tissue) and comprises of several stages which bring B cells to full functional maturity in secondary lymphoid tissue (e.g. lymph nodes) (LeBien and Tedder, 2008).

B cells originate from hematopoietic stem cells (HSCs) which, in the human foetus differentiate towards B cell progenitors (pro-B cells). The process of bone marrow cells (pro-B cells, CD34+/CD10+/CD22+) differentiation towards B cells, starts from rearrangements of three Ig gene segments: V, D and J, in the Ig heavy-chain (IgH), which results in presentation of CD34+/CD10+/CD19+ pre-B-1 cell-specific surface molecules. Pre-B1 cells then differentiate into CD34- large pre-B2 cells. Next, IgH pairs with light-chain (IgL), which present J and V rearranged gene segments, and create a complex called

pre-B cell receptor (pre-BCR) (Melchers, 2005). Pre-B2 cells with pre-BCR undergo several (4-6) cycles of cell division and a few more genetic rearrangements of the light chain of the receptor. B cell maturation is also accompanied by sequential activation and down-regulation of recombination activating genes 1 and 2 (RAG1 and RAG2), whose protein products are necessary for Ig rearrangement and generation of DNA strand breaks (needed for VDJ recombination) (Spicuglia et al., 2006). As a result of this whole process, a highly diverse repertoire of Ig genes is produced and a fully functional, developed BCR is presented in the immature B cell. Immature B cells possess several characteristic markers on their surface such as CD20, CD21, CD22 and CD40 (LeBien and Tedder, 2008). Immature B cells with BCR leave the bone marrow and transit towards secondary lymphoid organs, such as spleen, Peyer's patches, tonsils and lymph node. Mature, naïve B cells (CD24+/C38+) circulate through blood and lymphoid tissue, or reside in primary follicles in lymph node, where they wait for their first contact with a foreign antigen (Figure 1.1).

Antigen presentation to the BCR combined with signals from T helper cells, results in the activation of the germinal center (GC) reaction (Victora and Nussenzweig, 2012) (Figure 1.1). After entering the 'dark zone' of GC, naïve B cells start to rapidly proliferate (centroblasts). This robust clonal expansion is accompanied by somatic hypermutation (SHM) of centroblasts' VH genes, which leads to the production of antibodies with a higher affinity to antigen. B-cell lymphoma 6 (BCL-6) is a master transcriptional regulator of this stage (Basso and Dalla-Favera, 2012). Next, highly proliferating centroblasts differentiate into non-proliferating centrocytes in the 'light zone' of GC. Centrocytes

undergo selection, based on their affinity to the antigens presented by T cells and follicular dendritic cells. Low affinity interaction leads cells towards apoptosis. In this stage of B cell differentiation, cells (centrocytes) can undergo class switch recombination (CSR), which allows for changing of IgH class from IgM and IgD to IgG and IgA, and can therefore interact with different effector molecules (LeBien and Tedder, 2008). Both of these reactions, SHM and CSR, are driven by the enzyme activation-induced cytidine deaminase (AID), which, in cells is regulated by interferon regulatory factor 8 (IRF8) (Muramatsu et al., 2000) (Figure 1.1). These DNA modifications are necessary for normal B cell development; however, they also carry the risk of uncontrolled mutations, which can lead to the development of lymphomas.

The last stage of B cell development is a differentiation step, which establishes the GC B cell phenotype. This process is regulated by several transcriptional factors such as: BCL6, MTA3, SPIB, BTB domain and CNC homolog 2 (BACH2), OCT2, OCAB and IRF8 (Lenz and Staudt, 2010a). As mentioned before, BCL6 is the most important in the centroblast SHM reaction, but also down-regulation of this factor is essential for GC exit and final B cell differentiation. BCL-6 represses many genes connected with cell-cycle progression, cellular response to DNA damage, apoptosis and plasma cell differentiation (Shaffer et al., 2000). Differentiation of B cells towards plasma cells is connected with up-regulation of interferon regulatory factor 4 (IRF4), which increases activation of B lymphocyte induced maturation protein 1 (BLIMP1) (Klein et al., 2006), a master regulator of plasma cell differentiation. BLIMP1 regulates BCL6 repressor functions, and therefore favours B cell differentiation towards antibody-secreting plasma cells (Shaffer et al., 2000). In contrast

to this process, reduction of BCL-6 levels in combination with the activation of another transcriptional factor, PAX5, results in suppression of BLIMP1 and memory B cell development (Cobaleda et al., 2007).

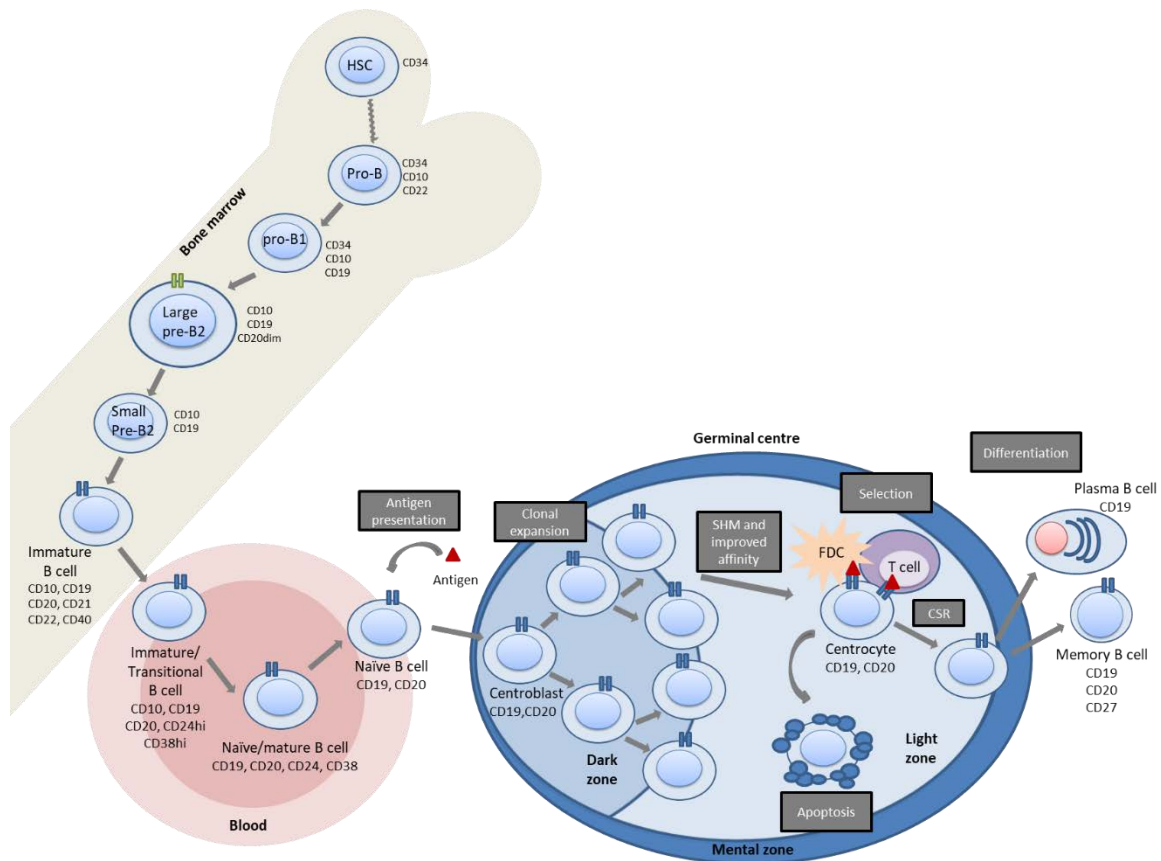


Figure 1.1 Normal B cell development.

B cells originate from hematopoietic stem cells (HSCs) which, after a few more stages of differentiation (indicated by dashed line) in bone marrow become pro-B cells and therefore initiate the process of development of the B-lineage. Large B cells which represent an incompletely developed BCR (green), undergo several rounds of proliferation, which results in the production of small pro-B2 cells, followed by immature B cells, with a fully functional BCR (blue). Immature B cells migrate from the bone marrow and circulate between marrow and lymphoid organs. Antigen (red triangle) presentation to naïve B cells, together with a signal from T helper cells (not shown), activate naïve B cell which then start rapidly proliferating in the dark zone of the germinal centre (clonal expansion). Centroblasts undergo somatic hypermutations (SEM) which helps to improve their affinity to the antigen. In the light zone of the germinal centre, centroblasts differentiate into non-proliferative centrocytes. Centrocytes are then selected by antigen presenting follicular dendritic cells (FDC) and T helper cells, for further differentiation, or if they have low affinity to the antigen, are mediated toward apoptosis. Next, chosen centrocytes undergo class switch recombination (CSR). As a consequence of the activation of specific transcriptional factors, centrocytes migrate outside the germinal centre and differentiate into plasma B cells or memory B cells.

1.1.2.2 DLBCL GCB and ABC subtypes

Two distinct molecular subtypes were identified in DLBCL NOS based on their gene expression profiles, which indicate that they originate from different stages of GC B cell development. These are, germinal centre B cell (GCB) and activated B cell (ABC) subtypes, with 15% of patients who remain unclassified (Alizadeh et al., 2000, Rosenwald et al., 2002). This classification seems to be very important in the context of therapeutic approaches, as these subtypes are driven by different signalling pathways (Shaffer et al., 2012, Roschewski et al., 2014) (Figure 1.2) and ABC type DLBCL is associated with the worst survival (Lenz et al., 2008b).

GCB type DLBCL

It is believed that GCB DLBCL is derived from GC B cells, as they express genes highly expressed in normal germinal centre B cells, such as CD10, LMO2 and BCL6 (Alizadeh et al., 2000, Rosenwald et al., 2002).

Several oncogenic pathways and genetic abnormalities were described as being characteristic of GCB DLBCL (Figure 1.2). For example, the t(14;18) translocation appears in approximately 30-40% of GCB DLBCL patients, but not in the ABC type of tumour. This translocation deregulates BCL2 (B-cell lymphoma 2) gene expression, which is responsible for the anti-apoptotic function in cells (Rosenwald et al., 2002, Lenz et al., 2008c). Overexpression of BCL2 in GCB DLBCL also has a negative prognostic impact on patients after R-CHOP treatment (Iqbal et al., 2011). Moreover, 20% of GCB DLBCL patients have a mutation of EZH2, a histone methyltransferase (Beguelin et al., 2013, Morin et al., 2010).

It was shown that EZH2 as a master regulator, in co-operation with BCL6, mediates lymphoma development in GCB type (Beguelin et al., 2013, Caganova et al., 2013). A somatic point mutation of the EZH2 gene (in exon 15), results in the replacement of tyrosine Tyr461 within the EZH2 protein. This change leads to a gain-of-function and increased methylation of histone 3, which promotes transcriptional silencing of key regulatory genes and therefore promotes lymphomagenesis (Sneeringer et al., 2010, Yap et al., 2011, Beguelin et al., 2013). Interestingly, in 10% of GCB DLBCL patients, deletions in the tumour suppressor gene PTEN (phosphate and tensin homologue) were described; in another 15%, amplification of miR-17-92 (microRNA cluster) which suppresses expression of PTEN, was identified (Xiao et al., 2008, Lenz et al., 2008c). The down-regulation of PTEN expression (by immunohistochemistry) was detected in 55% of GCB DLBCL patients, in comparison with only 14% of non-GCB cases. This results in constitutive activation of the PIK3/AKT signalling pathway and suggests it is important in GCB type DLBCL pathogenesis (Pfeifer et al., 2013).

ABC type DLBCL

Based on its gene expression profile, ABC subtype of DLBCL is believed to derive from B cells that are already differentiating into plasma cells. They express genes characteristic of normal mature plasma cells, such as X-box binding protein 1 (XBP1; the master regulator of Ig secretion) (Shaffer et al., 2004). The characteristic feature of ABC subtype is constitutive activation of NF κ B pathway, which mediates a signal promoting cell survival and proliferation, and inhibition of apoptosis due to constitutive activation of

CBM complex comprised of CARD11, BCL10 and MALT1 (Figure 1.2) (Davis et al., 2010). In normal lymphocytes, this complex is only activated by antigen stimulation; however, in ABC DLBCL it can be activated by several genetic aberrations. Approximately 10% of ABC DLBCL cases carry the mutation which activates CARD11, whereas the remainder of cases have sustained chronic activation of BCR signalling which influences the CBM complex (Davis et al., 2010, Lenz et al., 2008a). Constitutive BCR signalling was also discovered to be mediated by mutations in CD79A and CD79B in 20% of cases, but also by activation of downstream kinases SYK (spleen tyrosine kinase), PI3K, BTK (Bruton tyrosine kinase) and PKC β (protein kinase C β) (Davis et al., 2010). It was also shown that in more than 30% of ABC DLBCL patients, mutation of MYD88 results in upregulation of NF κ B and JUN pathways (Ngo et al., 2011). Constitutive activation of NF κ B in ABC DLBCL can be also caused by inactivation of the NF κ B negative regulator A20 (TNFAIP3), which occurs through its mutation and deletion (Compagno et al., 2009, Kato et al., 2009). Moreover, as a consequence of chronic activation of NF κ B, IRF4 transcriptional factor is activated which can direct centrocyte differentiation towards plasma cells (Davis et al., 2001). However, in the case of ABC DLBCL, this differentiation is not fully complete due to mutations and deletions of PRDM1 (PR domain zinc finger protein 1); this gene encodes BLIMP-1 (Tam et al., 2006, Pasqualucci et al., 2006). Additionally, in 25% of ABC DLBCLs, BCL6 translocation was observed, which also represses expression of BLIMP-1. These observations indicate a block in B cell differentiation to be important in the pathogenesis of the ABC subtype.

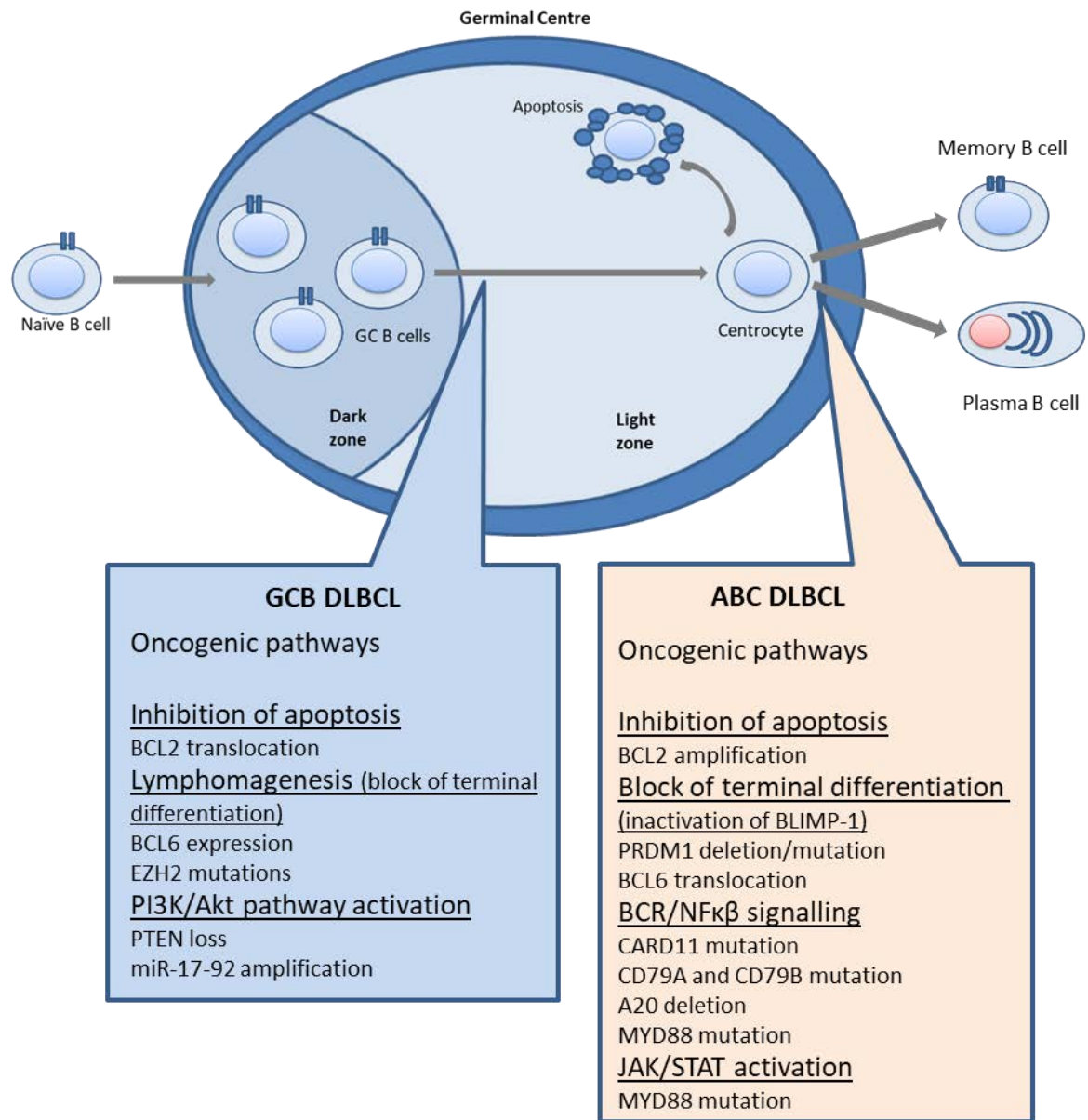


Figure 1.2 Molecular subtypes in DLBCL and their key oncogenic pathways.

Based on the gene expression profile of DLBCL, it can be divided into two main molecular subtypes: germinal centre B cell like (GCB) and activated B cell like (ABC) type. GCB is believed to derive from GC B cells, and ABC type from B cells which are differentiating into plasma cells, just before GC exit. The main oncogenic pathways, characteristic for these subtypes are listed.

1.1.2.3 Identification of GCB DLBCL and ABC DLCL subtypes

An accessible and reliable method to determine the molecular subtype of DLBCL is important from a prognostic and therapeutic point of view. Unfortunately, gene expression profiling is not available for every patient, due to the lack of a commercially available test and fresh-frozen tissue specimens. Nowadays, the common method to identify the DLBCL subtypes is IHC staining proposed by Hans et al., the so-called Hans algorithm. In this method, a combination of CD10, BCL-6 and MUM1/IRF4 IHC markers are used (Hans et al., 2004). According to this algorithm, DLBCL cases positive for CD10 marker are classified as GCB DLBCL type. DLBCL cases negative for CD10 and BCL6 markers are classified as non-GCB subtype, however if a case is negative for CD10 but positive for BCL6, staining for MUM1/IRF4 marker should be performed. Cases positive for MUM1/IRF4 are classified as ABC subtype, and cases negative for MUM1/IRF4 as GCB DLBCL subtype (Figure 1.3). This classification, due to its oversimplification and the poor reproducibility, only correlates with subgroups defined by gene expression profiling in approximately 87% of cases (Meyer et al., 2011, de Jong et al., 2007). Therefore, the IHC method of DLBCL classification still remains an imperfect substitution for gene expression profiling. Nevertheless, due to the unavailability of gene expression profiling as a standard test for every patient, WHO classification of lymphoid neoplasms (revision from 2016), considers Hans algorithm as an acceptable method for identification of DLBCL subtypes (Swerdlow et al., 2016). Novel studies based on quantification of RNA transcripts on paraffin-embedded tissue using NanoString technology, provides promising

gene expression-based methodology, which in the future could be successfully used for the reliable identification of DLBCL subtypes (Scott et al., 2014).

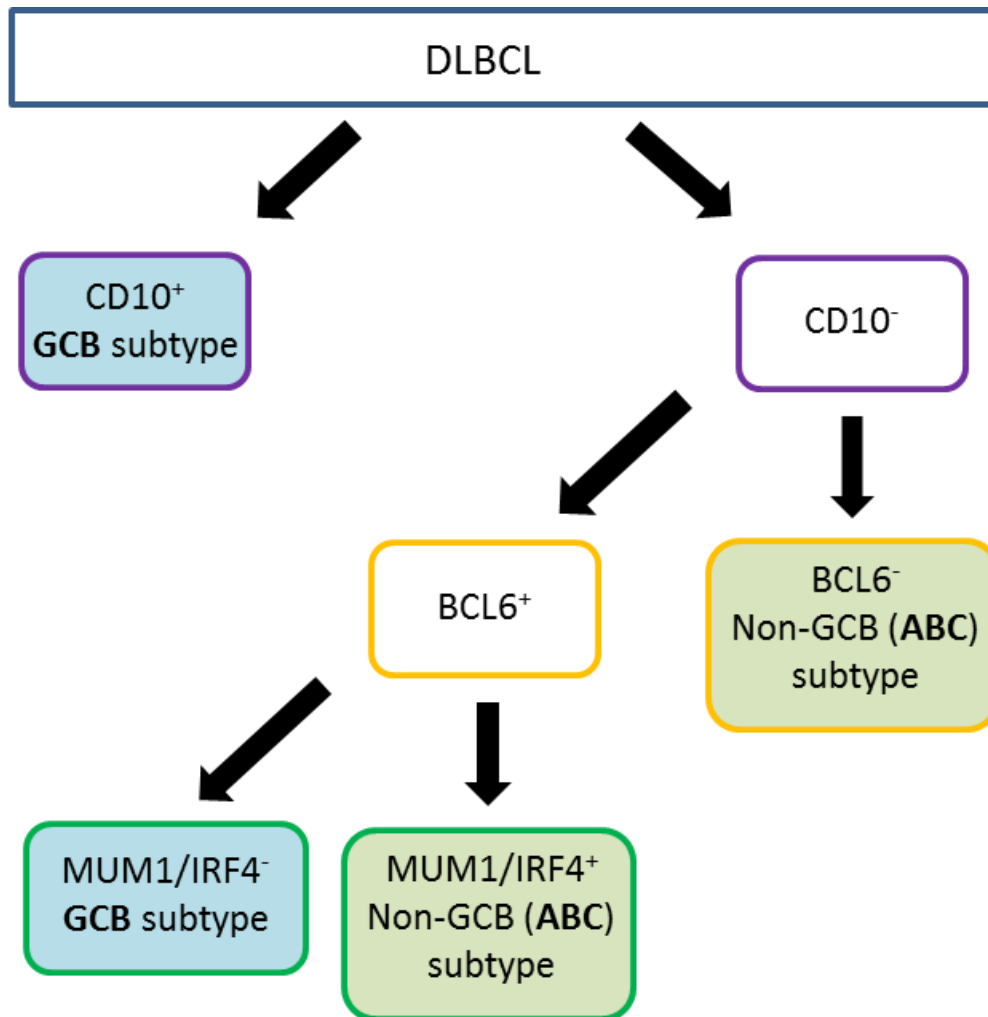


Figure 1.3. Hans algorithm for classification of DLBCL subtypes (Hans et al., 2004). IHC analysis of DLBCL cases based on the expression of 3 markers: CD10, BCL6 and MUM1.

1.1.3 Prognostic factors and DLBCL survival

1.1.3.1 Survival of DLBCL patients

The general 5-year overall survival (OS) in patients with DLBCL is approximately 46% (Smith et al., 2015). In the context of specific subtypes, OS seems to be more favourable towards GCB DLBCL patients, in comparison to the ABC subgroup (Alizadeh et al., 2000, Rosenwald et al., 2002, Shipp et al., 2002, Wright et al., 2003). The prediction of patients' survival has been attempted in several ways. The commonly used Hans algorithm predicts 5-year OS to be 76% of GCB type DLBCL, compared to 34% of ABC type DLBCL (Hans et al., 2004). Furthermore, gene expression analysis was used to identify specific genes which regulate OS in patients with DLBCL. Studies on patients with DLBCL after anthracycline-based therapy pointed at LMO2, BCL-6 and FN1 as genes which predict longer survival; whereas expression of CCND2, SCYA3 and BCL-2 genes, were connected with a shorter predicted survival (Lossos et al., 2004, Rosenwald et al., 2002, Shipp et al., 2002). However, the IHC method poses a 20% rate of misclassification with gene expression analysis, suggesting the need for improvement of this model.

The rearrangement of MYC oncogene (which appears in approximately 10% of DLBCL cases) in combination with BCL2 and/or BCL6 was shown to negatively affect DLBCL patient survival (Barrans et al., 2010, Savage et al., 2009), and therefore they are included as a new category of, "high-grade B-cell lymphoma, with MYC and BCL2 and/or BCL6 rearrangements", in the 2016 revised WHO classification (Table 1.1) (Swerdlow et al., 2016). A MYC and BCL2 translocation, referred to as "double hit lymphoma" occurs in

approximately 5% of DLBCL cases and has been shown to reside within GCB subtype; whereas MYC/BCL6 translocation is called “triple-hit lymphoma” and both of these signatures have a very poor prognosis with median OS of less than 12 months (Jedrzejczak, 2015, Menguy et al., 2018, Jaglal et al., 2012, Wang et al., 2015, Johnson et al., 2012). Moreover, overexpression of MYC (measured by IHC) in 25-30% of DLBCL cases is associated with BCL2 expression in 20-35% DLBCL cases (Johnson et al., 2012, Green et al., 2012). The majority of these cases are not connected with translocations of MYC and BCL2 genes, and are referred to as “dual-expressers”; they are more common in ABC subtype of DLBCL and are connected with a significantly poorer prognosis than patients who express only one or neither of these proteins (Hu et al., 2013).

Furthermore, it was shown that it was not only the molecular signature of tumour cells, but also the tumour microenvironment that affects survival in DLBCL patients following treatment (Lenz et al., 2008b). Two ‘stromal signatures’ were described to be variably present in both GCB and ABC subtypes. Stromal-1 signature is characterised by extracellular matrix deposition and infiltration of macrophages into the tumour, and was identified to be more favourable and connected with longer survival (Lenz et al., 2008b, Wels et al., 2008); whereas stromal-2 signature is characterised by a high density of blood vessels and is associated with a worse survival (Lenz et al., 2008b).

For years, the combination of cyclophosphamide, doxorubicin, vincristine and prednisone (CHOP) was the standard treatment for patients with DLBCL, independent of the subtype of the disease. The addition of rituximab, an anti-CD20 IgG1 monoclonal antibody, to

CHOP chemotherapy has significantly improved DLBCL patient survival (73% vs. 63%, $p=0.005$). However, more than 50% of ABC type DLBCL patients will still die from their disease without further improvements in treatment of this cancer (Lenz et al., 2008b, Coiffier et al., 2002).

1.1.3.2 Prognostic factors in DLBCL

Prognostic factors in DLBCL, which were shown to significantly influence survival of patients with this disease, can be considered in several categories; those related to the patient, such as age, presence of specific symptoms and status of performance; those related to the tumour, such as stage, proliferating fraction, tumour size, bone marrow and extranodal involvement; those related to aggressiveness of the disease, such as lactate dehydrogenase (LDH) level or β 2-microglobulin level, and those related to the treatment (Coiffier et al., 1991, Velasquez et al., 1991, Litam et al., 1991). In clinical practice, the commonly used tool to predict outcome in patients with aggressive non-HL is The International Prognostic Index (IPI) (Shipp et al., 1993, International Non-hodgkin's Lymphoma Prognostic Factors, 1993). It was developed before the availability of rituximab, and after revision to include rituximab in CHOP treatment, confirmed its prognostic usefulness (Sehn et al., 2007). Currently IPI does not include identification of distinct molecular subtypes of DLBCL.

The IPI consists of 5 negative prognostic factors:

- Age over 60
- Stage III to IV

- More than one extranodal site
- Elevated level of LDH (serum lactate dehydrogenase)
- ECOG (Eastern Cooperative Oncology Group) performance status of 2 or more

For each factor, one point is assigned and the total IPI score assigns patients into one of four outcome groups, with the 5-year OS being between 26% to 73% (Shipp et al., 1993).

More recently, a new updated NCCN-IPI score was proposed, which seems to be more successful in identifying high-risk patients (5-year OS of 33%) (Zhou et al., 2014). It included data from the National Comprehensive Cancer Network (NCCN) and incorporates the same 5 IPI factors; however further categorisation is based more on age, LDH level, and extranodal involvement in the bone marrow, liver, lung or central nervous system, rather than the number of extranodal sites (Zhou et al., 2014).

1.1.4 Treatment

1.1.4.1 Front-line therapy

For years, the standard front-line treatment for patients with DLBCL contained chemotherapy and radiotherapy, which in combination gave the best results (reviewed by: Friedberg et al., 2008)(Martelli et al., 2013). Three cycles of anthracycline (CHOP)-based drugs, followed by field radiation (40-50Gy), or 8 cycles of CHOP alone, were used as standard therapy for intermediate-high grade DLBCLs (Miller et al., 1998, Pfreundschuh et al., 2008). More recently, it was discovered that addition of the anti-CD20 monoclonal antibody rituximab to standard treatment with CHOP (R-CHOP), is successful in patients with DLBCLs. The results from an initial trial showed improvement

in 10-year OS in 16% of elderly patients (improving the disease-free survival rate from 40% with CHOP treatment alone, to 60% with R-CHOP therapy) (Coiffier et al., 2002, Coiffier et al., 2010). These observations were later confirmed by several additional trials, which resulted in R-CHOP being established as standard care for patients with DLBCL (Pfreundschuh et al., 2008, Pfreundschuh et al., 2006, Habermann et al., 2006, Sehn et al., 2005). It was shown that even 6 cycles of R-CHOP was sufficient for patients with advanced-stage disease (Pfreundschuh et al., 2008). In some advanced-stage patients with a potential risk of residual disease, consolidative radiotherapy is frequently used after completion of chemotherapy (recommended 3 cycles of R-CHOP for patients with stage I and non-bulky stage II disease), as several retrospective analyses indicated the possible benefits of this treatment (Aviles et al., 1994, Aviles et al., 2005, Dorth et al., 2012, Phan et al., 2010, Held et al., 2014, Nakamura et al., 2016). Although, no randomised trials from the 'rituximab era' have confirmed the role of consolidative radiation in treatment of DLBCL.

1.1.4.2 Treatment of relapse and refractory disease

Although the addition of rituximab to CHOP chemotherapy in standard treatment of DLBCLs has improved the disease-free survival of patients to approximately 60%, approximately 10% to 15% of patients still suffer from primary refractory disease and an additional 20% to 25% of patients who exhibit an initial response to treatment, relapse within the first 2 years (Coiffier et al., 2010, Friedberg, 2011).

It is established that less than 10% of patients who do not respond to first-line therapy and undergo currently available salvage therapy will achieve long-term disease-free survival (Hitz et al., 2015). Salvage treatment includes high dose chemotherapy and if possible, autologous stem cell transplantation (HDC/ASCT) (Philip et al., 1995); only around half of relapse/refractory DLBCL patients are eligible for this intensive treatment due to advanced age. The second-line chemotherapy treatment for these patients usually includes drugs such as ifosfamide, carboplatin and etoposide (ICE), in combination with rituximab (Kewalramani et al., 2004). Additionally, it was shown by correlative biomarker analysis that GCB subtype DLBCL patients may possibly benefit more from treatment with a combination of rituximab with several other drugs: dexamethasone, Ara-C and cisplatin (R-DHAP) as second-line therapy (Thieblemont et al., 2011).

Based on the very poor prognosis for relapse/refractory DLBCL, low effectiveness of currently available salvage therapy and high number of patients not eligible for such treatment, novel, more effective and less toxic agents are urgently needed.

1.1.4.3 Novel therapies for treatment of DLBCL

Gene expression studies on the molecular heterogeneity of DLBCL uncovered several new therapeutic targets which could be used for further improvement of DLBCL treatment.

NFκβ and BCR signalling as potential targets for novel DLBCL therapies

As mentioned before, NFκβ and BCR signalling have been described as constitutively active in ABC subtype of DLBCL. Therefore, several therapies targeting these pathways are currently under assessment. For example, bortezomib which blocks the degradation

of $I\kappa\beta\alpha$ (an inactive protein for $NF\kappa\beta$), was successfully used in combination with chemotherapy as a second-line treatment in relapsed ABC type DLBCL patients (Dunleavy et al., 2009). The example of the drug targeting BCR cascade is ibrutinib. This inhibitor of BTK, which is currently in clinical trials (phase 3, PHOENIX), induced positive response in 41% of relapsed ABC type DLBCL patients compared to 5% response in patients with GCB type DLBCL (Wilson et al., 2012). In phase 1 and 2 trial, fostamatinib disodium, a SYK inhibitor, also showed response in more than 20% of tested refractory DLBCL patients (Friedberg et al., 2010). Everolimus, is another drug proposed to target important component of BCR pathway - PI3K signalling, by selective inhibition of mTOR. It is currently in phase III trial and showed positive response in various lymphomas, including 30% of DLBCL patients (Witzig et al., 2011).

BCL2 targeting therapies

Overexpression of BCL2 is observed in both subtypes of DLBCL, and was described as a negative prognostic factor for GCB type DLBCL and for “dual expresser” lymphomas (Johnson et al., 2012, Green et al., 2012). Phase I clinical study on selective BCL2 inhibitor, known as ABT-199, showed successful improvement in 38% of relapsed DLBCL patients (Souers et al., 2013, Davids et al., 2014).

Targeting microenvironment of DLBCL

The known importance of the tumour microenvironment in the development of cancer also provides opportunities for lymphoma therapies. Lenalidomide is a drug belonging to the group of immunomodulating agents able to inhibit angiogenesis and stimulate

immune response; and therefore also able to influence tumour enriched for the stromal-2 signature of DLBCL (Thieblemont et al., 2012). It was shown to be effective in approximately 35% of relapsed aggressive B-cell non-HL patients (Wiernik et al., 2008) and was shown to be safely combined with R-CHOP treatment (Nowakowski et al., 2011, Vitolo et al., 2014); therefore the phase III ROBUST clinical trial is investigating the impact of the addition of this drug to R-CHOP treatment of ABC DLBCLs.

1.2 Receptor tyrosine kinases (RTKs)

RTKs are a large and diverse group of transmembrane proteins, whose main function is extracellular signal transduction into the cell, and therefore control of the most important intracellular pathways responsible for basic cellular functions, such as proliferation, differentiation and apoptosis (Ullrich and Schlessinger, 1990, Blume-Jensen and Hunter, 2001). In normal cells, these functions are under tight control. However, the observation that increased proliferation and immortality of cells are amongst the most important features in cancer, led to the investigation of deregulation of RTKs in tumorigenesis (Bennasroune et al., 2004).

One of the first RTKs observed to be up-regulated in the human genome was the HER2/neu gene. A 100-fold amplification of this receptor was discovered in around 30% of tested patients with invasive breast cancer, and this over-expression correlated with a poor prognosis (Slamon et al., 1989). This discovery highlights the importance of finding new therapeutic targets among receptor tyrosine kinases, and confirming the role of this receptor family in the process of tumorigenesis.

1.2.1 RTK structure and general mechanisms of action

The RTK family accounts for around 20 subfamilies, which in total include 58 different receptors (Robinson et al., 2000, Manning et al., 2002). All of them are similar in structure and mechanism of activation. Activation of the receptor is usually due to a glycosylated hydrophilic extracellular ligand-binding domain, which is connected with the cytoplasmic part of the receptor by single α -helix transmembrane region (20 amino acids). Inside the

cell, receptor is built of a juxtamembrane domain (40-80 amino acids), a conserved protein tyrosine kinase domain, and finishes with a C-terminus (carboxyl terminal tail). In addition to general structure these receptors also contain sub-domain motifs, which are responsible for substrate-binding, receptor phosphorylation and dimerization (Figure 1.4) (Hanks et al., 1988, Hunter, 1998, Hubbard, 1997).

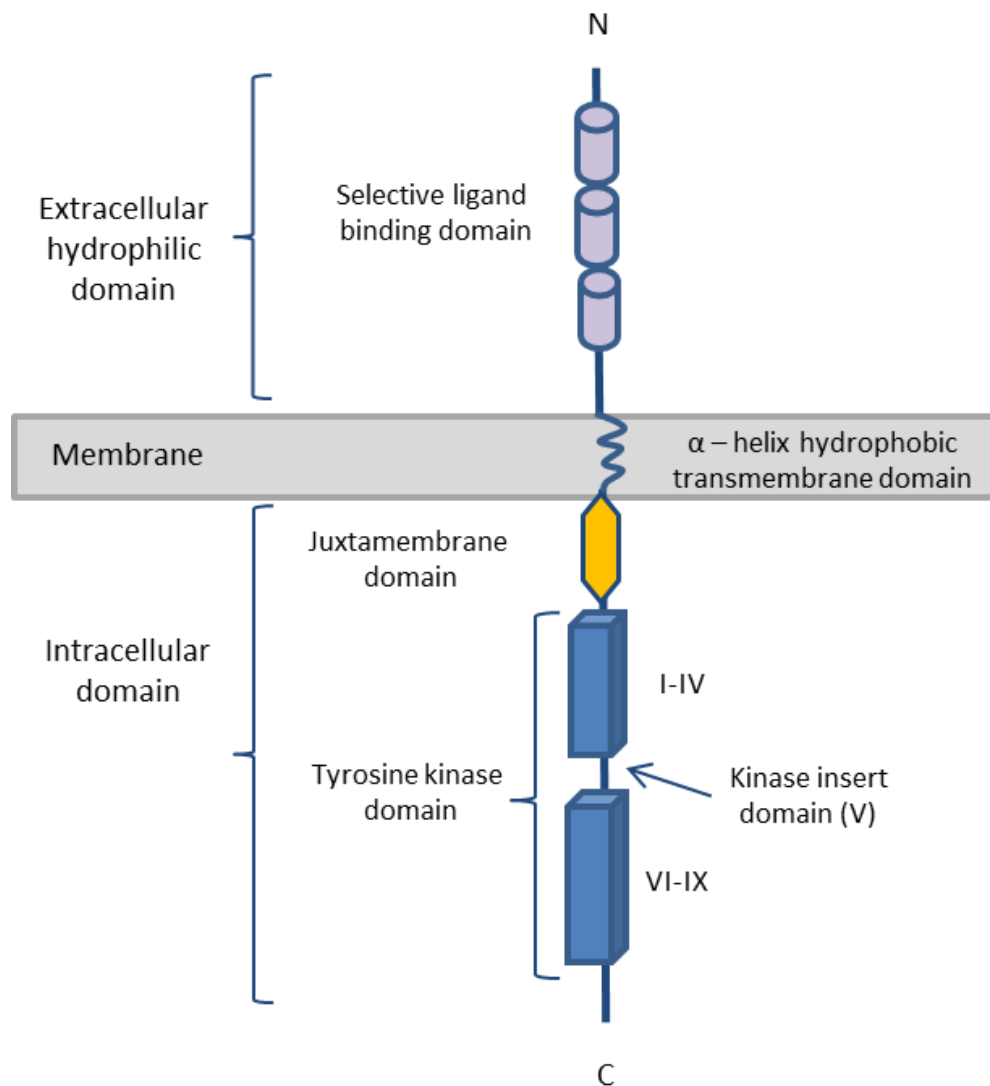


Figure 1.4 Structure of receptor tyrosine kinases (RTKs).

RTKs are built of an N-terminal selective ligand-binding extracellular domain, whose structure varies amongst different RTK subfamilies; a single α -helix transmembrane domain, which is important for stabilisation of the receptor; and an intracellular C-terminal domain, which is composed of a juxtamembrane region, tyrosine kinase domains – composed of 12 subdomains connected by one kinase insert domain (subdomain V) and C-terminal tail. The intracellular domain is directly responsible for receptor activation and downstream signal transduction by phosphorylation of tyrosine kinase domains.

The activation of the receptor cannot take place without its earlier dimerization. Here, the α -helix transmembrane domain helps with formation and stabilization of a dimer by non-covalent oligomerisation of α -helices in a lipid cell membrane (Arkin, 2002, Moriki et al., 2001). The pre-dimerized receptor is able to recognise its ligand, which binds to N-terminus of the receptor. This ligand-receptor interaction is very specific for each RTK subfamily and requires a large number of low-energy bonds such as ionic, hydrophobic or Van der Waals (Segaliny et al., 2015). Signals from the activated extracellular domain by successful ligand-binding cause further stabilisation of a dimer, and conformational changes to the tyrosine kinase domain, which results in receptor auto-phosphorylation and change to an 'open' conformation of the activation loop (located on the tyrosine kinase domain) (Lemmon and Schlessinger, 2010). Receptor orientation and phosphorylation determine the active state of a kinase domain. Phosphorylation of two tyrosine residues in an activation loop is necessary for a functional receptor and to stabilize its 'open structure'. This conformation is necessary for successful ATP binding. The phosphorylation of tyrosine kinases requires ATP which is stored in between two tyrosine kinase lobes and is provided by Mg^{2+} -ATP complexes. ATP is then bound to the protein substrate, which contains a tyrosine target, and initiates the transfer of the phosphate group from ATP to the receptor domain. Phosphorylated tyrosine kinases are then able to recruit cytoplasmic proteins, which then allows for activation of downstream signalling pathways (Hubbard and Till, 2000) (Figure 1.5). RTKs can affect signalling pathways directly by recruiting enzymatic effectors, or indirectly through their adapter proteins. The spectrum of RTKs is very broad; therefore many different pathways

can be affected. However, the most common pathways activated by RTKs and responsible for cellular functions such as cell proliferation, death, differentiation, migration or angiogenesis, are MSPK (Cargnello and Roux, 2011); PI3K/Akt/mTOR (Song et al., 2005); and Src (Bromann et al., 2004) pathways.

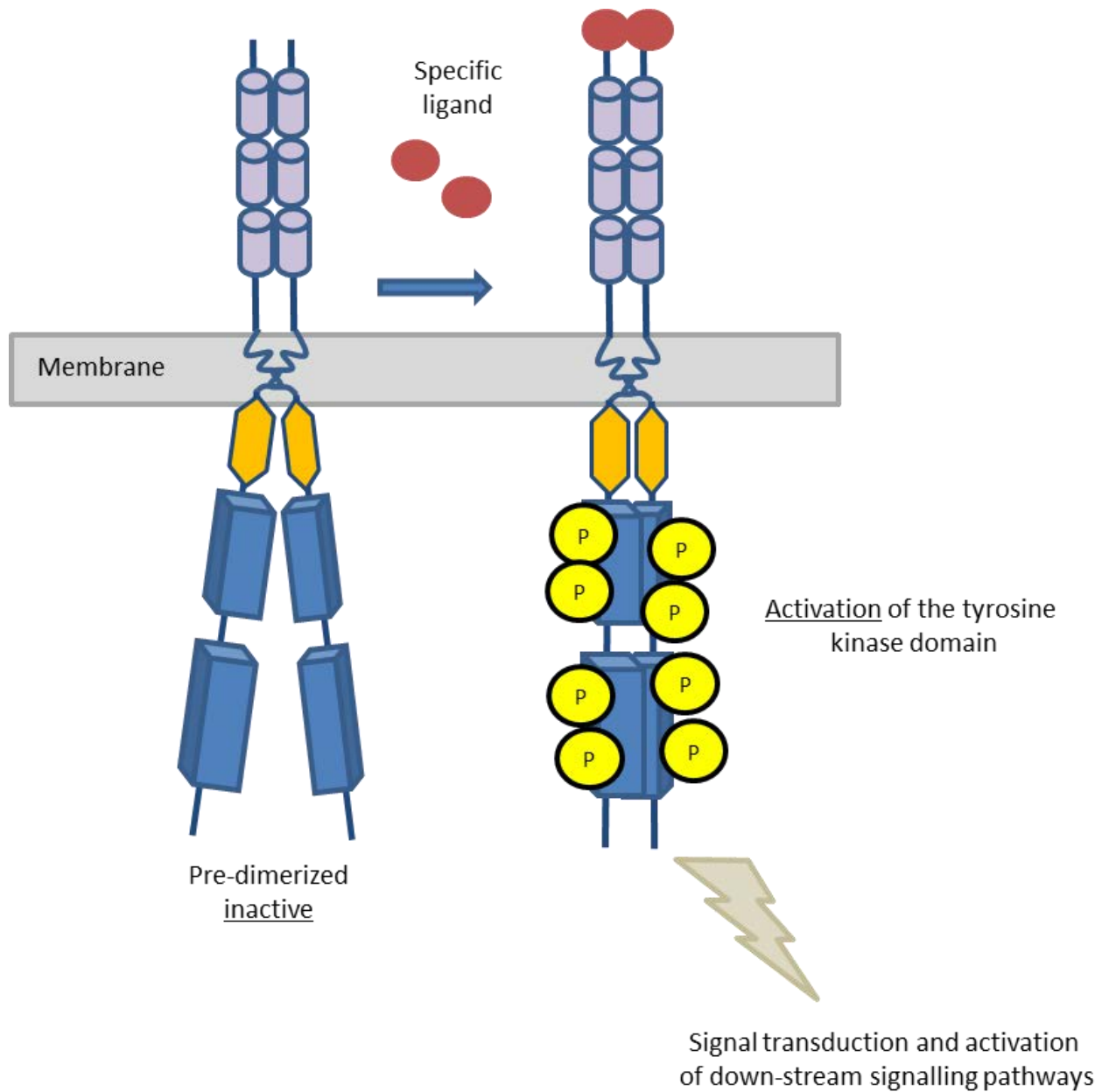


Figure 1.5 Dimerization and activation of receptor tyrosine kinases (RTKs).

A stable dimer, consists of two α -chains, and is created thanks to strong interactions between α -helix transmembrane domains in the cell membrane. This inactive form changes its conformation after binding of a specific ligand to the N-terminal of the receptor. Ligand binding initiates changes in the intracellular tyrosine kinase domain and release of ATP, and in that way phosphorylation of tyrosine kinases. Activation of the receptor cause attachment of intracellular proteins to phosphor-tyrosine docking sites and further signal transduction and activation of down-stream signalling pathways.

1.3 Discoidin domain receptor (DDR) family

Discoidin domain receptors are a relatively new (only discovered in the early 1990s), subfamily of RTKs. In the human genome it is represented by two members: DDR1 and DDR2 (Vogel et al., 2006). Their function is typical for RTKs and includes regulation of proliferation, adhesion and differentiation (Leitinger, 2011, Lemmon and Schlessinger, 2010). DDRs though can influence ECM structure and take part in its remodelling, owing to their ability to control matrix metalloproteinases (MMPs) (Leitinger, 2014). What makes them different from other RTKs is their mechanism of activation. DDRs can only be activated by one type of non-soluble ligand; collagen, and activation of the receptor is characterised by slow kinetics; the maximal activity of DDRs is observed several hours after collagen treatment (Vogel et al., 1997). What is more, Leitinger and co-workers, showed that dimerization of the extracellular domains of the DDRs is necessary for collagen binding; this stands in opposition to the widely known paradigm of ligand induced dimerization of RTKs. DDRs already exist as a dimers on the cell surface and ligand binding activates their signalling by changes in dimer conformation; however, ligand binding does not induce receptor oligomerisation, as has been observed in many RTKs (Leitinger, 2003, Lemmon and Schlessinger, 2010).

1.3.1 DDRs' expression and functions

DDRs are widely expressed in normal developing organisms. High levels of DDR1 mRNA was reported in lung, keratinocytes, spleen, kidney, placenta and brain (Sakamoto et al., 2001, Dimarco et al., 1993, Curat and Vogel, 2002, Shackel et al., 2002, Bhatt et al., 2000).

Whereas DDR1 expression is predominantly in epithelial cells (Alves et al., 1995), DDR2 dominates in tissues developing from embryonic mesoderm and is found in muscle, skin, kidney and lung (Alves et al., 1995, Lai and Lemke, 1994, Labrador et al., 2001). DDR expression was also noted in cells of both the nervous and immune systems (Zerlin et al., 1993, Lai and Lemke, 1994, Chetoui et al., 2011, Kamohara et al., 2001, Sanchez et al., 1994).

DDR1 plays important role in the process of organogenesis, while DDR2 is crucial for bone growth. In a DDR1-knockout mouse model, it was shown that lack of DDR1 affects several reproductive functions, including lactation and blastocyst implantation (Vogel et al., 2001). Lack of DDR1 in mice was also connected with defects in kidneys and inner ear structure of these animals (Torban and Goodyer, 2009). What is more, as mentioned previously, DDR1 is very important for cellular differentiation and motility, and also for collagen synthesis and signalling. DDR2 is involved in early development for controlling several aspects of bone growth (Zhang et al., 2011) and dysregulation of DDR2 function in mice resulted in defective bone growth as expected (Labrador et al., 2001, Kawai et al., 2014). In humans, DDR2 mutations leads to spondylo-meta-epiphyseal dysplasia (SMED-SL), a rare genetic disorder characterised by disproportions in body structure (short stature and limbs, broad fingers) and bone abnormalities (Borochowitz et al., 1993, Bargal et al., 2009). Although DDRs' functions in early embryo development appear clear, the role of their expression in healthy adult tissue is not fully established. Some evidence has found roles for the DDRs in wound healing (DDR2) and immune response (DDR1). Expression of DDR1 was reported in mononuclear cells of peripheral blood and in

activated T cells (Kamohara et al., 2001, Chetoui et al., 2011), whereas DDR2 was found in human circulating neutrophils (Afonso et al., 2013). The ability of neutrophils to migrate in 3D collagen matrices, suggests an important role for DDRs in immune responses. It is also postulated that DDRs can mediate migration of activated leukocytes toward the site of inflammation (Afonso et al., 2013). Interestingly, the observation of dysregulation of DDRs' expression in many pathological conditions has generated much interest in cancer research, and DDR1 over-expression has been described in breast, ovarian, brain and lung cancer, acute lymphocytic leukaemia and Hodgkin lymphoma (Chiaretti et al., 2005, Cader et al., 2013, Johnson et al., 1993, Heinzelmann-Schwarz et al., 2004, Weiner et al., 2000, Yang et al., 2010). What is more, DDR1 was found to be associated with the development of several other diseases such as atherosclerosis and fibrosis (Hou et al., 2001, Roberts et al., 2011). The role of DDRs in the regulation of expression and activation of metalloproteinases (MMPs), and its ability to degrade ECM components and tissue remodelling, seems to be very important for development of these diseases (Vogel et al., 1997, Valiathan et al., 2012). The over-expression of DDR1 across multiple diseases, including cancer, makes it a good therapeutic target.

1.3.2 Discoidin domain receptor 1 (DDR1) structure and isoforms

DDR1 possesses the typical structure of RTKs. However, interesting differences were noted in the extracellular part of the receptor. Like no other RTKs, DDR1 is a compound of an extracellular discoidin homology domain (DS), which is responsible for ligand binding; and DS-like domain which after ligand binding, participates in receptor activation (Vander

Kooi et al., 2007, Carafoli et al., 2009). What is more, it seems that loose packing of these DS and DS-like domains creates more space for possible alterations in structure, and might explain conformational changes seen in the DDR1 dimer (Carafoli et al., 2009). It was shown that DDR1 forms ligand-independent dimers, separately for extracellular and intracellular part of the receptor. Two motifs have been identified in the transmembrane part of DDR1: leucine zipper and GXXXG, which seem to be responsible for the appearance of DDR1 as a stable dimer in the absence of a ligand. Furthermore, a leucine zipper appears to be responsible for DDR1 self-association in biological membrane (Noordeen et al., 2006).

Its remaining structure comprises of an extracellular juxtamembrane region, which is built of 50 amino acids and contains N-, O- glycosylation and matrix metalloproteinase sites, a transmembrane domain, which is responsible for ligand independent dimerization of the receptor; a large intracellular juxtamembrane region (169 amino acids) with tyrosine kinases able to phosphorylate, one intracellular tyrosine kinase domain and C-terminal tail (Perez et al., 1994, Noordeen et al., 2006, Lemeer et al., 2012, Carafoli et al., 2012).

The DDR1 gene is found on human chromosome 6 (6p21.2) and is made up of 17 exons (Perez et al., 1994, Playford et al., 1996). It encodes 5 different transcripts, which raise 5 different DDR1 isoforms called DDR1a – e, generated by alternative splicing. DDR1 isoforms differ from each other by tyrosine kinase activity. Isoforms DDR1a – c have fully functional kinase activity, out of which DDR1c is the longest one, and possesses 919 amino acids. DDR1a and DDR1b in comparison to the c – isoform, lack 37 and 6 amino

acids in the intracellular juxtamembrane region or kinase domain, respectively. In contrast, DDR1d and DDR1e, are truncated proteins lacking the kinase region, and therefore have no kinase activity at all (Alves et al., 2001) (Borza and Pozzi, 2014, Rammal et al., 2016) (Figure 1.6). DDR1 isoforms analysis in adult tissues, suggests the DDR1b isoform is the most common (Perez et al., 1996). Interestingly, DDR1a was found to dominate in several cancer cell lines including Hodgkin lymphoma, breast and glioma tumour cell lines (Cader et al., 2013, Perez et al., 1996, Ram et al., 2006).

Not much is known yet about the mechanism regulating DDR1 transcription. However, in a few cases it was found that DDR1 transcription can be regulated by the Ras/Raf/ERK signalling pathway in human T cells (Chetoui et al., 2011) or in primary lung carcinoma. Here, DDR1 expression is regulated by DDR2 activation mediated by type I collagen which must be accompanied by ERK1/2 activation (Ruiz and Jarai, 2011). Interestingly, in breast and colon cancer cells, activation of DDR1 regulates its own expression by further Ras/Raf/ERK signalling (Ongusaha et al., 2003).

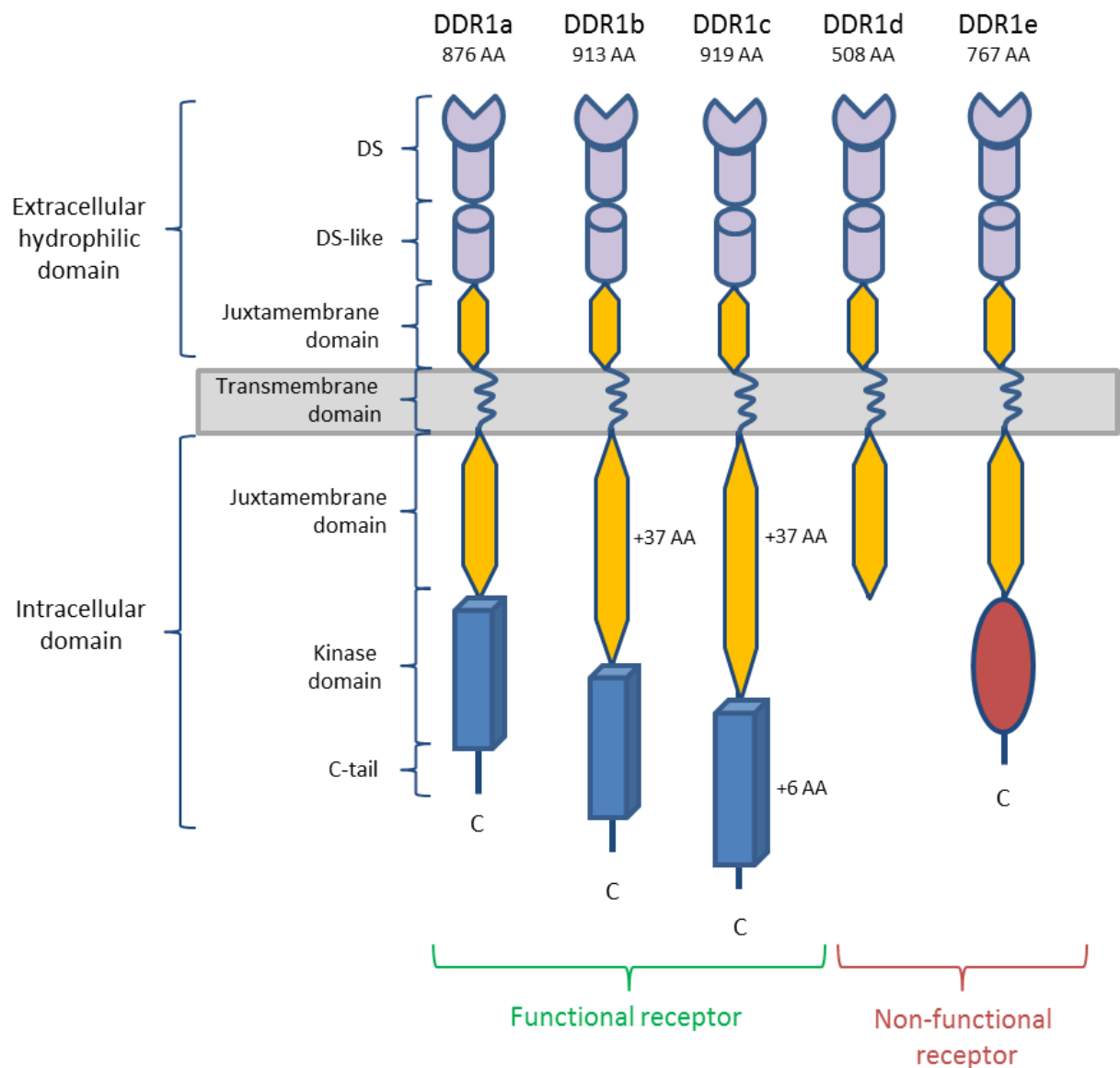


Figure 1.6 Structure of different DDR1 isoforms.

DDR1a, DDR1b and DDR1c are enzymatically functional receptors, whereas DDR1d and DDR1e do not present functional activity. The extracellular part of the DDR1 receptor is the same for all isoforms. Differences in structure and length are detected in the intracellular domain which determines the functionality of the receptor. DS- discoidin domain; DS-like – discoidin like domain; AA – amino acids.

1.3.3 DDR1 activation by collagen

Activation of DDR1 starts with collagen binding to the DS domain of the receptor. DDR1 activation appears to happen only in the presence of native, triple-helical collagen. It has been shown that denatured forms of collagen, like gelatin, are not able to induce kinase activity (Vogel et al., 1997, Kadler et al., 2007). Several types of collagen have been confirmed to induce DDR1 activation; this includes fibrillar collagens types I – III and network forming collagens type IV, VI and VIII (Vogel et al., 1997, Shrivastava et al., 1997).

The specificity of ligand binding to DDR1 is connected to the fact that DDRs are able to recognise only a specific amino acid sequence of collagens. This selective ligand recognition is possible due to highly conserved motifs, created by five surface-exposed loops at the top of the DS domain of DDRs. On DDR1, GVMGFO (O, hydroxyproline) sequence defines the main collagen binding residue. It is composed of six highly conserved in DDR1 amino acids (Trp53, Thr57, Arg105, Glu113, Asn175 and Asp69) and presents high affinity to fibrillary collagens I-III, but not to collagen IV (Abdulhussein et al., 2004, Leitinger, 2003). This observation suggests that DDR1 has to present another motif to bind non-fibrillar collagens, however this is not yet well characterised (Xu et al., 2011, Carafoli et al., 2009).

How DDRs are activated by collagen is still poorly understood. What is known is that by binding to the pre-formed DDR dimers, collagen causes the conformational changes necessary for receptor activation (Leitinger, 2003, Lemmon and Schlessinger, 2010). This process is characterised by slow kinetics and in some cases can take up to 18h from initial

exposure to collagen for full receptor autophosphorylation (Vogel et al., 1997, Mihai et al., 2009). This slow phosphorylation of kinase residues in DDR1 might be connected with the prolonged time needed for full receptor internalization on the cell surface. Thus far, only a single study has proposed that collagen binding to the receptor might cause its rapid aggregation, followed by receptor internalization into early endosome vesicles and after that, internalized DDR1 is recycled back to the cell surface (Mihai et al., 2009). These observations suggest that DDR1 phosphorylation can take place in the cytoplasmic compartment of the cell, rather than on the cell surface, and that DDR1 signalling can be controlled by endocytosis. This model would also provide an explanation for the unusually slow kinetics of DDR1 activation, however further studies are required to confirm these observations (Mihai et al., 2009).

Like other RTKs, DDR1 ligand-mediated phosphorylation of tyrosine residues leads to activation of several downstream signalling pathways. It is not yet known how the signal is translated from the collagen binding domain towards the tyrosine residues of DDR1. In total DDR1 possesses 15 tyrosine residues, which can be phosphorylated upon receptor stimulation with collagen. In the activation loop of all DDR1 isoforms (region containing 20-35 residues, beginning with the conserved Asp-Ohe-Gly motif), 3 major tyrosine residues were localised: Tyr792, Tyr796 and Tyr797, which seem to be critical for receptor activation (Perez et al., 1994). Additionally, several tyrosine residues in the juxtamembrane region (in DDR1b: Tyr513, Tyr484, Tyr 521) (Lemeer et al., 2012) and in the cytoplasmic domain, can be phosphorylated and work as docking sites for adaptor molecules. These residues differ between DDR1 isoforms. DDR1a isoform contains only

13 tyrosine residues and lacks Tyr513 and Tyr520. It was shown that activation of DDR1 is accompanied by p85 (subunit of PI3K) binding to Tyr881 residue and SHP-2 to Tyr703, Tyr796 and Tyr740 (Koo et al., 2006, Wang et al., 2006). Tyrosine residues also interact with several other proteins, such as RasGAP, SHIP-1/2 or STAT family members (Lemeer et al., 2012). However, detailed information about which tyrosine kinase domains became activated after collagen stimulation is lacking.

1.3.4 DDR-mediated signalling

DDR1 presents signalling typical of RTKs; it is often dependent on the cell or ligand type, and is still not fully understood (Borza and Pozzi, 2014). 30 different proteins have been identified, that potentially interact with DDR1 tyrosine phosphorylation residues (Lemeer et al., 2012). Most of those proteins possess a SH2 or PTB (phosphotyrosine binding) domain, through which they attach to the receptor. DDRs can recruit their enzymatic effectors directly by binding them to tyrosine domains, or indirectly using adapter proteins (e.g. Grb2, Shc, JAK2, STAT3, and CDC42). Two main signalling pathways are activated after receptor phosphorylation; MAPK/ERK and PI3K/Akt. Additionally, NF κ B and Notch 1 pathways have also been described as being activated by DDR1. DDR1 phosphorylation drives pro-survival signalling in breast and colon cancer cell lines via the NF κ B pathway, and in colon carcinoma through Notch-1 signalling (Ongusaha et al., 2003, Das et al., 2006, Kim et al., 2011). Recent discoveries in colorectal cancer point towards a new ability of DDR1 to phosphorylate BCR protein on Tyr177 and through this regulate β -catenin signalling responsible for cell motility (Jeitany et al., 2018).

MAPK/ERK signalling pathway

The main functions of the MAPK (mitogen-activated protein kinase)/ERK (extracellular signal-regulated kinase) signalling pathway are to control cell proliferation, differentiation, apoptosis, migration and angiogenesis.

As mentioned before, DDRs' activation after collagen binding results in phosphorylation of their tyrosine domains. This phosphorylation allows for recruitment of Grb2 adaptive protein, which binds to phosphorylated tyrosine residues by its SH2 domains. The second adaptive protein, SOS, binds to Grb2 by its SH3 domain. Due to this complex, RAS protein can be activated (SOS allows for exchange of GDP for GTP). Activated RAS transduces signals through recruitment and phosphorylation of Raf kinases (Cseh et al., 2014). Activated Raf phosphorylates MEK1 and MEK2 (MAP2K 1/2), which catalyse the phosphorylation on ERK1/ERK2. Activated ERK1/2 is then responsible for activation of transcriptional factors in the cell nucleus, such as, STAT, Elk-1 or CREB. These regulators activate transcription of genes regulating specific intracellular functions (Roskoski, 2012) (Figure 1.7).

The MAPK pathway additionally activates three other pathways: p38, JNK and ERK5. Activation of p38 pathway by MAP2K results in transcription of genes controlling cell proliferation, inflammation, angiogenesis and production of cytokines. Through the JNK pathway, DDR1 can control cell apoptosis and development of the immune system (Shintani et al., 2008), and in ERK5 pathway activation of MEKK2/3 by WNK1 results in phosphorylation and translocation of ERK5, which, in the nucleus activates cyclin D1 and

by this controls cell proliferation and survival (Raman et al., 2007, Cargnello and Roux, 2011).

DDR1 was observed to differentially affect the ERK pathway in different cell types. For example, DDR1 was described to activate ERK in smooth muscle cells (Lu et al., 2011), whereas the opposite effect was observed in mesangial cells, where the ERK pathway seems to be inhibited by DDR1 (Curat and Vogel, 2002). What is more, in T47D breast cancer cell line, high expression of DDR1 does not affect ERK pathway activation at all (L'Hote C et al., 2002).

PI3K/Akt pathway

The PI3K pathway mainly controls the cell cycle and through this maintains the cell survival-apoptosis balance. It plays a role in cell proliferation, migration and metabolism of glucose. PI3K pathway activation by DDR1 has been reported in a variety of normal and cancerous human cell lines (Ongusaha et al., 2003).

PI3K pathway can be activated similarly to the MAPK pathway, by binding of Grb2 and SOS adaptor proteins. PI3K catalytic activation starts with its recruitment by activated RTKs. PI3K is a kinase able to phosphorylate membrane lipids through its p110 subunit. Its activation transfers phosphate groups from PIP2 (phosphatidylinositol 4,5-bisphosphate) to PIP3 (phosphatidylinositol 3,4,5-triphosphate), which then allows for recruitment of Akt and PDK-1 to the membrane. PDK-1 is then activated by PIP3; this results in phosphorylation of Akt protein. Active Akt opens a spectrum of possibilities for further protein binding, and activation of processes responsible for cell survival, such as

degradation of pro-apoptotic BAD or p53 proteins, or expression of anti-apoptotic Bcl-2 protein. Additionally, Akt affects cell proliferation by inhibiting cell cycle repressors like p21 or p27, and induces angiogenesis by transcription of VEGF and HIF-1 α genes. Regulation of glucose and lipid metabolism by Akt is possible through suppression of GSK3 and activation of mTOR protein (Song et al., 2005) (Figure 1.7).

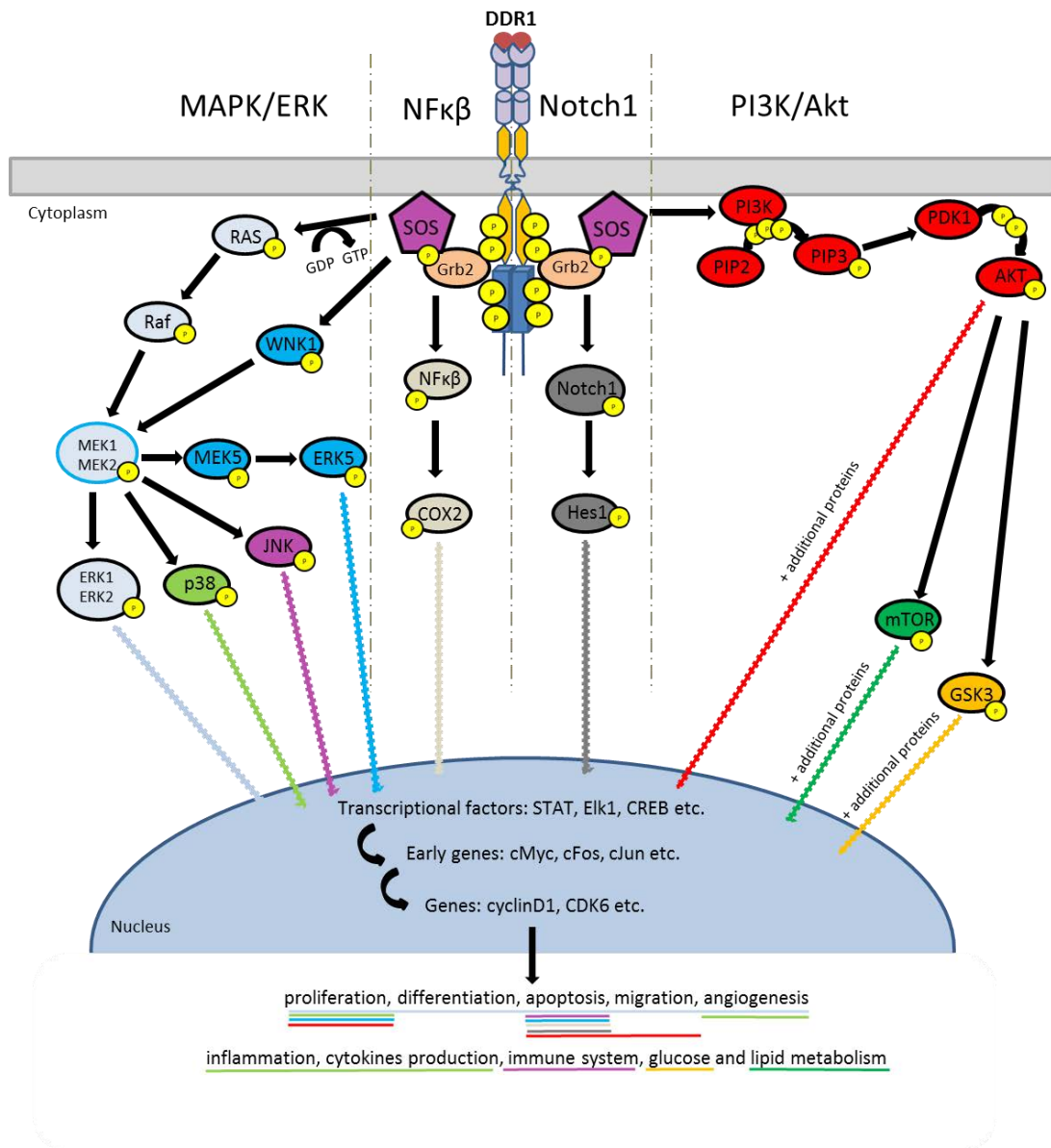


Figure 1.7 Main signalling pathways activated by DDR1.

Activation of DDR1 by collagen binding, causes its autophosphorylation on tyrosine residues (P) which allows for Grb2 – SOS adaptive protein binding. This complex is able to recruit further proteins, which are translating phosphorylated signals towards the nucleus. The MAPK/ERK pathway leads to activation of ERK1/ERK2 protein, which later activates transcriptional factors and is responsible for transcription of genes involved in regulation of proliferation, apoptosis, differentiation, migration and angiogenesis (blue on graph). MAPK/ERK is also activating p38 (green; proliferation, angiogenesis, inflammation, cytokine production), JNK (purple; apoptosis, development of immune system) and ERK5 (blue; proliferation, apoptosis) pathways. NFκβ and Notch1 pathways activated by DDR1 induce pro-survival functions in the cell (cream and grey; apoptosis). PI3K/Akt pathway activation starts from PI3K lipid kinase binding to Grb2/SOS complex and transfer of phosphate groups to PIP3. This whole process leads to Akt activation which is a binding site for many other proteins that regulates cell cycle progression and cell survival (red; proliferation, apoptosis, migration). Akt also controls glucose and lipid metabolism by activating mTOR (green; lipid metabolism) and GSK3 (orange; glucose metabolism) (for details see text in Section 1.3.4).

1.3.5 DDR1 cooperation with other receptors and growth factors

In addition to signal transduction by DDR1 after direct collagen activation of the receptor, DDR1 also seems to affect cell signalling induced by other receptors, such as integrins, Wnt5a/Frizzled, Notch1 or TM4SF1 tetraspanin, but also by growth factors, e.g. TGF- β .

It was shown that TM4SF1 tetraspanin helps with recruitment of syntenin2 and PKC α to the DDR1 kinase domain, which results in the activation of JAK2 and STAT3 proteins. The consequences of this activation are associated with increased metastatic properties of several breast cancers (Gao et al., 2016).

Integrins

DDR1 activation by collagen binding has been shown to occur independently of integrins (Vogel et al., 2000); however there is evidence that DDR1 and integrins can modulate each other's signals. Crosstalk between these receptors has been reported in the β 1 integrin subfamily; four members of this family were found to be activated by collagen in a similar way to DDRs (Leitinger, 2011). This cooperation can enhance signal transduction or cell adhesion, but can also inhibit specific functions of both receptors in a cell dependent manner. In a mouse model, crosstalk between DDR1 and α 2 β 1 integrin maintained undifferentiated embryonic stem cell renewal by selective activation of specific pathways which control Bim-1 (self-renewal controlling molecule) (Suh and Han, 2011). Overexpression of DDR1 in cells possessing α 1 β 1 and α 2 β 1 integrins was also shown to enhance the integrin-dependent adhesion to collagen, due to increased activation of integrins (Xu et al., 2012). Moreover, in pancreatic cancer cells, cooperation

of DDR1 and $\alpha 2\beta 1$ result in JNK pathway activation and through this, promote cell scattering (Shintani et al., 2008).

In MDCK cells, DDR1-integrin interactions had the opposite effect. In these cells, DDR1 activation by collagen I mediated a suppressive effect on cell migration and adhesion, induced by $\alpha 2\beta 1$ (Wang et al., 2005). In human adipose stromal cells in 3D culture, it was observed that DDR1-mediated transcription of stromal aromatase is inhibited by $\beta 1$ integrins (Ghosh et al., 2013).

Collagen-independent activation of DDR1

Although DDR1 is clearly activated by collagen, there is evidence to suggest that under specific conditions, DDR1 might also undergo collagen-independent activation.

DDR1 activation can, in some cases, be mediated by growth factors. Cooperation of DDR1 and TGF- β seems to be critical for normal mammary gland development in mice (Roarty and Serra, 2007). Wnt5a was also found to interact with DDR1, causing its phosphorylation in human mammary epithelial cells, and through this influence cell adhesion and migration (Jansson and Andersson, 2001). Moreover, in carcinoma cells expressing p53, DDR1 was shown to be activated by genotoxic stress (DNA damage or ionising radiation) (Ongusaha et al., 2003).

1.4 DDR1 expression in diseases

It is already well established that DDR1 expression is dysregulated in a variety of human cancers and other diseases. It has been linked with the development and progression of atherosclerosis, lung and kidney fibrosis and a number of cancers.

1.4.1 Atherosclerosis

Atherosclerosis is a disease in which smooth muscle cells (SMC) are highly proliferating and are characterised by increased migration, MMP and ECM synthesis. This pathological activity of SMCs causes thickening of the neointimal lesions in vessel walls and atherosclerotic plaque formation – the hallmark of this disease. The first observation of the role of DDR1 in atherosclerosis was made by Hou et al. in a mouse model. They showed that DDR1 plays an important role in collagen accumulation in atherosclerotic plaques. Mice with DDR1 knocked out demonstrate less intimal layer thickening and collagen accumulation after blood vessel injury than wild type controls (Hou et al., 2001). Additionally, DDR1 seems to also drive the migration of SMC cells and collagen remodelling (Ferri et al., 2004). Studies with *Ldlr*^{-/-} (low-density lipoprotein receptor) mice (this represents a more complicated model of human atherosclerosis) confirmed a critical role of DDR1 in plaque formation. DDR1 drives both inflammation and fibrosis during early stages of plaque formation. This pro-inflammatory role of DDR1 was confirmed by the observation of a reduced number of plaque infiltrating macrophages in *Ldlr*/*DDR1* knockout mice, in comparison to the DDR1 positive control (Franco et al., 2008).

1.4.2 Fibrosis

DDR1 upregulation was found to be a cause of fibrosis in several tissues. In lung, it has been shown that deficiency of DDR1 in mice decreases the fibrotic response by decreased inflammation. An observed reduction in the number of CD3-positive lymphocytes and F4/80-positive cells in lung infiltrate, but also decreased activation of p38 kinase in MAPK signalling, known to be involved in the lung fibrosis, suggests DDR1 is an important regulator of this disease (Underwood et al., 2000, Avivi-Green et al., 2006). Furthermore, the expression of DDR1 in human lung tissue was confirmed and the role of DDR1 in epithelial repair in lung was also investigated *in vitro*, which confirmed the results seen in the mouse model (Roberts et al., 2011). Therefore, DDR1 could be a good target for the treatment of idiopathic pulmonary fibrosis (IPF), which is characterised by continuous epithelial injury.

DDR1 overexpression is also well established in patients with kidney fibrosis, as well as in the mouse model of this disease. Observations from the DDR1 knockout mouse model concluded that DDR1 drives development of hypertension-induced kidney disease, by modulating both inflammation and fibrosis (Flamant et al., 2006). High levels of DDR1 expression were also described in other kidney disorders such as lupus nephritis, Goodpasture syndrome and Alport syndrome. DDR1 knockout in the Col4a3 mouse model (for progressive renal scarring) improved kidney function by reducing inflammation and fibrosis (Gross et al., 2010).

1.4.3 Cancer

The mutation and expression of DDRs is found in many tumours, for example, breast, lung, brain, head and neck, liver, pancreatic, prostate and ovarian cancers, and in a broad range of lymphomas and leukaemias (Valiathan et al., 2012, Rammal et al., 2016). DDRs have been shown to regulate cell proliferation, migration and therefore tumour invasiveness. Their activation in cancer is also linked with malignant transformation and epithelial to mesenchymal transition (EMT), which plays a crucial role in tissue differentiation and repair, but can also cause tissue fibrosis and in tumours is associated with poor survival, resistance to therapy and increased cell motility (Thiery et al., 2009). Depending of type and stage of cancer, DDR1 can act in a pro- or anti-tumorigenic manner, which makes the process of understanding their role in the development and progression of cancers more complex.

Breast cancer

One of the first studies about DDR expression in cancer tissue originated from cells isolated from breast cancer in mice and suggests a critical function of these receptors in breast cancer progression. In the mouse model, DDR1 knockout was connected with abnormalities in mammary phenotype (Vogel et al., 2001).

DDR1 is also known to be highly expressed in the human breast carcinoma cell lines T47D and BT-20 (Johnson et al., 1993). However, analysis of different types of primary human breast cancers resulted in conflicting observations. In primary invasive carcinoma with lymph node metastases, DDR1 expression in mRNA was elevated (Barker et al., 1995),

whereas a study on human breast carcinomas (grade intermediate to high) showed reduction of DDR1 mRNA expression relative to normal tissue (Neuhaus et al., 2011). Some studies in human breast cancer cell lines suggest that in breast cancers with elevated DDR1 expression, activation of the receptor can promote cell proliferation, resistance to chemotherapy (Das et al., 2006)(T47D, MDA-MB-435 cell lines), migration (Neuhaus et al., 2011)(MDA-MB-468,T47D cell lines) and invasion (Juin et al., 2014)(MDA-MB-231 cell line). However, in other studies opposite effects were observed depending on the cell line (Assent et al., 2015)(proliferation: MCF-7, ZR-75-1 cell lines) (Koh et al., 2015)(migration: MDA-MB-231, Hs578T cell lines). These observations once again indicate a DDR1-cell dependent function in cancer and are suggestive of DDR1's involvement in regulation of cell proliferation, migration and invasion in breast carcinoma, although the exact role of DDR1 in breast cancer progression is still not fully understood (Jing et al., 2018).

Lung cancer

NSCLC is characterised by dysregulation of DDR expression, phosphorylation, and in some cases even mutation. DDR1 was found to be overexpressed in a cohort of primary NCLCs from a few independent studies (Ford et al., 2007, Yang et al., 2010, Valencia et al., 2012). Moreover, DDR1 overexpression was found to be negatively associated with overall survival (Yang et al., 2010, Valencia et al., 2012). High levels of activation of DDR1 were confirmed in a study of 150 primary NSCLC tumours, where DDR1 was found to be among the most phosphorylated RTKs (third after Met and Alk) (Rikova et al., 2007). These

observations, taken together suggest that DDR1 might be associated with the development and progression of NSCLC. Interestingly, genetic analysis of DDRs in NSCLC from several studies identified three somatic mutations of DDR1 (A496S in cytoplasmic JM region, W385C in extracellular JM region and F866Y in kinase domain) (Davies et al., 2005, Ding et al., 2008) and 11 mutations in the DDR2 gene, among which L239R and I638F were found to regenerate cellular sensitivity to the RTK inhibitor dasatinib (Hammerman et al., 2011).

Hodgkin lymphoma

It is known that the pathogenesis of haematological malignancies is associated with dysregulation of tyrosine kinase function. However, the number of studies which focus on DDR function in blood cancers is very limited. Until now, only a few studies have been published which confirm disruptions in DDR1 expression in adult acute lymphocytic leukaemia (ALL) (Chiaretti et al., 2005) and DDR1 expression (Favreau et al., 2012) and gene mutations in acute myeloid leukaemia (AML) (Tomasson et al., 2008, Loriaux et al., 2008). Recently, DDR1 was also shown to be expressed in chronic lymphocytic leukaemia (CLL). DDR1 mRNA expression was confirmed in CLL by three published datasets, which showed that the high level of DDR1 correlates with three independent prognostic markers for CLL (time-to-first-treatment (TTFT), ZAP70 and IGVH status), suggesting that expression of DDR1 in CLL might be connected with poor prognosis. Furthermore, DDR1 cell surface expression was also confirmed on peripheral blood leukaemia cells in a small

cohort of CLL cases; however the functional role and mechanisms controlling DDR1 expression in this cancer has not been confirmed (Barisione et al., 2017).

So far, Hodgkin lymphoma seems to be the best studied haematological malignancy in the context of DDR expression and functions. Upregulation of DDR2 expression was demonstrated in 30-70% of Hodgkin-Reed-Sternberg (HRS) cells from lymph nodes of HL patients, which were shown to remain in close contact with collagen I (Renne et al., 2005, Willenbrock et al., 2006). Over-expression of DDR1 in HRS cells was described by Cader et al., together with the observation of the close association of HRS cells with collagen. In primary HL, DDR1 in HRS cells was localised to the cell membrane and cytoplasm. Upregulation of DDR1 expression (both in protein and mRNA) was also described in 4 HL-derived cell lines (L591, L428, L1236, KMH2), followed by the discovery that the DDR1a isoform is predominantly expressed in these cells (Cader et al., 2013). Moreover, it was also shown that collagen activates DDR1 in HL lines, which was seen by robust phosphorylation of the receptor after collagen stimulation. Activation of DDR1 by collagen was then shown to protect L428 cells from apoptosis, and in DG75 cells, DDR1 phosphorylation protected cells from death induced by the addition of the chemotherapeutic drug, etoposide (Cader et al., 2013).

Other cancers

DDR1 expression was also described in several other cancers (Valiathan et al., 2013). Overexpression of DDR1 in mRNA was reported in different types of brain tumours in children and adults (Weiner et al., 2000, Ram et al., 2006). DDR1 expression at the

protein level was shown to be elevated and strongly correlated with poor prognosis in gliomas. DDR1 has also been shown to play an important role in the regulation of proliferation, (Yamanaka et al., 2006), migration and invasiveness of glioma cells (Ram et al., 2006).

Some studies in ovarian and endometrial cancers indicated that DDR1 may be a useful target and biomarker for these diseases, as its high expression has been correlated with a poor prognosis (Quan et al., 2011, Colas et al., 2011). DDR1 and PCA1 (prostate cancer antigen 1) are highly expressed in primary prostate cancers, and it was shown that PCA1 regulates DDR1 expression in prostate cancer cell lines (Shimada et al., 2008).

In liver cancer, DDR1 was found to be among the most phosphorylated RTKs and its over-expression was connected with advanced stage of the tumour (Shen et al., 2010, Gu et al., 2011). Moreover, DDR1 over-expression was also confirmed in pancreatic (Couvelard et al., 2006) and head and neck cancer (Squire et al., 2002). In both cancers, the in vitro studies proposed a role for DDR1 in increased tumour migration (Park et al., 2007, Rudra-Ganguly et al., 2014) and EMT (Shintani et al., 2008, Maeyama et al., 2008).

1.5 DDR1 as a therapeutic target in cancer

The contribution of DDR1 signalling to the pathogenesis of many different cancers indicates that blocking of DDR1 activity or expression might be a good therapeutic approach. DDR1 can be affected by several strategies which could lead to down-regulation of the receptor or to the inhibition of DDR1 activation. For example, genetic mutation of DDR1 expression was shown in mice model of glomerulonephritis (Kerroch et al., 2012). The latter approach was already successfully tested on cancer cells. This could work via several mechanisms; thus, the activation of intracellular pathways by DDRs can be prevented by: disruption of DDRs-collagen interaction, inhibition of DDR activation by affecting extracellular domains of receptor and by inhibition of DDR kinase activity by small molecules inhibitors (Figure 1.8) (Borza and Pozzi, 2014).

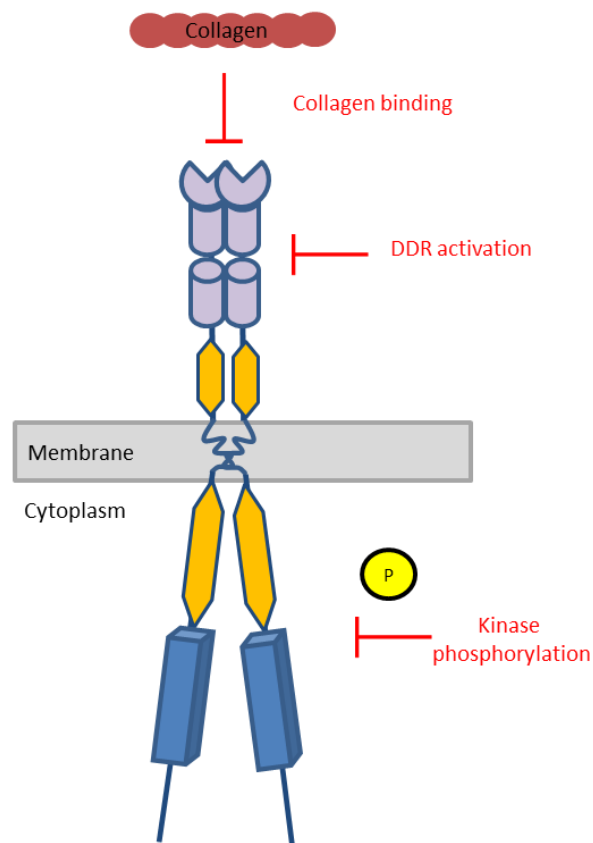


Figure 1.8 DDRs therapeutic therapy strategy in cancer.

Preventing DDRs activation can be achieved by: blocking collagen/DDR interactions, inhibition of DDR activation by specific antibodies which prevents receptor oligomerisation and transformation caused by collagen binding and by specific small molecule inhibitors which block phosphorylation of the tyrosine kinases of the receptor.

1.5.1 DDR1 inhibitors

DDR1 activation can be inhibited by broad range of antibodies which bind to the DS-like domain of receptor, but do not influence collagen binding (Carafoli et al., 2012), they include the monoclonal antibodies Fab 3E3 (Carafoli et al., 2012), 48B3 (Ram et al., 2006) and H-126 (Castro-Sanchez et al., 2010).

Another approach is to use small molecule inhibitors targeting directly the kinase domain of the receptor. Small molecule inhibitors are divided into three groups. Type I inhibitors target the highly conserved DFG motif at the beginning of the activation loop of the kinase domain in its active DFG-IN conformation, and they work as ATP competitors. Their action is described as promiscuous; however their advantage lies in their ability to inhibit kinases that are resistance to type II inhibitors (Eglen and Reisine, 2009, Tokarski et al., 2006). Nowadays, most of the kinase inhibitors belong to this group. Type II inhibitors seem to be more selective because of more specific binding to the kinase domain in its non-active conformation - DFG-OUT. This conformation allows for binding of the inhibitor to additional sites in the kinase domain and therefore stabilizes it in an inactive form (Kothiwale et al., 2015). The type III inhibitors target allosteric sites responsible for the regulation of kinase activity, rather than ATP binding site itself (Taylor and Kornev, 2011).

Three small molecule inhibitors, are currently in use for treatment of patients with chronic myelogenous leukaemia (CML): imatinib (Gleevec®, STI571, type II) which is used as a first line treatment, and two second-generation inhibitors: nilotinib (Tasigna®,

AMN107, type II) and dasatinib (Sprycell®, BMS354825, type I), which are supporting imatinib treatment in patients with some resistance to this drug (Weisberg et al., 2005). All these inhibitors were originally designed to target the tyrosine kinase activity of the fusion oncogene Breakpoint Cluster Region-Abelson kinase (BCR-ABL) and nilotinib's and imatinib's specificity to this kinase was confirmed. However, dasatinib was described to potentially inhibit many more kinases including those belonging to Src family. Therefore, the probability of observing off-target effects during in vivo treatment with dasatinib is high (Shah et al., 2004, Weisberg et al., 2007). Interestingly, the ability of these drugs to inhibit the phosphorylation of DDR1 was also identified, with nilotinib showing the strongest affinity for DDR1 in chronic myelogenous leukaemia (Day et al., 2008). Recent studies confirmed the effectiveness of nilotinib in inhibiting DDR1 in colorectal cancer (CRC). Treatment of colorectal cancer cell lines with nilotinib resulted in reduction of cell metastasis and invasion, as a result of an effect on the newly discovered DDR1-BCR signalling. These observations were also confirmed in CRC liver metastasis mouse model (Jeitany et al., 2018). Two more BCR-ABL kinase inhibitors able to inhibit DDR1 activity were reported; Bafetanib (INNO-406) is a structural analogue of imatinib and nilotinib, but its specificity is not comparable to those drugs. Ponatinib, another type II selective ABL inhibitor was also described to effectively block DDR1 activation (Canning et al., 2014). Bafetanib was reported to interfere with other kinases, including PDGFR, KIT and LYN (Rix et al., 2010). Similar properties were described for the LCB 03-0110 inhibitor, which in HEK293 cells successfully blocked collagen induced activation of DDR1 and DDR2 (Sun et al., 2012).

These inhibitors were designed against BCR-ABL and so are not specific for DDR1. The functional effects of DDR1 inhibition by anti-BCR-ABL drugs in cancers, pointed at the importance of inhibitory treatment of DDR1 in cancer therapies. Therefore, the need of specific blocking of DDR1 phosphorylation, led to the discovery of few novel and selective DDR1 inhibitors.

Gao and co-workers reported 3-(2(pyrazolo[1,5- α]-pyrimidin-6-yl)ethynyl)benzimidides as novel and selective DDR1 inhibitors, which tightly capture the ATP binding domain. By screening around 2000 compounds previously designed to inhibit BCR-ABL and other RTKs, they reported a group of 24 pyrazolopyrimidine compounds called 7a-7x, which showed the highest affinity to DDR1/DDR2. After some structural optimisations, two compounds, 7rh and 7rj, were reported to show high specific inhibitory activity against DDR1, but much less towards DDR2, BCR-ABL, c-Kit kinases and to a further 456 tested kinases. The initial tests on the NCI-H23 non-small cell lung cancer cell line, characterised by high expression of DDR1, showed a decrease in total DDR1 protein levels, which was suggested to be caused by the inhibition of the proliferative signals from Ras/Raf/ERK and PI3K/Akt pathways. Moreover, inhibition of DDR1 resulted in decreased level of produced metalloproteinase 2 (MMP2), indicating a possible role for 7rh and 7rj inhibitors in the down-regulation of migration and invasion of cancer cells. The anti-proliferative effect of 7rh and 7rj inhibitors, already in low μ M concentrations, was also confirmed in several other cell lines. 7rh and 7rj also reduced adhesion and colony formation in NCI-H23 lung cancer cells (Gao et al., 2013).

Independently, another potent and selective type II DDR1 inhibitor: DDR-IN-1, which currently is also commercially available, was designed and synthesised (Kim et al., 2014). The ability of DDR-IN-1 inhibitor to block (with a high selectivity) DDR1 kinase phosphorylation after exposure to collagen was confirmed in U2OS cells. It was also shown that DDR1-IN-1 affects kinases such as EGFR, Src, Cdk1, mTOR and PI3K. Treatment of several cancer cell lines with DDR1-IN-1 resulted in inhibition of cell proliferation, but not at concentrations lower than 10 μ M, perhaps surprising in light of the suggested very high selectivity of this inhibitor (Kim et al., 2014).

Selective DDR1 inhibitors described above were mostly designed based of the known structure of BCR-ABL inhibitors (nilotinib, imatinib, dasatinib) and their mechanism of action. A new approach to the discovery of small molecule inhibitors of DDR1 was presented by Murray and co-workers (Murray et al., 2015). Their discovery of novel DDR1/DDR2 inhibitors was based on the analysis of fragments (protein complexes) on the crystal structure of DDR1, which are targeted by specific inhibitors. It was found that most of the fragments were localised on the hinge region, at the front of ATP binding motif of DDR1. However, 10 fragments were localised in the back pocket of DDR1, which is accessible only when activation loop is in DFG-OUT conformation. The design of the new drugs was then based on specific fragments binding, starting from those which were discovered to bind to the back pocket of DDRs. This approach resulted in construction of 9 DDRs inhibitors with a very high selectivity to DDR1 or/and DDR2 receptors (Murray et al., 2015).

1.6 Chromosomal instability and cancer

1.6.1 Mitosis

Understanding how equal chromosomal division occurs into two daughter cells was a challenge since the first observation of chromosome separation during mitosis of fertilized eggs of sea urchin by Theodor Boveri in 1902 (Kops et al., 2005, Boveri, 1902).

The aim of mitosis is to produce two identical daughter cells containing equal numbers of chromosomes. Mitosis has several phases, controlled by mitotic checkpoints. The beginning of mitosis is defined by chromosome condensation and mitotic spindle (separation of duplicated centrosomes) formation during prophase (Rieder, 2011, Kops et al., 2005, Rosenblatt, 2005). At this stage, the process of chromosome condensation is still reversible. However, after passing this point, the cell enters the next stage of mitosis called late prophase, and from now on the cell is committed to mitosis and the process of division can be stopped only by cell death. After nuclear envelope breakdown (NEB) the cell enters prometaphase. Chromosomes, which are now loose in the cytoplasm, become attached to microtubules, what is driven by microtubule motor protein CENPE (Mitchison, 1988). If any of the kinetochores is not attached, the mitotic checkpoint (SAC; spindle assembly checkpoint) is activated and process of mitosis is stopped. Microtubule capture by all kinetochores results in silencing of the mitotic checkpoint and the continuation of mitosis. Duplicated sister chromatids captured by microtubules are then aligned into mitosis plate (metaphase), and pulled apart in anaphase (Mitchison, 1988, Wadsworth et al., 1988). In the last phase of mitosis the nuclear envelope is reproduced

and chromosomes decondense (telophase), leading to final division of the cell in cytokinesis (Rieder, 2011, Kops et al., 2005) (Figure 1.9).

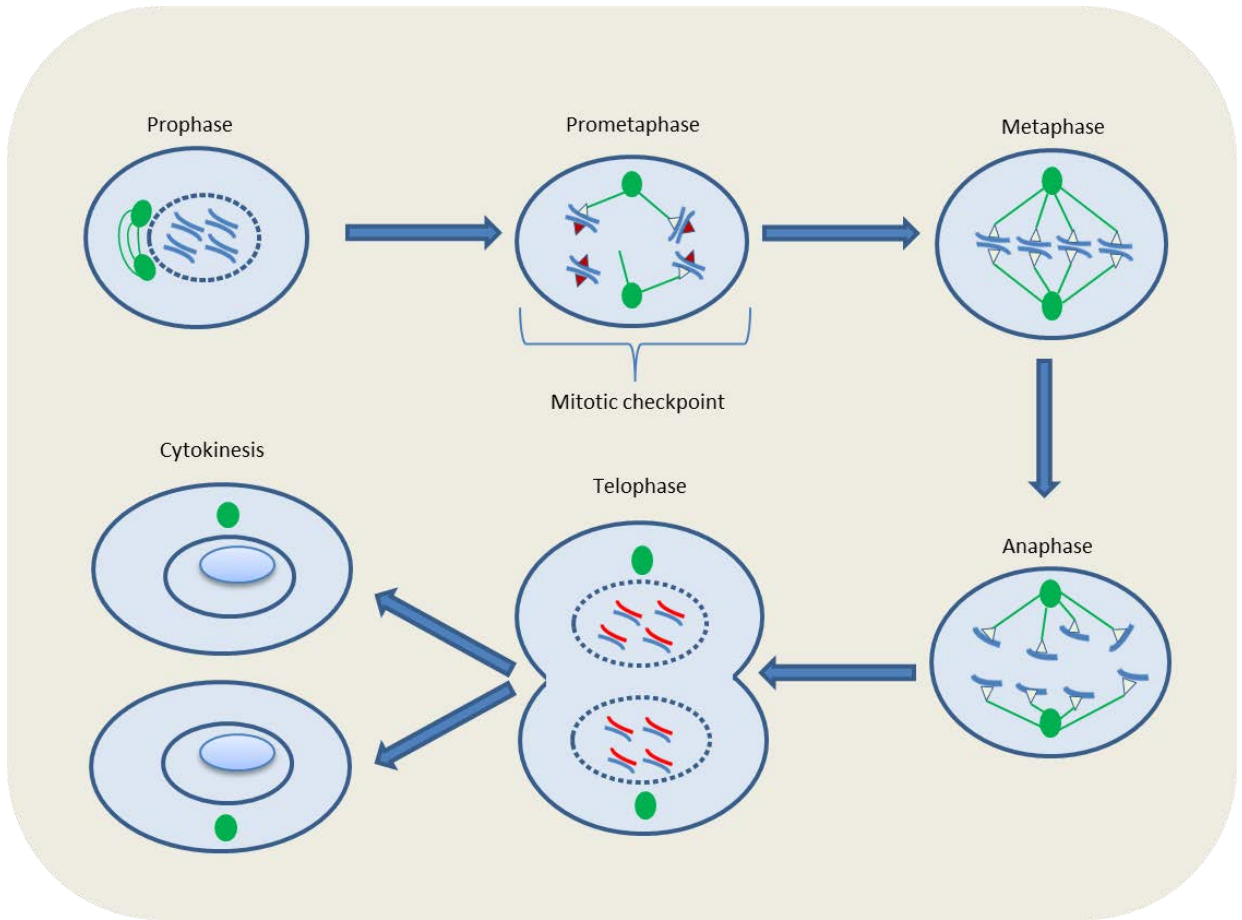


Figure 1.9 Phases of mitosis.

Chromosomes condensation, centrosomes (green circles) separation and nuclear envelope breakdown (the dashed circle) in prophase starts process of mitosis. Chromosomes are attached to microtubules in prometaphase. Single error in attachment of kinetochores (red triangle) to microtubules results in activation of mitotic checkpoint and by that blockade of the progress of mitosis. Capture of all kinetochores (white triangles) on duplicated chromosomes by microtubules, inactivates mitotic checkpoint and allows for mitotic plate formation in metaphase. Aligned sister chromatids are then pulled apart in anaphase. In telophase, cell is preparing for final division and cytokinesis, by reformation of nuclear envelope and decondensation of chromosomes.

1.6.2 Mitotic checkpoints

The process of proper segregation of chromosomes during mitosis is controlled by a primary cell cycle control mechanism called the mitotic checkpoint (SAC, spindle assembly checkpoint). Its activation by the signal generated in the event of a mistake in the attachment of kinetochores, prevents progression of the cell division process through anaphase. The first components of the mitotic checkpoint were initially discovered in budding yeasts (Bub1-3, Mad1-3 and MPS1) and the importance of its orthologues were also confirmed in vertebrates (Mad1, Mad 2, Bub3, kinase Bub1 and Mps1) (Shin et al., 2003, Abrieu et al., 2001, Jin et al., 1998, Li and Benezra, 1996, Taylor et al., 1998). The vertebrate mitotic checkpoint is additionally comprised of the kinase BUBR1, the microtubule motor protein CENPE (centromere protein E), the protein complex ZW10-ROD-zwilch and MAPK (mitogen-activated protein kinase) (Abrieu et al., 2000, Chan et al., 1999, Chan et al., 2000, Mao et al., 2003, Minshull et al., 1994) (Table 1.2).

The signal transduction in SAC starts from CENPE which is the microtubule motor protein responsible for chromosome capture during metaphase. The signal from unattached kinetochores, driven by CENPE, activates the SAC and promotes recruitment of the mitotic checkpoint components. It has been shown that MPS1 (monopolar spindle 1) kinase activation may contribute to kinetochore capture by CENPE protein and controls the phosphorylation of MAD1 protein (Abrieu et al., 2001) (Faesen et al., 2017, Mattison et al., 2007). Phosphorylation of MAD1 is subsequently required for its association with MAD2 protein (Chen et al., 1999, Faesen et al., 2017). Binding of the CENPE protein to its

direct binding partner, BUBR1, causes activation of CENPE which is necessary for further attachment of the MAD1/MAD2 complex. Therefore, MPS1 and CENPE seems to be necessary for MAD1/MAD2 complex recruitment to the kinetochores during activation of the SAC. In return, this complex is responsible for changes in the MAD2 conformation to its active form (Chan et al., 1999, Shah et al., 2004). Activated MAD2 binds with BUBR1 and BUB3, and in creating this complex, is able to prevent CDC20 (cell-division-cycle 20 homologue) from activating a multi-subunit E3 ubiquitin ligase, APC/C (anaphase promoting complex/cyclosome). A few other proteins supporting this process include BUB1 and MPS1, which, when missing, weakens mitotic checkpoint signalling (Abrieu et al., 2001). All these proteins together form an active complex, and have the capacity to block mitosis in prophase because of the lack of ubiquitination of securin and cyclin B1, normally mediated by active APC/C (Figure 1.10a) (Cleveland et al., 2003, Sudakin et al., 2001) (Hwang et al., 1998). However, when kinetochore attachment is completed by microtubule capture (mediated mostly by CENPE), inhibitory complex production is hindered and the mitotic checkpoint is silenced (Figure 1.10b) (Putkey et al., 2002, Weaver et al., 2003). Degradation of cyclin B1 by APC/C, known as a 'master regulator of mitosis', results in inactivation of CDK1 (cyclin-dependent kinase 1) and initiates mitotic exit; whereas degradation of securin causes activation of separase. Active separase influences cohesin links which keep sister chromatids together, and cause their separation (Peters, 2002). It has been shown in one cell type (PtK1, vertebrate somatic cells), that a signal from a single unattached kinetochore, can delay progression of mitosis for at least 3 hours (Rieder et al., 1994).

Table 1.2 Mitotic checkpoint components (Kops et al., 2005; Faesen et al., 2017; modified)

Protein	Size/Description	Binding partners	Function in checkpoint
BUB1	122 kDa; serine/threonine kinase	BUB3	Inhibits CDC20 by phosphorylation
BUBR1	120 kDa; serine/threonine kinase	CENPE, BUB3, CDC20	Part of APC/C inhibitor complex. Directly binds to CDC20 and inhibits APC/C activity
BUB3	37 kDa	BUB1, BUBR1	Part of APC/C inhibitory complex. Localizes BUB1 and BUBE1 to kinetochores
MAD1	83 kDa	MAD2	Directly recruits MAD2 to unattached kinetochores
MAD2	23 kDa	MAD1, CDC20, CMT2/p31 ^{comet}	Part of APC/C inhibitory complex. Directly binds to CDC20 and inhibits APC/C activity
CMT2/p31 ^{comet}	31 kDa	MAD2	Inhibits mitotic checkpoint signalling by antagonizing MAD2
MPS1	97 kDa	CENPE, MAD1, BUB1	Spindle poles duplication; phosphorylation of MAD1 protein, targeting MAD1:MAD2 complex; recruitment of BUB1 and BUB3
CENPE	312 kDa; plus-end directed microtubule motor	BUBR1	Activates BUBR1 at the unattached kinetochore
ZW10	89 kDa	ROD, Zwilch	Part of complex that recruits the MAD1-MAD2 heterodimer to unattached kinetochores
ROD	251 kDa	ZW10, Zwilch	
Zwilch	67 kDa	ROD, ZW10	

APC/C, anaphase promoting complex/cyclosome; BUB, budding uninhibited by benzimidazole; BUBR1, BUB1-related protein; CDC20 – cell-division-cycle20; CENPE, centromere protein E; MAD, mitotic arrest deficient; MPS1, monopolar spindle 1.

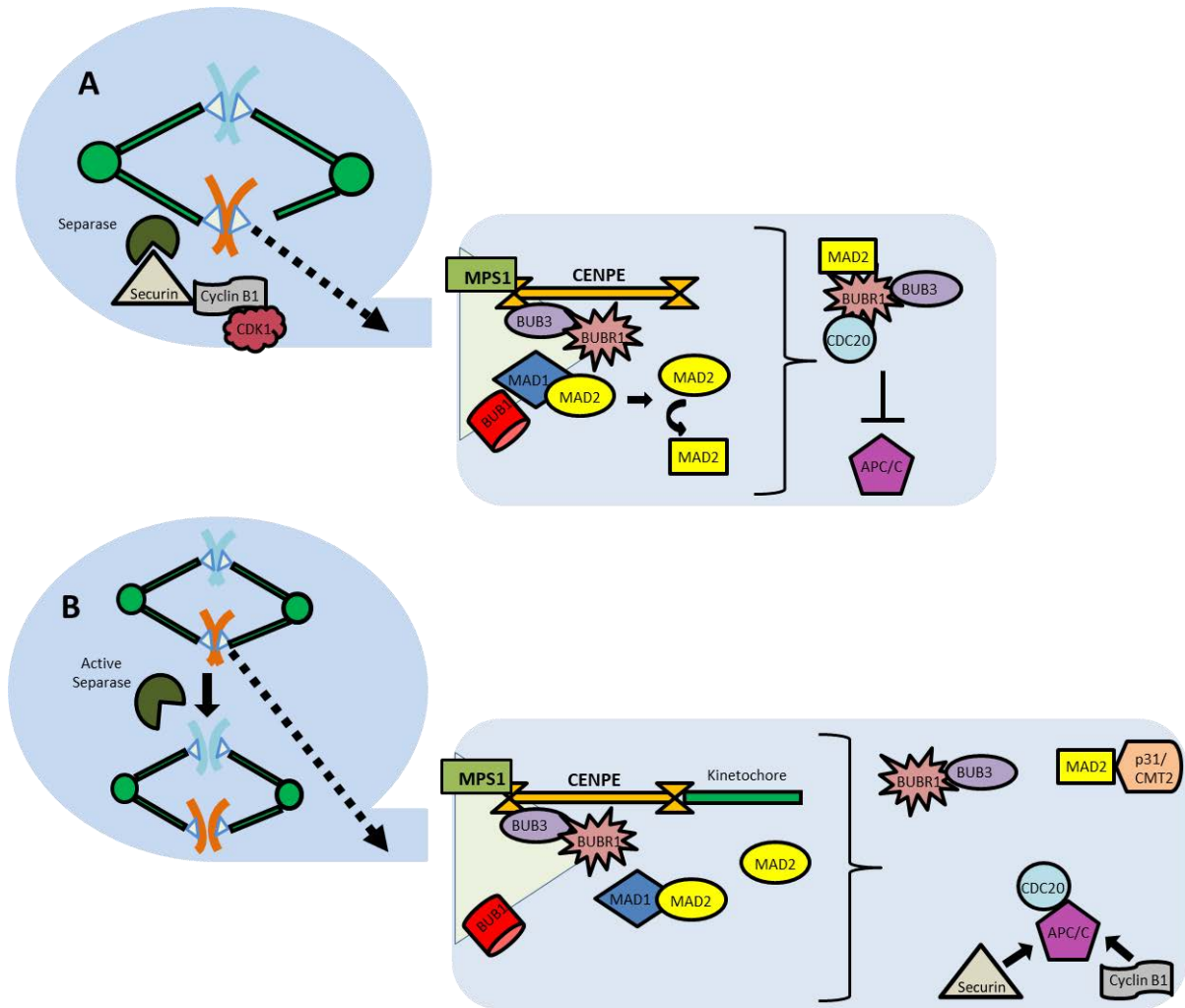


Figure 1.10 Mitotic checkpoints in mammals – activation and deactivation.

A) Activation of the mitotic checkpoint is caused by lack of attachment of all kinetochores to a chromosome. CENPE, a microtubule motor protein, binds directly to BUBR1, which causes its activation and further attachment of MAD1/MAD2 complex. Activation of MAD1/MAD2 is then responsible for the conformational changes in MAD2 structure towards its active form. This process is supported by other proteins such as MPS1 and BUB1. Connection of active MAD2, with BUBR1 and BUB3 creates a complex which is able to capture CDC20 and in this way prevents activation of APC/C. As a consequence of this action, securin and cyclin B1 are not degraded by APC/C; they then bind to separase and in combination with CDK1 block its activity. B) Deactivation of the mitotic checkpoint starts from attachment of kinetochore microtubules to CENPE. This connection prevents binding of MAD1/MAD2 complex and stops production of the active form of MAD2 protein. The remaining active MAD2 is captured by the p31/CMT2 complex, which releases CDC20 and allows for its binding to APC/C. This connection activates APC/C, allows ubiquitination of securin and cyclin B1 and in the same way allows for further activation of separase and progression of mitosis towards anaphase.

1.6.3 Aneuploidy and chromosomal instability (CIN)

Chromosomal instability is a pathological persistent state of chromosome mis-segregation during cell division, in which whole chromosomes are (randomly) lost or gained (Orr et al., 2015) (Lengauer et al., 1997). Chromosomal instability is closely connected with aneuploidy and usually arises as a consequence of abnormal mitosis. Several mistakes in the process of cell division, such as mitotic timing, microtubule dynamic, centrosome relocation within the cell or telomere maintenance can lead to CIN (Schvartzman et al., 2010). However, growing evidence indicates that disruption of the mitotic checkpoint is the main cause of CIN (Cahill et al., 1998). As chromosomal instability seems to be a hallmark of most of human cancers, understanding its role in tumour initiation and progression is at the centre of research.

The history of research on aneuploidy dates to almost a century ago, when Theodor Boveri performed the first systematic analysis of the influence of aneuploidy on cells (Orr et al., 2015, Boveri, 1902). This was subsequently followed by many studies which concluded that aneuploidy causes serious abnormalities in an organism. The term aneuploidy describes a disrupted number of chromosomes in a cell, which is either more or less than the usual 46 chromosomes. It is estimated that during normal development of a multicellular organism, the possible rate of developing aneuploidy by chromosome missegregation is 1 in every 10^5 cell divisions (Hartwell et al., 1982). Therefore, the effect of this rare event in a normally developing organism is usually eliminated by apoptosis of the aneuploid cells. However, if this event occurs more frequently, and the organism is

not able to eliminate all cells with an abnormal chromosome number, it can lead to disruption in cellular function (Torres et al., 2008, Orr et al., 2015). In contrast to polyploidy (chromosome set number greater than normal $2n$), which in many plants or animals is a normal condition necessary for organism development, aneuploidy is usually associated with serious pathological conditions such as sterility, diseases or tumour formation. There are many genes in the human genome, which when present in only one copy causes serious abnormalities. It is also known that a loss of chromosomes is less well-tolerated by an organism than a gain (Torres et al., 2008, Fisher and Scambler, 1994). In humans, examples of non-lethal aneuploidy are trisomies 13, 18 and 21. Individuals with trisomies of 13 and 18 carry serious developmental defects and their survival is usually below one year. Trisomy of chromosome 21, known as Down syndrome, is quite common (approximately 1 in 750 births) and affected individuals have both physical and mental disabilities. Survival of affected individuals though, is much longer than trisomies 13 and 18. The most common human somatic aneuploidy disease is cancer. It is known that over 90% of solid tumours possess features of aneuploidy, which are consequences of defects during cell division (Orr et al., 2015).

1.6.4 The road to whole chromosomal aneuploidy

Normal cell division requires equal separation of chromosomes into daughter cells. Certain events must take place for this process to be successfully completed. These are correct organisation of microtubules into mitotic spindles and proper attachment of chromosomes to kinetochores, at the appropriate time in mitosis. Defects in these

processes can result in cell aneuploidy. There are several ways in which this can happen (Orr et al., 2015, Kops et al., 2005).

a) Aberrant mitosis

For correct cell division, kinetochores must be attached to microtubules from the opposite spindle poles. However, this process often generates several mistakes, which, if not fixed by the spindle assembly checkpoint (SAC), can lead to chromosome or structural aneuploidy, affecting the process of cell division or even life of the cell (Orr et al., 2015).

The process of aberrant mitosis happens when cells enter mitosis with a multipolar spindle; this can be a consequence of the over-production of centrosomes in previous cytokinesis (cell polyploidization - 8N) or errors during centrosome duplication (Storchova and Pellman, 2004). This division creates aneuploid daughter cells. It was found that the genetic changes underlying this process are connected with amplification of STH15/aurora kinase A (Zhou et al., 1998) and inactivation of p53 and BRCA1 which are tumour suppressors (Fukasawa et al., 1996, Deng, 2002).

b) Cohesion defects

The cohesion between two sister chromatids is extremely important for successful cell division and allows for synchronous separation after passing the SAC (Orr et al., 2015).

The control of the cohesion between sister chromatids is dependent on regulation of one of the proteases, separase. Separase is inhibited by securin (pituitary tumour transforming gene 1, PTTG1) (Pei and Melmed, 1997). Any disruption in cohesion leads to chromosome mis-segregation, and in the same way might contribute to aneuploidy in

human cancers (Orr et al., 2015). There is a described correlation between the level of securin and the invasiveness of pituitary tumours (Zhang et al., 1999). It has also been shown that removing securin in human cancer cells resulted in the elevation of CIN (Jallepalli et al., 2001).

c) Mistakes in centrosome attachment to spindle microtubules

The constitutive attachment of one kinetochore to the microtubules from both spindle poles is another possible cause of aneuploidy (Cimini et al., 2001). The inhibition of aurora kinase B, borealin, survivin or INCENP (Inner centromere protein), which belong to the attachment-error-correction mechanism, promotes this type of attachment in cells (Gassmann et al., 2004).

d) Mitotic checkpoint defects

SAC is a complicated signalling network with the ability to delay the mitotic progression until all kinetochores are correctly attached to microtubules. Its role is to control this connection and at the same time minimise the likelihood of errors. Therefore, errors in this mechanism lead to the possibility of mistakes during cell division, and at the same time can cause whole chromosome missegregation which will lead to aneuploidy (Orr et al., 2015, Kops et al., 2005).

1.6.5 Aneuploidy and CIN in cancer

David Hansemann was the first scientist who, in 1890 discovered mitotic defects in cancer cells (Rajagopalan and Lengauer, 2004, Kops et al., 2005). He analysed chromosome

architecture in various carcinomas and noticed abnormal changes in their sizes and structure. His discovery raised the idea of a possible link between aneuploidy and the process of tumorigenesis. There is increasing evidence suggesting that numerical and structural aneuploidy in cancer is caused by chromosomal instability, reflected by frequently observed defects in mitotic segregation during cell division (Rajagopalan and Lengauer, 2004). Most cancer cells contain an abnormal number of chromosomes (in between 60 and 90) and what is more, in the same tumour this number usually differs between cancer cells. These chromosomes also usually carry some structural changes which are rarely seen in normal cells. Chromosomal instability (CIN) is a common feature of many cancers. The cause of this is not yet known, but there is growing evidence which emphasizes the importance of defects in the mitotic checkpoint in the process of tumorigenesis. It was found that defects in the mitotic checkpoint are possible causes of CIN in cancers, and can contribute to tumour growth and progression. Complete inactivation of mitotic checkpoint signalling is lethal for the cell. However, it was shown that many tumour cells are characterised by down-regulation of mitotic checkpoint genes, and when tested in mice, this down-regulation caused spontaneous tumour formation (Kops et al., 2005). Mice cells deficient in CENPE were not able to recruit enough checkpoint proteins and generate a strong enough signal; as a result, few unattached chromosomes were not able to inhibit mitosis progression. In addition, high, frequent rates of mis-segregation were observed both in vivo and in vitro (Weaver et al., 2003). Similar results were seen in mice with down-regulation of Mad2, BUBR1 or Bub3.

In all cases, a higher level of aneuploid fibroblasts and a small increase in tumour development was observed (Babu et al., 2003, Michel et al., 2001, Dai et al., 2004).

The basis of our understanding of the process of tumour formation is based on observations of genetic alterations in specific genes of individual cells (Nowell, 1976, Fearon and Vogelstein, 1990). It is also clear that it is not only aneuploidy which is a common signature of most solid tumours, but also several mutations in oncogenes and tumour suppressor genes, for example KRAS, tumour protein p53 (TP53) and breast cancer 1 (BRCA1) (Kops et al., 2005). In 1998, it was first discovered that mutations in mitotic checkpoint proteins BUBR1 and BUB1, are common in a subset of colorectal cancer cell lines (4 out of 19) (Cahill et al., 1998). Different studies confirmed mutations of other mitotic checkpoint proteins (MAD2, MAD1, BUB1, BUBR1, ZW10-ROD-zwilch) in different types of cancers including: lung, pancreatic, rectal, lymphoid, breast, prostate and bladder (Gemma et al., 2000, Hempen et al., 2003, Ohshima et al., 2000, Imai et al., 1999, Hernando et al., 2001, Nomoto et al., 1999, Percy et al., 2000, Tsukasaki et al., 2001, Wang et al., 2004a); However, the changes in mitotic checkpoint function are not only affected by mutations of specific proteins; oncogene products and tumour suppressors also significantly affect mitosis by regulating mitotic checkpoints. The evidence suggests that a weakened mitotic checkpoint, especially if it appears in conjunction with a mutation in a tumour suppressor gene, might facilitate cancer development (Kops et al., 2005, Rao et al., 2005). Loss of tumour suppressors such as APC, p53, or BRCA1, as well as overexpression of oncogenes (MSM2, AURA, RAS) play an important role in microtubule instability and centrosome amplification (Nigg, 2002,

Fukasawa et al., 1996, Deng, 2002). What is more, mitotic entry or suppression could also be regulated by tumour suppressors (CHFR, LATS1, RASSF1A) (Scolnick and Halazonetis, 2000, Tao et al., 1999, Song et al., 2004). Some oncogenes and tumour suppressors (BRCA1, BCSG1, RB, E2F, p53) can also affect and weaken mitotic checkpoints by direct influence on checkpoint proteins (Wang et al., 2004a, Ren et al., 2002, Chun and Jin, 2003, Iwanaga and Jeang, 2002); It is known that mutations appear during the clonal evolution of cancer, but it is not clear how many mutations in a single cell must take place to make it develop into a metastatic cell. Mathematical analysis suggests six to ten clonal mutations in a single cell, to develop a mature cancer cell (Knudson, 2001, Nowak et al., 2002).

1.6.6 The causes of aneuploidy in tumours

There are two separate theories which may explain why aneuploidy is so common in cancer. The first theory is that aneuploidy is simply necessary for the process of tumorigenesis (Duesberg et al., 1999). It was observed that patients with trisomy 21 are more likely to develop childhood leukaemia (Hasle et al., 2000). Based on previous studies, Torres et al. proposed another way in which aneuploidy could generate tumorigenesis. As mentioned previously, during normal cell proliferation, aneuploidy can appear approximately once per every 10^5 cell divisions. For most of these cells, the aneuploidy state is lethal. However, in some of the aneuploid cells which do not die, the process of cell division appears to be much slower than in the normal cells. In this way, aneuploid cells are usually outcompeted by normal cells, and the effect of aneuploidy in

an organism is blocked. The problem appears when, around slowly proliferating aneuploid cells, there are not enough normal dividing cells. In this situation, aneuploid cells will overcome diploid cells, and tumour formation begins. They also proposed that cell stress (caused by the process of aneuploidy) and the changes this generates increases genomic instability in aneuploid cells to strongly encourage the process of tumorigenesis. Their analysis led them to the conclusion that the first gene mutations caused by aneuploidy in cells, are those which let aneuploid cells tolerate the negative effects of aneuploidy itself. Aneuploidy could cause genomic changes and promote mechanisms, which will now promote the growth and proliferation of cells in a particular environment. What is more, it could also protect cells from lethal mutations by providing extra copies of genes necessary for tumorigenesis (Torres et al., 2008).

The second theory puts less emphasis on aneuploidy in cancer development, and explains changes in the number of chromosomes as a consequence of uncontrolled growth of tumour cells. In this way, aneuploidy would be an echo of previous events in the cell which are more important for the process of tumorigenesis. Bunz et al. proposed that aneuploidy might be the effect of inactivation of p53 pathways, which appear late during tumour development and result in cell tetraploidization – a state which can promote aneuploidy (Bunz et al., 2002). Several other studies support this theory, and even suggest that aneuploidy suppresses rather than promote the process of tumour formation. One piece of evidence to support this theory is an observation that individuals with an extra copy of chromosome 21 are 50% less likely to develop a solid tumour than healthy individuals (Hasle et al., 2000, Satge et al., 2003). Weaver et al. showed that in a

mouse model, the induction of low levels of aneuploidy prevents tumorigenesis in most tissues, and postpones tumour formation in others (Weaver et al., 2007).

Although very interesting, both these theories still do not have enough evidence for their confirmation, and the science world is still divided in its opinion about the reasons for aneuploidy in tumours.

1.6.7 Prognosis and treatment

Cancers carrying aneuploidy and/or chromosomal instability were found to be associated with a poorer prognosis than diploid cancers (Watanabe et al., 2001, Zhou et al., 2002). What is more, there is some evidence suggesting that chromosomal instability (CIN) may contribute to the development of chemotherapy resistance in cancer (Sawyers, 2001).

CIN might influence changes in intracellular and extracellular environments and through this contribute to cellular resistance to some drugs commonly used as chemotherapy like imatinib (Gleevec) and 5-fluorouracil (Wang et al., 2004b, Sawyers, 2001). There are already several drugs in use or in clinical studies which aim to block mitosis by affecting the mitotic checkpoint. Chemotherapeutic drug groups called taxanes and vinca alkaloids are currently in use as part of standard treatment regimens for patients with lung, breast, ovarian and prostate cancers, lymphomas and myelomas (Jordan and Wilson, 2004) (Orr et al., 2015). They provoke long term cell cycle arrest in mitosis by affecting production of unattached kinetochores and influencing microtubule dynamics. The new drug Ispinesib is currently in clinical trials and its function is to block EG5 which is needed for spindle-pole separation. Preclinical tests in mouse xenografts resulted in total regression of

tumours (Purcell et al., 2010). Several other new drugs in clinical trials are also targeting mitotic spindle proteins, such as aurora kinase A and B (Dar et al., 2010), and certain cyclin dependent kinases (CDKs) (Malumbres and Barbacid, 2009). Blocking mitotic check point by drugs is usually followed by cell death (Jordan and Wilson, 2004). Several researchers are also in the process of discovering a way to completely block mitotic checkpoints in cancer cells, leading tumour cells toward apoptosis. The potential treatment of cancer using its aneuploidy signature, could include selective elimination of aneuploid tumour cells, based on their stress-induced phenotype, which differs from normal diploid cells (Orr et al., 2015). In theory, the idea of blocking mitosis to kill tumour cells sounds very promising, but there is a high risk of increasing aneuploidy in healthy cells as a consequence of this treatment.

1.6.8 CENPE - a mitotic checkpoint gene in cancer

Cell proliferation is a well-known target of cancer chemotherapy. Influencing dividing cells and leading them towards apoptotic pathways, seems to be an obvious move towards treating cancer. Therefore, it is not a surprise that there is interest in the kinesins family of motor proteins as potential cancer drug targets (Wood et al., 2001). The superfamily of kinesins contains more than 650 members, of which 45 are found in the human genome (Hirokawa et al., 2010). The main function of this group of proteins is to control different stages of cell division and intracellular transport. Currently, 16 kinesins which play important role in the process of mitosis and cytokinesis are known; among them is centromere-associated protein E (CENPE) (Rath and Kozielski, 2012). CENPE is a

protein responsible for binding spindle microtubules to kinetochores at the earliest stages of this process (Yao et al., 1997). Therefore, its importance in correct cell division seems to be obvious. Interestingly, it was discovered that the hallmark of some tumours is disrupted CENPE expression, indicating its possible role in tumorigenesis and therefore as a potential drug target in cancer treatment. However, the role of CENPE dysregulation in tumour development and progression is not very well studied. Since our knowledge about the localisation and function of CENPE in healthy cells is expanding, there is also growing interest in this protein in the context of tumorigenesis. Liu et al. showed that downregulation of CENPE in HepG-2 human hepatoma cells causes numerical chromosomal abnormalities and possibly also plays an important role in the development and progression of hepatocellular carcinoma (Liu et al., 2015). On the other hand, overexpression of CENPE in combination with overexpression of cyclin B1 correlated with a poor prognosis in breast cancer (Agarwal et al., 2009, Kung et al., 2014). What is more, it was discovered in a mouse model of high risk neuroblastoma, that CENPE is a promising therapeutic target for this disease, based on genetic analysis of tumour progression (Balamuth et al., 2010). In clinical trials there are currently several CENPE inhibitors being tested, of which GSK923295 (in Phase I clinical trials), seems to provide promising results in patients with refractory cancer; partial response in one patient; stable disease in one-third of patients with mild side effects (Chung et al., 2012). Despite the fact that there is still much to investigate in relation to CENPE as a therapeutic target in different types of cancers, current results are promising, confirming its importance and possible future use as a target in cancer treatment.

1.7 Study aims

Nowadays, treatment of all DLBCL patients is based on standard R-CHOP therapy, but this is only curative in approximately 60% of cases and is complicated by the diversity of this disease. Therefore, individual treatment of patients based on the targeting of specific molecular abnormalities is required. DDR1 is highlighted as an oncoprotein, which is an important regulator of tumour cell growth, survival, metastasis and invasiveness. A broad spectrum of pathways mediates DDR1 signalling, make it an important, but not an easy, target for cancer therapy. Therefore, despite growing research on DDR1, our knowledge about this receptor still needs improvement. This thesis explores the contribution of DDR1 signalling to the pathogenesis of DLBCL, and considers its potential therapeutic reversal using small molecule inhibitors of DDR1.

The specific aims of this thesis are to:

1. Identify the DDR1 mediated transcriptional changes that follow collagen stimulation in germinal centre B cells, and examine their relevance to B cell lymphomagenesis.
2. Investigate the potential role of activation of DDR1 by collagen in mediating aneuploidy in DLBCL.
3. Investigate the potential therapeutic use of DDR1 inhibitors in vitro and in vivo.

CHAPTER TWO

MATERIALS AND METHODS

2. Materials and methods

2.1 Cell culture

2.1.1 Maintenance of the cell lines

All used suspension cell lines were cultured in growth media (summarised in Table 2.1), at 37°C in a humidified atmosphere containing 5% of carbon dioxide (Galaxy R CO₂ Incubator; RS Biotech). Twice a week, to replenish nutrients and remove waste, cells were pelleted by centrifugation at 1700rpm for 5min (Eppendorf Centrifuge 5810R; Eppendorf UK Limited). The supernatant was aspirated using a VACUSAFE aspirator (INTEGRA Biosciences AG) and cells were re-suspended in fresh media, pre-warmed to 37°C (Heratherm™ Compact Microbiological Incubator; Thermo Fisher Scientific). Cells were counted and seeded in new culture flask, at a concentration of 5×10^5 cells/ml.

Adherent cell lines were maintained in the growth media described in Table 2.1. To prevent over growth, cells were passaged at 80% confluency, as estimated by visual microscopic inspection. Prior to sub-culturing, media was aspirated (VACUSAFE aspirator; Integra Biosciences AG) and cells were washed twice with PBS (phosphate buffered saline, pH 7.4; Life Technologies Ltd). PBS was then removed and trypsin solution (Gibco; Life Technologies Ltd) was added to the cells and incubated at 37°C for 3 min, to allow cells to detach from the culture flask. To neutralise trypsin, fresh media was added to cells. To remove the trypsin, cells were pelleted by centrifugation at 1700rpm for 5min and re-suspended in fresh, pre-warmed media to the desired concentration.

Table 2.1 Summary of cell lines and the culture conditions.

Cell line	Growth characteristic	Cancer type	Origin	Culture media
L591	Suspension	Nodular sclerosis, HL (human)	B cell derived lymphoma cell line, established from 31 years old female with diagnosed Hodgkin lymphoma in 1982 (Diehl et al., 1982); EBV positive.	RPMI-1640 (Gibco, Life Technologies Ltd) supplemented with 10% v/v fetal bovine serum (FBS, Gibco; Life Technologies Ltd) and 1% v/v penicillin/streptomycin (P/S, Gibco; Life Technologies Ltd)
L1236	Suspension	Mixed cellularity, HL (human)	EBV negative cell line established in 1994, from peripheral blood of 34 years old male patient (Kanzler et al., 1996).	
L428	Suspension	Nodular sclerosis, HL (human)	Established from 37 years old woman with Hodgkin lymphoma in 1978 (Schaadt et al., 1980); EBV negative (Schaadt et al., 1979).	
L540	Suspension	T cell derived nodular sclerosis, HL (human)	Hodgkin lymphoma cell line from the bone marrow of 20 years old woman; EBV negative (Diehl et al., 1981).	
KMH2	Suspension	Mixed cellularity, HL (human)	Established in 1974 from 37 years old male patient with Hodgkin lymphoma; EBV negative (Kamesaki et al., 1986)	
U2932	Suspension	DLBCL (human)	Cell line derived from 29 years old female patient with DLBCL, who previously was diagnosed with Hodgkin lymphoma; ABC-like subtype; EBV negative (Amini et al., 2002).	
Ocily 7	Suspension	DLBCL (human)	GCB-like lymphoma subtype; established from peripheral blood sample of a 48-year-old man with B-cell non-Hodgkin lymphoma (DLBCL), EBV negative (Tweeddale et al., 1987).	
HT	Suspension	DLBCL (human)	Established in 1983 from 70 years old male patient with DLBCL; GCB-like lymphoma subtype; EBV negative (Beckwith et al., 1990)	
Karpas 422	Suspension	DLBCL (human)	GCB-like lymphoma subtype; established from 72 years old woman with DLBCL in 1986; EBV negative (Dyer et al., 1990).	
Farage	Suspension	DLBCL (human)	GCB-like lymphoma subtype, established in 1990 from the lymph node of female	

			patient with DLBCL; EBV positive (Benbassat et al., 1992).	
SUDHL4	Suspension	DLBCL (human)	Established From 38 years old male patient with DLBCL in 1975; GCB-like lymphoma subtype; EBV negative (Epstein et al., 1978).	
SUDHL5	Suspension	DLBCL (human)	GCB-like lymphoma subtype; established from the lymph node of the 17 years old woman with DLBCL; EBV negative (Epstein et al., 1978).	
BJAB	Suspension	DLBCL (human)	GCB-like lymphoma subtype; derived from bone marrow, nowadays classified as DLBCL (Wennborg et al., 1987). Previously known as Burkitt lymphoma; EBV-negative; established from 5 years old girl (Klein et al., 1974).	
DG75	Suspension	BL (human)	Established in 1975 from 10 years old boy with Burkitt lymphoma; EBV negative (Benbassat et al., 1977).	
Hela	Adherent	Human epitheloid cervix carcinoma	Established in 1951 from 51 years old woman (Scherer et al., 1953). Later diagnosis – adenocarcinoma; EBV negative.	
Ocily 3	Suspension	DLBCL (human)	ABC-like lymphoma subtype; bone marrow of a 52-year-old man with B-cell non-Hodgkin lymphoma (DLBCL), EBV negative (Tweeddale et al., 1987).	IMDM (Gibco, Life Technologies Ltd) supplemented with 20% v/v fetal bovine serum (FBS, Gibco; Life Technologies Ltd) and 1% v/v penicillin/streptomycin (P/S, Gibco; Life Technologies Ltd)
Ocily 1	Suspension	DLBCL (human)	GCB-like lymphoma subtype; bone marrow of a 44-year-old man with B-cell non-Hodgkin lymphoma (DLBCL), EBV negative (Tweeddale et al., 1987).	IMDM (Gibco, Life Technologies Ltd) supplemented with 10% v/v fetal bovine serum (FBS, Gibco; Life Technologies Ltd) and 1% v/v penicillin/streptomycin (P/S, Gibco; Life Technologies Ltd)
A20	Suspension	Murine B cell lymphoma	Mouse derived lymphoma cell line, established in 1979. Presents B cell properties (Kim et al., 1979).	RPMI-1640 (Gibco; Life Technologies Ltd) supplemented with 2mM L-glutamine, 10% v/v FBS (Sigma), 10mM HEPES (Sigma), 1mM sodium pyruvate (Sigma), 200mg/l glucose (Sigma) and 0.05mM 2-mercaptoethanol (Gibco; Life Technologies Ltd)

2.1.2 Cryopreservation of cells and recovery of frozen cells

To cryopreserve cell lines, 5×10^6 cells were pelleted by centrifugation in 4°C , at 1700rpm for 10min (Eppendorf Centrifuge 5810R; Eppendorf UK Limited) and re-suspended in 500 μl of cold freezing solution (90% v/v FBS (Gibco, Life Technologies Ltd) and 10% v/v dimethyl sulphoxide (DMSO; Sigma). Cells were transferred into cryopreservation vials (Nunc[®] Cryo Tubes; Sigma) and slowly frozen down to -80°C in a cryo container (Nalgene[®] Mr. Frosty; Sigma). Cells were subsequently stored at -80°C .

To recover frozen cells for cell culture, cryopreserved cells were thawed quickly to minimize the exposure to DMSO, and re-suspended in 5ml of fresh pre-warmed media. Cells were pelleted by centrifugation at 1700rpm for 5 min and immediately re-suspended in 7ml of complete medium. Cells were grown in 25cm³ flasks at 37°C in the humidified incubator with 5% CO₂.

2.1.3 Cell counting

Cell concentration was determined by mixing equal volume of cell suspension and Trypan Blue (Sigma) (1:1; 10 μl each). 10 μl of this solution was then pipetted onto a Naubauer haemocytometer (Marienfeld), and live (bright) cells were counted using Olympus CK30 inverted light microscope in four separate zones of the grid. The concentration of the cells (number of cells per ml of culture) was calculated by multiplying the average number of counted cells by 10^4 and the dilution factor of Trypan Blue (2).

2.2 Isolation and maintenance of primary human GC B cells from tonsils

2.2.1 Tonsil specimens

Paediatric tonsil tissues were obtained from the [REDACTED]. All work using tonsils was performed under local ethics committee approval (Ref No. 06/Q2702/50). Fresh tonsils were transported in phosphate buffered saline (PBS, Life Technologies Ltd) on ice.

2.2.2 Purification of tonsillar mononuclear cells (TMCs)

Work on tonsils was started immediately after arrival of tissue and processed with help of [REDACTED]. All steps of isolation were carried out in sterile conditions on ice, using cold reagents, to prevent apoptosis (as described previously by (Vockerodt et al., 2008)). Tonsils were placed in cold RPMI 1640 medium (Gibco; Life Technologies Ltd) supplemented with 1% v/v penicillin/streptomycin solution (Gibco; Life Technologies Ltd) and 0.5% v/v ciproxin (Bayer). Using a scalpel, tonsils were minced to release the tonsillar cells into the medium. The cell suspension was collected in 50ml falcon tubes (Corning® Self-standing Centrifuge tubes; Sigma) and kept on ice.

Mononuclear cells were then isolated by gradient separation using Lymphoprep™ solution (Axis-Shield Diagnostics Ltd). 15ml of lymphoprep solution was transferred into 50ml tubes then 35ml of tonsillar cell suspension in medium layered on top, followed by 30 min centrifugation at 2200rpm, at room temperature with the break off. This procedure created the visible layers of: plasma (top), mononuclear cells (middle),

lymphoprep solution (bottom) and erythrocytes (pellet). Mononuclear cells were transferred to a new tube, topped up with cold RPMI 1640 media and washed twice in medium and once in autoMACS solution (Miltenyi Biotec Ltd) supplemented with 0.5% v/v ciproxin (Bayer), 1% v/v penicillin/streptomycin solution (Gibco; Life Technologies Ltd) and 5% v/v MACS[®] BSA stock solution (Miltenyi Biotec Ltd), by centrifugation at 4°C, 1000rpm for 10 min. Tonsillar mononuclear cells were counted using Trypan Blue (Sigma) as previously described.

2.2.3 Purification of CD10 positive GC B cells

Isolated mononuclear cells were re-suspended in autoMACS solution (Miltenyi Biotec Ltd) to a concentration of 10^7 cells/100 μ l. Anti-CD10-Phycoerythrin (PE) antibody (eBioscience) was added to cell suspension at 1:50 dilution, and incubated for 10 min at 4°C in the dark. After this time, cells were washed with 10x staining volume of autoMACS solution and re-suspended again with autoMACS, at the concentration of 10^7 cells/100 μ l. Anti-PE microbeads (Miltenyi Biotec Ltd) at the dilution 1:10 were added and incubated for 15 min at 4°C in the dark. Cells were washed with 10x of staining volume of ice cold autoMACS solution.

As the last step, cells were re-suspended in autoMACS solution to the concentration 10^8 cells/500 μ l (assuming that max 40% of cells are labelled) and LS columns (Miltenyi Biotec Ltd) with 50 μ m cell filters (CellTrics[®]; Partec), were prepared for cell loading by being placed on a pre-cooled separation magnet (Miltenyi Biotec Ltd) and rinsed with 3ml of autoMACS solution. 500 μ l of cell suspension was applied to the column and left to fully

pass through, followed by 3 separate washes with 3ml of autoMACS solution. To release CD10+ cells from the column, LS columns were removed from the magnet and placed into 15ml tubes. 5ml of autoMACS buffer was added and the contents forced through by gentle pressure with the plunger. Cells were counted using trypan blue and kept on ice until further use or frozen at -80°C .

2.3 Plasmid preparation

2.3.1 Broth and agar preparation

Luria-Bertani (LB) broth was prepared using 2g LB-Broth Base powder (Invitrogen) in 100ml distilled water, autoclaved and stored at room temperature.

LB agar was prepared by dissolving 1.5g select agar powder (Invitrogen) and 2g LB-Broth Base powder in 100ml of filtered water and autoclaved. Prepared agar was kept at RT. Before pouring on plates, agar was heated up in microwave and antibiotic ($100\mu\text{g}/\text{ml}$ ampicillin (Sigma)) was added. Ready plates were then stored at 4°C , until further use.

2.3.2 Preparation of plasmid from glycerol stock

Glycerol stock of pIRES2-EGFP plasmid with and without DDR1a insert was a gift of [REDACTED]
[REDACTED] Details of the plasmid used are summarised in Table 2.2. A small portion (pipette tip) of the plasmid glycerol stock was transferred into 2ml of freshly prepared LB broth with $50\mu\text{g}/\text{ml}$ kanamycin monosulphate (Sigma) and placed in a shaking incubator at 37°C , 150rpm for 8 hours. After this time, the mixture was transferred into conical flask with 100ml of LB broth and incubated

overnight with shaking at 37°C, 150rpm. Next day the content of the flask was transferred into 50ml conical tubes and pelleted by centrifugation at 4°C, 7000rpm for 15 min. Pellets were immediately lysed with 8ml of Lysis Buffer LYS-EF (part of the Nucleobond kit) and the plasmid was purified using Nucleobond Xtra Midi Plus EF kit, according to manufacturer's protocol (MACHEREY-NAGEL) or frozen at -80°C. Plasmid concentration was determined using a NanoDrop™ 1000 spectrophotometer (Thermo Scientific).

2.3.3 Transformation of bacteria

pCDH-mDIV-DDR1 and pCDH-DIV-DDR1 plasmids were gifts from [REDACTED] ([REDACTED]). mDIV-DDR1 and DIV-DDR1 plasmids were cut from Whatman paper and incubated in RNA free water at 4°C overnight. XL1-Blue competent cells were thawed on ice. 50µl of bacteria was mixed with 1µl of plasmid and incubated on ice for 30min. After this time tube was transferred to 40°C water bath and heat shock for 1min. Cells with plasmid were then moved straight back on ice for 1min. To let bacteria grow, 250µl of LB media without antibiotic was added and cells were incubated for 1h at 37°C on shaker. After required time, 100µl of cells were plated on selective agar plate (100µg/ml ampicillin (Sigma)) and left over night in 37°C incubator. Next day, picked colonies were transferred into 2ml of LB broth with 100µg/ml ampicillin and incubated for 8h at 37°C, on shaker. Glycerol stock was prepared by mixing 850µl of grown bacteria with 150µl of glycerol (Sigma) or bacteria were transferred into 100ml of LB broth and incubated for plasmid extraction as described in Section 2.3.2. Glycerol stock was frozen and stored at -80°C.

2.4 Transfection of cell lines and primary GC B cells

All procedures were performed in sterile conditions.

2.4.1 Nucleofection

2.4.1.1 DDR1 expression plasmid

Cell lines

DG75 cells were transfected by nucleofection at room temperature. For the procedure, Cell Line Nucleofector® Kit V (Lonza) and Nucleofector device (first generation; Lonza) was used. One day before transfection cells were seeded in fresh RPMI 1640 medium, supplemented with 1% v/v penicillin/streptomycin solution (Gibco; Life Technologies Ltd) and 10% v/v fetal bovine serum (FBS, Gibco; Life Technologies Ltd), at a concentration of 5×10^5 cells/ml. Cells were pelleted by centrifugation at 750rpm for 10 min at room temperature and re-suspended at 1×10^6 cells/100 μ l of nucleofector solution V per reaction. Cells in solution were then mixed with 2 μ g of plasmid (Table 2.2) and transferred into the nucleofection cuvettes supplied with the kit (Lonza). Cells were nucleofected using the R-013 program on the Nucleofector device, and immediately transferred into 2ml of fresh pre-warmed medium. Before further analysis, cells were incubated for 24h at 37°C in a humidified atmosphere with 5% CO₂.

Primary germinal centre B cells

The nucleofection of primary GC B cells was carried directly after isolation from tonsils tissue. The whole protocol was performed at room temperature and Human B Cell

Nucleofector® Kit (Lonza) was used. Cells were pelleted by centrifugation in 720rpm for 10 min at room temperature and re-suspended in a concentration of 5×10^6 cells/100µl of nucleofector solution B per reaction. 10µg of pIRES2-EGFP vector (Clontech Laboratories) as a control or 10µg of pIRES2-EGFP vector containing DDR1a (gift of [REDACTED]) per reaction was added. Cells were nucleofected in Nucleofector device (first generation, Lonza), using program U-15. Cells were immediately transferred to fresh, pre-warmed RPMI 1640 medium supplemented with 5% v/v FBS and 1% v/v penicillin/streptomycin, and incubated at 37°C in 5% CO₂, for 8h.

2.4.1.2 Knock down of CENPE gene using siRNA

Silencer® Select Validated siRNA from Ambion was used for the silencing of CENPE in cell lines (Table 2.3). DG75 cells were seeded 24h before nucleofection in the fresh supplemented medium at a concentration of 5×10^5 cells/ml. Cells were nucleofected with 2µg of Silencer® Select Validated CENPE siRNA (Ambion) or with 2µg of Negative Control Silencer® Select #1 siRNA (Ambion), using Nucleofector device and solutions as described above. Cells were incubated for 24h at 37°C in a humidified atmosphere with 5% CO₂.

Table 2.2 Details of used plasmids.

Plasmid	Selectable marker	Note	Company
pIRES2-EGFP	Kanamycin	Express EGFP	Clontech Laboratories – ██████████ ████████████████████ ████████████████████ ████████
DDR1a-pIRES2-EGFP	Kanamycin	Express EGFP and DDR1a	████ █████ █████ █████ █████ ████████████████████ ████████████████████
pCDH-mDIV-DDR1	Ampicillin	Not active DDR1 mutant	████████████████████ ████████████████████
pCDH-DIV-DDR1	Ampicillin	Constitutively active DDR1	████████████████████

Table 2.3 CENPE siRNA information.

siRNA information	Sense	Antisense
Sequence (5'→ 3')	GGUUGACUCAGAUACUACAtt	UGUAGUAUCUGAGUCAACctt
Length	21	21
Molecular Weight	6700	6600

2.4.2 Electroporation

24h prior to transfection BJAB cells were seeded in fresh medium at a concentration of 5×10^5 cells/ml. Cells were pelleted by centrifugation at 4°C , 1000rpm for 10 min and re-suspended at a concentration of 1×10^7 cells/250 μl of cold medium per reaction, supplemented with 25mM 4-(2-hydroxyethyl)-1-piperazineethanesulfonic acid (Hepes; Sigma). Cell suspension was then mixed with 20 μg of plasmid, as detailed above (Table 2.2) and transferred to 4mm electroporation cuvettes (Geneflow Limited). Cells were electroporated using BioRad Gene Pulser II electroporator (Bio-Rad Laboratories Ltd) at 250V and high capacity of 950 μF . Following this procedure cells were immediately transferred into 10ml of fresh, pre-warmed medium and incubated for 24h at 37°C in the incubator with 5% CO_2 .

2.5 Stimulation with collagen and cell harvest

All procedures were performed in sterile conditions.

Cell lines

DG75 or BJAB cells after transfection were collected into separate tubes for DDR1a and empty vector control. Non-transfected L591 cells were counted and seeded the day before stimulation, at 5×10^5 cells/ml.

Cells were pelleted by centrifugation at room temperature, 1000rpm for 10 min and re-suspended in the same volume of fresh pre-warmed RPMI 1640 medium supplemented with 1% v/v of penicillin/streptomycin, without FBS. Cells were seeded in equal volume

(5ml) in separate Petri dishes for each time point of stimulation and were 'serum starved' for 2h at 37°C in 5% CO₂ conditions. After this time, soluble type I collagen (extracted from rat tail; Millipore Ltd) or 0.5% acetic acid as a control (Fisher Scientific), was added directly to the cell suspension at a concentration of 100µg/ml and incubated at 37°C in 5% CO₂ condition, for the required time.

Stimulated cells were harvested by centrifugation at 4°C, 1700rpm for 7min. The supernatant was removed from the cell pellet using VACUSAFE aspirator and cells were washed with cold PBS supplemented with 1mM of activated sodium vanadate (SOV; Sigma). In the next step PBS with SOV was removed and cell pellets frozen in -20°C.

Germinal centre B cells isolated from tonsil

Transfected GCB cells were stimulated with 100µg/ml of soluble type I collagen (Millipore) added directly to the cell suspension and incubated for 4h at 37°C in a humidified atmosphere with 5% CO₂. Cells were harvested by addition of 250µl/ml of collagenase (Sigma) and 10 min incubation at 37°C. After this time, cells were mixed with cold PBS and transferred into two tubes: one for cells transfected with the plasmid containing DDR1a insert and one for the control plasmid. Cells were pelleted by centrifugation at 4°C in 900rpm for 10min. To fully remove collagen, cells were washed again with 35ml of autoMACS solution. Cells treated this way were ready for the immediate cell sorting.

2.6 Cell sorting

Transfected GC B cells were re-stained using anti CD10-phycoerythrin (PE) antibody (eBioscience) by mixing the cell pellet with 250µl/sample of antibody dilution (25µl of CD10-PE in 250µl of AutoMACS solution) and incubated for 10min in the dark at 4°C. Cells were washed once with autoMACS and re-suspended in 250µl of the solution. As a last stage, cells were passed through 50µm cell filters (Miltenyi Biotec Ltd) straight into a FACS tubes.

At the same time sorting controls were prepared. 1ml of tonsillar mononuclear cells (TMC) each was stained (as described above) separately for: anti CD10-PE as a positive control for GC B cells and anti CD4-FITC as a control for GFP-positive cells. An unstained negative control was also prepared by mixing 50µl of TMC with 200µl of autoMACS solution.

Immediately prior to sorting, Hoechst dye (Cell Signalling; prepared from powder to working solution of 20µg/ml) was added to transfected GC B cells and to control TMC. Live (Hoechst negative) transfected GC B cells (CD10+GFP+) were sorted using MoFlo Astrios (Beckman-Coulter) into cold PBS. Cells were pelleted by centrifugation at 4°C in 1700rpm for 7min and frozen at -80°C.

2.7 Treatment of the cells with inhibitors

Discoidin domain receptor 1 (DDR1) inhibitors

Three different DDR1-specific small molecule inhibitors were tested. All were dissolved in DMSO (Sigma) at different stock concentrations: 7rh (7-4104) inhibitor (500 μ M), 7rj (7-4109) inhibitor (5mM) ([REDACTED]) and DDR1-IN-1 dihydrochloride (R&D Systems) (Kim et al., 2014) (10mM). Stock solutions were stored in aliquots at 4 $^{\circ}$ C.

Transfected BJAB cells were seeded 24h prior to treatment in a concentration of 5x10⁵ cells/ml in fresh medium supplemented with 10% serum. The next day cells were 'serum starved' for 2h. Inhibitors were diluted to the required concentrations in serum-free medium and added to the cells in suspension, which was immediately followed by collagen stimulation. Cells with inhibitor and collagen were incubated for 1h and harvested by centrifugation at 4 $^{\circ}$ C in 1700rpm for 5min. Cell pellets were then frozen at -20 $^{\circ}$ C, until further use.

CENPE inhibitor (GSK923295)

CENPE inhibitor (GSK923295; Cayman Chemical) was dissolved in DMSO, to 1mM stock concentration (Bennett et al., 2015).

DG75 and Hela cells were seeded 24h prior to treatment in fresh medium supplemented with 10% FBS. Next day cells were 'serum starved' for 2h, followed by 4h incubation at 37 $^{\circ}$ C with 50nM CENPE inhibitor. Dividing Hela cells were released to media supernatant

by gentle mechanical tapping on a flask. DG75 and HeLa cells in suspension were then harvested by 10min centrifugation at RT, 1000rpm, followed by PBS wash. Cell pellets were re-suspended in PBS, counted and cytopins were prepared (as described in Section 2.10.2.1). Cells were fixed on glass slides in 100% ice cold methanol (Sigma) for 15min, followed by immunofluorescent staining.

MPS1 kinase inhibitor (AZ3146)

MPS1 kinase inhibitor (AZ3146; ApexBio) was dissolved in DMSO to 50mM stock solution. DG75 cells treated with CENPE inhibitor (as described above), were incubated with 2 μ M of AZ3146 for 2 hours at 37°C. Cells were then harvested by centrifugation for 10min at RT, 1000rpm and washed twice with PBS. After second wash, cell pellet was re-suspended in culture media supplemented with 10%FBS and cells were cultured for 24h at 37°C and in 5% CO₂ conditions. Next day, cells were stained for metaphase spread (section 2.10.3).

2.8 Trypan blue viability assay

To check toxicity of DDR1 inhibitors, DDR1a transfected BJAB cells were seeded 24h prior to treatment in 5x10⁵ cells/ml, in fresh medium supplemented with 10% FBS. Next day, cells were 'serum starved' for 2h. After this time, cells were treated with different concentrations of inhibitors for 1, 2 and 3h. Untreated and DMSO treated cells were included as a control baseline of cell viability. Cells were harvested, centrifuged at 1500rpm for 5min at RT and re-suspended in 100 μ l of serum free media. 10 μ l of cells were then mixed 1:1 with 0.4% trypan blue solution (Sigma). Live and dead cells were then counted using haemocytometer, under the bright field microscope.

2.9 RNA analysis

All RNA work was performed using RNase-free equipment and reagents on ice, to minimise the risk of contamination. The work space and pipettes used for RNA work were decontaminated with RNaseZap® Rnase Decontamination Solution (Ambion) and RNase free filter tips (Starlab) were used.

2.9.1 RNA extraction and purification

Cell lines and control non-transfected GC B cells

Cells were seeded in fresh medium, 24h before harvesting at a concentration of 5×10^5 cells/ml. The next day 5×10^6 cells was transferred to fresh tubes and pelleted by centrifugation at 4°C , in 1700rpm for 5min. The cell pellet was then washed once with cold PBS. Non-transfected GC B cells were pelleted straight after isolation (as described above) and stored at -80°C . Prior to RNA extraction, pellets were taken out of the freezer and kept on ice.

Total RNA was extracted from cell pellets using QIAGEN mini RNeasy kit, according to the manufacturer's protocol (QIAGEN Ltd). Cells were lysed in RLT buffer supplemented with β -mercaptoethanol (Sigma). To degrade contaminating DNA in samples, DNase digestion was performed using RNase-Free DNase Set (QIAGEN Ltd), as recommended in the manufacturer's protocol. RNA was eluted from columns by addition of $30\mu\text{l}$ of nuclease-free water (Promega UK Ltd) directly to the column membrane and a short centrifugation. RNA concentration of the samples was determined using NanoDrop ND-1000 spectrophotometer and samples were stored at -80°C .

Primary transfected GC B cells

Cell pellets from sorted, transfected GC B cells were lysed in 100µl of RLT buffer supplemented with 1µl of 14.3M β-mercaptoethanol (Sigma) and 1µl of N-carrier (AmpTec). Next steps of RNA extraction were performed as per manufacturer's protocol for the QIAGEN RNeasy micro kit (QIAGEN Ltd). The quality and concentration of RNA was measured using the Bioanalyser 2100 (Agilent) with the Agilent RNA 6000 Pico Kit according to the manufacturer's protocol (Agilent Technologies). For RNA amplification, only samples in which RNA integrity (RIN) was >7 were chosen.

2.9.2 cDNA preparation

RNA was reverse transcribed to complementary DNA (cDNA) using qScript cDNA SuperMix (Quanta Biosciences). 500ng of RNA from cell lines and 200ng of RNA from primary DLBCL ([REDACTED]) was mixed in sterile, thin walled 0.2ml PCR tubes, with 4µl of SuperMix and topped up with nuclease free water to a total volume of 20µl. The samples were immediately transferred to a Verti Thermal Cycler (Applied Biosystems) and incubated with the following protocol: 5min at 25°C, 30min at 42°C and 5min at 85°C. After this time cDNA samples were placed on ice and stored at -20°C.

2.9.3 Amplification of cDNA for gene expression analysis

Amplification of cDNA from total RNA extracted from isolated, transfected, stimulated and sorted GC B cells was performed using NuGEN Ovation® RNA-Seq system V2 kit

(NuGEN Ltd), according to manufacturer's protocol. The final product of this reaction – amplified SPIA® cDNA, was stored at -80°C, until it was sent for RNA sequencing.

2.9.4 RNA sequencing (RNAseq)

RNA from three biological replicates of GC B cells described above, was isolated, cDNA amplified and samples were sent to Edinburgh Genomics (UK) for RNAseq. All samples passed quality control test and TruSeq Nano gel-free library (350bp insert) was produced from the amplified cDNA. Six samples were sequenced in one lane using HiSeq 4000 HO 125 base paired end platform. Resulting data was analysed by [REDACTED]

2.9.5 Quantitative real time polymerase chain reaction (qRT-PCR)

All qRT-PCR reactions were prepared on 96 well optical reaction plates (Applied Biosystems, Life technologies Ltd) in a total volume of 20µl/reaction. Each reaction was a mixture of: 5µl of diluted 1:20 in nuclease free water cDNA, 10µl of FastStart Universal Probe Master Mix (Roche Diagnostic Limited), 1µl of 20x primer/probe of gene of interest (FAM labelled), 1µl of 20x primer/probe endogenous control (GAPDH; VIC TAMRA labelled) (Applied Biosystems) and 3µl of nuclease free water. All primers and probes used are listed in Table 2.4. The plate was set as a multiplex reaction, each sample was run in triplicate and water control (no target; cDNA free) was included. The plate was sealed with an optical clear adhesive film (STARLAB Ltd), centrifuged briefly to remove air bubbles and samples were amplified using ABI Prism 7700 Sequence Detection System (Applied Biosystems) according to standard relative quantification method in following

conditions: enzyme activation at 50°C for 2min, denaturation at 95°C for 10min, 40 cycles of amplification at 95°C for 15s and extension at 60°C for 1min.

2.9.6 Fluidigm®48.48 Fast Real Time PCR

2.9.6.1 Fluidigm® Gene Expression Specific Target Amplification

The amplification of the specific target genes in cDNA samples was performed according to the manufacturer's protocol (Fluidigm). In the first step, 'pooled assay mix' was prepared by mixing 2µl of each 20x primer/probe (including endogenous control) (TaqMan™, Applied Biosystems) with TE Buffer Low (ThermoFisher Scientific) to a total volume of 200µl.

The sample mixture was prepared in thin walled 0.65ml PCR tubes by combining separately for each sample: 2.5µl of TaqMan PreAmp Master Mix (2x) (Applied Biosystem), 1.25µl of 'Pooled assay mix' and 1.25µl of cDNA. The reactions were mixed and amplified in MasterCycler® Gradient Thermal Cycler (Eppendorf) using the following settings: 95°C for 10min followed by 14 cycles of 95°C for 15s and 60°C for 4min. The amplified product was diluted 1:5 by adding 20µl TE Buffer Low and kept at -20°C until required.

2.9.6.2 Fluidigm®48.48 real time polymerase chain reaction

The assay was prepared according to the Fluidigm 48.48 Fast Real Time PCR Workflow Quick Reference protocol, provided by the manufacturer. Briefly, 10x assay mix and sample mix were prepared separately in two 96 well optical reaction plates. To prepare

10x assay mix for each targeted gene, 2.5µl of 20x primer/probe was combined with 2.5µl of 2x Assay Loading Reagent (Fluidigm). On the second plate, sample mix was prepared by adding 2.5µl of 2x TaqMan Fast Advanced Master Mix (Applied Biosystems) and 0.25µl of 20x GE Sample Loading Reagent (Fluidigm) to 2.25µl of amplified cDNA.

After priming the Fluidigm 48.48 Dynamic Array™ IFC for Gene Expression chip (Fluidigm), samples and assays were loaded, all eventual air bubbles were removed and the chip was run in IFC Controller MX machine (Fluidigm) for 1h. After this time the IFC chip was transferred to the BioMark™ HD instrument for real time PCR reaction using GE 48X48 Standard v1 specific protocol (Fluidigm). The data and colour-coded expression heat map were collected using BioMark HD Data Collection Software v3.0.2 and analysed using Fluidigm Real-Time Software.

Table 2.4 List of TaqMan® Gene Expression Assays used for qRT-PCR and Fluidigm®.

Gene	Assay ID
ADAM12	Hs01106101_m1
AGAP3	Hs01553093_m1
ANKRD50	Hs00379454_m1
ARHGEF19	Hs01584221_g1
CILP	Hs00173647_m1
DDR1	Hs01058433_g1
FBP1	Hs00983323_m1
GMIP	Hs00213126_m1
HSPB1	Hs00356629_g1
LDLR	Hs00181192_m1
OBSCN	Hs00405789_m1
PLN	Hs01848144_s1
PSD4	Hs00202892_m1
RAB34	Hs01094510_g1
SIRPA	Hs00388953_g1
SMPD3	Hs00920354_m1
SYDE2	Hs00410961_m1
SYNPO	Hs00702468_s1
SYTL4	Hs00299039_m1
UNC5B	Hs00900710_m1

ZSWIM5	Hs01123837_mH
KLHL15	Hs00399541_m1
SRSF4	Hs00900675_m1
GCSAM	Hs00381190_m1
LMNB2	Hs00383326_m1
NAA40	Hs00227062_m1
CCNF	Hs00171049_m1
CENPE	Hs01068241_m1
RAD54L	Hs00269177_m1
GAPDH	Hs02758991_g1
β2M	Hs00187842_m1
PGK1	Hs99999906_m1
TBP	Hs00427620_m1
HPRT1	Hs02800695_m1

2.9.7 qRT-PCR and Fluidigm data analysis

The threshold cycle (Ct value) data generated by both ABI Prism 7700 sequence detection system and BioMark™ HD instrument were created based on amplification plots of fluorescent intensity analysed for each signal. Based on these values, the delta-delta ($\Delta\Delta$) Ct method (described previously by Livak and Schmittgen, 2001 (Livak and Schmittgen, 2001)) was used, to quantify the relative levels of transcripts normalised against an endogenous control (β 2M, TBP, HPRT1, GAPDH, PGK1). The difference between target Ct value and control Ct value was calculated for each sample (target Ct - endogenous control Ct) and the resultant value was presented as a relative gene expression, determined based on reference sample which was assigned a value of 1. These calculations resulted in an absolute value of fold change for each sample which was used for further analysis and data presentation.

2.10 Protein analysis

2.10.1 Western blotting

2.10.1.1 Protein extraction

Fresh cells were prepared for protein extraction 24h before, by counting and re-suspending in fresh warm supplemented medium at a concentration of 5×10^5 cells/ml. The following day, cells were pelleted by centrifugation at 4°C in 1700rpm for 5min.

Most of the samples were also analysed for the phosphorylation of proteins. Therefore, all the cell pellets prior to lysis were washed once in cold PBS supplemented with 1mM SOV to preserve any phosphorylated proteins, before being transferred to 1.5ml micro

centrifuge tubes (Eppendorf) and kept on ice. Cell pellets were then re-suspended in RIPA (Radio-Immuno-Precipitation Assay) lysis buffer (Sigma) supplemented with 1mM of activated SOV and 4% v/v protease inhibitor cocktail (cOmplete tablets, EDTA-free; Roche Diagnostic Limited), and incubated on ice for 30min. To obtain pure protein extract, cells with lysis buffer were then centrifuged in Heraeus Pico 17 Microcentrifuge (Thermo Fisher Scientific) at full speed, at 4°C for 15min. The supernatant was transferred to clean 1.5ml tubes and stored at -20°C.

2.10.1.2 Determination of protein concentration

To quantify protein concentration, the Bio-Rad Protein Assay (Bio-Rad Laboratories Ltd) was used. To plot a calibration curve, five standards were prepared from 1mg/ml stock bovine serum albumin (BSA, Sigma) by dilution in distilled water to 0.1, 0.2, 0.3, 0.4 and 0.5mg/ml. 2.5µl of each sample was mixed with 22.5µl of sterile distilled water. 10µl of standards and samples was then loaded in duplicate in a 96 well flat bottom plate. Bio-Rad Protein Assay Reagent was diluted 1:5 in distilled water and 200µl was added to each well. The plate was then transferred to a Bio-Rad 680 microplate reader and absorbance read as an end point reaction at 595nm. The protein concentration was obtained from calculations based on the calibration curve.

2.10.1.3 Sodium dodecyl sulphate polyacrylamide gel electrophoresis (SDS-PAGE)

Proteins were separated by SDS-PAGE using 8% resolving acrylamide gels. Small gels designed for 10 samples were made according to Lab FAQs booklet (Roche Diagnostic Limited) in a two-step process. To run >10 samples, ready-made Criterion TGX Stain Free Gel, 7.5%, 12+2-well (Bio-Rad) was used. Gels were transferred to Mini/Midi Trans-Blot®

Cell tank (Bio-Rad Laboratories Ltd.) and fully submerged in Tris-Glycine-SDS PAGE Buffer (Geneflow Ltd.). Typically, 50µg of protein was diluted 1:1 in 2x Laemli sample buffer (Bio-Rad Laboratories Ltd.) supplemented with 1M dithiothreitol (DTT). To denature proteins, samples were boiled at 95°C for 10min. Samples were loaded on pre-made gels alongside a Spectra Multicolor Broad Range Protein ladder (Thermo Fisher Scientific) or for bigger proteins, Color-coded Prestained Protein Marker High Range (43-315 kDa) (Cell Signaling) and separated at 120V for 2h.

2.10.1.4 Protein transfer

Transfer of protein from acrylamide gel to a polyvinylidene fluoride (PVDF) membrane was performed using ready-to-use Trans-Blot Turbo Mini or Midi PVDF Transfer Packs and Trans-Blot Turbo Transfer System (Bio-Rad Laboratories), with the standard built-in settings for high molecular weight proteins (1.3A, 25V for 7min).

2.10.1.5 Immunoblotting

The membrane with transferred protein was incubated for 1h at room temperature on a shaking platform in 5% BSA (Sigma) dissolved in TRIS buffered saline-tween (BSA/TBST; milk/TBST) to block non-specific protein binding. TBST buffer was prepared by dissolving 1.21g TRIS, 8.77g NaCl and 0.5ml Tween20 (Thermo Fisher Scientific) in 1l of distilled water. Membranes were then incubated overnight on a rocker at 4°C with primary antibodies diluted to the appropriate concentration in 5% v/v BSA/TBST. The membrane was washed 3 times with TBST with shaking for 10min, followed by 1h incubation with corresponding HRP-conjugated secondary IgG antibodies (Dako), diluted in 5% v/v

BSA/TBST (Table 2.5). After incubation, the membrane was washed again 3 times for 10min each in TBST as before.

Antibody-protein complexes were visualised using Bio-Rad Clarity Western enhanced chemiluminescence (ECL) (Bio-Rad Laboratories Ltd.) by 1min incubation of membrane with ECL mixture and visualising with ChemiDoc MP imaging system (Bio-Rad Laboratories Ltd.). The blots were analysed using ImageLab 4.1 software.

Some membranes were probed for other proteins of interest by first stripping bound antibodies with 1x mild stripping solution (Millipore) in RT on a shaker for 10min. The membrane was then blocked for 1h in 5% v/v BSA/TBST and re-probed as described above.

Following detection of the protein of interest, the membrane was then probed with housekeeping proteins as a protein loading control. The membrane was washed 3 times at RT for 10min each wash, in TBST. Then the membrane was re-probed as described above at RT on a shaker for 30min in β -actin or β -tubulin HRP-conjugated (Cell Signaling) antibody, diluted 1:1000 in 5% v/v BSA/TBST.

Table 2.5 List of used primary and secondary antibodies.

Antibody	Supplier	Clone	Species	WB dilution	IHC dilution and condition	IF dilution and condition
DDR1 (D1G6) XP(R)	Cell Signaling	5583S	Rabbit	1:1000	1:50; 4°C, O/N	1:200; 4°C O/N
DDR1 (Tyr792)	Cell Signaling	11994S	Rabbit	1:1000	-	-
Collagen VI	LsBio	LS-B696	Rabbit	-	1:200; 4°C, O/N	1:600; RT, 1h
Senpe	Sigma	HPA042294	Rabbit	1:1000	1:1800; 4°C, O/N	1:6000; (tissue), 1:400 (cytospin) 4°C, O/N
CD20	Dako	L26	Mouse	-	Ready to use; 1h RT	
CD30	Dako	Ber-H2	Mouse	-	Ready to use; 1h RT	
α-Tubulin	Sigma	T5168	Mouse	-	-	1:2000 (cytospin) RT; 1h
B actin (13E5) (HRP)	Cell Signaling	5125	Rabbit	1:1000	-	-
B tubulin (9F3) (HRP)	Cell Signaling	5146	Rabbit	1:1000	-	-
Polyclonal Goat anti-Rabbit (HRP)	Dako	P0448	Goat	1:1000	-	-
Polyclonal Goat anti-mouse (HRP)	Dako	P0447	Goat	1:3000	-	-
ImmPRESS HRP reagent Universal Anti Mouse/Rabbit IgG	Vector Laboratories Ltd.	MP-7500	Horse	-	Ready to use; 30min, RT	-
Clean Blot IP Detection Reagent (HRP)	Thermo Fisher Scientific	21230	-	1:500	-	-

2.10.2 Sample preparation for immunohistochemistry (IHC) and immunofluorescence (IF)

2.10.2.1 Preparation of cytopins

Cultured cells were counted (as described above) and the appropriate number was pelleted by centrifugation at 4°C, at 1700rpm for 5min. Cells were re-suspended in cold PBS (Life Technology Ltd) to a concentration of 2×10^6 cells/ml. A thin layer of cells was then placed on a glass slide (X-tra positive charged Adhesive; Surgipath) using the Cytospin™ 4 Cytocentrifuge (centrifuge, Cytofunnel™ disposable sample chambers, filter cards and Cytoclips™; Thermo Fisher Scientific). 100µl of cell suspension was centrifuged at 1000rpm for 5min. Cytopins were left to air dry for 10min and fixed by immersing in 10% v/v buffered formaldehyde solution (Fernaedale Pharmaceutical) for 10min or in ice cold 100% methanol (Sigma) for 15min. After this time slides were washed in distilled water or PBS and left to air dry for 30min. Cytopins were used fresh for further experiments or stored at -20°C.

2.10.2.2 Preparation of Poly-Lysine coated slides and Hela cells seeding

Cover slips were washed twice in 70% ethanol (Sigma), followed by single wash in PBS. Slides were left to air dry for 15min. 0.1% poly L-lysine solution (Sigma) was diluted 1:10 in PBS and 200µl was applied on prepared cover slip. Coated slides were left to dry for 1h at 65°C and rinsed in PBS before seeding cells.

Dividing Hela cells were released to suspension by tapping culture flask. Cells released to culture medium were collected by centrifugation at RT in 100rpm for 10min. Supernatant was removed, pellet was re-suspended in 2ml of culture media and cells were counted.

2×10^4 cells/slide was seeded on prepared poly L-lysine cover slips and incubated for 10min prior to fixation with ice cold methanol for 15min. Fixed cover slips with cells were stored at 4°C until further use.

2.10.2.3 Primary paraffin embedded samples

Paraffin-embedded blocks of reactive tonsils were obtained from [REDACTED]. Sections were cut to $4\mu\text{M}$ in thickness and placed onto X-tra Adhesive micro slides (Surgipath Europe) by the pathology department at [REDACTED].

Paraffin-embedded tumour microarray (TMA) blocks of DLBCL were prepared by a pathologist, [REDACTED] based on a cohort of DLBCL patient samples with full clinical annotation, retrieved from the pathology department at [REDACTED]. Each TMA section contains 30 different DLBCL cases including tonsil as a control. Other set of DLBCL TMA's used, were a gift of [REDACTED].

The paraffin embedded sections of mouse tissue were prepared by [REDACTED].

2.10.3 Metaphase spread

Cells were seeded the day before in the concentration of 5×10^5 cells/ml. Next day, 5mln cells were incubated with $200\mu\text{l}$ of colcemide ($10\mu\text{g/ml}$; Sigma) for 3h. Cells were transferred into 50ml tubes and spin at 1500rpm for 5min at RT, followed by wash with 10ml of PBS. After centrifugation, supernatant was removed and 1.5ml of fresh PBS was

added to re-suspend cell pellet, by tapping the bottom of the tube. In next step, 10ml of pre-warmed (37°C) and freshly made hypotonic buffer (5ml of FBS, 5ml of 75mM KCl, 25ml of H₂O) was slowly added to the cell suspension, and incubated for 30min at 37°C. After incubation, 1ml of freshly made fixation buffer (25% of volume of acetic acid (Sigma) and 75% of volume of ethanol (Sigma)) was added – drop by drop, while shaking gently. Tube was inverted once to mix and spin down at 1200rpm for 5min. Supernatant was removed, leaving around 1-2ml of hypotonic buffer at the bottom of the tube. By gently tapping, cells were re-suspended in remaining buffer, 10ml of fresh fixation buffer was added and cells were centrifuge at 1200rpm for 5min. This step was repeated 3 times. After third time, supernatant was removed leaving around 1ml of fixation buffer at the bottom of the tube. Re-suspended cells were then frozen at -20°C. Next day, two microscope slides per cell line were immersed in acetic acid and 20µl of the fixed cells were dropped on the slide from arm length. Slides were then left to dry overnight. Dry slides where stained for 15min in Giemsa solution (1:20 dilution in water; Scientific Laboratory Supplies), washed in water for 5min and left to dry. Slides were mounted using Entellan New (VWR International Marketplace) mounting media and analysed under the bright field microscope, using 100x lense. Chromosome counting was performed in Fiji ImageJ program.

2.10.4 Van Gieson staining method

For Van Gieson's method for collagen fibres, slides were first de-waxed in xylene for 10min, followed by re-hydration in 100% ethanol then in 90% ethanol, 10min each. Slides were then washed in distilled water for 5min and placed on a slide tray. Sections were

circled with PAP-PEN. Weigert's Working Haematoxylin solutions A & B (Polyscience Inc.) were mixed 1:1 and 100µl of mixture was incubated on the slide for 10min. Slides were washed in distilled water, dried and stained by Van Gieson's solution for 5min. Slides were then dehydrated by immersing in 100% ethanol for 30s followed by 5min incubation in histoclear. Stained samples were mounted with coverslips using DPX mounting medium (Invitrogen) and analysed under the microscope.

2.10.5 Immunohistochemistry (IHC)

2.10.5.1 Preparation of slides for immunohistochemistry (IHC)

Cytospins

Cytospins were taken out of the freezer, thawed at room temperature for a few minutes and the endogenous peroxidase activity blocked by immersing slides in 0.3% v/v hydrogen peroxidase (Sigma) for 15min. After incubation, slides were rinsed in cold running tap water for 5min.

Tissue sections

Slides were de-waxed by immersing in HistoClear (National Diagnostics) for 10min and re-hydrated in 100% ethanol (Sigma) for another 10min. The slides were then washed in cold running tap water for 5min and endogenous peroxidase activity was blocked by immersing slides in 0.3% v/v hydrogen peroxidase for 15min. Before the antigen retrieval step, slides were rinsed for 5min in cold running tap water.

2.10.5.2 Antigen retrieval

The citric buffer microwave antigen retrieval method was used. 1.26g of sodium citrate and 0.25g of citric acid were dissolved in 1l of distilled water and pH was adjusted to 6.0 with 0.1M sodium hydroxide. Before immersing slides, the buffer was boiled in a glass beaker for 10min at microwave full power. Immediately after this, slides were placed in the buffer ensuring that the slides were fully submerged and boiled for another 10min at moderate power, followed by 10min at low power. The buffer was then left to cool for around 30min, before removing the slides and washing in running tap water.

2.10.5.3 Detection and visualisation of antigen by immunohistochemistry (IHC)

Slides were placed on a metal microscope slide staining tray (Richardson of Leicester Ltd), the section was circled with the PAP-PEN (Dako) and washed with 0.1% PBS-Tween (PBST) for 5min. To block non-specific background staining, samples were incubated in 5x casein blocking solution (Vector Laboratories Ltd) for 10min. Casein was removed and primary antibodies were applied. Samples were incubated with primary antibody diluted in PBS to the desired concentrations (Table 2.5). After incubation, samples were washed 3 times in PBST for 5min each; ImmPRESS HRP reagent Universal Anti Mouse/ Rabbit IgG (Vector Laboratories Ltd) secondary antibodies were applied and incubated for 30min at room temperature. For visualisation of staining, ImmPact DAB substrate system (diaminobenzidine) (Vector Laboratories Ltd) was added which bound to the antibody-antigen complex and converted the substrate into a brown insoluble product. Sections were then washed for 5min in cold running tap water and counterstained in Mayer's haematoxylin (Sigma) for 2min, followed by another 2min wash in hot running tap water.

Samples were then dehydrated by immersing in 100% ethanol for 10min, followed by 10min incubation in histoclear. Stained slides were mounted with coverslips using DPX mounting medium (Invitrogen) or Omnimount™ Histological Mounting Medium (National Diagnostics) and analysed under the microscope with help of [REDACTED]

2.10.5.4 Slides scoring

Stained slides were then analysed under the microscope and scored by [REDACTED]. In case of DDR1 staining, samples were recorded as positive if $\geq 25\%$ of cells were positive for each marker. For CENPE staining, samples were recorded as negative, positive (if tumour cells were stained with the same intensity as in control germinal centre B cells and non-malignant cells in the tumour microenvironment), or weakly positive (if tumour cells were stained less intensely than control germinal centre B cells and non-malignant cells in the tumour microenvironment). Collagen VI staining was classified as positive, when $\geq 25\%$ of tumour cells were in contact with collagen.

2.10.6 Detection of antigen by single/multiple immunofluorescence (IF) staining using Opal™ kit

Immunofluorescence staining was performed using the Opal™ kit (PerkinElmer). The protocol used was provided by manufacturer for the Opal™ Fluorophore kit. Staining using Opal fluorescent dyes provided strong and specific binding to the antigen and enabled multi-labelling on fixed tissue or cells, as re-heating the sample does not affect the previously constructed covalent bond between fluorophore and antigen (PerkinElmer

Assay development guide booklet). This method allowed visualisation of several different markers of interest on a single slide.

2.10.6.1 Preparation of slides

Cytospins

Cytospin slides were prepared in the same way as described above for IHC, with the difference in the final washing step, which was performed in distilled water.

Tissue sections

Paraffin-embedded sections were de-waxed using xylene (Fisher Scientific) for total of 30min and re-hydrated by immersing slides in different dilutions of ethanol: 100% ethanol for 5min, 95% ethanol for 3min and 70% ethanol for 3min. Sections were washed for 5min in running distilled water and endogenous peroxidase activity was blocked as described above. Slides were washed again for 5min in distilled water.

2.10.6.2 Opal™ fluorophore staining

After citric buffer (pH6.0) antigen retrieval, slides were placed on a staining tray and the section was marked by PEP-PEN (Dako). Samples were washed with PBST for 5min and blocked for 10min in 5x casein blocking solution (Vector Laboratories Ltd) or 1h in 10% FBS. Primary antibodies were applied and incubated for the required time (Table 2.5). Slides were washed with PBST and ImmPRESS HRP reagent Universal Anti Mouse/Rabbit IgG (Vector Laboratories Ltd) secondary antibody was added. After 30min incubation, slides were washed in PBST, as described above.

For the visualisation step, the chosen fluorophore was optimally diluted in amplification diluent (part of Opal™ 3-plex kit; FP1135) (Table 2.6) and incubated on the section, at room temperature, in the dark for 10min. Slides were then washed with PBST.

For multiple labelling, after fluorophore dye application and the first wash in PBST, second antigen retrieval step was performed. Slides were boiled again in pre-heated (5min on high power) pH 6.0, citric buffer, for 15min at microwave low power, to strip the antigen-antibody complex. All the following steps were repeated (as described above), making sure that different fluorophore dye (Table 2.6) was used for each primary antibody applied.

As a final step, DAPI (Life Technology) diluted 1:1000 in PBS was applied and incubated for 5min, followed by 5min wash with PBST. Slides were mounted with a coverslip using Vectrashield Hard Set (Vector Laboratories Ltd) mounting medium. Cells were analysed with help of [REDACTED] using a Nikon E600 UV microscope or Vectra Slide Scanning System.

Table 2.6 Fluorophores used for multiplex immunofluorescence staining.

Fluorophore	Company	Dilution	Conditions
Cyanine 5	Perkin Elmer	1:400	Diluted in amplification diluent (FP1135), part of Opal™ Fluorophore kit; Incubation for 6min
Cyanine 3	Perkin Elmer	1:200	Diluted in amplification diluent (FP1135), part of Opal™ Fluorophore kit; Incubation for 10min
FITC	Perkin Elmer	1:200	Diluted in amplification diluent (FP1135), part of Opal™ Fluorophore kit; Incubation for 10min
DAPI	Life Technology	1:1000	Diluted in PBS; incubation for 5min

2.10.7 Flow cytometry

With help of [REDACTED], flow cytometry was used to detect DDR1 cell surface expression. 1×10^6 cells in media were transferred to each flow cytometry tube. At the same time, an extra tube for each stain of compensation beads (BD Bioscience) was prepared, with 1 drop of relevant anti-species Ig and negative control each. Cells were then pelleted by centrifugation at room temperature at 1500rpm for 3min. To fully remove the media, cells were re-suspended in 1ml of 1% v/v FBS/PBS and centrifuged again. The pellets were re-suspended in 100 μ l of 1% v/v FBS/PBS with 2 μ l of each antibody (DDR1-PE, CD20 APC CY7, CD30 PerCP (Ebioscience)) and incubated for 20min at 4°C, in the dark. Cells and compensation beads were then washed in 1% v/v FBS/PBS and fixed by re-suspension in 1% paraformaldehyde. Cells were run through a BD LCR II Cell Analyser (BD Bioscience) and the results were analysed using Flowjo software (TreeStar Inc).

2.11 Mouse model

2.11.1 L591, BJAB, A20 xenograft

Cells were maintained as described in section 2.1.1. Prior to injection, cells were counted and seeded to a concentration of 5×10^5 cells/ml. The following day, cells were harvested by brief centrifugation at 1700rpm for 5min. Cells were re-suspended in PBS to 3×10^7 cells/ml. Immunodeficient NSGTM Mice (The Jackson Laboratory) were injected with 100 μ l of cells (3×10^6 cells/mouse) subcutaneously in the right flank, N=3 mice/cell line (carried out by [REDACTED]). Mice were monitored weekly and tumours measured as soon as they were visible. After 39 days, mice were killed by cervical dislocation and the tumour was collected in RPMI-1640. A small portion of the tumour was fixed in 10% formalin for further use in immunohistochemistry staining. The rest of the tissue was minced and cells were analysed by flow cytometry.

A20 xenograft samples were a gift of [REDACTED]

2.12 Statistical analysis

2.12.1 RNA sequencing data analysis from GC B cells

Statistical analysis of RNA sequencing data from GC B cells transfected with DDR1a and EV, was performed by [REDACTED]. Sequence reads were aligned to hg19 reference sequence using Rsubread aligner (Liao et al., 2013). Mapped sequencing reads were assigned to individual genes using featureCounts function. Gene symbol and description were obtained from NCBI gene database. The data was then normalized using TMM (trimmed mean of M values) method and converted into counts-

per-million (CPM) reads using the edgeR package (Robinson et al., 2010). edgeR was also used for differential expression analysis with criteria: $p < 0.05$ and fold change < 1.5 . Genes with read counts-per-million < 2 in more than three samples were removed.

2.12.2 Re-analysis of published datasets

The re-analysis of published RNAseq data and microarray datasets were performed by 

RNAseq data of 105 DLBCL cases, among which 32 had been categorised as ABC-type and 54 as GCB-type DLBCL, were downloaded from the controlled access area of NIH database (dbGap; <http://www.ncbi.nlm.nih.gov/gap>; accession code phs000532.v5.p2) (Morin et al., 2011). RNA-seq data for four GC B cell samples were downloaded from Gene Expression Omnibus (<http://www.ncbi.nlm.nih.gov/geo/>; accession GSE45982 – GSM1129344, GSM1129345, GSM1129346 and GSM1129347) (Beguelin et al., 2013). CPM was generated by using the same methodology as described above.

The global gene expression microarray data from GSE10846 of 414 DLBCL cases, among which 167 were classified as ABC type and 183 as GCB type DLBCL (Lenz et al., 2008b), and from GSE12453 for several types of lymphoma, including 11 DLBCL, 12 HL and 10 normal GC B cells (5 centrocyte and 5 centroblast) (Brune et al., 2008), were downloaded from the Gene Expression Omnibus (GEO) website. Data from both datasets were normalised using the affy package in R (Bolstad et al., 2003, Irizarry et al., 2003). Differential expression analysis was performed using limma (Smyth, 2004) in R.

2.12.3 Measurement of aneuploidy index

Clinical data, level 3 copy number data and level 3 RNA-sequencing (v2) data for the DLBCL dataset were downloaded from TCGA's data portal and analysed by [REDACTED]. In total there were 48 tumour samples for which both copy number and RNA-sequencing data were available. Copy number data were also available for 46 matched normal (blood or bone marrow) samples. Segmented copy number data based on the hg19 human reference genome were used. For each sample, a copy number "index" value was calculated separately for each chromosomal arm, as the weighted (by length of segment) average of the copy number values for each segment. Total autosomal aneuploidy was then calculated for each sample as the sum across all autosomal arms of the absolute value of two minus index value. Allowance for tumour purity was made using the "percent_tumor_nuclei" item available in the clinical data. The un-normalized gene-level RNA-sequencing data were used. Raw read counts were normalized (trimmed mean of M-values method) between samples and converted to counts-per-million reads for each gene using the edgeR package in R (Robinson et al., 2010), as described above.

2.12.4 Overall survival analysis in DDR1 positive DLBCL

Clinical data for the DLBCL samples used to determine the overall survival in DDR1 positive and negative DLBCL were a kind gift of [REDACTED]. These comprised 29 DLBCL cases which after scoring were described as DDR1 positive, 46 cases described as DDR1 negative (described in Section 2.10.5.4) and 7 cases classified as indeterminate and excluded from further

analysis. From DDR1 positive cases, 18 patients and from DDR1 negative cases, 19 patients didn't survive first 1000 days from diagnosis. Kaplan-Meier analysis was performed by [REDACTED] using survival package in R. P value was calculated using log-rank test.

CHAPTER THREE

Results part I

INVESTIGATING THE CONTRIBUTION OF DDR1 TO THE PATHOGENESIS OF DIFFUSE LARGE B CELL LYMPHOMA

3. Investigating the contribution of DDR1 to the pathogenesis of diffuse large B cell lymphoma

3.1 Expression of DDR1 receptor and its ligand collagen in DLBCL

3.1.1 Over-expression of DDR1 in primary diffuse large B cell lymphoma

To investigate the expression of DDR1 in DLBCL, with a help of [REDACTED], a re-analysis of three datasets that had analysed global gene expression in DLBCL was performed (Brune et al., 2008, Lenz et al., 2008b, Morin et al., 2011). The first analysis was done with the dataset published by Brune et al. This dataset consists of microarray analysis of 11 DLBCL (subset unknown), 12 HL and 10 normal GC B cells (centrocytes, centroblasts from 5 healthy tonsils) (Brune et al., 2008). This revealed that when compared to primary germinal centre B cells (GCB), DDR1 was significantly over-expressed in a subset of DLBCL ($p=0.01129$; Figure 3.1A and raw data provided in Appendix 1). To further investigate DDR1 expression, separately in ABC and GCB types of DLBCL, I next analysed datasets reported by Morin et al. (Morin et al., 2011) and Lenz et al (Lenz et al., 2008b). The Morin dataset was created by analysing gene expression by RNA sequencing of 117 tumour samples, which included 32 ABC and 54 GCB type of DLBCL. DDR1 expression in cpm in both types of DLBCL was then compared to 4 normal GC B cell controls (controls taken from RNAseq results published by Beguelin et al. (Beguelin et al., 2013). Lenz et al. published a microarray analysis of 414 newly diagnosed DLBCL, among which 167 were classified as ABC type and 183 as GCB type DLBCL. The re-analysis of both datasets showed statistically significantly higher expression of DDR1 in

GCB type, in comparison to ABC type of DLBCL (Morin $p=0.00083$, Lenz $p=0.00008431$) (Figure 3.1B and 3.1C; raw data in Appendix 2 and 3).

I next used Fluidigm®48.48 Fast Real Time PCR (as described in Materials and Methods, section 2.9.6) to study the expression of DDR1 mRNA in a separate cohort of DLBCL, provided by [REDACTED]

This analysis revealed that, 20/44 DLBCL samples had significantly higher levels of DDR1 compared with normal GC B cells (Figure 3.1D, raw data in Appendix 4).

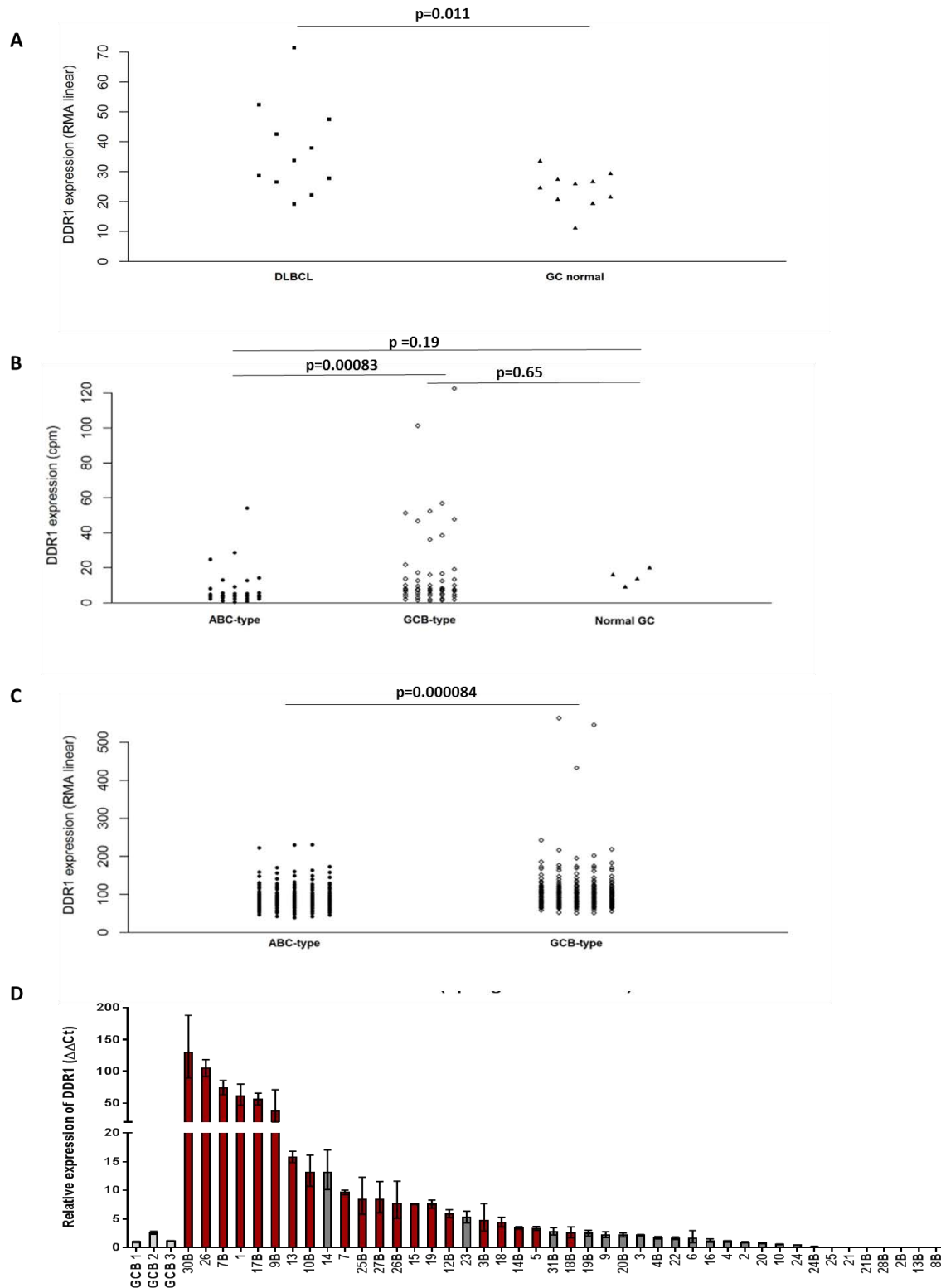


Figure 3.1 Over-expression of DDR1 in diffuse large B cell lymphoma.

A) Re-analysis of datasets reporting global gene expression in DLBCL and normal GC B cells revealed that when compared to primary germinal centre B cells, DDR1 mRNA was significantly over-expressed in a subset of DLBCL, including cases of both ABC and GC type ($p=0.02011$). Comparison of DDR1 expression in a series of DLBCL reported by B) Morin and C) Lenz separately, reveals that DDR1 expression is significantly higher in GCB type, when compared to ABC type DLBCL (Lenz $p=0.00008431$; Morin $p=0.01782$) D) qRT-PCR confirms the over-expression of DDR1 mRNA in a separate cohort of DLBCL. 20/44 DLBCL samples showed significantly higher levels of DDR1 compared with normal GC B cells. Students T test, where red bars indicates significant up-regulation of DDR1 ($p\leq 0.05$).

To study DDR1 protein expression, I next performed immunohistochemistry on primary DLBCL. To do this, I first confirmed the specificity of a rabbit monoclonal antibody to DDR1 (D1G6) XP[®] (Cell Signaling). I used the DG75 Burkitt lymphoma cell line, which expresses very low endogenous levels of DDR1. I transfected DG75 cells with DDR1a plasmid or with empty vector (EV) as a control (Materials and Methods section 2.4). Both immunohistochemistry and immunoblotting, showed specific detection of DDR1 in transfected cells, in comparison to EV control (Figure 3.2A and 3.2B). As a last level of confirmation, I performed immunofluorescent staining on primary HL, which is already known to express high levels of DDR1 in HRS cells (Cader et al, 2013). My results confirmed high DDR1 expression in tumour cells, in comparison to DDR1 negative GC cells in tonsil control (Figure 3.2C).

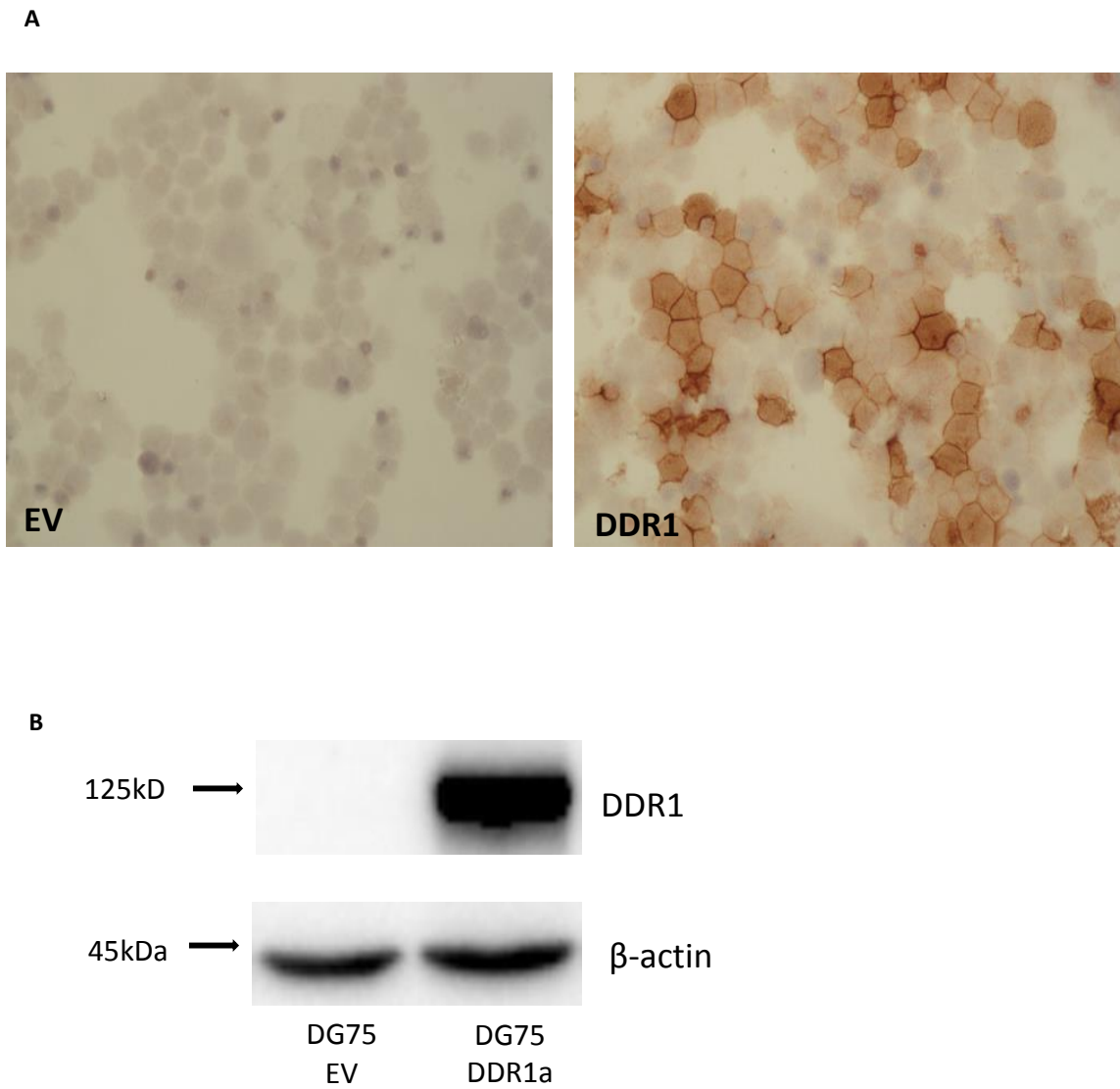


Figure 3.2. Validation of DDR1 antibody.

A) Immunohistochemistry shows DDR1 staining in DG75 cell line, transfected with DDR1 or EV as a control, using rabbit monoclonal DDR1 (D1G6) XP® antibody (Cell Signaling). B) Immunoblotting confirming DDR1 expression in DDR1 expressing DG75 cells (MW of protein 125kDa). Equal loading of the protein is shown using β -actin antibody (MW of protein 45kDa).

c

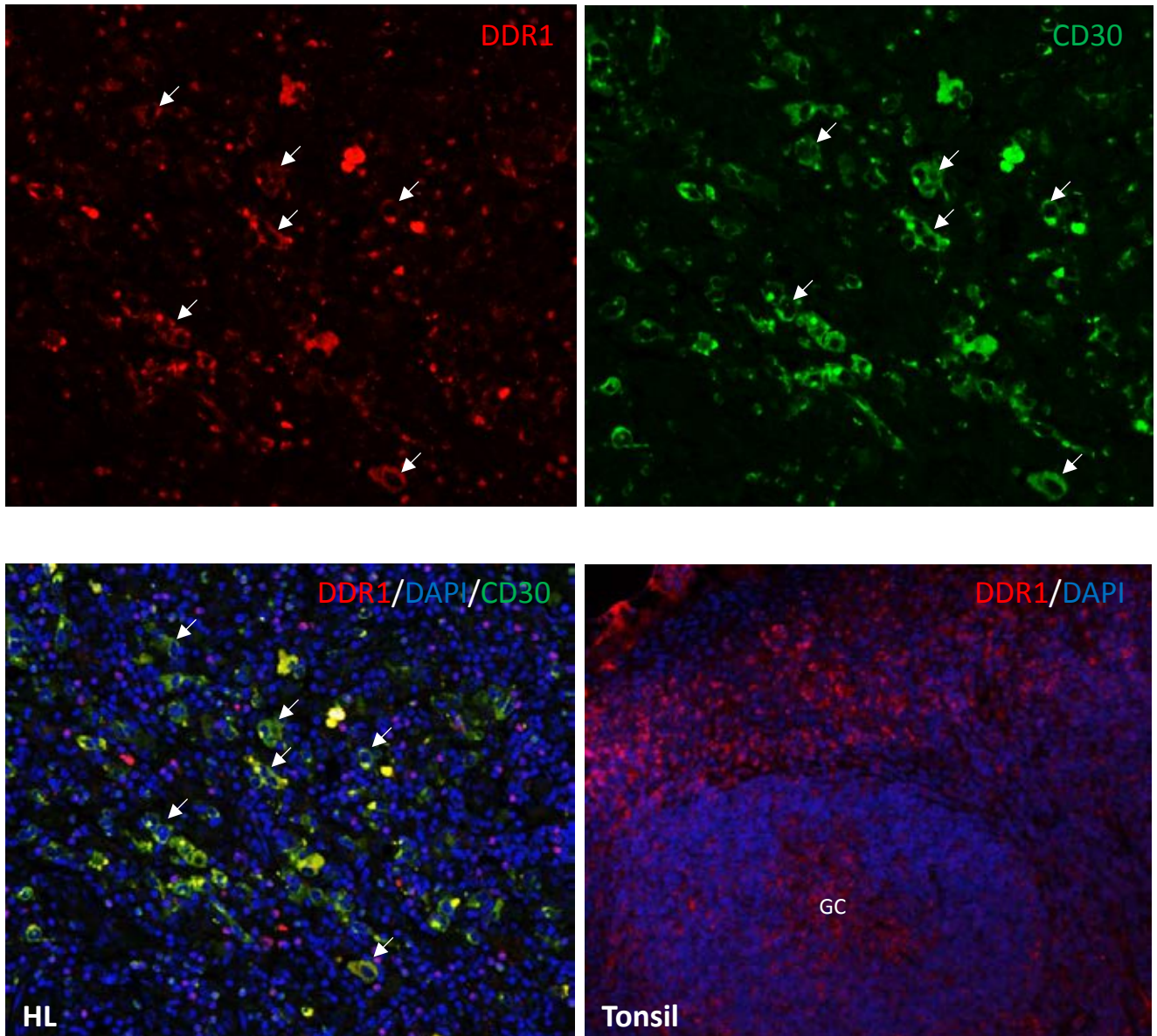


Figure 3.2C. Immunofluorescent staining with DDR1 antibody in primary HL (top panels) shows expression of DDR1 in HRS cells (DDR1+CD30+; marked with arrows, bottom left panel), in contrast to germinal centre negative control (bottom right panel). GC- germinal centre.

Having confirmed the specificity of the DDR1 antibody, I tested a separate cohort of 75 cases of DLBCL by immunohistochemistry. Stained sections were analysed under the microscope and scored by [REDACTED]. DDR1 expression was recorded as positive if $\geq 25\%$ of cells were positive for DDR1 marker. In contrast to normal GC B cells which did not express detectable DDR1, 29/75 cases of DLBCL showed DDR1 expression in tumour cells (Figure 3.2D). Data was already available on those cases for BCL6, CD10 and IRF4 staining and the Hans algorithm had been used to defined each case as either GC or non-GC type (Hans et al., 2004). 20/29 DDR1 positive DLBCL were of ABC type and 9/29 of GCB type.

I next examined the impact of DDR1 expression on survival in this cohort (statistical analysis performed by [REDACTED]). DDR1 positive cases appear to have worse survival; however this was not statistically significant (Figure 3.3). I conclude that DDR1 is over-expressed in a subset of DLBCL, which includes cases of both GC and ABC type DLBCL.

D

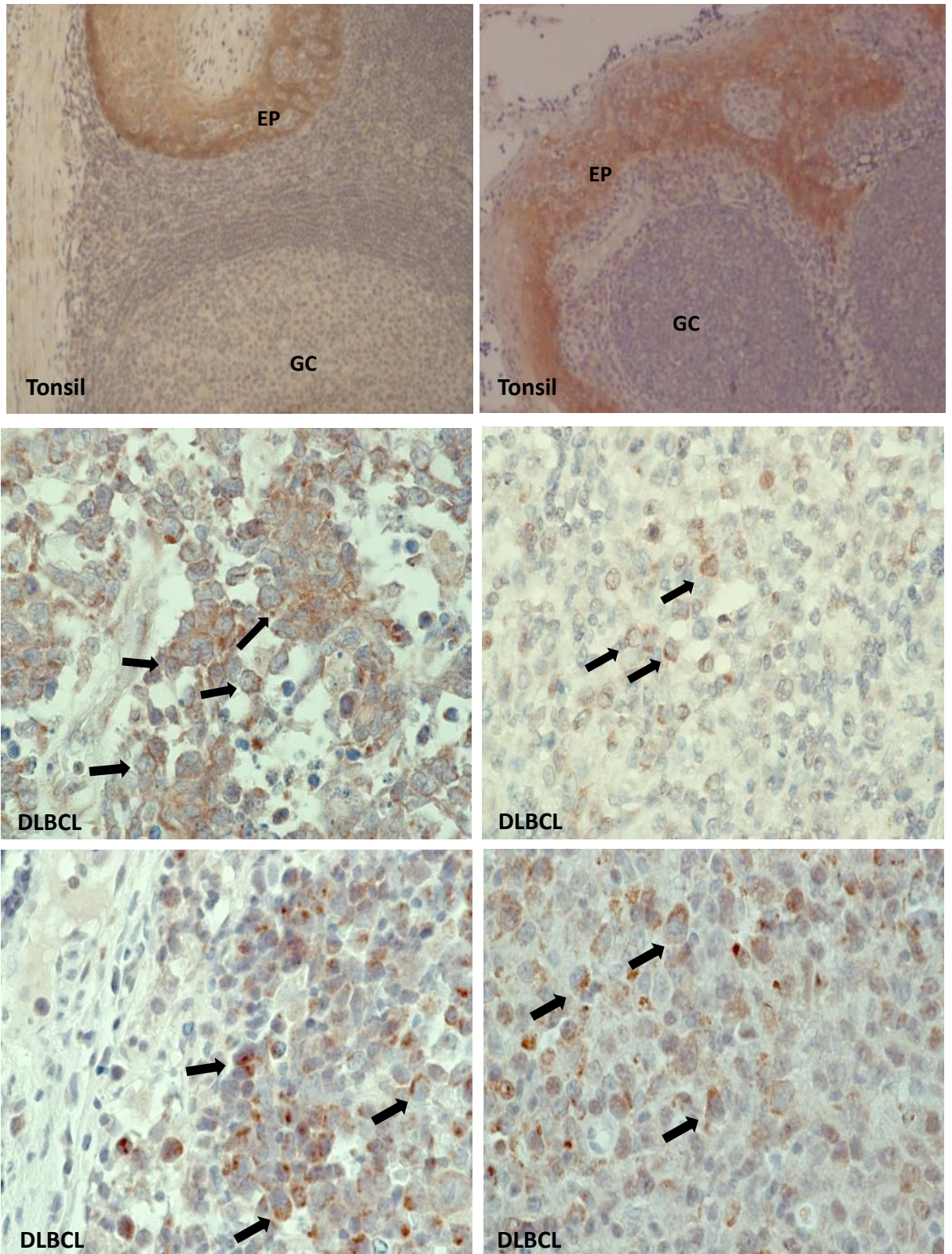


Figure 3.2D DDR1 expression in diffuse large B cell lymphoma.

Immunohistochemistry shows representative examples of DDR1 staining in normal tonsil (two top panels) and four representative cases of DLBCL showing tumour cell expression (bottom panels). GC-germinal centre, EP - tonsillar epithelial cells. GC B cells did not stain for DDR1. DDR1-positive tumour cells are arrowed.

DLBCL database - KM analysis by DDR1 status (1000 days)

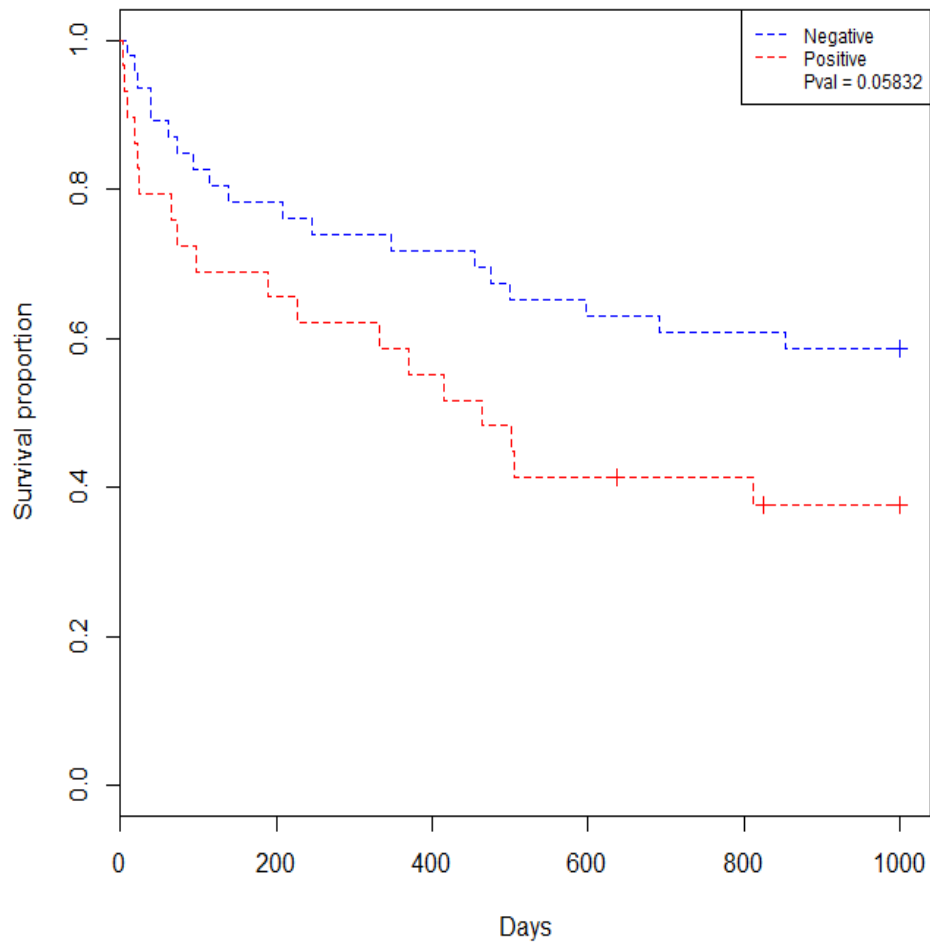


Figure 3.3 Overall survivals in DDR1 positive and negative DLBCL patients.

Kaplan-Meier plot is showing overall survival in patients with DLBCL in first 1000 days from diagnosis. Although not statistically significant ($p=0.05832$), DDR1 positive cases (red) appear to have worse survival in comparison to DDR1 negative (blue) cases.

3.1.2 DDR1-expressing DLBCL are enriched for the expression of collagen genes

To explore the relationship between DDR1 expression and that of its collagen ligands in DLBCL, I next interrogated a meta-analysis of 11 DLBCL gene expression datasets comprising over 2000 cases of DLBCL, data provided by [REDACTED] [REDACTED] (Care et al., 2015). For each data set, the variance for each gene was used to order them by patient sample and Spearman's rank correlations compared to that of DDR1 were calculated from the top 80% of the genes. The correlation matrices and p values were merged across all datasets using median values. A DDR1-correlated gene set was created by taking all genes present in at least six datasets with a median $p < 0.05$. This meta-analysis revealed that the expression of 1446 unique genes was positively correlated, and that of 1295 unique genes negatively correlated, with DDR1 expression in primary DLBCL. I then compared these gene sets to a list of all known collagen genes (source: <http://www.genenames.org/genefamilies/COLLAGEN>) (46 genes; Appendix 5). This analysis showed that collagen genes were significantly enriched among genes that were positively correlated with DDR1 expression in primary DLBCL (odds ratio=5.69; $p < 0.0001$), and depleted among genes negatively correlated with DDR1, although this did not reach statistical significance (odds ratio= 0; $p = 0.075$) (Figure 3.4A). I noted that collagen genes enriched among genes positively correlated with DDR1 in DLBCL included a number of subunits of type VI collagen, including COL6A1, COL6A2, COL6A3, and COL6A5. Immunohistochemistry of normal lymphoid tissues and the same cohorts of DLBCL described above revealed that while normal germinal centre B cells lacked type VI collagen, all 22 DDR1-expressing DLBCL as well as 10 DDR1 negative DLBCL cases, showed a prominent deposition of type VI collagen surrounding tumour cells (Figure 3.4B).

I confirmed the co-expression of DDR1 and type VI collagen in tonsil and in two cases of DDR1 positive DLBCL by multiplex immunofluorescent staining (Figure 3.4C and 3.4D). These observations suggest that DDR1 and collagen are expressed in close proximity in DLBCL.

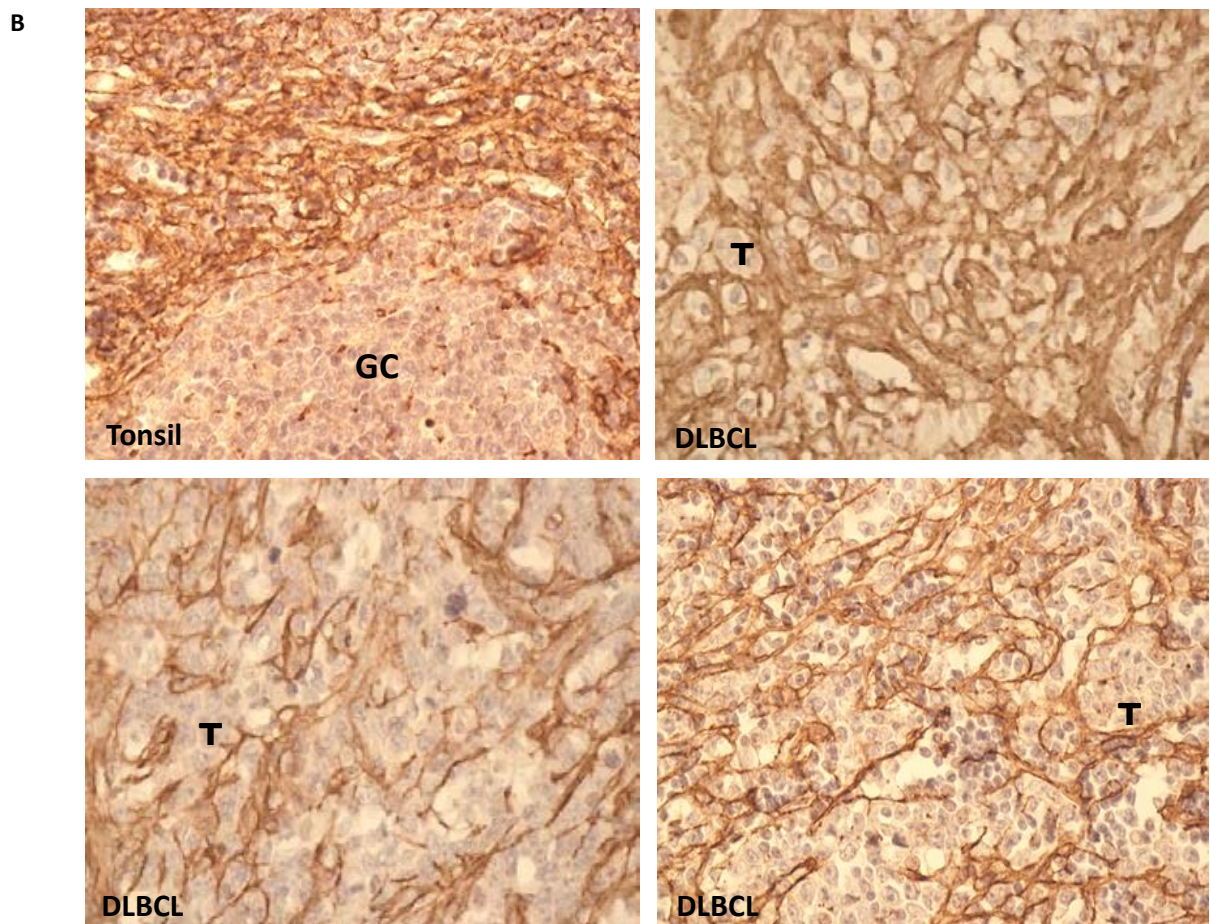
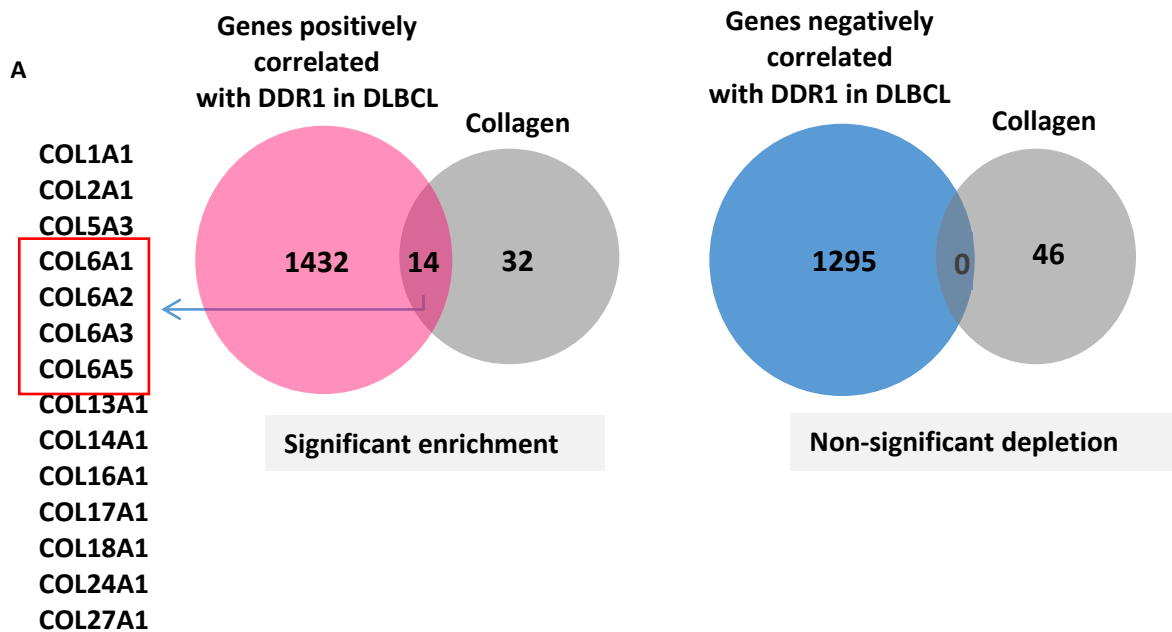


Figure 3.4 DDR1-expressing DLBCL are enriched for the expression of collagen genes.
 A) A meta-analysis of 11 DLBCL gene expression datasets comprising over 2000 cases of DLBCL revealed that collagen genes were significantly enriched among those genes that were positively correlated (left panel; $p < 0.0001$), and depleted among those genes that were negatively correlated (right panel; p value=0.08), with DDR1 in primary DLBCL. Collagen genes enriched among genes positively correlated with DDR1 included COL6A1, COL6A2, COL6A3, and COL6A5 (red box). B) Representative examples of staining for type VI collagen in tonsil (left upper panel) and primary DLBCL. Type VI collagen was mostly absent from normal germinal centres (GC), whereas DDR1-expressing primary DLBCL displayed prominent type VI collagen deposition surrounding tumour cells (T).

c

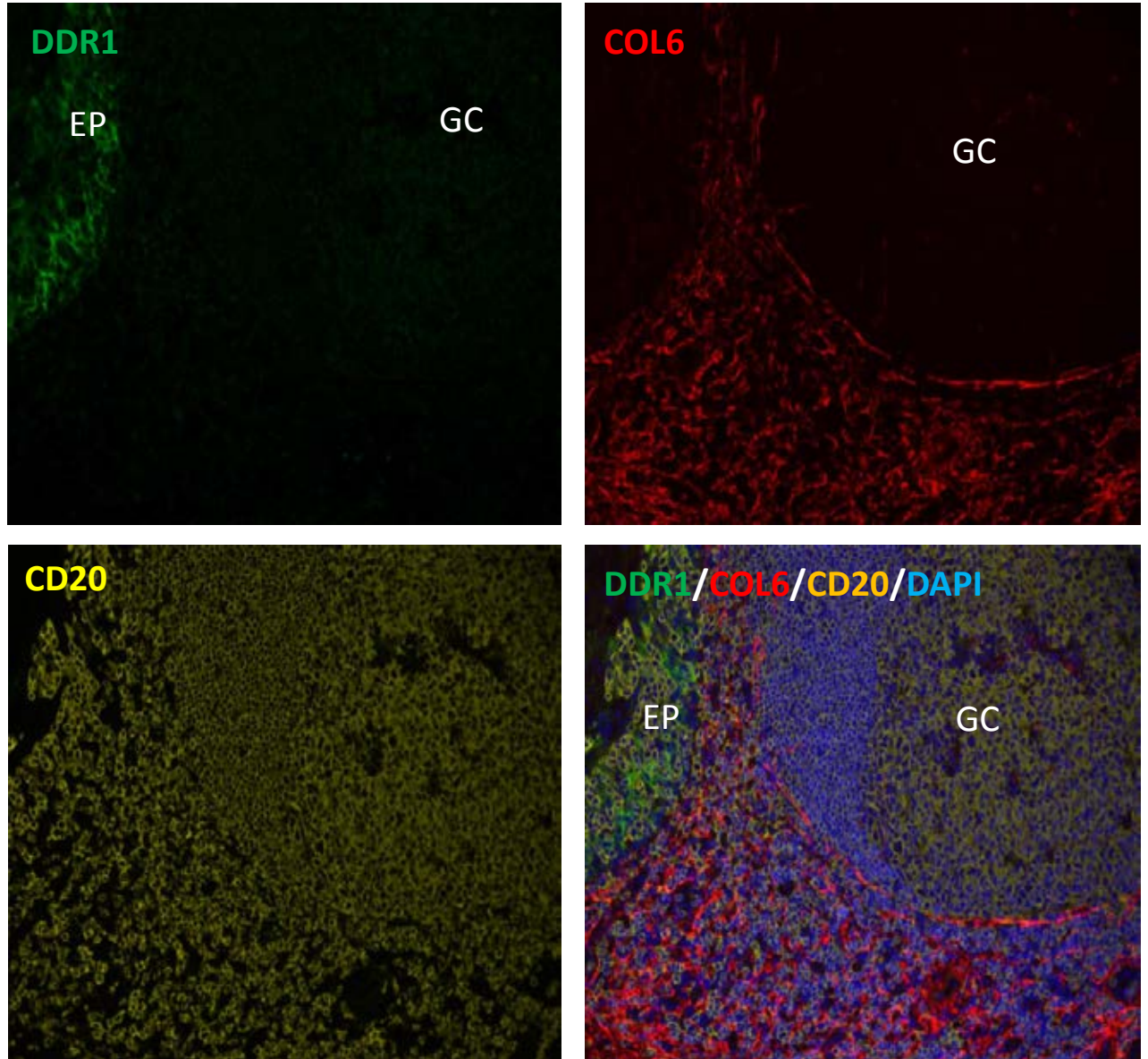


Figure 3.4C Multiplex immunofluorescence staining with DDR1, COL6 and CD20 in tonsil control. EP-epithelium, GC – germinal centre.

D

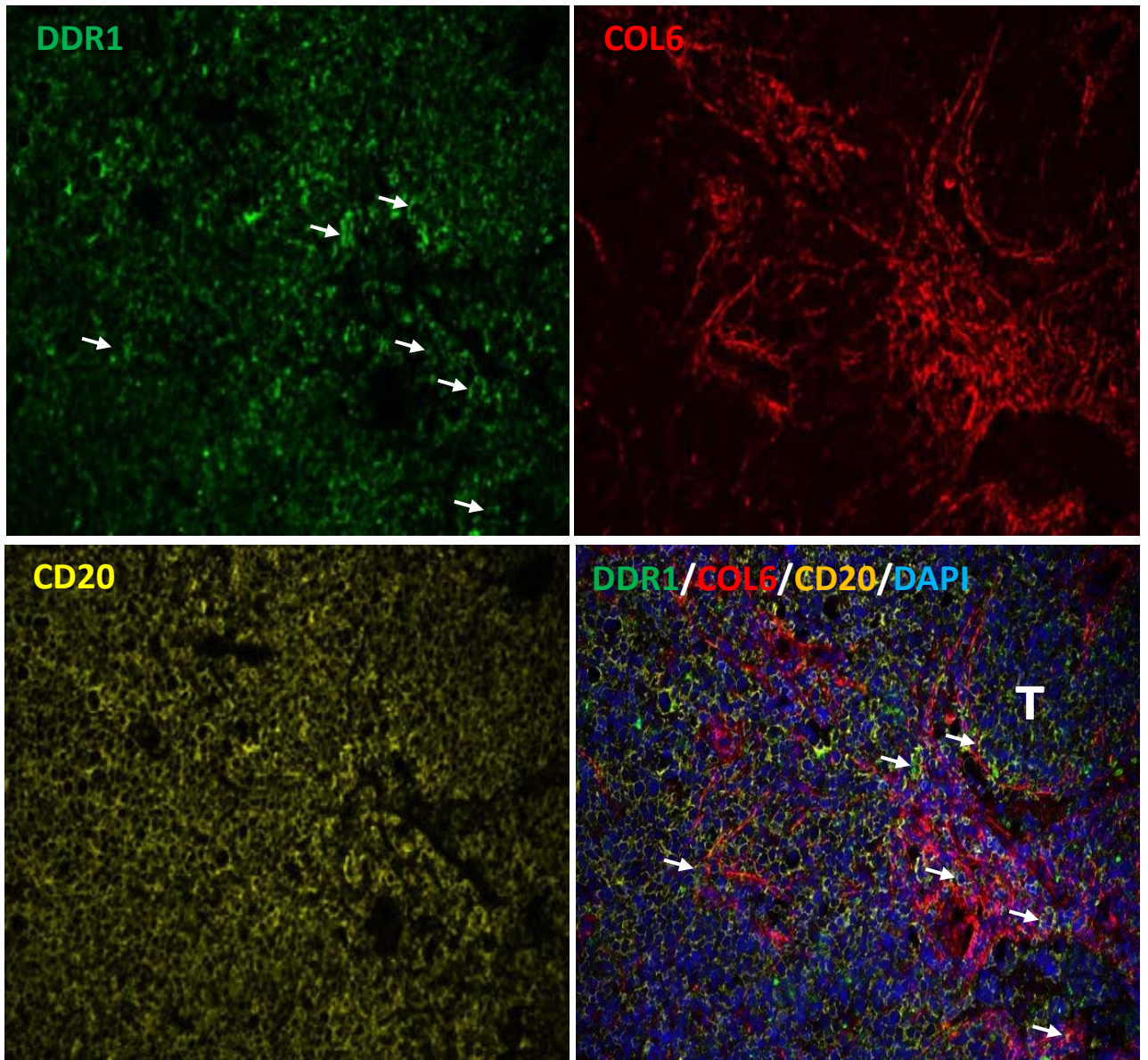


Figure 3.4D Multiplex immunofluorescence confirmed that DDR1-expressing tumour cells (CD20 positive) were intimately associated with stromal type VI collagen in DLBCL (marked by arrows). T- tumour cells.

3.2 Genes negatively correlated with DDR1 expression in DLBCL are enriched for mitotic spindle associated genes

Next, using an online gene functional classification tool, DAVID (<https://david.ncifcrf.gov/>)(Dennis et al., 2003), I performed an ontology analysis of the genes whose expression was either positively or negatively correlated with that of DDR1 in primary DLBCL. I found that genes positively correlated with DDR1 expression in DLBCL were significantly enriched for the GO terms 'collagen catabolic process', 'collagen metabolic process' and 'wound healing' as well as 'regulation of apoptosis' and 'cell migration' reflecting the known functions of DDR1 (Figure 3.5A). On the other hand, genes negatively correlated with DDR1 were enriched for GO terms associated with the regulation of mitotic integrity, including 'mitotic spindle organisation' and 'mitotic sister chromatid segregation' (Figure 3.5B).

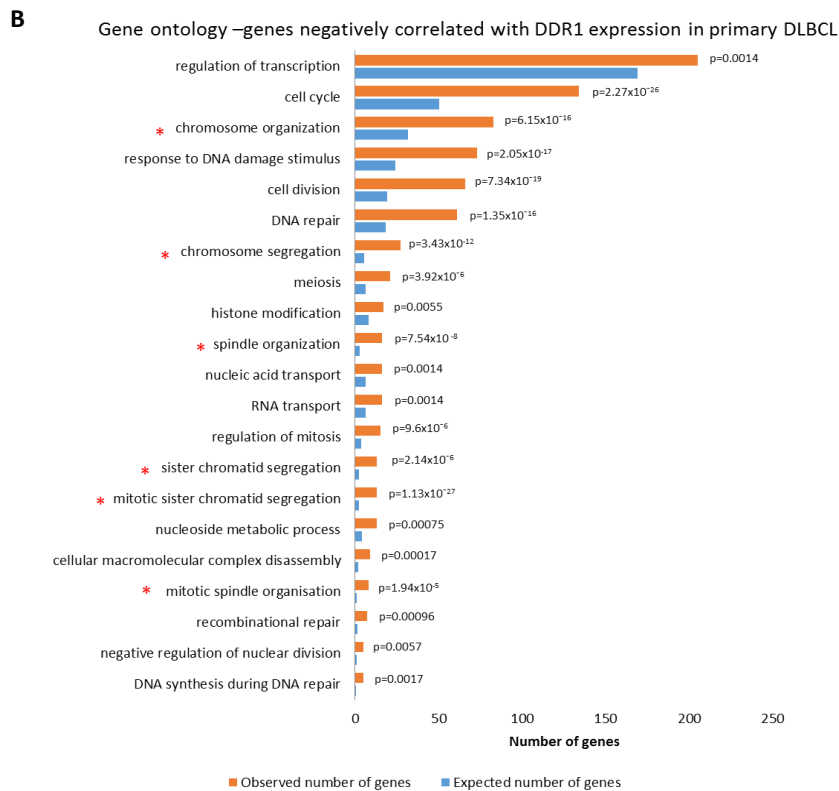
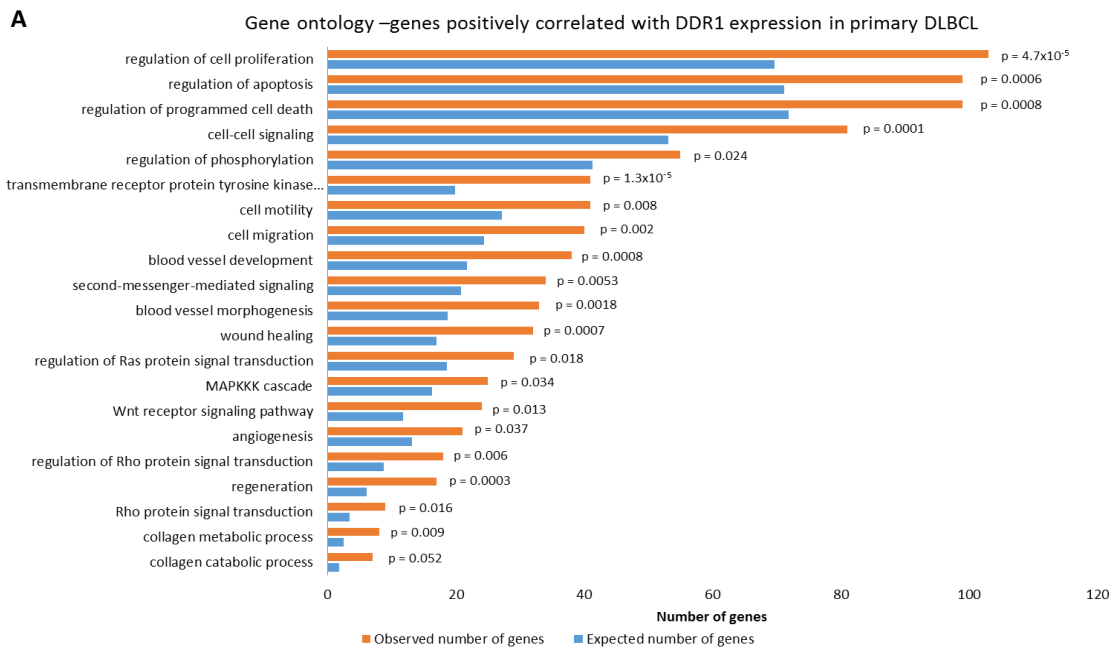


Figure 3.5 Genes negatively correlated with DDR1 expression in DLBCL are enriched for mitotic spindle associated genes.

A) Selected GO terms from the ontology analysis of genes positively correlated with DDR1 expression in DLBCL included ‘collagen catabolic process’, ‘collagen metabolic process’ and ‘wound healing’ as well as ‘regulation of apoptosis’ and ‘cell migration’, reflecting known DDR1 functions. B) Selected GO terms from the ontology analysis of genes negatively correlated with DDR1 expression in DLBCL included ‘chromosome organisation’, ‘mitotic sister chromatid segregation’, and ‘chromosome segregation’. Red asterisks shows GO terms associated with mitotic spindle functions.

To further explore the possibility that genes with mitotic spindle functions might be down-regulated in DDR1-expressing DLBCL, I used a comprehensive list of 513 'mitotic spindle associated' genes that was compiled by our group (Ramagiri et al., manuscript in preparation), which included those classified under the GO terms listed above, as well as those that had been identified in an unbiased Pubmed search using the search term 'mitotic spindle'. I found a significant enrichment of 'mitotic spindle associated' genes among genes negatively correlated with DDR1 expression in DLBCL (odds ratio=3.67; $p < 0.0001$; Figure 5C upper panel), and a significant depletion among those positively correlated with DDR1 (odds ratio=0.43; $p = 0.0015$; not shown). I also used a comprehensive mitotic spindle checkpoint signature comprising 103 genes which included those classified under the GO term 'GO:0031577' (Ramagiri et al., manuscript in preparation). I found a significant enrichment of 'mitotic spindle checkpoint' genes among genes negatively correlated (odds ratio=7.03; $p < 0.0001$; Figure 3.5C, lower panel), but not among those positively correlated (odds ratio=1.35; $p = 0.245$; not shown), with DDR1 expression. I conclude that genes negatively correlated with DDR1 expression in DLBCL are enriched for mitotic spindle associated genes.

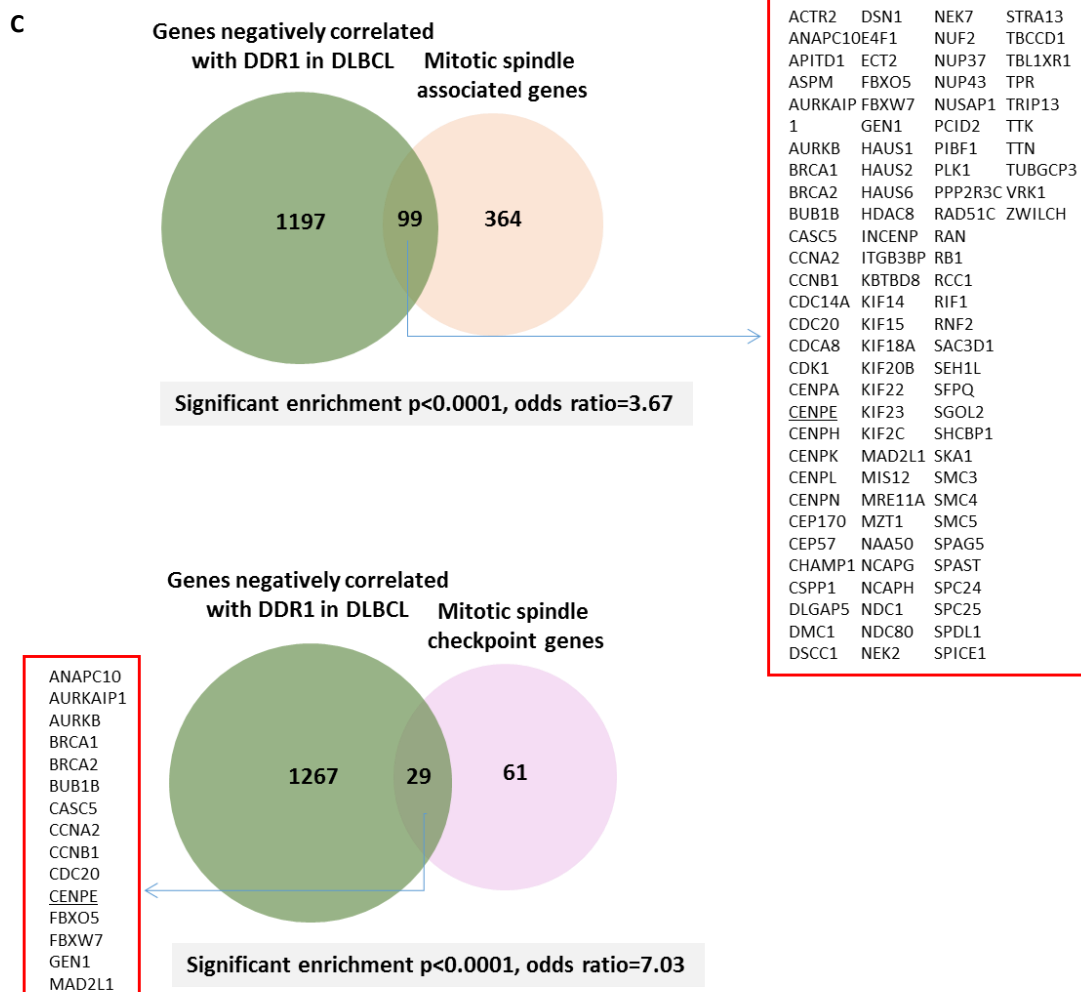


Figure 3.5C: Using a comprehensive list of 513 ‘mitotic spindle associated’ genes which included those classified under the GO terms listed above, as well as those identified in an unbiased Pubmed search using the search term ‘mitotic spindle’, I found that 463 of these genes were also on the human genome build used to derive the genes sets positively and negatively correlated with DDR1 in DLBCL. I found a significant enrichment of ‘mitotic spindle associated’ genes among genes negatively correlated with DDR1 expression in DLBCL (odds ratio=3.67; $p < 0.0001$; upper panel), and a significant depletion among those positively correlated with DDR1 (odds ratio=0.43; $p = 0.0015$; not shown). I also used a comprehensive mitotic spindle checkpoint signature, comprising 103 genes which included those classified under the GO term ‘GO:0031577’, as well as those reported by Bieche et al., and those identified in an unbiased Pubmed search using the search term ‘mitotic spindle checkpoint’. 90 of these genes were also on the human genome build used to derive the genes sets positively and negatively correlated with DDR1 in DLBCL. I found a significant enrichment of ‘mitotic spindle checkpoint’ genes among genes negatively correlated (odds ratio=7.03; $p < 0.0001$; lower panel), but not among those positively correlated (odds ratio=1.35; $p = 0.245$; not shown), with DDR1 expression.

3.3 DDR1 expression correlates with aneuploidy in primary DLBCL

Given that the loss or reduced expression of mitotic spindle associated genes contributes to aneuploidy, I next explored if DDR1 expression was directly associated with aneuploidy in DLBCL. To do this I first utilized a gene set known as TRI70, which contains 50 genes that display the strongest absolute negative correlation with aneuploidy in trisomic MEFs (Sheltzer, 2013) (Appendix 6A). I found that 25/50 genes from TRI70 aneuploidy signature, were also negatively correlated with DDR1 in DLBCL. This represents significant enrichment ($p < .0001$; odds ratio=7.92; Figure 3.6A, left panel). No genes from TRI70 aneuploidy signature were found among genes positively correlated with DDR1 in DLBCL; this represent a significant depletion ($p = 0.037$; odds ratio=0, Figure 3.6A right panel). Next, I used a second aneuploidy signature, referred to as HET70, which consists of the genes displaying the strongest positive correlation with karyotype heterogeneity in the NCI60 panel of cell lines (Sheltzer, 2013) (Appendix 6B). 17/65 HET70 genes were significantly enriched among genes positively correlated with DDR1 ($p < .0001$; odds ratio=3.74; Figure 3.6B right panel), but not among those negatively correlated ($p = 0.22$; odds ratio=0.51; Figure 3.6B left panel), with DDR1. To further confirm this association, I used a third transcriptional signature derived from multiple aneuploid vs. diploid datasets (Duerrbaum et al., 2014). I found that genes up-regulated in the Core aneuploidy signature were significantly enriched among genes positively correlated with DDR1 ($p = 0.0061$; odds ratio=4.04; Figure 3.6C, left panel), but not among those negatively correlated ($p = 0.15$; odds ratio=0; Figure 3.6C, right panel), with DDR1. Finally, total autosomal aneuploidy was measured by [REDACTED], in a cohort of 48 DLBCL samples available from the TCGA for which both copy

number and RNA-sequencing data were available. For each sample, a copy number “index” value was calculated separately for each chromosomal arm, as the weighted (by length of segment) average of the copy number values for each segment. Total autosomal aneuploidy was then calculated for each sample as the sum across all autosomal arms of the absolute value of two minus index value. Allowance for tumour purity was made using the “percent_tumor_nuclei” item available in the clinical data. A statistically significant positive correlation was found between the aneuploidy index and DDR1 expression in this cohort (Pearson correlation coefficient: $r=0.33$, $p=0.023$; Figure 3.6D). Taken together these data show that DDR1 expression is associated with aneuploidy in primary DLBCL.

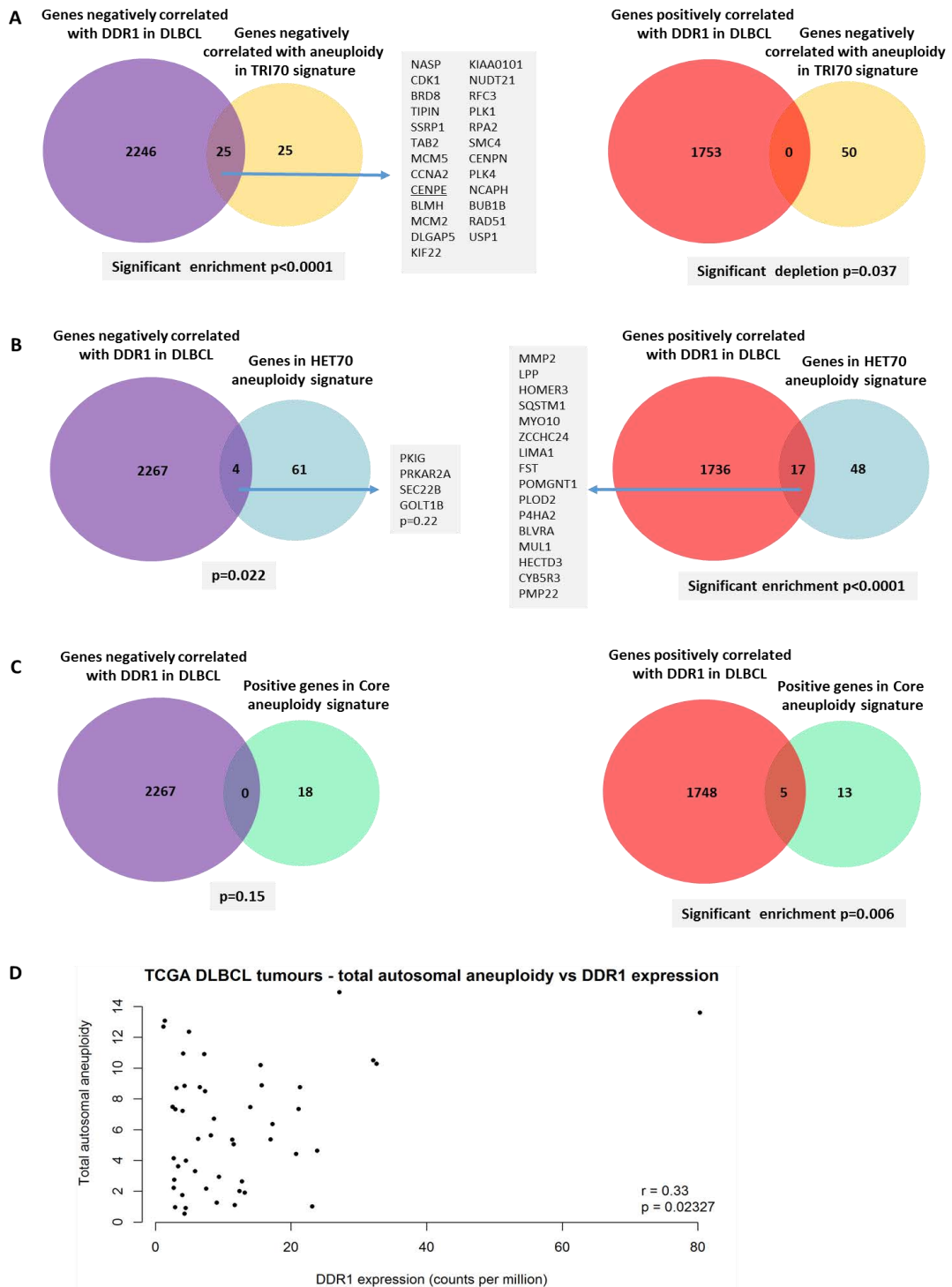


Figure 3.6 DDR1 expression correlates with aneuploidy in primary DLBCL.

A) Genes negatively correlated with DDR1 expression in DLBCL were enriched among genes negatively correlated with aneuploidy in the TRI70 signature ($p < 0.0001$; odds ratio=7.92; left panel), and significantly depleted among genes positively correlated with DDR1 in DLBCL ($p = 0.037$; odds ratio=0; right panel). B) Genes positively correlated with DDR1 in DLBCL were enriched among those displaying the strongest positive correlation with karyotype heterogeneity in the NCI60 panel of cell lines (HET70 signature) ($p < .0001$; odds ratio=3.74; right panel), but not among those negatively correlated ($p = 0.22$; odds ratio=0.51; left panel), with DDR1. C) Genes positively correlated with DDR1 in DLBCL were also enriched among those genes up-regulated in a core aneuploidy signature derived from multiple aneuploid vs. diploid datasets ($p = 0.006$; odds ratio=4.04). D) Total autosomal aneuploidy is positively correlated with DDR1 expression in primary DLBCL (Pearson correlation coefficient: $r = 0.33$, $p = 0.023$).

3.4 Regulation of lymphoma-associated genes by DDR1 in primary and transformed GC B cells

Given that DDR1 is a receptor tyrosine kinase that can engage multiple cell signalling pathway to regulate cellular gene expression, I next focused on the possibility that DDR1 might induce an aneuploidy phenotype through one or more of its transcriptional targets.

3.4.1 Optimization of conditions for the transfection and analysis of DDR1-transfected primary GC B cells

To identify the transcriptional targets of DDR1 relevant to lymphoma development, I used primary GC B cells, the presumed progenitors of DLBCL, isolated from fresh paediatric tonsils. To isolate GC B cells I used a method which was already optimized in our group by [REDACTED] (Vockerodt et al., 2008). With help from [REDACTED], I next optimized the protocol for the transfection of isolated primary human germinal centre B cells with DDR1. First, I transfected freshly isolated GCB cells with 10µg of pIRES2-EGFP with DDR1a insert and with pIRES2-EGFP plasmid as a control (EV), using Human B Cell Nucleofector® Kit (Lonza). Next, I wanted to determine the time point at which I obtained maximum DDR1 expression. I tested different time points post-transfection (8, 10, 12 and 16 hours of incubation). Immunoblotting revealed maximal DDR1 protein expression 8 hours after transfection (Figure 3.7). I then used flow cytometry to study DDR1 expression in transfected cells. My results showed that, by using nucleofection as a method of transfection and 8 hours post-transfection cells incubation, I was able to obtain around 30% of live cells, from which around 14% was successfully transfected. 12 hours of incubation reduced number of live cells by half (Figure 3.8A and 3.8B).

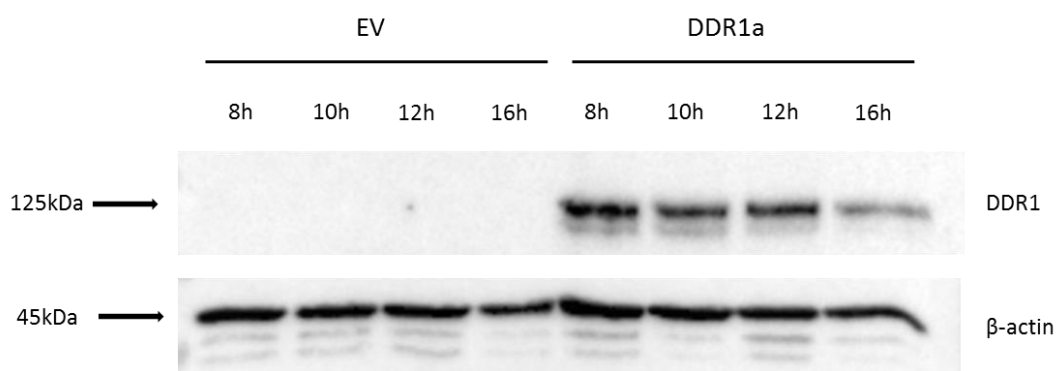


Figure 3.7 Optimization of the time of post-transfection of GCB cells.

GC B cells transfected by nucleofection with DDR1a and EV as a control were harvested 8, 10, 12 and 16 hours after transfection. Immunoblotting showed the DDR1 expression at 8 hours. β -actin confirmed equal loading of the samples. Data shown is representative of two independent experiments from two different donors.

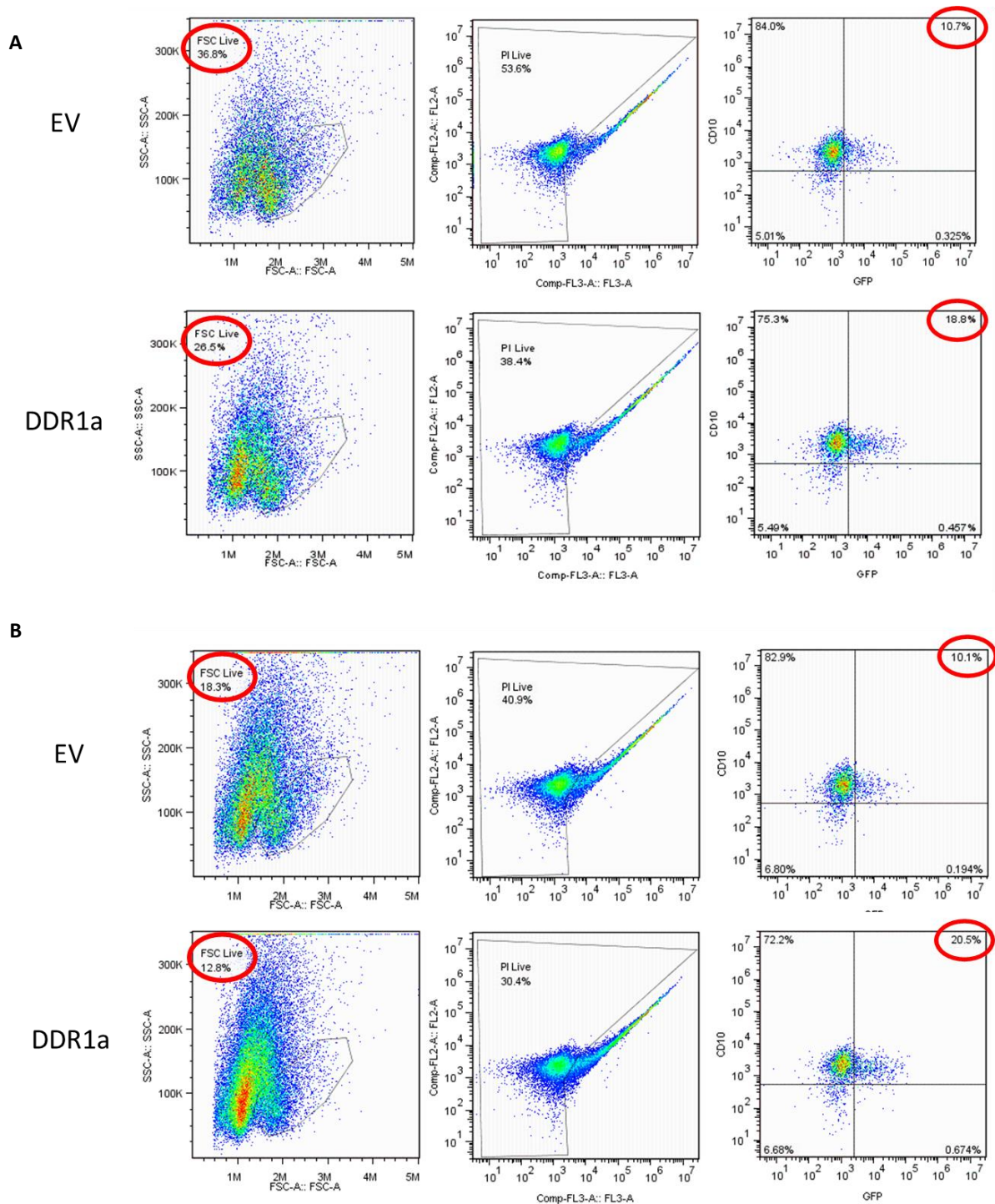


Figure 3.8 Optimization of the method of GC B cells transfection.

GC B cells transfected by nucleofection with DDR1a (bottom panels) and EV (top panels) as a control. 8 and 12h after transfection cells were tested by flow cytometry, based on inserted GFP marker. A) The results revealed that after 8 hours, around 30% of cells survives the process of transfection (36.8% for EV and 26.5% for DDR1; left panels, red circle), from which 10.7% for EV and 18.8% for DDR1 (CD10⁺GFP⁺; right panels, red circle), were successfully transfected with pIRES2-EGFP plasmid with DDR1a insert or without, as a control (EV - empty vector). B) After 12 hours of incubation the number of life cells were reduced by half: 18.3% for EV and 12.8% for DDR1 (left panels, red circle), when compared to 8 hours time point. Data shown are representative from two independent experiments.

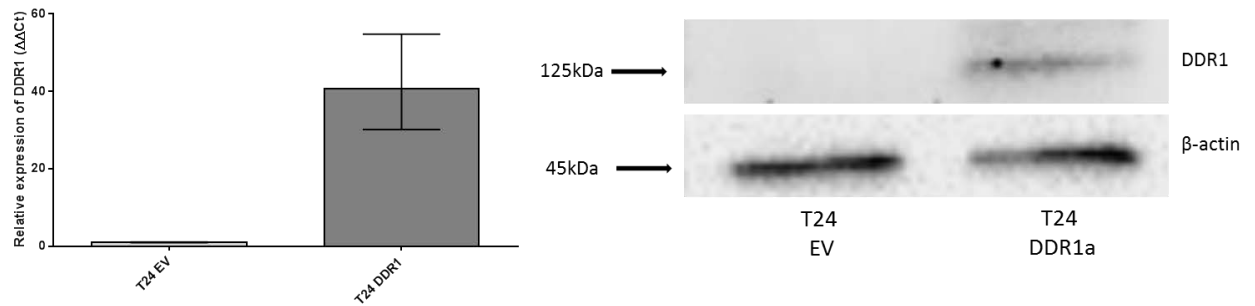
3.4.2 Optimization of collagen stimulation of DDR1 transfected GC B cells

To activate the DDR1 receptor in primary GC B cells, I used soluble collagen type I, which was already shown to activate DDR1 in cell lines (Cader et al., 2013). I stimulated cells transfected either with DDR1 or EV as a control with 100µg/ml collagen (as described by Cader et al., 2013) for 4 and 8 hours. With the help of [REDACTED], I checked cell viability by flow cytometry. This showed higher number of alive transfected cells after 4h of stimulation, in comparison to the other tested time point. These results were confirmed by measurement of RNA on a Bioanalyzer; RNA quality was the highest in tonsil samples after 4h stimulation (Appendix 7).

3.4.3 Identification of DDR1 target genes in primary GC B cells

Having successfully optimized the transfection of GC B cells and their stimulation with collagen, I prepared three replicates of GC B cells (from three different donors), transfected with DDR1 or EV for 8 hours, followed by collagen stimulation for 4 hours (Materials and Methods Sections 2.4.1.1 and 2.5). Cells were then flow sorted as described in Materials and Methods (Sections 2.6).

Due to low number of cells after transfection and sorting, I amplified extracted RNA using NuGEN Ovation® RNA-Seq system V2 kit (NuGEN Ltd) (Figure 3.9B). Having confirmed the expression of DDR1 in transfected GC B cells by qPCR and immunoblotting (Figure 3.9A), I used RNAseq (performed by Edinburgh Genomics, UK), to measure cellular gene expression in DDR1-expressed or control primary GC B cells treated with collagen. After quality checks and successful library preparation, samples were sequenced using Illumina HiSeq 4000 HO 125 base paired end platform.

A**B**

Tonsil	Plasmid transfection	Number of cells sorted	RNA concentration [pg/μl]	RNA concentration [pg/5μl]	RNA integrity (RIN)	cDNA concentration after amplification [μg/20μl]
T20	EV	4.7 x 10 ⁴	2444	12.220	8.2	5.28
	DDR1a	3.8 x 10 ⁴	1585	7.925	7.5	6.14
T22	EV	2.15 x 10 ⁴	303	1.515	8.5	3.74
	DDR1a	1.19 x 10 ⁴	1023	5.115	8.5	6
T24	EV	1.56 x 10 ⁴	114	570	8.5	2.12
	DDR1a	1.6 x 10 ⁴	221	1.105	8.5	0.56

Figure 3.9 Summary of data from GC B cells transfected with DDR1 or EV and harvested for RNAseq analysis.

A) DDR1 expression in transfected cells was confirmed by qRT-PCR (left panel) and immunoblotting (right panel). Data shown (T24) are representative of the three donors used. B) Table presents information from cell sorting, RNA concentration and post-amplified cDNA concentration of GC B cells isolated from three separate donors (T20,T22,T24) and transfected with DDR1a or EV (empty vector). Samples were sent for RNAseq.

RNAseq raw data, received from Edinburgh Genomics, was analyzed by [REDACTED]. Data was aligned to the human hg19 reference sequence using Rsubread aligner. Mapped sequencing reads were assigned to hg19 refGene using featureCounts. Genes with read counts < 2 in more than three samples were removed. The data were normalized using TMM (trimmed mean of M values) method. Differentially expressed cellular genes were identified using edgeR and DDR1 targets were identified by comparing DDR1 transfected versus EV transfected germinal centre B cells with the criteria of absolute fold change > 1.5 and p value < 0.05. I found that compared to control cells, collagen stimulation of DDR1-expressing GC B cells was followed by the up-regulation of 400 unique genes (raw data available on request) and by the down-regulation of 260 unique genes (raw data available on request).

Analysis of the DDR1a sequence in RNAseq confirmed that the ectopically expressed DDR1a was a wild type (performed by [REDACTED]).

3.4.4 Validation of DDR1 target genes.

I next compared the lists of genes generated by RNAseq with the lists of genes correlated with DDR1 in DLBCL (Care et al., 2015) for up-regulated and down-regulated genes separately (gene list generated as described in Results section 3.4.3). I found that genes positively correlated with DDR1 in DLBCL, were significantly enriched in the group of genes up-regulated by collagen treatment of DDR1-expressing GC B cells (45 genes, $p < 0.001$; odds ratio=2.1) (Figure 3.10, top panel). However, I did not observe an enrichment of genes negatively correlated with DDR1 among genes down-regulated by DDR1 in GC B cells. Rather, the overlap was only 6 genes which represent a significant

depletion ($p=0.04$; odds ratio=0.44) (Figure 3.10, bottom panel). Note: downregulated genes include CENPE (see later).

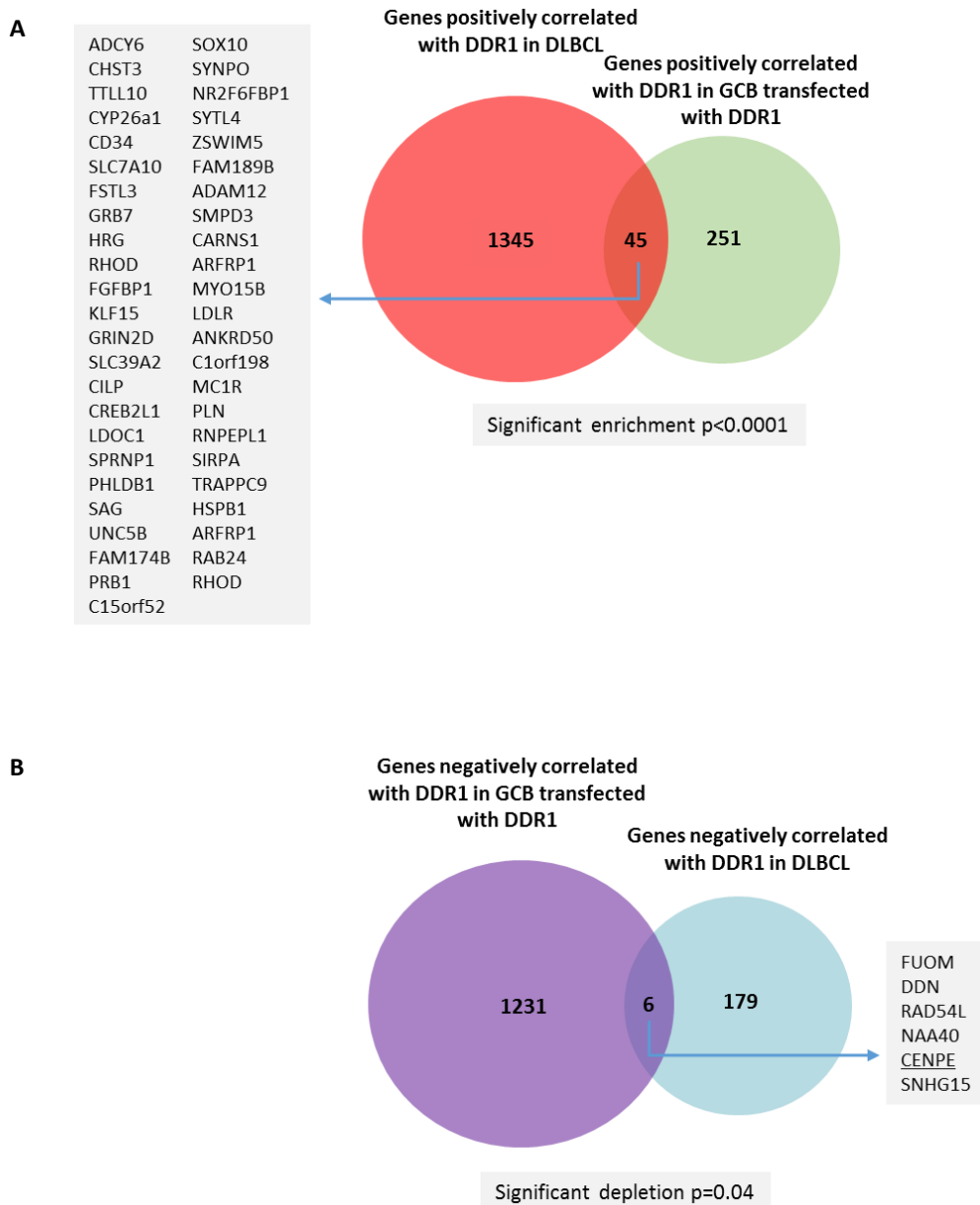


Figure 3.10 Overlap between genes correlated with DDR1 in DLBCL and differentially expressed following collagen stimulation of DDR1-expressing GC B cells.

A) Overlap between genes positively correlated with DDR1 in DLBCL and genes upregulated by DDR1 in GC B cells transfected with DDR1. B) Overlap between genes negatively correlated with DDR1 and downregulated by DDR1 in GC B cells.

To select genes for validation, I then compared the expression of the 45 up-regulated genes found in the RNAseq data from transformed GC B, with two other DLBCL datasets, reported by Morin et al. (Morin et al., 2011) and Brune et al (Brune et al., 2008). This analysis revealed 21 up-regulated genes (including DDR1) that were common between those DLBCL databases and these were selected for further validation. The list of 8 down-regulated genes for validation was also created based on genes in common across the DLBCL databases and according to the strongest down-regulation in GC B cells transfected with DDR1 (based on fold change; Table 3.1).

Table 3.1 DDR1 target genes selected for validation by Fluidigm®48.48 Fast Real Time PCR.

Genes upregulated	Genes downregulated
DDR1	KLHL15
ADAM 12	SRSF4
AGAP3	GCSAM
ANKRD50	LMNB2
ARHGEF19	CENPE
CILP	NAA40
FBP1	RAD54L
GMIP	CCNF
HSPB1	
LDLR	
OBSCN	
PLN	
PSD4	
RAB34	
SIRPA	
SMPD3	
SYDE2	
SYNPO	
SYTL4	
UNC5B	
ZSWIM5	

To validate the differential expression of selected DDR1 targets in collagen-treated DDR1 or empty vector-transfected primary GC B cells I used Fluidigm®48.48 Fast Real Time PCR. This method allows high throughput quantification of target genes combining 48 samples and 48 assays into 2304 parallel PCR reactions. What is more, it requires only 1.25µl of cDNA per sample. Samples were loaded onto a plate in triplicate and analyzed for all 29 target genes and 5 different 'housekeeping' genes at the same time. To choose the correct endogenous control, results from 5 'housekeeping' genes were analyzed. My initial panel of housekeeping genes included GAPDH, β2M, PGK1, TBP, HPRT1. I excluded β2M from the analysis of primary DLBCL samples, as it is known to be mutated in a subset of DLBCL (Challa-Malladi et al., 2011, Morin et al., 2011). Next, I analyzed the 4 remaining housekeeping genes according to the level of expression and variability in replicates of samples. This analysis revealed that PGK1 showed the least variation and the highest consistency in between samples. Results were analyzed as described in Materials and Methods, section 2.9.7, using the delta-delta ($\Delta\Delta$) Ct method in which the relative levels of transcripts are normalized against the PGK1 endogenous control.

DDR1 expression in GC B cells transfected with DDR1 or EV was confirmed (Figure 3.11). 14/28 of the target genes were validated in at least 2 out of 3 replicates (Figure 3.12, left panels), including 7/20 genes up-regulated by DDR1 (Figure 3.12A, left panel) and 7/8 genes down-regulated by DDR1 (Figure 3.12B, left panel). Data for genes not validated are presented in Appendix 8.

I next investigated the expression of these target genes in primary DLBCL, analyzing 44 different DLBCL samples for all 28 target genes (Figure 3.12A and 3.12B, right panels).

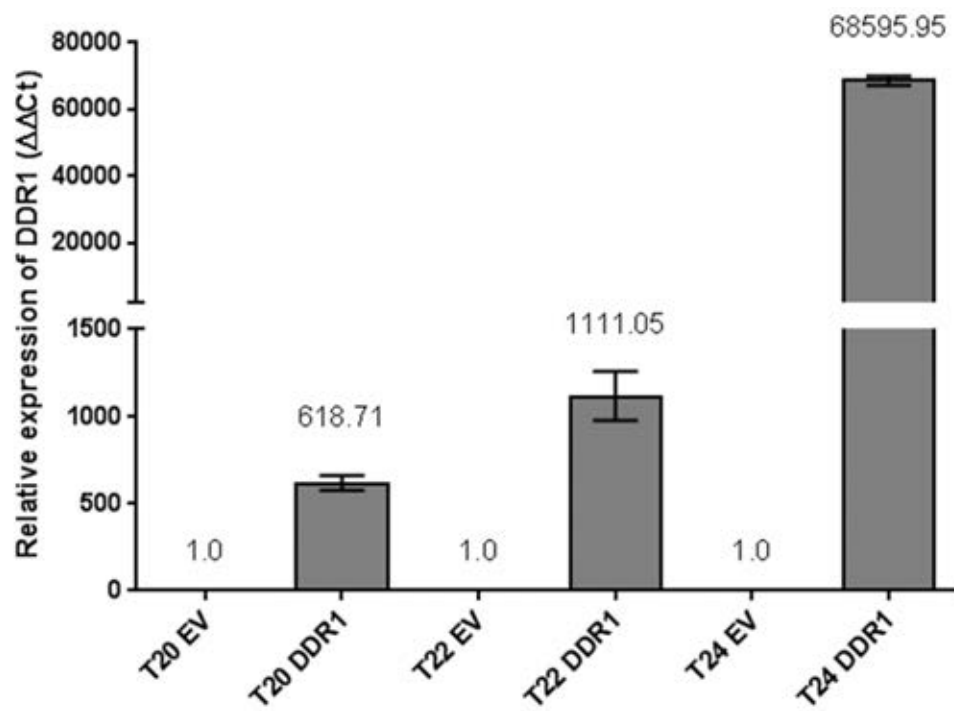
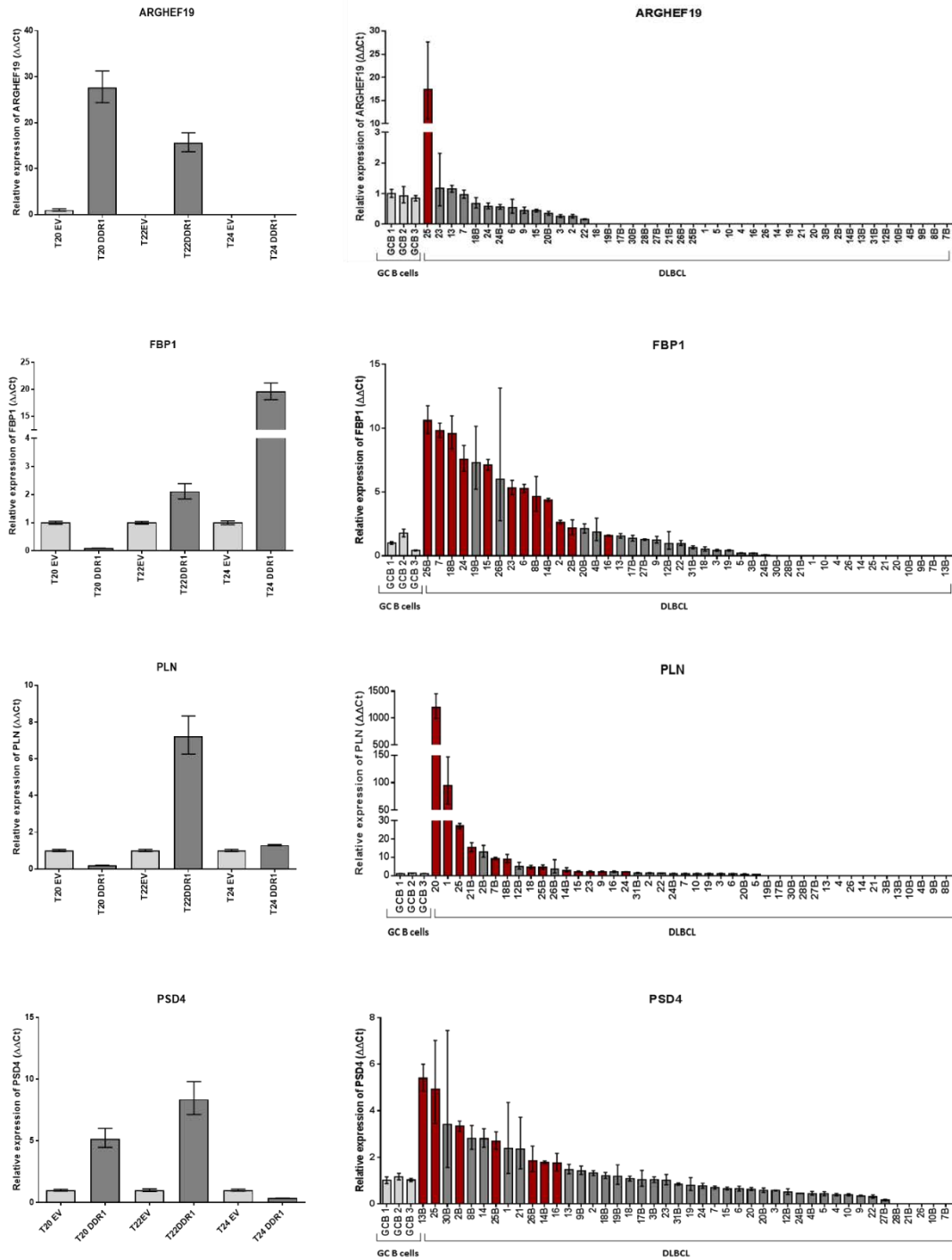


Figure 3.11 DDR1 expression in primary GC B cells transfected with DDR1a and EV as a control, in 3 separate donors.

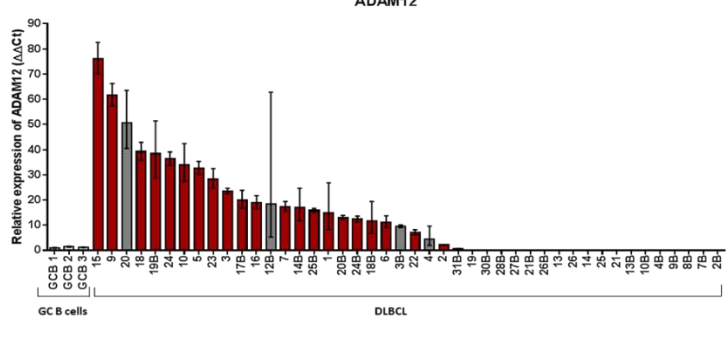
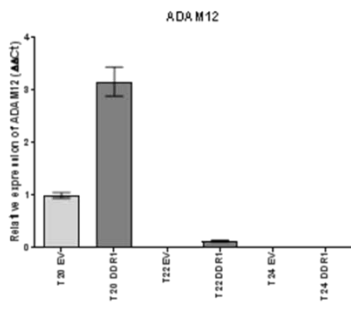
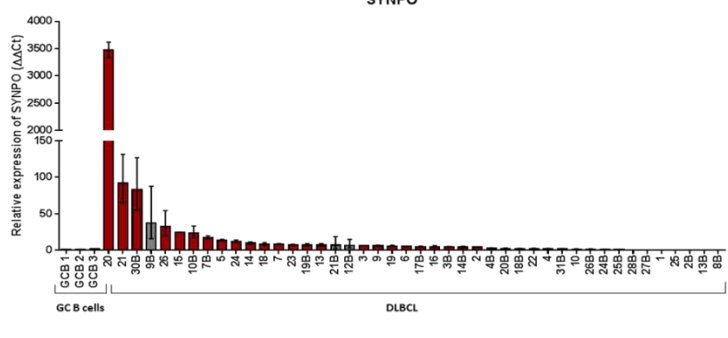
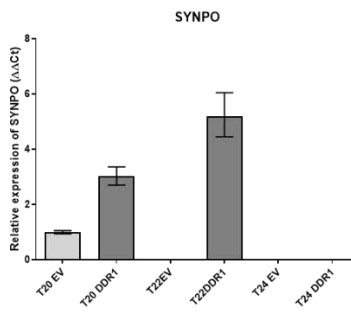
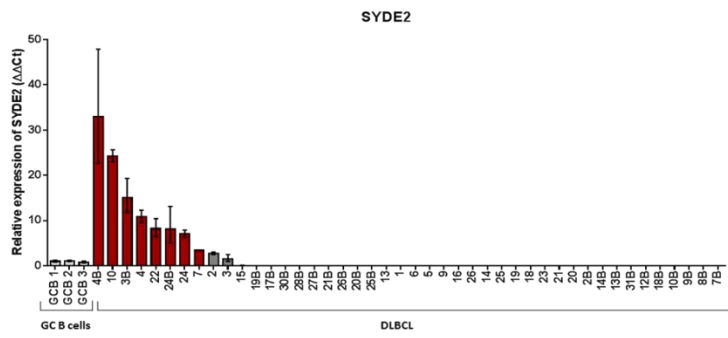
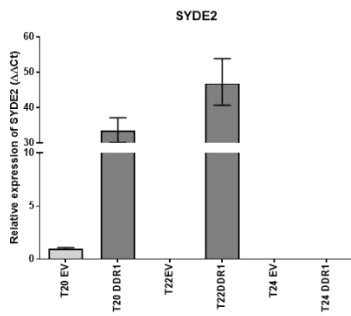
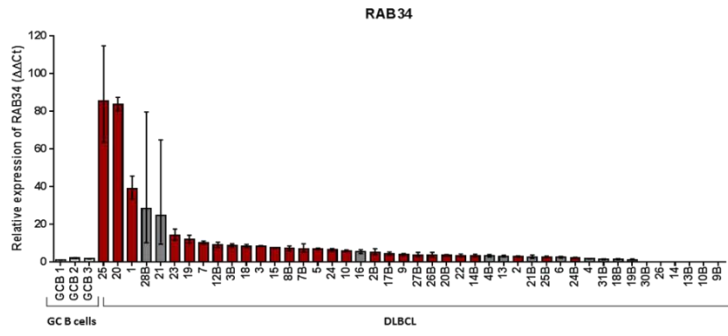
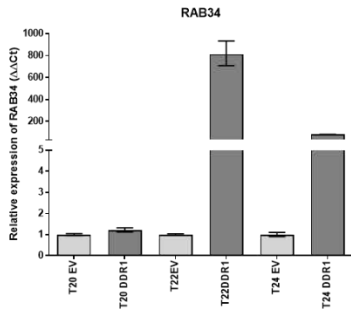
DDR1 expression in transfected cells was confirmed by qRT-PCR. Data shown are from three separate donors.

Figure 3.12A Analysis of the expression of genes up-regulated in collagen-treated DDR1 compared with empty vector-transfected primary GC B cells and in primary DLBCL versus normal GC B cells.

Differential expression of genes upregulated in DDR1a expressing GC B cells, compared to EV-transfected GC B cells is shown in the left panels. Right panels show expression of those genes in DLBCL vs normal GC B. Significant upregulation is marked by red colour.



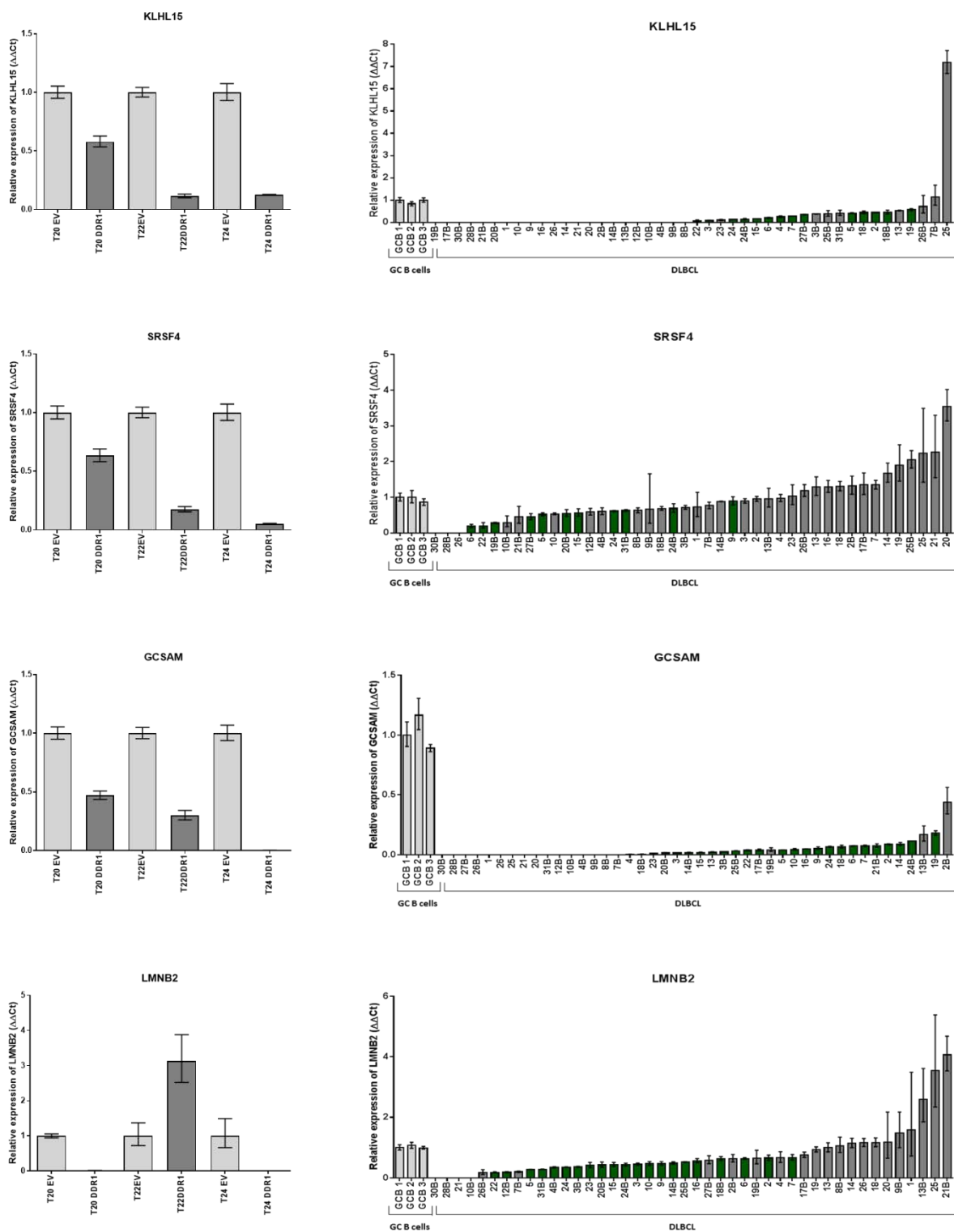
■ Significant up-regulation

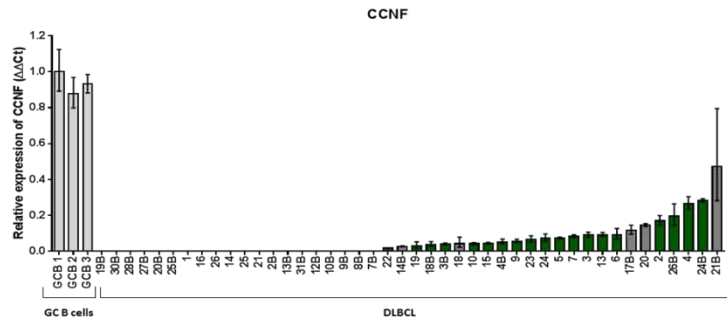
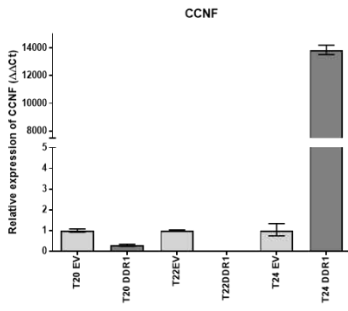
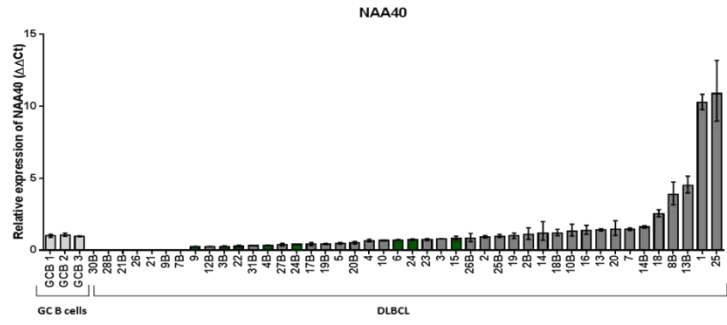
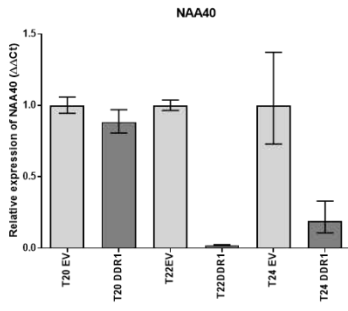


Significant up-regulation

Figure 3.12B Analysis of the expression of genes down-regulated in collagen-treated DDR1 compared with empty vector-transfected primary GC B cells and in primary DLBCL versus normal GC B cells.

Differential expression of genes down regulated in DDR1a expressing GC B cells, compared to EV-transfected GC B cells is shown in the left panels. Right panels show expression of those genes in DLBCL vs normal GC B.





Significant down-regulation

3.4.5 Validation of DDR1 target genes in lymphoma cell lines and the establishment of cell line model for in vivo and in vitro studies

Having shown the differential expression of DDR1 target genes in primary DLBCL, I next wanted to measure the expression of these genes in lymphoma cell lines and establish a cell line model suitable for future testing of DDR1 inhibitors and in vivo studies.

To do this, I first investigated the expression of DDR1 in HL and DLBCL cell lines by qRT-PCR and immunoblotting. As DDR1 expression in HL was already reported by Cader et al (Cader et al., 2013), I enclosed those cell lines in my study as a positive control. This analysis showed that DDR1 mRNA is expressed in all DLBCL cell lines tested but levels were generally not higher than in GC B cells. However, the level of endogenous DDR1 expression in HL cell line is much higher than in GC B cells and tested DLBCL cell lines (Figure 3.13A and B).

I first used BJAB cells, a DDR1-negative GC DLBCL line. I tested the optimum concentration of collagen required for DDR1 activation, based on the results already published by Cader et al. on HL cell lines (Cader et al, 2013). I found that 100µg/ml of soluble collagen type I for 1h was sufficient for the activation of DDR1 (Figure 3.14A).

I then transfected with DDR1a another cell line - DG75 and used L591 cells which endogenously express DDR1. I found that 1h of 100µg/ml collagen induced the robust phosphorylation of DDR1 (Figure 3.14B and C).

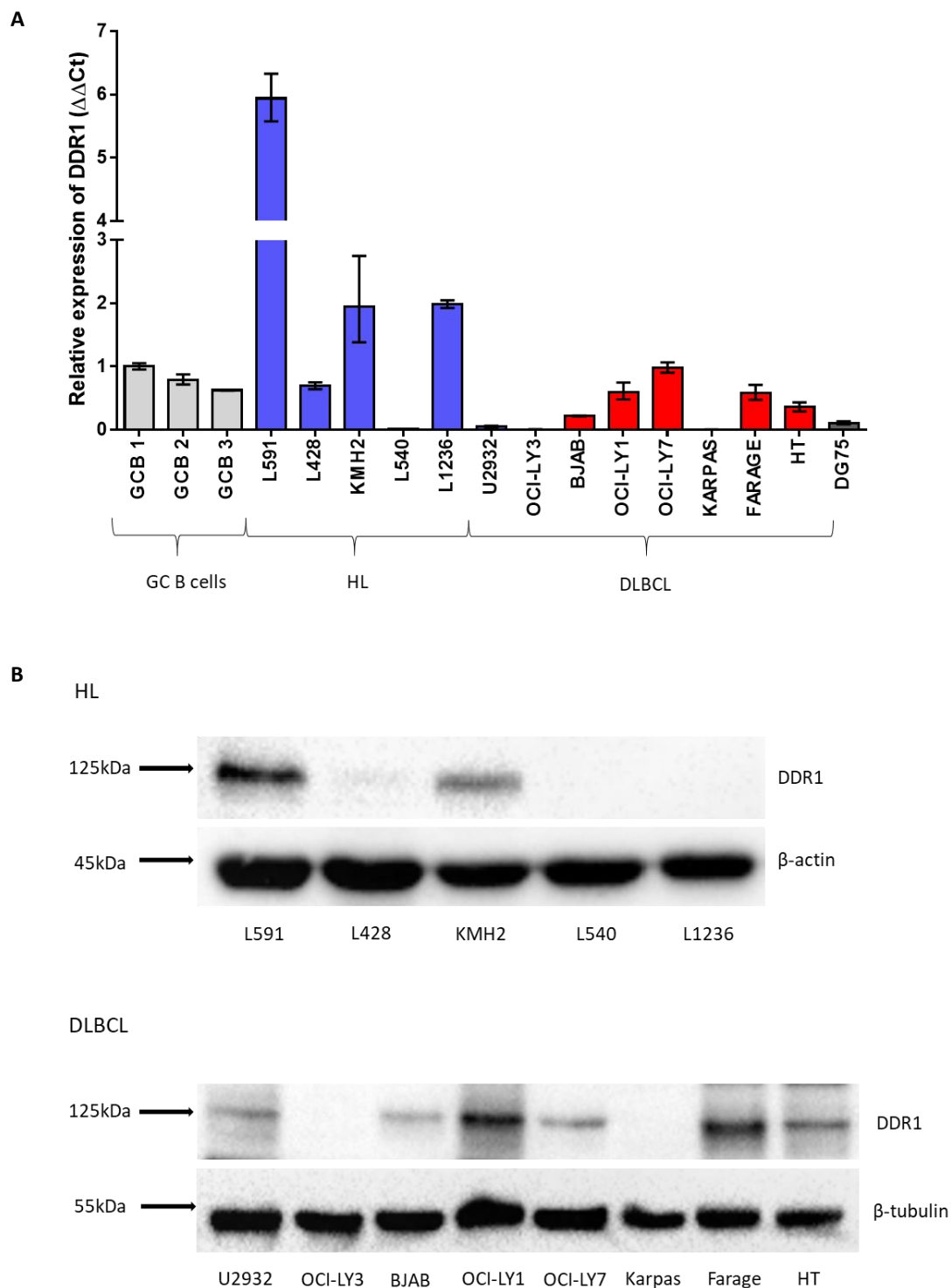


Figure 3.13 DDR1 expression in HL and DLBCL cell lines.

A) DDR1 expression in one HL and 6 DLBCL cell lines was shown by qRT-PCR in comparison to three normal GC B cell samples. B) Immunoblotting results of endogenous expression of DDR1 in HL and DLBCL cell lines, detected by specific DDR1 antibody (MW=125kDa). β -actin in HL and β -tubulin in DLBCL, confirmed equal loading of the sample. Data shown are representative of three independent experiments.

A

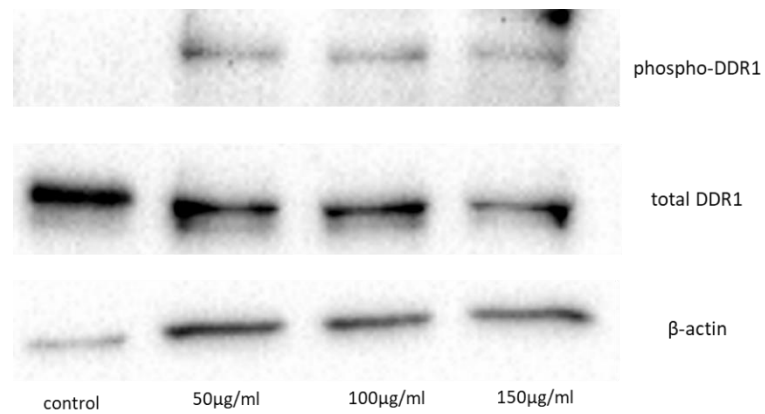


Figure 3.14A Optimisation of the collagen concentration for DDR1 activation.

A) Immunoblotting results of endogenous expression of DDR1 in BJAB cell line transfected with DDR1a and receptor phosphorylation after collagen stimulation, with detectable band after 50, 100 and 150µg/ml collagen concentration, in comparison non-stimulated control (MW=125kDa). β-actin confirmed equal loading of the sample. Data shown are representative of two independent experiments.

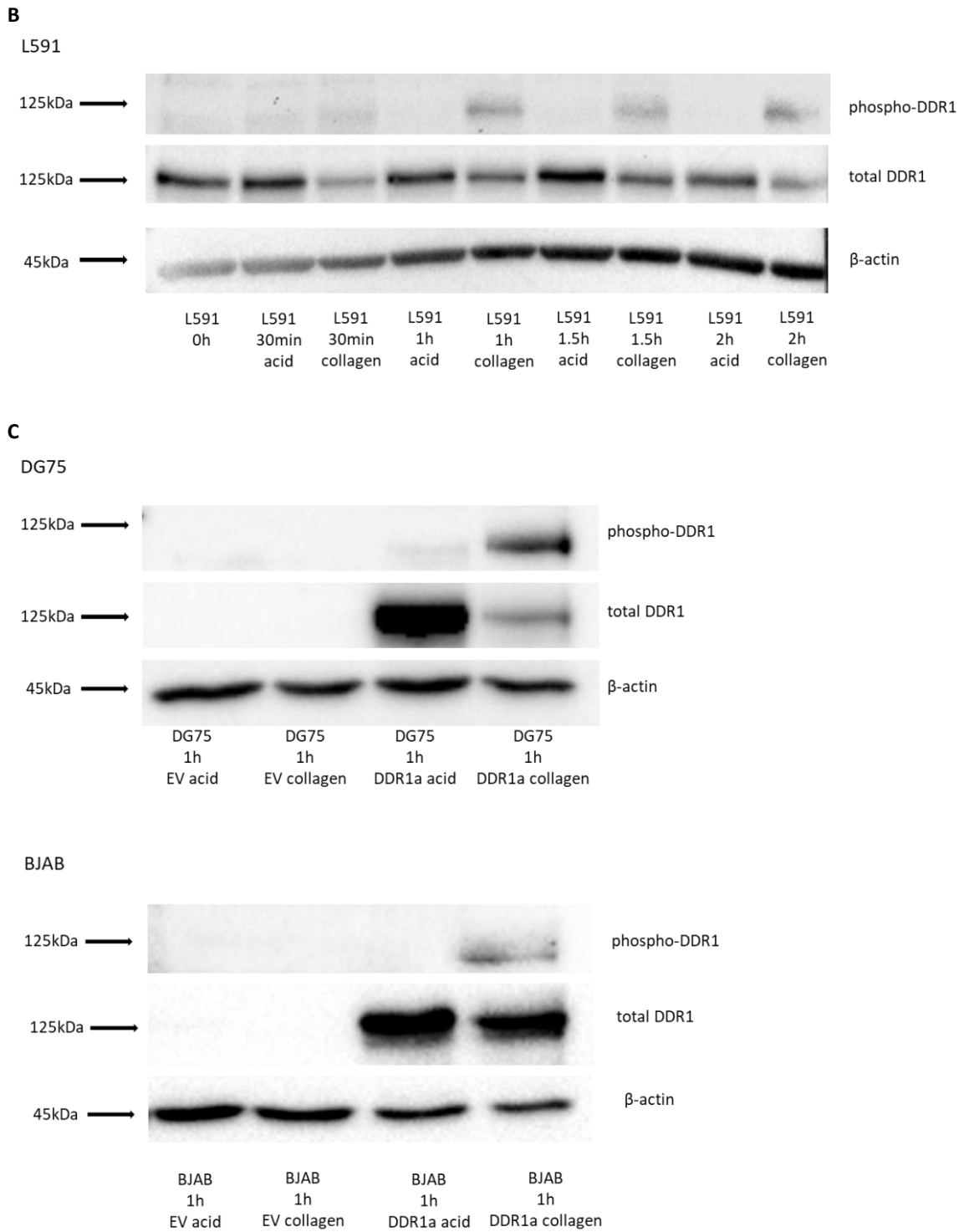


Figure 3.14B and C. DDR1 expression and phosphorylation after collagen stimulation in HL and DLBCL cell lines.

B) Immunoblotting results of endogenous expression of DDR1 in HL L591 cell line and receptor phosphorylation after collagen stimulation, with detectable band after 1 hour in comparison to 0.5% acetic acid control (MW=125kDa). C) Immunoblotting results of DDR1 expression and phosphorylation status after activation of DDR1 by collagen in DG75 and BJAB cell lines transfected with DDR1a and EV as a control. One hour DDR1 stimulation by collagen resulted in its activation. β-actin confirmed equal loading of the sample. Data shown are representative of three independent experiments.

I next analysed the expression of DDR1 target genes in these three collagen-stimulated cell lines, at four time points: 1h, 2h, 4h and 6h, using the Fluidigm®48.48 Fast Real Time PCR for all 21 up-regulated (Figure 3.15C) and 8 down-regulated (Figure 3.16B) DDR1 target genes. The 5 different 'housekeeping genes' (GAPDH, β 2M, PGK1, TBP, and HPRT1) were included. For L591 cells the data was normalized against HPRT1, and for DG75 and BJAB cell lines GAPDH appeared to be the best endogenous control. DDR1 expression was confirmed by qRT-PCR (Figure 3.15A). Genes with the relative expression >1.1 were classified as up-regulated and with relative expression <0.9 as down-regulated, in comparison to EV (for BJAB and DG75) or 0.5% acetic acid (for L591) control which had a normalised value of 1. This analysis revealed differences in the regulation of DDR1 target genes expression between cell lines at different time points. After 1h collagen stimulation, 3 genes: SYTL4, UNC5B and ADAM12, were up-regulated (Figure 3.15B) and 4 genes: CENPE, GCSAM, SRSF4 and KLHL15 were down-regulated in all three lines (Figure 3.16A).

A

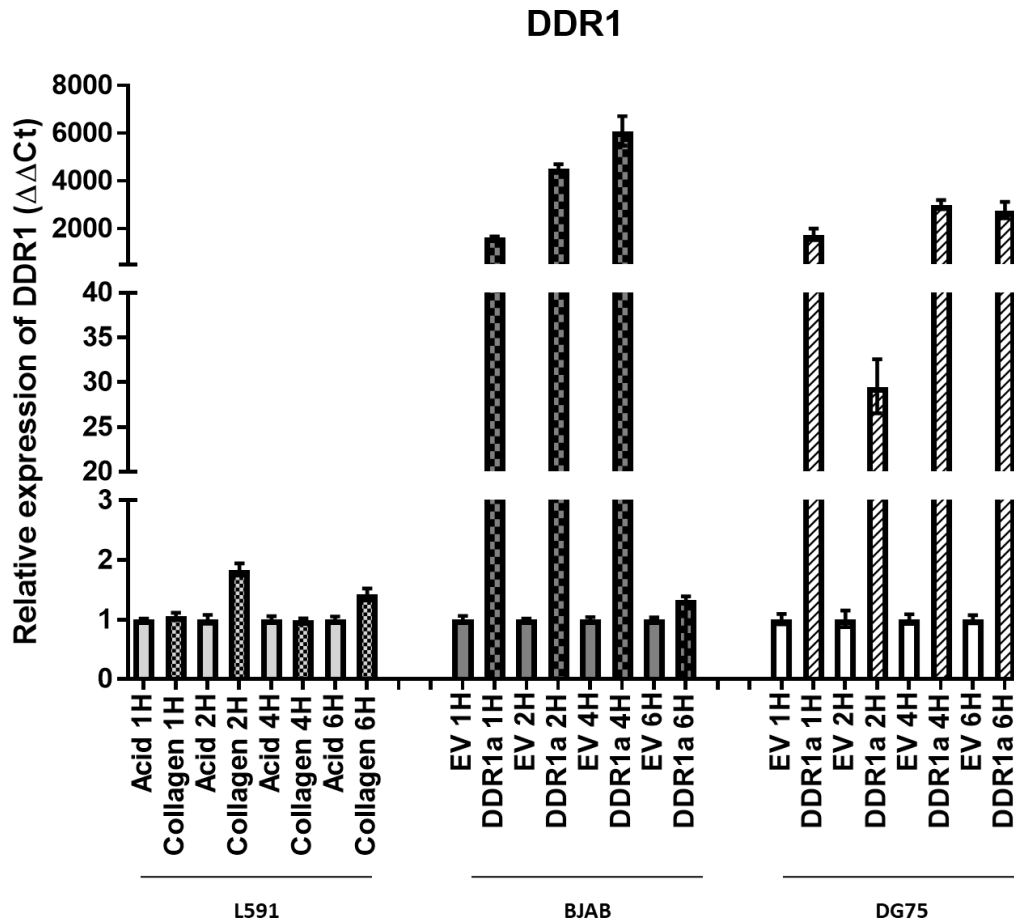


Figure 3.15A DDR1 expression in cell lines treated with collagen.

DDR1 expression in L591, Hodgkin lymphoma cell line – endogenous level of DDR1, and in two DDR1a and EV control transfected cell lines: BJAB, DLBCL cell line and DG75, Burkitt lymphoma cell line, after collagen stimulation for 1, 2, 4 and 6 hours. L591 cells were treated with 0.5% acetic acid as a control.

B

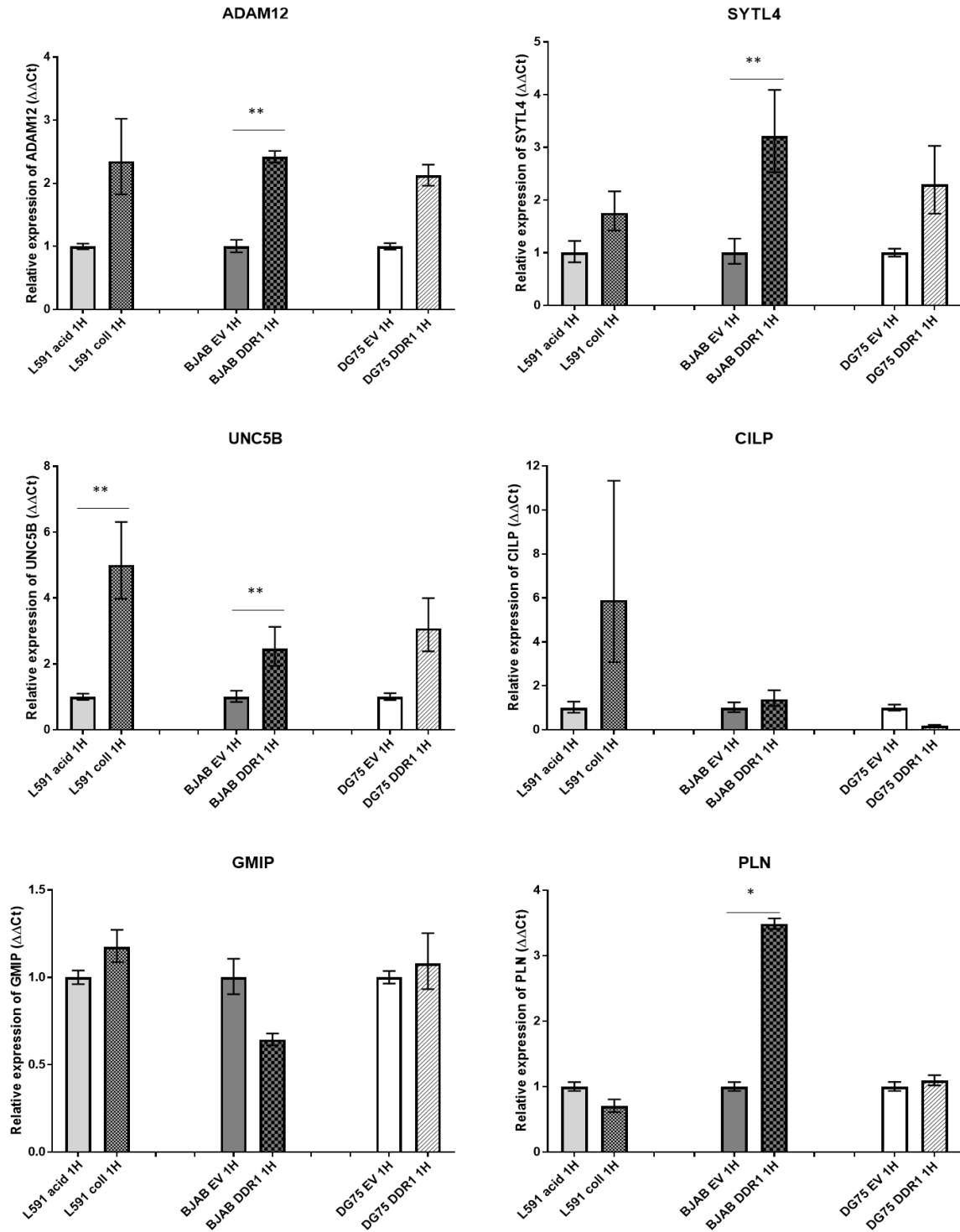
		BJAB	DG75	L591
Up – regulated genes (relative expression >1.1)	1h	PLN SYTL4 UNC5B ADAM12 ARHGEF19 CILP	UNC5B SIRPA SYNPO SYTL4 ADAM12 PSD4	ZSWIM5 CILP UNC5B SIRPA ADAM12 OBSCN SYTL4 AGAP3 GMIP
	2h	CILP ARHGEF19 OBSCN PLN	-	ZSWIM5 UNC5B GMIP PSD4 AGAP3 LDLR SMPD3 SYDE2 SYNPO PLN SYTL4 ARHGEF19 OBSCN ANKRD50 SIRPA
	4h	CILP ZSWIM5 PLN ADAM12 SYTL4	SIRPA SYNPO FBP1	HSPB1
	6h	-	SYNPO PSD4 SMPD3 GMIP FBP1 AGAP3 OBSCN ARGHEF19 LDLR SYDE2 ADAM12 RAB34 ANKRD50	SYNPO HSPB1 PSD4 AGAP3 GMIP SYDE2 ANKRD50 LDLR

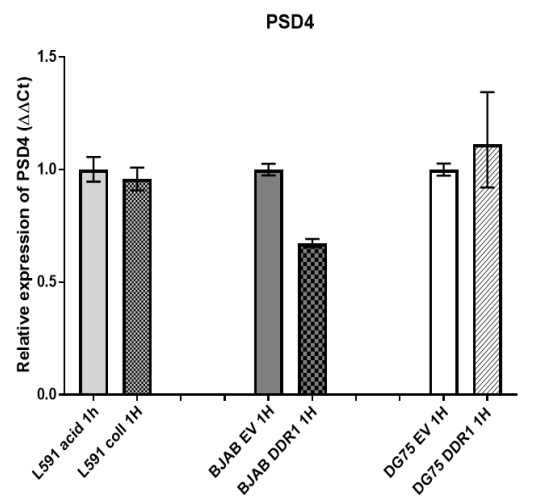
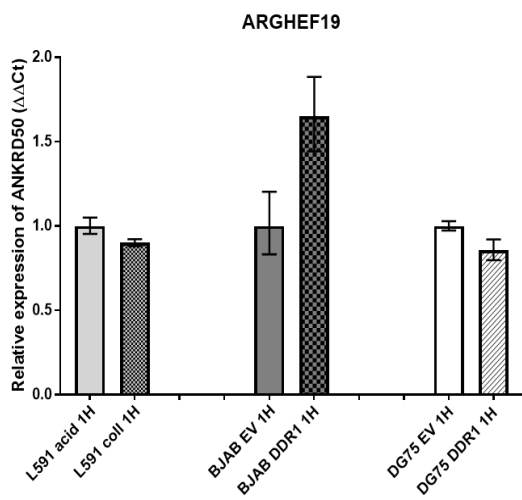
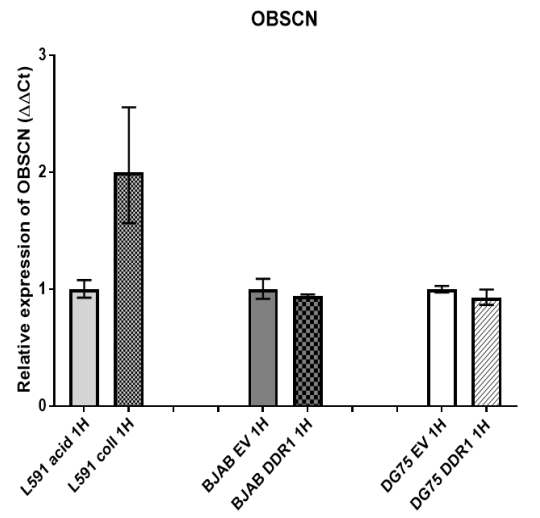
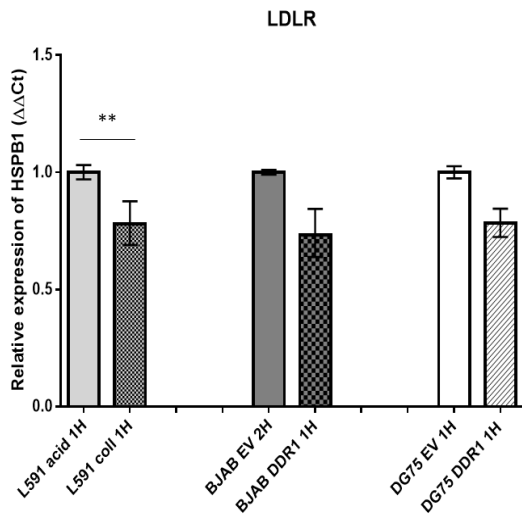
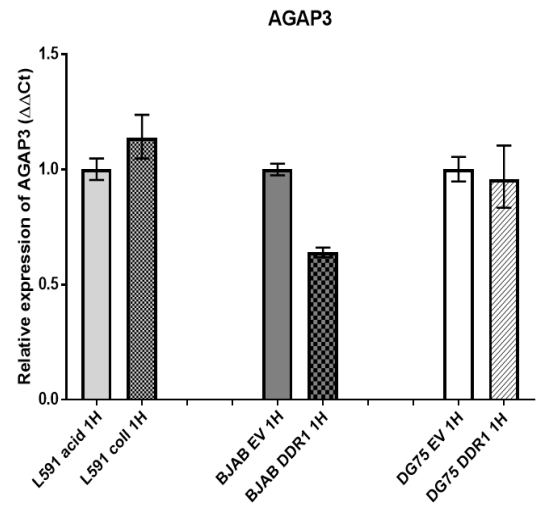
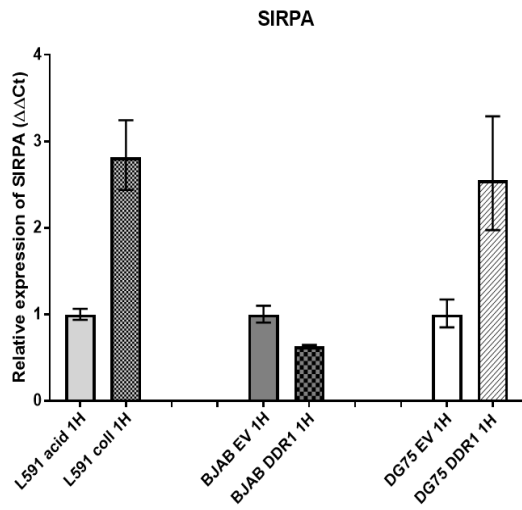
Figure 3.15B Summary of the analysis of the expression of genes up-regulated in collagen-treated cell lines.

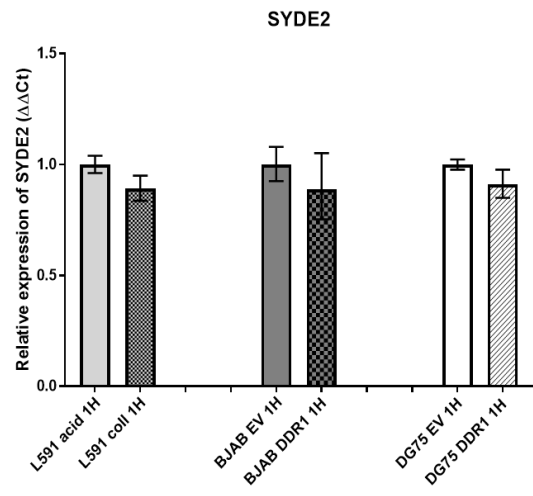
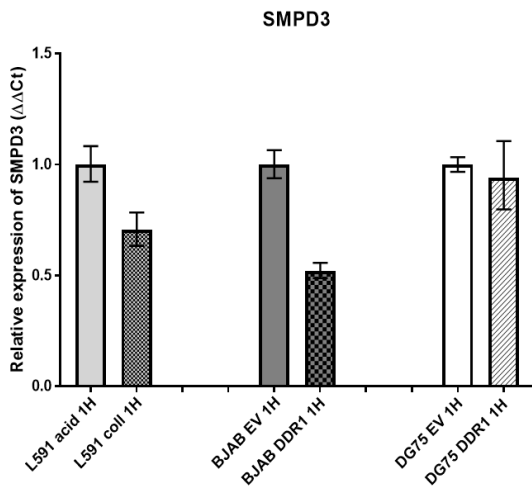
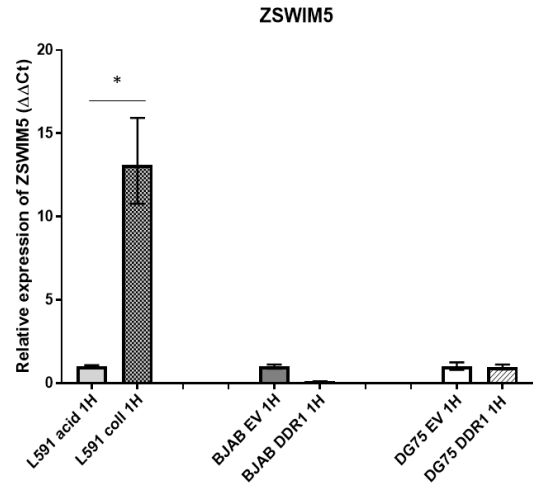
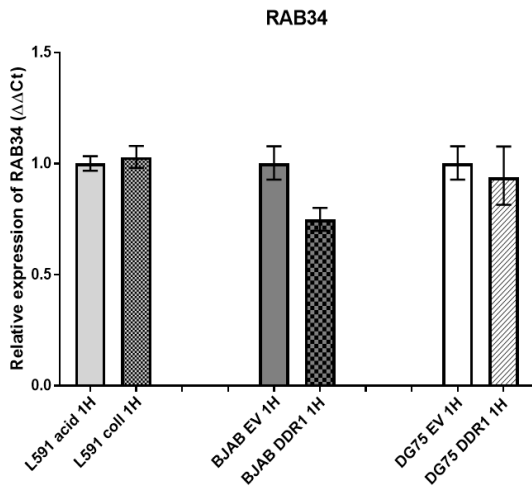
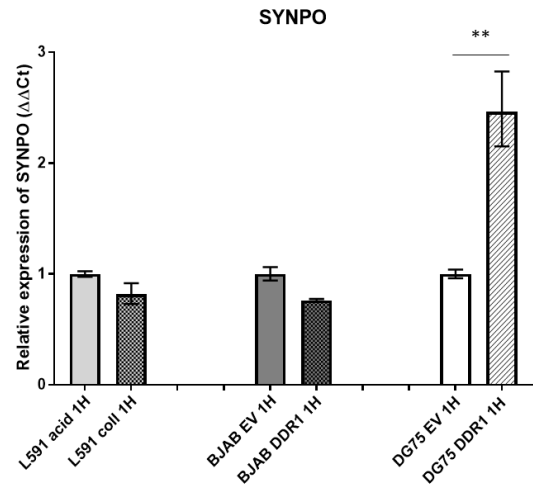
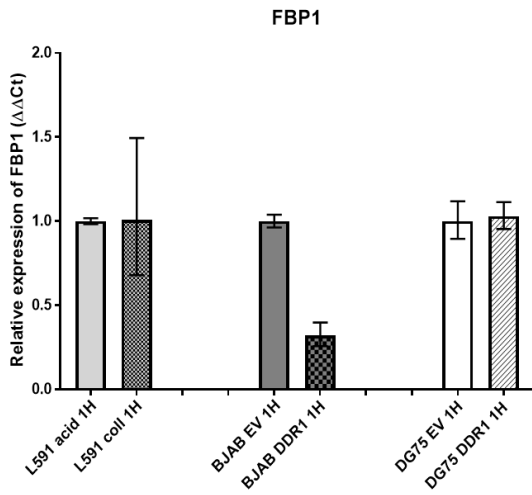
Table presents the summary of genes upregulated (relative expression calculated using $\Delta\Delta C_t$ method >1.1) in all three tested cell lines after 1, 2, 4 and 6 hours of collagen stimulation. After 1 hour of collagen treatment the highest number of genes were up regulated in all 3 cell lines (3 genes), when compared with other time points.

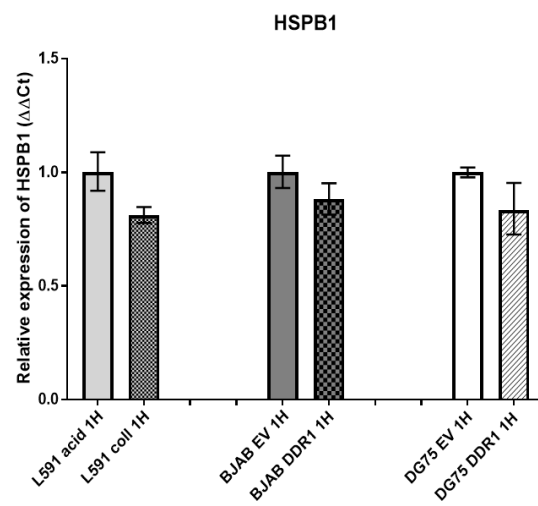
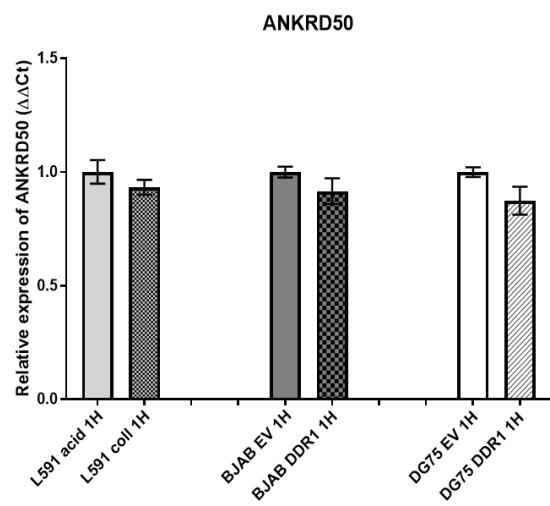
Figure 3.15C Analysis of the expression of genes up-regulated in collagen-treated cell lines.

Differential expression of genes up-regulated in DDR1-expressing cell lines, after 1h collagen stimulation. L591, Hodgkin lymphoma cell line, endogenously expressing DDR1 and two DDR1a and EV control, transfected cell lines: BJAB, DLBCL cell lines and DG75, Burkitt lymphoma cell line. L591 cells were treated with 0.5% acetic acid as a control.









A

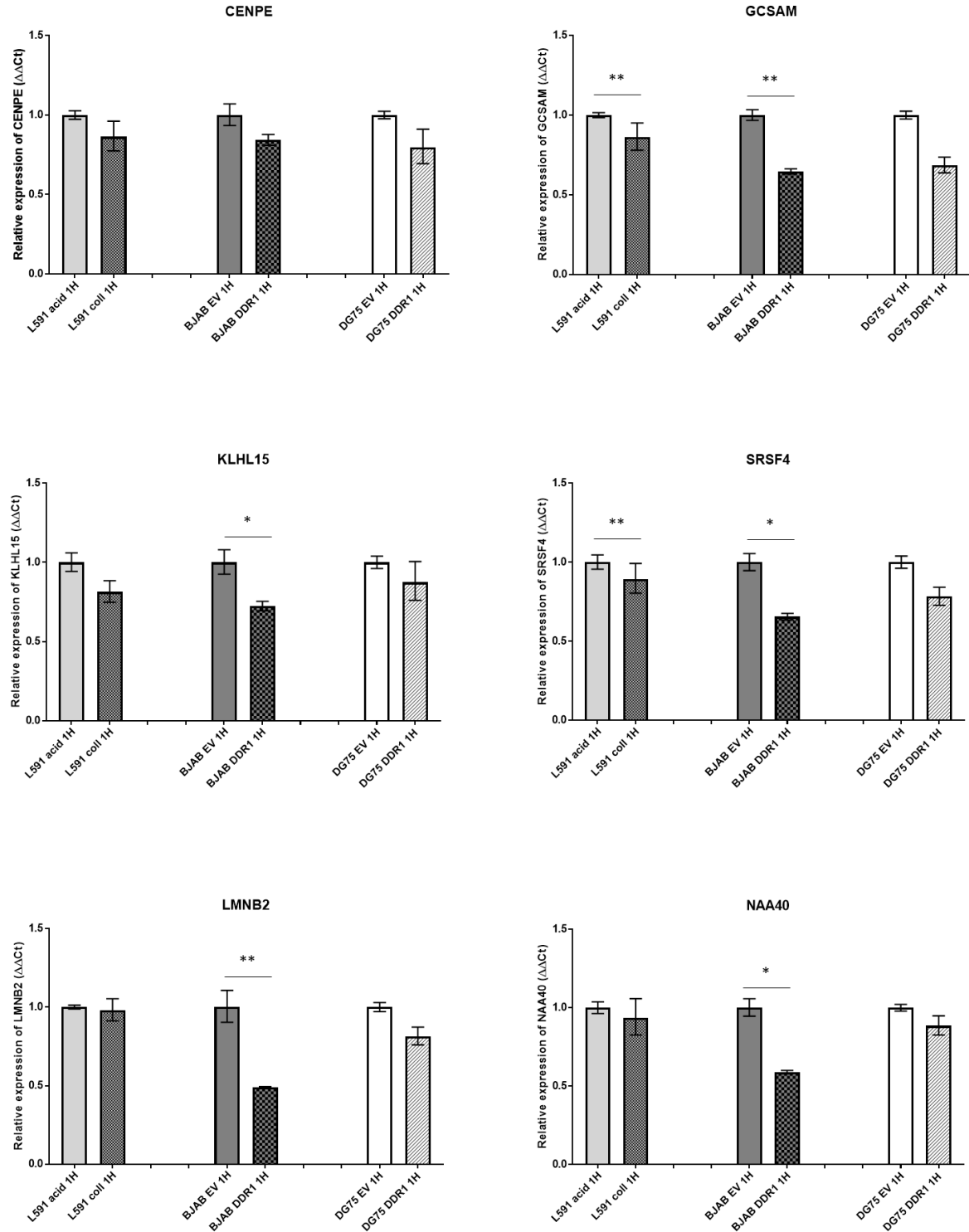
		BJAB	DG75	L591
Down – regulated genes (relative expression <0.9)	1h	LMNB2 NAA40 CCNF GCSAM SRSF4 KLHL15 CENPE RAD54L	KLHL15 SRSF4 GCSAM LMNB2 CENPE NAA40 RAD54L CCNF	KLHL15 SRSF4 GCSAM CENPE
	2h	NAA40 LMNB2 CCNF SRSF4 GCSAM KLHL15 RAD54L	RAD54L GCSAM SRSF4 NAA40 LMNB2 CCNF CENPE KLHL15	CENPE
	4h	SRSF4 GCASM RAD54L LMNB2 CCNF NAA40	KLHL15 SRSF4 GCSAM NAA40 RAD54L CCNF LMNB2	SRSF4 RAD54L
	6h	RAD54L GCSAM SRSF4 NAA40 LMNB2 CCNF CENPE KLHL15	-	-

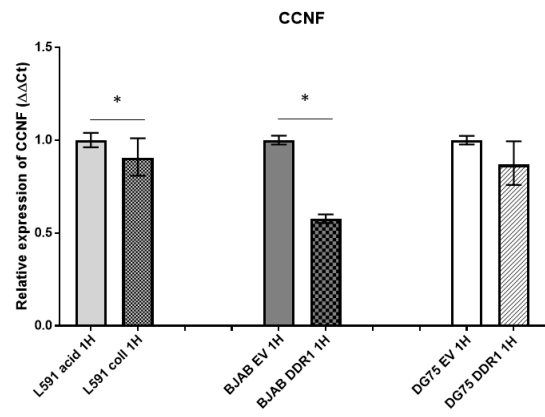
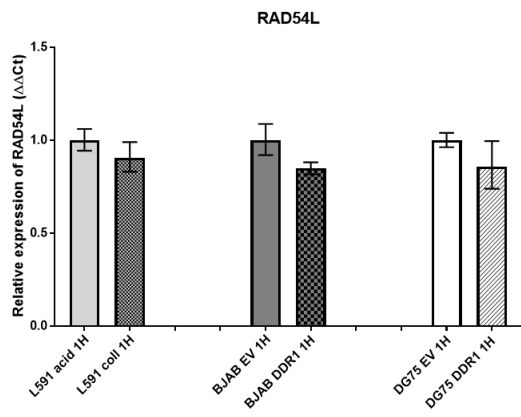
Figure 3.16A Summary of the analysis of the expression of genes down-regulated in collagen-treated cell lines.

Table presents the summary of genes down regulated (relative expression calculated using $\Delta\Delta\text{Ct}$ method <0.95) in all three tested cell lines after 1, 2, 4 and 6 hours of collagen stimulation. After 1 hour of collagen treatment there were found 2 genes down regulated in all 3 cell lines: GCSAM and CENPE, when compared with other time points.

Figure 3.16B Analysis of the expression of genes down-regulated in collagen-treated cell lines.

Differential expression of genes down regulated in DDR1 expressing cell lines after 1h collagen stimulation. L591, Hodgkin lymphoma cell line, endogenously expressing DDR1 and two DDR1a and EV control, transfected cell lines: BJAB, DLBCL cell lines and DG75, Burkitt lymphoma cell line. L591 cells were treated with 0.5% acetic acid as a control. Students T test where * indicates $p \leq 0.05$, ** $p \leq 0.01$ and *** $p \leq 0.001$.



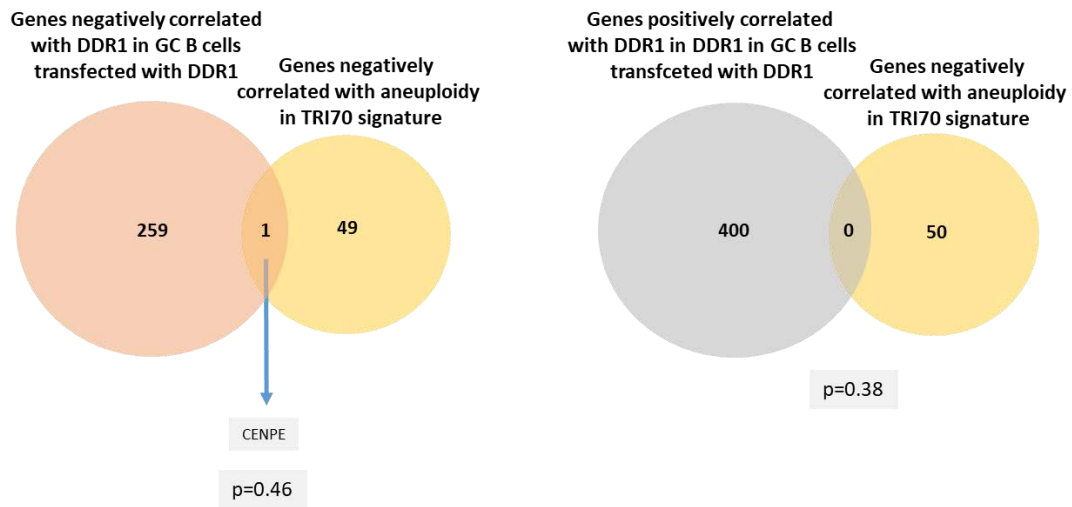


3.5 CENPE is down-regulated in primary DLBCL and transformed GC B cells

I decided to focus on CENPE which was down-regulated by collagen treatment of DDR1-expressing GC B cells, compared to control cells (fold change=-2.31; p value=0.032). Moreover, as I showed earlier during the re-analysis of existing datasets, CENPE was among the genes negatively correlated with DDR1 in DLBCL and down-regulated by DDR1 in DLBCL cell lines. CENPE was also of particular interest because it has been shown to be essential for the proper functioning of the mitotic checkpoint signal at individual kinetochores and because reduced expression of CENPE has been shown to induce aneuploidy (Bennett et al., 2015).

I next analysed the two previously described aneuploidy signatures, TRI70 and HET70 (described in Section 3.2.3). CENPE was the only DDR1-regulated gene among genes that were negatively correlated with the TRI70 aneuploidy signature (p=0.46, odds ratio=2.05, Figure 3.17A, left panel). From the second analysed aneuploidy signature HET70, 1/70 genes was negatively correlated with DDR1 (p=0.7, odd ratio=0.14, Figure 3.17B left panel) and 3/70 HET70 genes were positively correlated with DDR1 in transformed GC B cells (p=0.057, odd ratio=2.93, Figure 3.17B right panel), however CENPE was not among them.

A



B

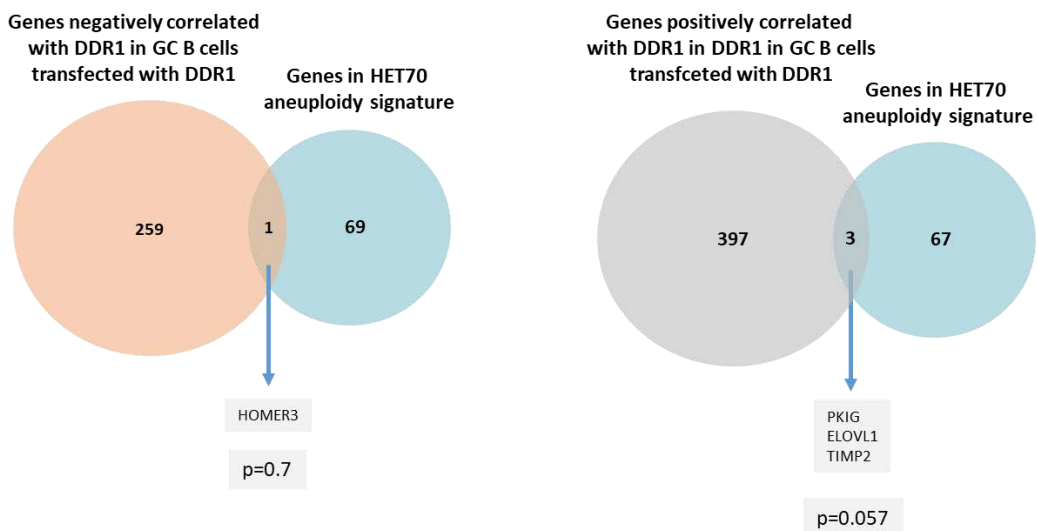


Figure 3.17 DDR1 expression correlates with aneuploidy in primary DDR1- expressing GC B cells.

A) CENPE was the only gene among genes negatively correlated with TRI70 aneuploidy signature that was negatively correlated with DDR1 in transfected GC B cells ($p=0.46$, odds ratio=2.05, left panel). No genes in common were found in between genes positively correlated with DDR1 in transfected GC B cells and genes negatively correlated with TRI70 aneuploidy signature ($p=0.38$; odds ratio=0; right panel). B) Genes positively correlated with DDR1 in transfected GC B cells, were enriched among those displaying the strongest positive correlation with karyotype heterogeneity in the NCI60 panel of cell lines (HET70 signature) ($p<.0001$; odds ratio=3.74; right panel), but not among those negatively correlated ($p=0.7$; odds ratio=0.14; left panel), with DDR1. This was not statistically significant.

With help of bioinformatician, [REDACTED], the existing DLBCL database published by Morin et al. was re-analyzed (Morin et al., 2011), to investigate the expression of CENPE in primary cases of ABC and GCB type of DLBCL. The re-analysis of this dataset showed statistically significantly lower expression of CENPE in GCB type, in comparison to ABC type of DLBCL ($p=0.04712$). Those results also suggest the possible down-regulation of CENPE in both types of DLBCL, when compared with 4 normal GC B cells [(Beguelin et al., 2013); GSE45982], however this change appeared to be not statistically significant (ABC vs normal $p=0.09851$; GCB vs normal $p=0.07006$) (Figure 3.18A).

I used qRT-PCR to investigate CENPE mRNA expression in collagen treated DDR1-expressing GC B cells and a cohort of 44 primary DLBCL. This analysis showed that CENPE expression was decreased in three out of four transformed GC B cells (Figure 3.18B), and in 42/44 tested primary DLBCL, compared to primary GC B cells (Figure 3.18C).

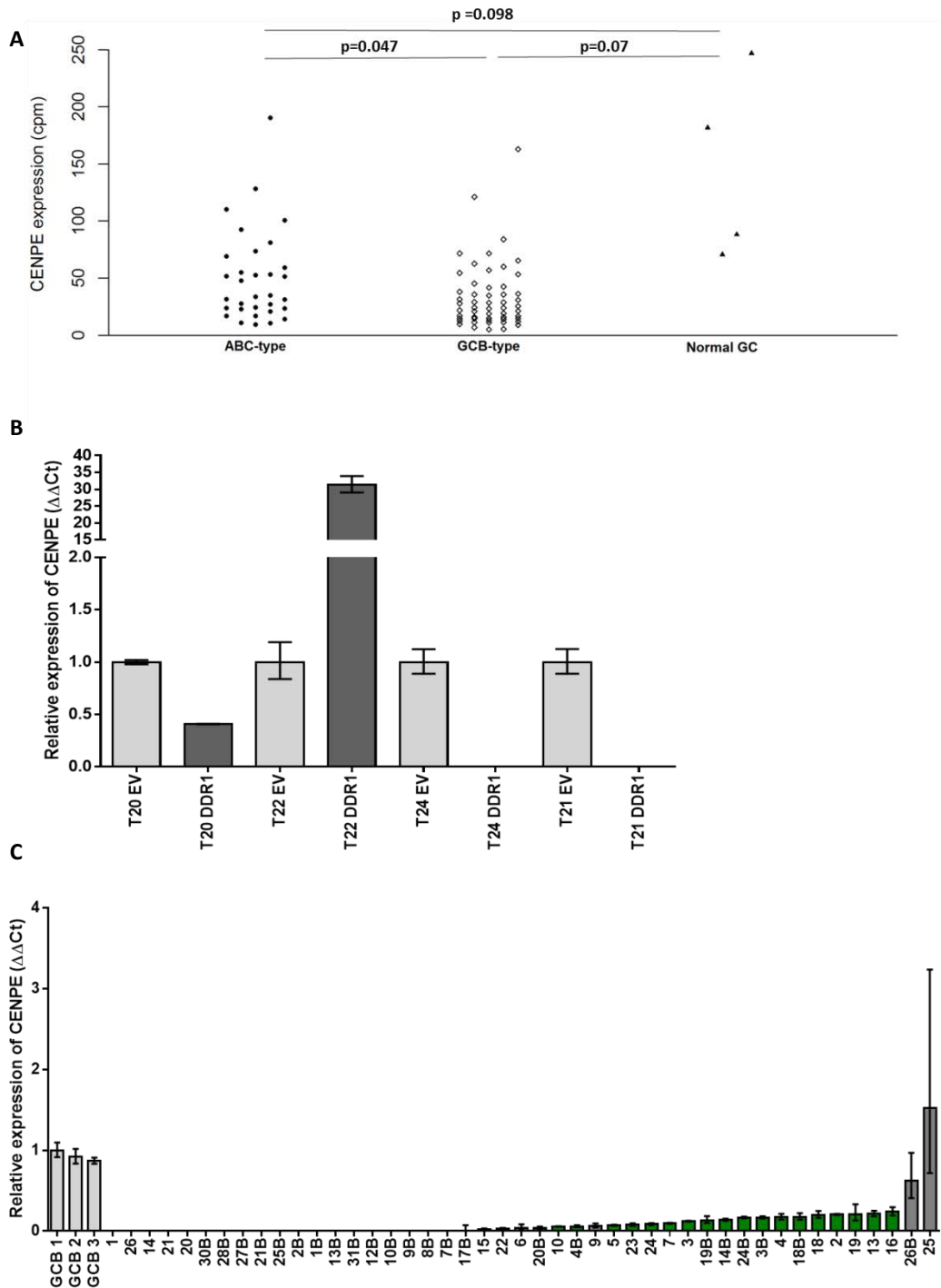


Figure 3.18 Down - regulation of CENPE in diffuse large B cell lymphoma.

A) Morin reveals that CENPE expression is significantly down-regulated in GCB type, when compared to ABC type DLBCL ($p=0.04712$) B) qRT-PCR confirms the down-regulation of CENPE mRNA in three out of four collagen treated DDR1a-expressing GC B cells, in comparison to EV control and C) in a separate cohort of DLBCL, when compared with normal GC B cells. Students T test, where green bars indicates significant down-regulation of CENPE.

Having shown downregulation of CENPE mRNA in primary DDR1-expressing GC B cells and DLBCL by qRT-PCR, I next performed immunohistochemistry on primary DLBCL sections. To do this, I first validated the specificity of CENPE antibody. I tested several lymphoma cell lines for their endogenous expression of CENPE using qRT-PCR and immunoblotting (Figure 3.19A and B). I next validated an antibody against CENPE, by knocking down CENPE gene expression in the DG75 cell line, which had detectable levels of endogenous CENPE expression at both the RNA and protein level. To do this, I transfected DG75 cells with CENPE Silencer® Select Validated siRNA (Ambion) (Materials and Methods section 1.4.1.2) and checked protein expression by immunoblotting. Results showed specific detection of CENPE in DG75 transfected with Negative Control Silencer® Select #1 siRNA, in comparison to cells transfected with CENPE Silencer®, which did not show CENPE expression (Figure 3.19C).

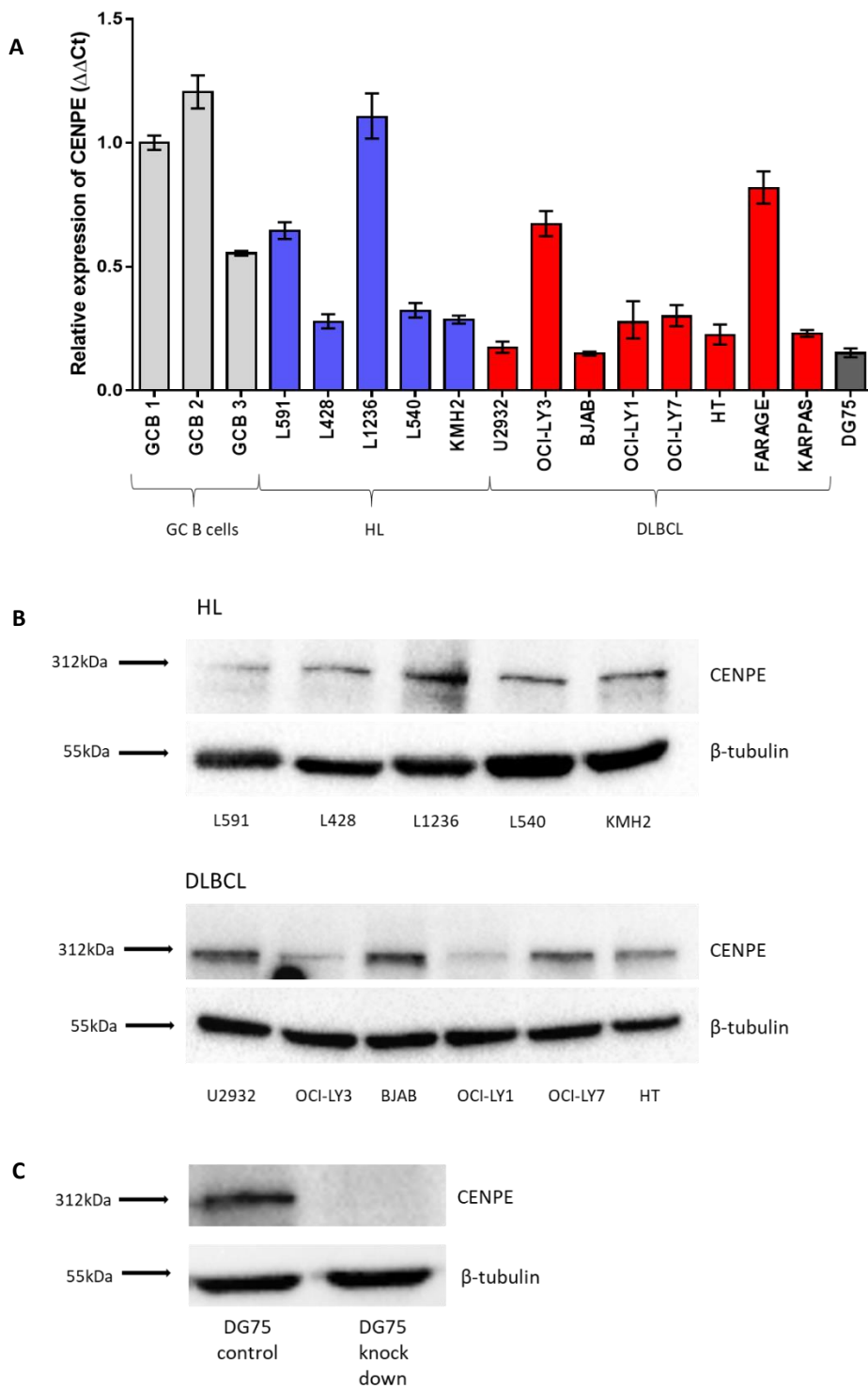


Figure 3.19 CENPE expression in lymphoma cell lines.

A) qRT-PCR shows CENPE mRNA level in one HL, 6 DLBCL and DG75 cell lines in comparison to three normal GC B cells samples.

B) Immunoblotting results of endogenous of CENPE on chosen HL, DLBCL and DG75 cell lines, detected by specific CENPE antibody (Sigma, MW=312kDa). β tubulin confirmed equal loading of the sample. C) Validation of CENPE antibody (Sigma) on DG75 with knocked down CENPE gene expression, by transfection with CENPE Silencer® Select Validated siRNA (Ambion), in comparison to DG75 transfected with Negative Control Silencer® Select #1 siRNA as a control. Data shown are representative of three independent experiments.

Having confirmed the specificity of the CENPE antibody, I next investigated CENPE expression by immunohistochemistry in 33 primary DLBCL that were previously tested for DDR1. Stained for CENPE expression sections were analysed and scored by [REDACTED]. For CENPE, samples were recorded as negative, positive (if tumour cells were stained with the same intensity as in control germinal centre B cells and non-malignant cells in the tumour microenvironment), or weakly positive (if tumour cells were stained less intensely than control germinal centre B cells and non-malignant cells in the tumour microenvironment). This analysis revealed that 20/33 cases showed downregulation of CENPE in tumour cells (compared to non-malignant cells). 13/33 cases showed expression of CENPE that was equivalent to non-malignant cells (Figure 3.20). I also performed co-staining on two DLBCL cases positive for DDR1. This confirmed the down-regulation of CENPE (red) in tumour cells (positive for CD20; yellow) expressing DDR1 (green) (Figure 3.21A), in comparison to tonsil control (Figure 3.21B). I conclude that DDR1 downregulates CENPE expression and that CENPE is downregulated in primary DLBCL.

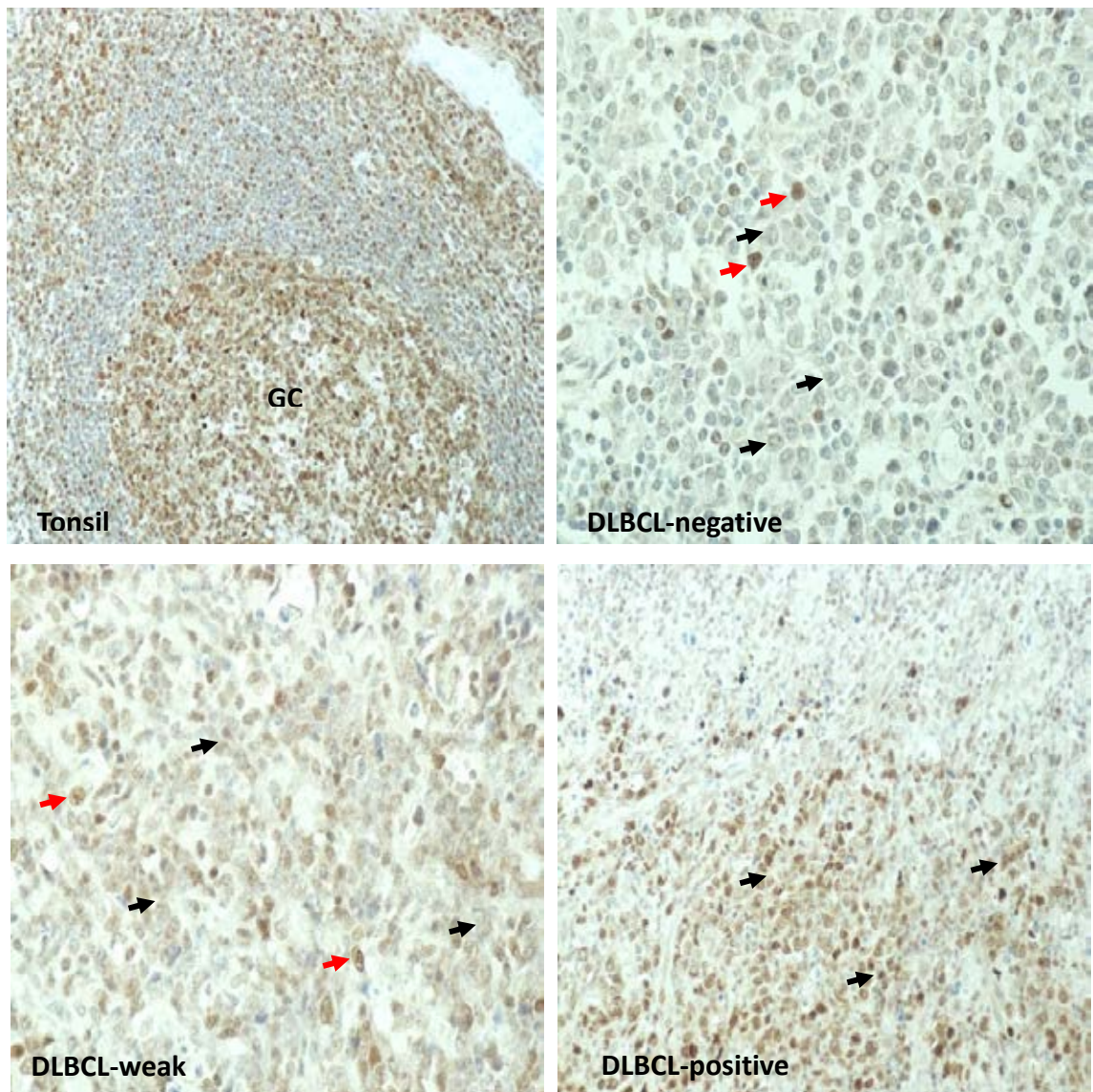


Figure 3.20 CENPE is down-regulated in primary DLBCL.

Representative examples of staining for CENPE. Top left panel shows strong expression of CENPE in a normal germinal centre (GC) of tonsil. Remaining panels show examples of CENPE staining including cases in which CENPE was not detected in tumour cells (top right), a case with weak expression in tumour cells (bottom left), and a case showing strong staining (bottom right). Black arrows show tumour cells. Red arrows indicate non-malignant cells that are positive for CENPE.

A

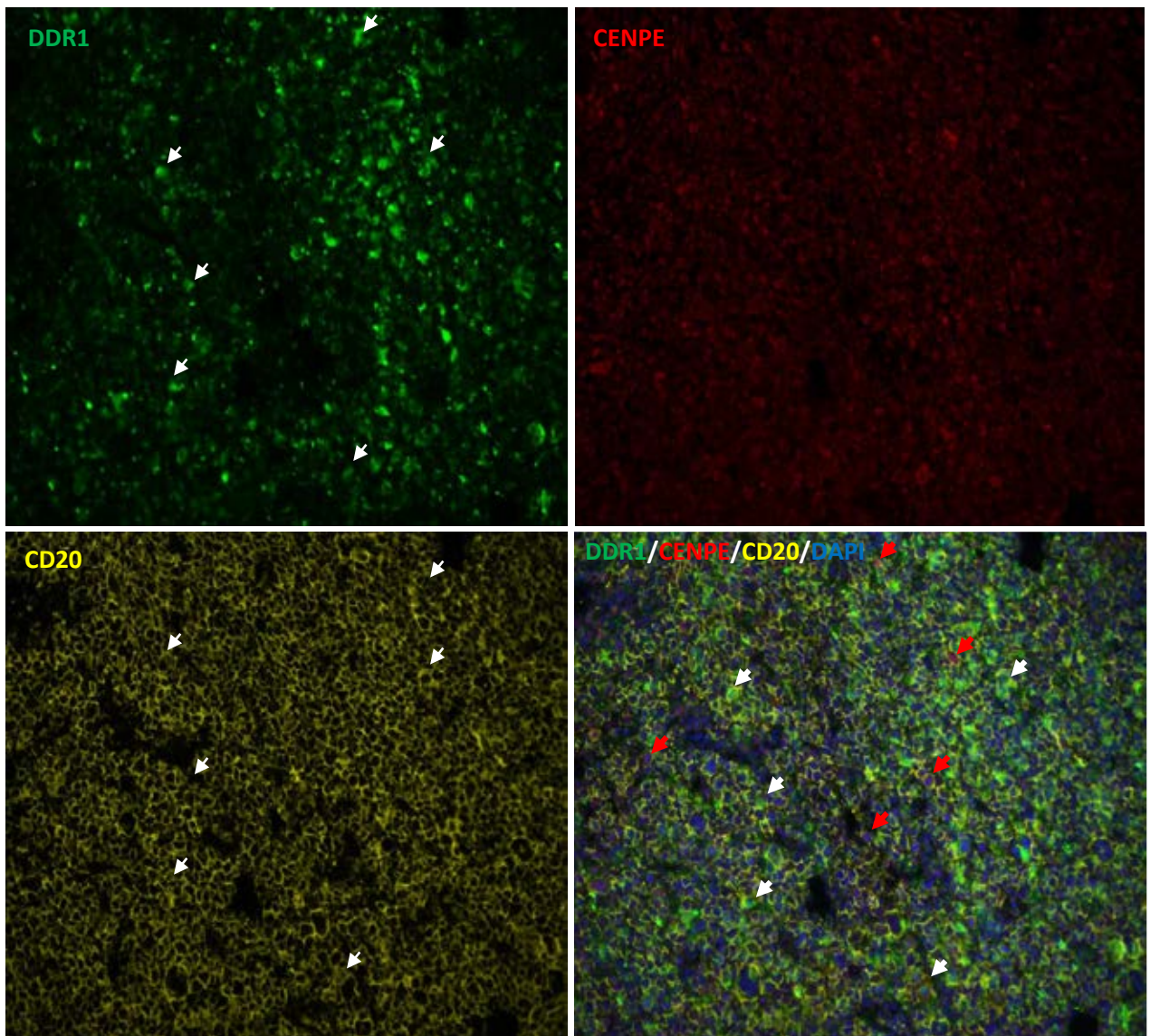


Figure 3.21A CENPE and DDR1 expression in DLBCL - multiplex immunofluorescence. Multiplex immunofluorescence confirmed that CENPE (red) expression is decreased in DDR1-expressing (green) tumour cells (CD20 positive, yellow) in comparison to tonsil control (Figure 3.22 B). Top left panel present DDR1 expression on tumour cells (white arrows), right top panel represent downregulation of CENPE in tumour cells and middle panel shows CD20 positive tumour cells (white arrows pointing at DDR1 positive tumour cells). Bottom panel present co-expression of DDR1, CENPE and CD20 on DLBCL case. Tumour cells expressing DDR1 and with decreased level of CENPE are marked by white arrows. Red arrows pointing at tumour cells negative for DDR1 and with high expression of CENPE.

B

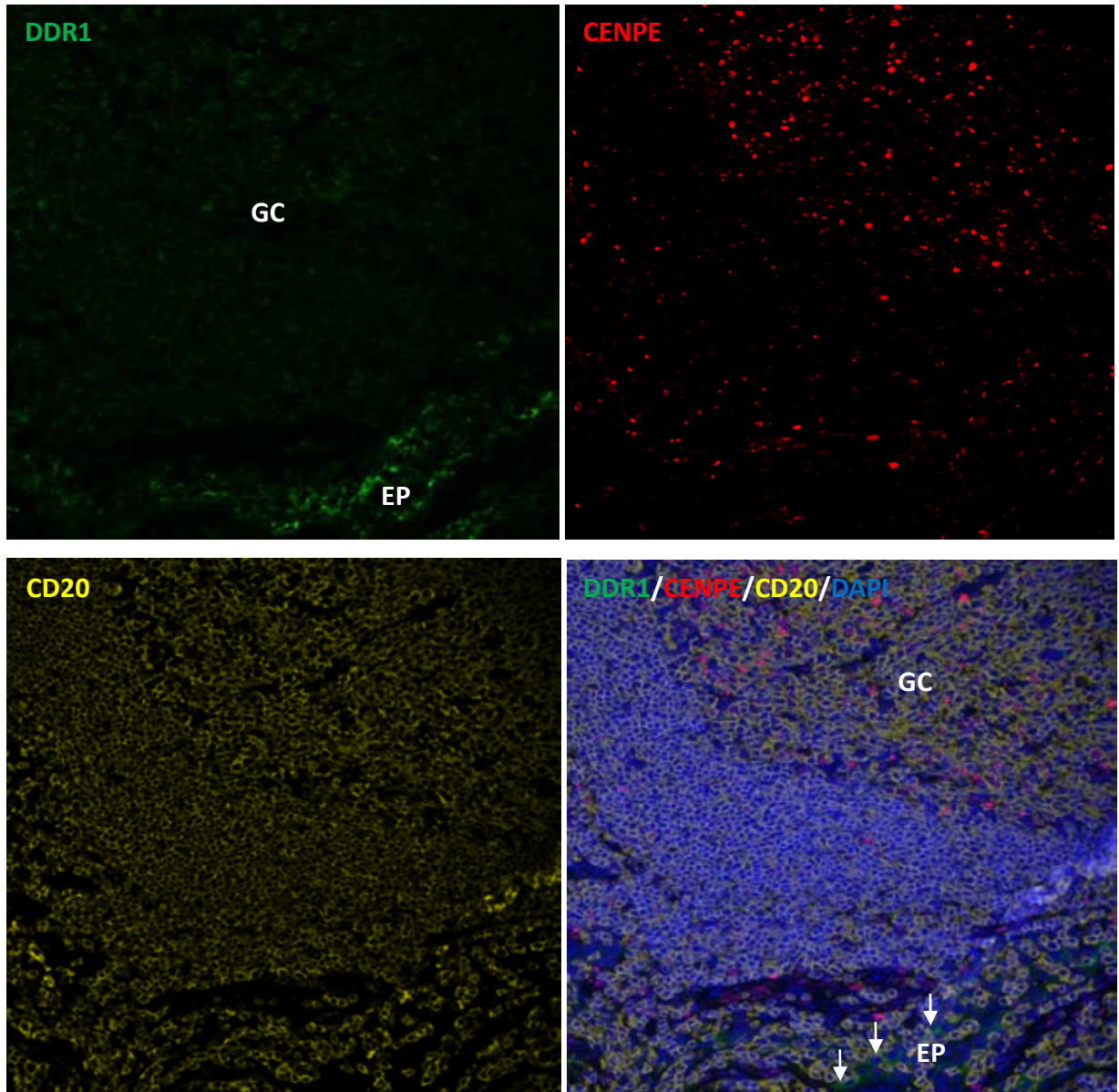


Figure 3.21B CENPE and DDR1 expression in Tonsil - multiplex immunofluorescence. Multiplex immunofluorescence on Tonsil control. CENPE (red) expression is strong in germinal centre (GC) (top right panel). DDR1 level (green) is very low in GC but highly expressed by epithelial cells (top left panel). Presence of B cells was confirmed by CD20 staining (yellow, bottom left). Bottom right panel present DDR1, CENPE and CD20 staining in tonsil control. EP - epithelium, GC – germinal centre. DDR1 positive and CD20 negative epithelial cells are marked by white arrows (bottom right panel, DDR1/CENPE/CD20/DAPI).

3.6 CENPE expression is down-regulated following collagen stimulation of DDR1a transfected BJAB and DG75 cells.

I next wanted to investigate the effect of DDR1 activation on CENPE expression in cell lines.

To do this, I transfected BJAB and DG75 cell lines with DDR1a, and stimulated them with collagen or 0.5% acetic acid as a control, for 1, 2, 4 and 6h (as described in Materials and Methods, sections 2.4 and 2.5). CENPE expression was measured by qRT-PCR and immunoblotting. I found that collagen treatment of these cells led to a decrease in the expression of CENPE in both cell lines. Down-regulation of CENPE mRNA was detected already after 1h of DDR1 stimulation with collagen (Figure 3.22A), whereas the strongest effect on protein expression was detected by immunoblotting after 2h of collagen stimulation (Figure 3.22B).

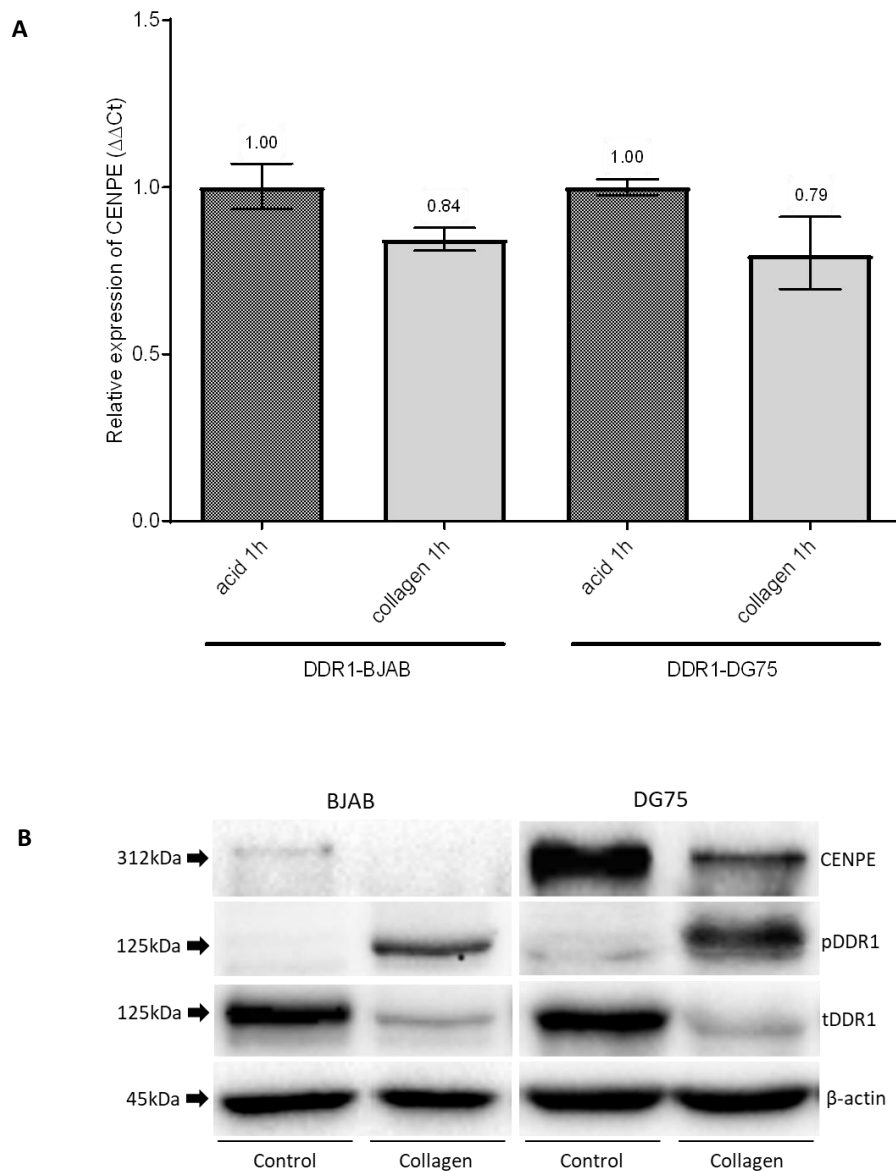


Figure 3.22 CENPE expression in lymphoma cell lines after activation of DDR1 by collagen.

A) qRT-PCR shows down-regulation of CENPE mRNA in DDR1a transfected BJAB and DG75 cell lines after 1h collagen stimulation, in comparison to 0.5% acetic acid treated control cells. B) Immunoblotting for CENPE in BJAB and DG75 cell lines, detected by specific CENPE antibody (Sigma, MW=312kDa). Blot also shows successful transfection and activation of DDR1 receptor by 2h collagen stimulation. β actin confirmed equal protein loading. Data shown are representative of three independent experiments.

3.7 DG75 cell line as a model to investigate the impact of DDR1 on the development of aneuploidy in vitro.

Decreased CENPE expression is known to induce aneuploidy. The next set of experiments was designed to test if the downregulation of CENPE by DDR1 could induce aneuploidy in B cells.

With the help of [REDACTED], I stained metaphase spreads of three cell lines: L591, DG75 and BJAB with Giemsa. For each cell line, 220 cells were counted and based on cell size, divided into three groups: normal (2N), hyperploid (>2N), and hypoploid (<2N). DG75 cells showed the smallest variability in cell size – 78.28% of cells were normal (2N), compared to 59.82% for BJAB and 71.36% for L591. Only 4.53% of DG75 were classified as hypoploid (<2N); as opposed to 15.98% for BJAB and 15.91% for L591 (Figure 3.23A).

I next counted the exact number of chromosomes in 35 metaphase cells for each cell line. DG75 showed the least variation in the number of chromosomes, with a mean chromosome number of 44.5 (Figure 3.23B).

Based on those observations I decided to use the DG75 line as a karyotypically stable model for my further experiments.

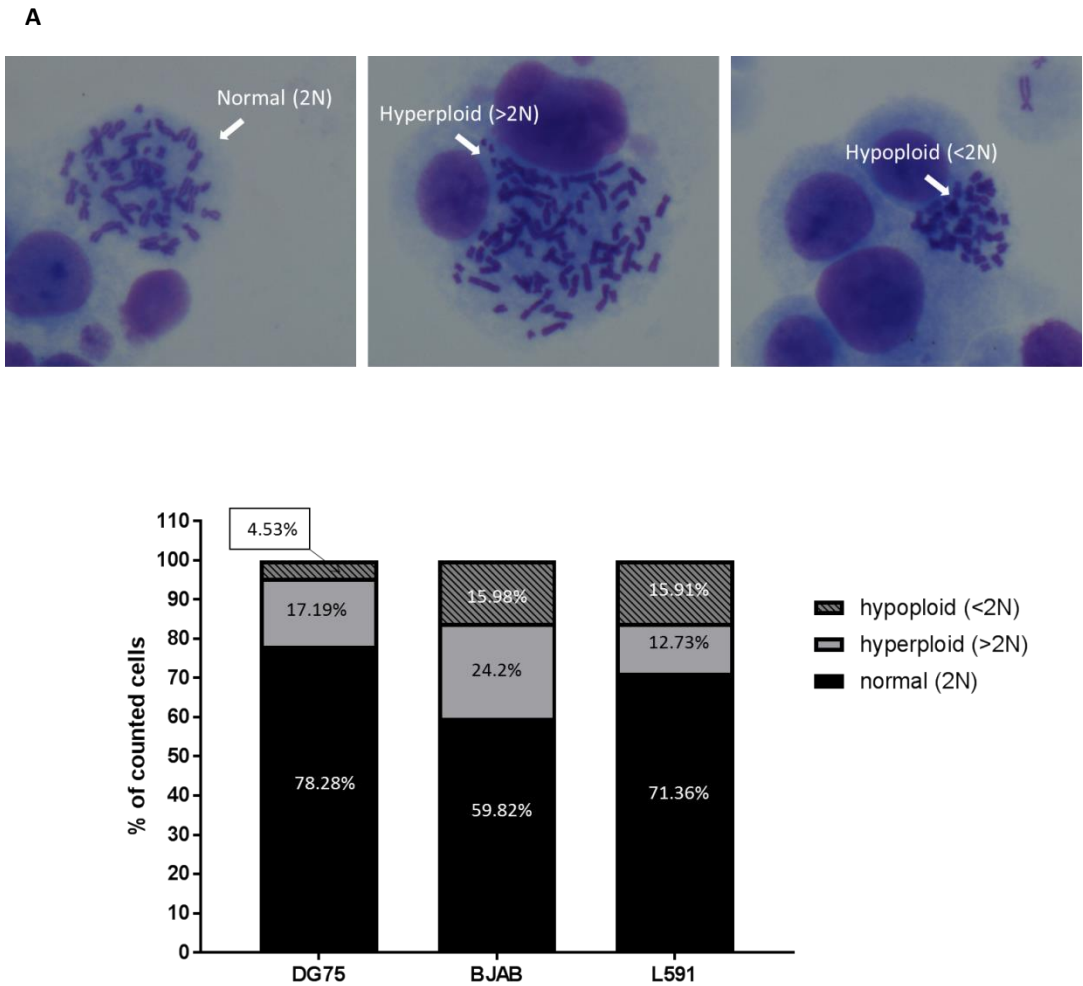


Figure 3.23A Analysis of cell sizes based on metaphases of DG75, BJAB and L591 cells.

Metaphase spreads of DG75, BJAB and L591 cell lines were stained and the size of the cells analysed. An example of normal (2N), hyperploid (>2N), and hypoploid (<2N) BJAB cells are shown. 220 cells were analysed for each cell line. Graphs show percentages of normal, hyperploid and hypoploid cells.

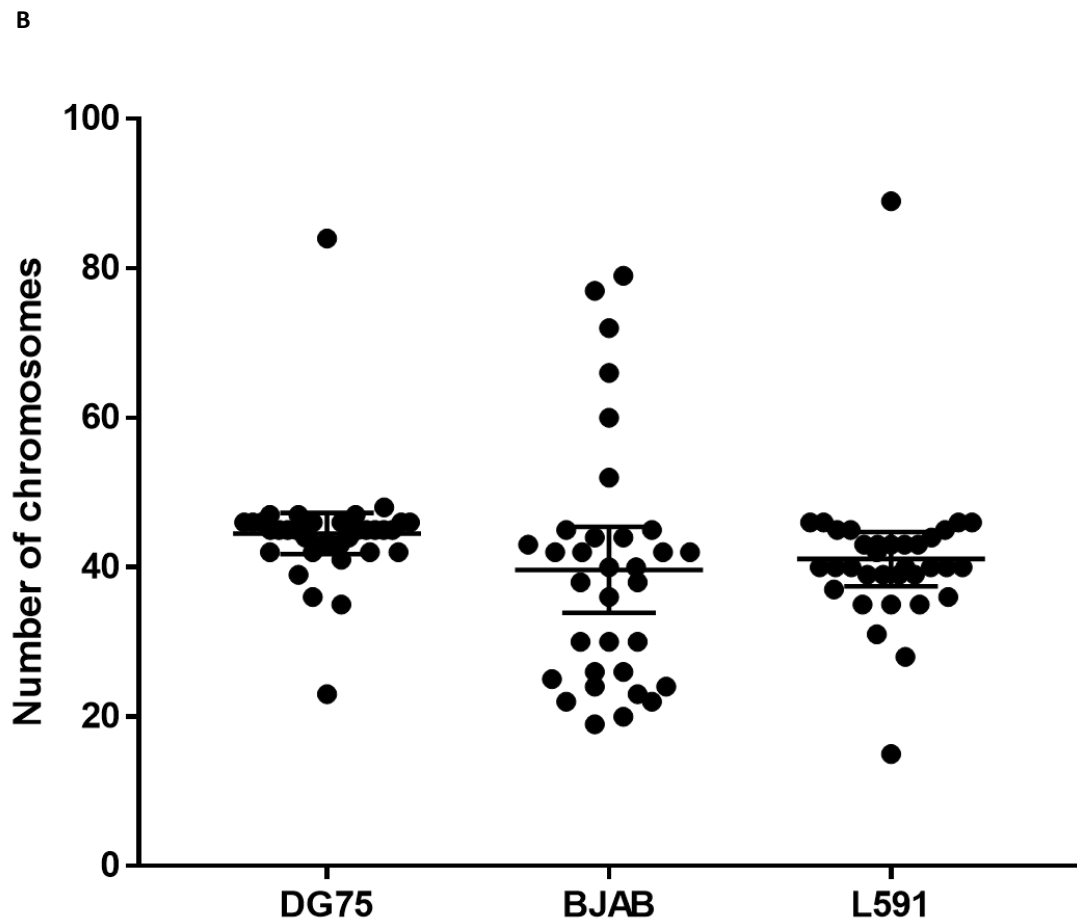


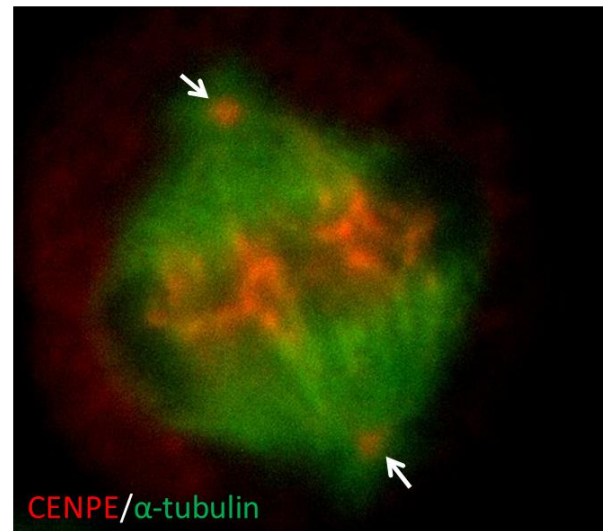
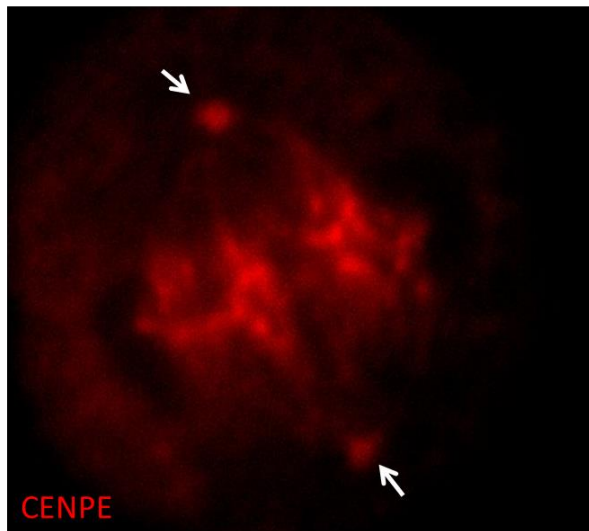
Figure 3.23B Analysis of chromosome number in metaphase spreads of DG75, BJAB and L591 cell lines.
 Metaphase spreads were stained and chromosomes in each metaphase counted. Chromosomes from 35 cells were counted for each cell line. DG75 had a mean chromosome number of 44.7 and the least variability in chromosome number. Lines on a graph represent mean value and standard errors.

Previously, Bennet et al., showed that the inhibition of CENPE with GSK923295 generated aneuploidy in HeLa and DLD-1 cell lines (Bennett et al., 2015). GSK923295 is an allosteric inhibitor which disrupts the ATPase activity of CENPE, which is needed for microtubule activation and their interactions with kinetochores during mitosis. This inhibitor has a high specificity for the CENPE motor domain and stabilise the CENPE protein in a conformation that highly increase its affinity for microtubule binding (Wood et al., 2010).

I first wanted to confirm that I could block CENPE localisation in HeLa cells.

To do this, I treated HeLa cells with or without 50nM of GSK923295 inhibitor for 4h, fixed in ice cold methanol and stained for CENPE and α -tubulin. As expected, GSK923295 treatment resulted in the dislocation of CENPE proteins during metaphase. Thus, in untreated HeLa cells, CENPE proteins were located exactly at the end of each kinetochore in a correctly formatted metaphase plate (Figure 3.24, top panel). However, in cells treated with GSK293295, CENPE proteins were dislocated from kinetochores, or were fully blocked at spindle poles, preventing proper formation of metaphase plates (Figure 3.24, bottom panel).

Control



GSK923295

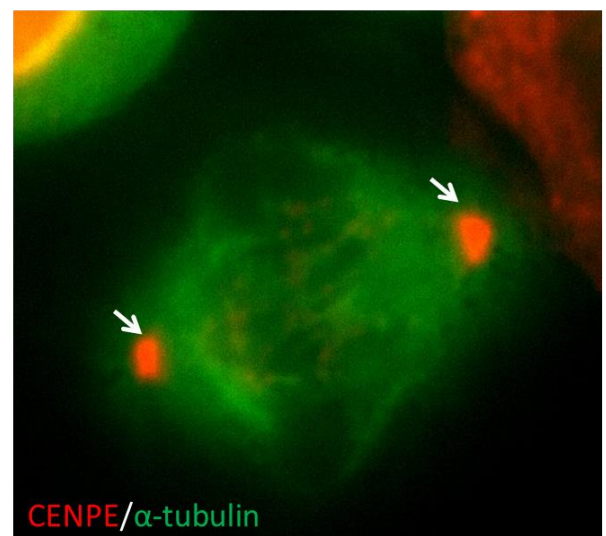
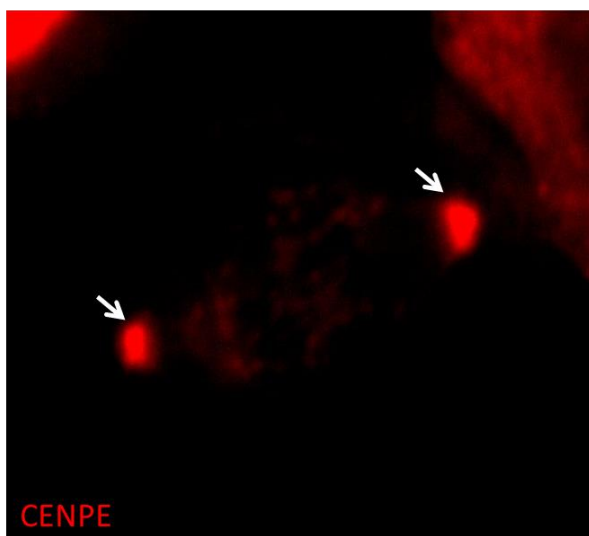


Figure 3.24 Dislocation of CENPE protein in HeLa cells after treatment with GSK923295.

HeLa cells were treated with 50nM of GSK923295 for 4 hours. CENPE and α -tubulin were visualised by immunofluorescent staining. Location of CENPE protein (red) in metaphase cell treated with inhibitor (bottom panels), was different in comparison to non-treated control (top panels). GSK923295 inhibitor prevented CENPE protein from binding to kinetochores, and formation of proper metaphase plate. This effect was detected as strong red staining in mitotic spindle poles (bottom panels). α -tubulin (green) staining was performed to detect metaphase cells. Mitotic spindle poles are marked with white arrows.

Having confirmed that GSK923295 disrupts CENPE localisation in HeLa cells, I next wanted to investigate its effects in DG75 cells. Inhibition of CENPE by GSK923295 has been shown to result in a delay in mitosis, lack of mitosis plate formation and activation of the SAC, which if prolonged results in apoptosis. To avoid apoptosis after CENPE inhibition, I treated cells with an inhibitor of the MPS1 kinase, known as AZ3146, which helps override SAC, and by this allowing anaphase to proceed. Inhibition of MPS1 during mitosis inactivates the SAC, by releasing MAD1-MAD2 complex which prevents production of the active form of MAD2 and therefore activation of APC/C which mediates further progression of mitosis (Hewitt et al., 2010) (Figure 3.25).

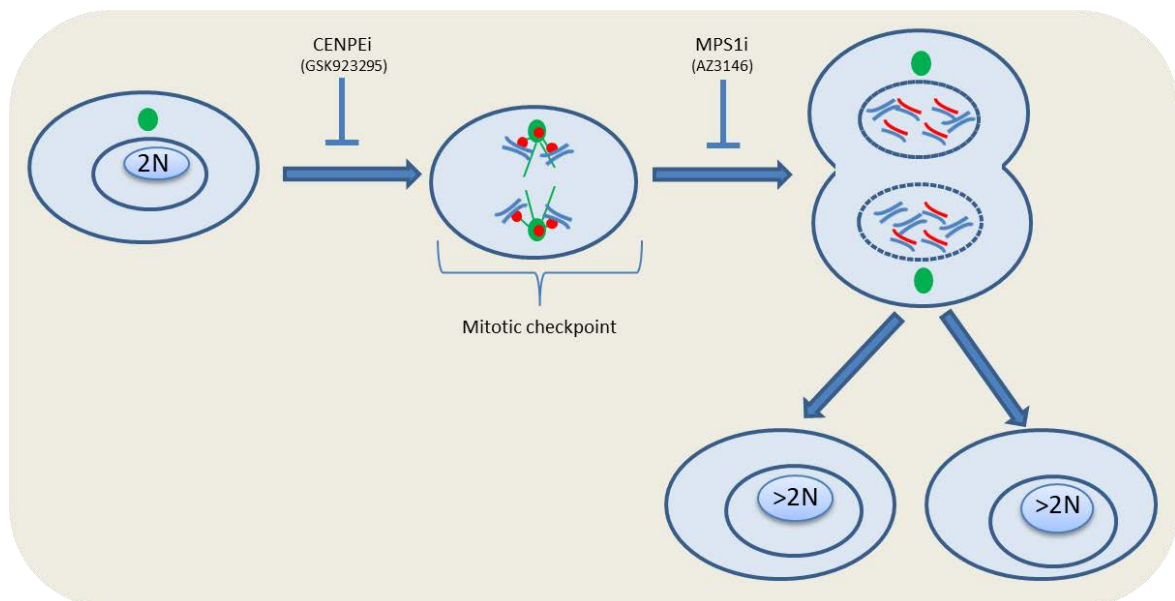


Figure 3.25 Experimental plan for induction of aneuploidy in DG75 cells.

DG75 cells (2N) treated with CENPE inhibitor (GSK923295) should result in misalignment of chromosomes at the metaphase plate. CENPE proteins (red dots) on chromosomes are clustered close to, or in centrosomes/mitotic spindles (green circles). Lack of chromosome alignment activates the spindle assembly checkpoint (SAC). Addition of MPS1 inhibitor (AZ3146) results in release of MAD1-MAD2 complex and inactivation of SAC, allowing mitosis progression. As a result of these treatments, aneuploid cells (>2N) should be produced.

I incubated DG75 cells with GSK923295 for 4h, followed by AZ3146 for 2h. Cells were then incubated in fresh media supplemented with 10% FBS for 24 hours and metaphase spreads stained with Giemsa.

225 cells were counted for control or GSK923295/AZ3146 treated cells and divided into three groups based on cell size as before. Compared to control cells, GSK923295/AZ3146 treatment of DG75 cells increased the percentage of hyperploid cells (>2N) (21.3% to 45.8%) and decreased the percentage of normal cells (2N) (73.37% to 52.9%) (Figure 3.26A).

These observations were confirmed by chromosome counts. 100 cells were analysed in control and treated cells. Compared to control cells, GSK923295/AZ3146 treatment of DG75 cells significantly increased chromosome number ($p=0.028$) (Figure 3.26B).

A

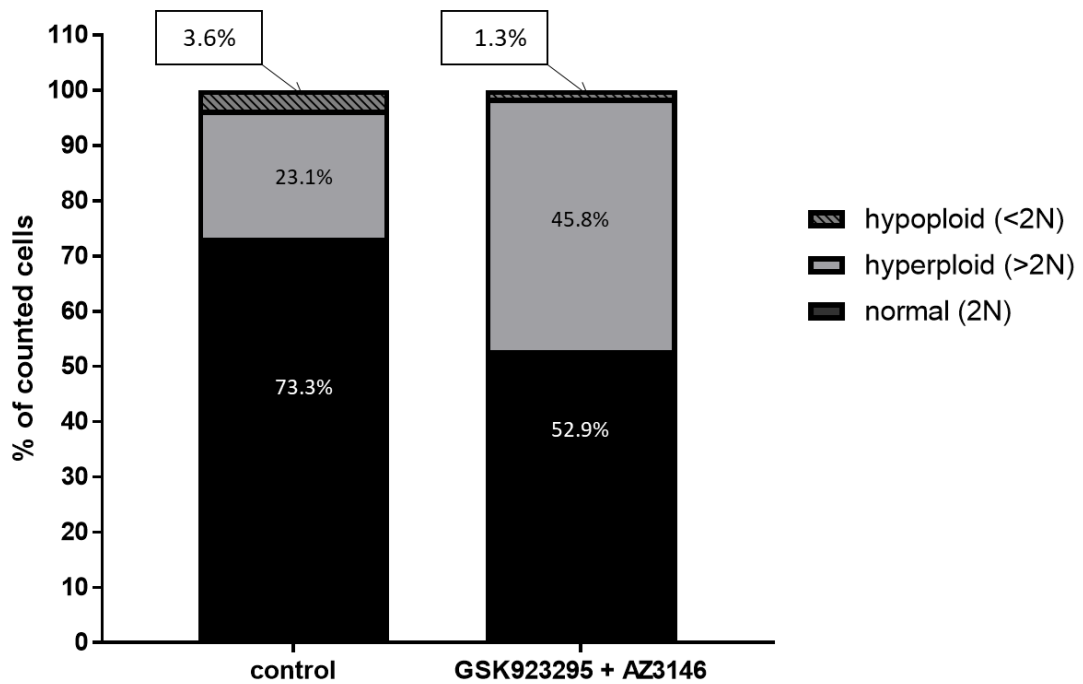


Figure 3.26A Aneuploidy in DG75 cells after CENPE/MPS1 kinase inhibition, as measured by metaphase cell size.

DG75 cells were treated with 50nM of GSK923295 for 4 hours, followed by 2 μ M of AZ3146 for 2 hours. Metaphase spreads were stained after 24h and cell size measured as before. 225 cells were analysed. Graphs show percentages of normal (2N) (black), hyperploid (>2N) (grey) and hypoploid (<2N) (grey patterned) cells. Results are based on a single experiment.

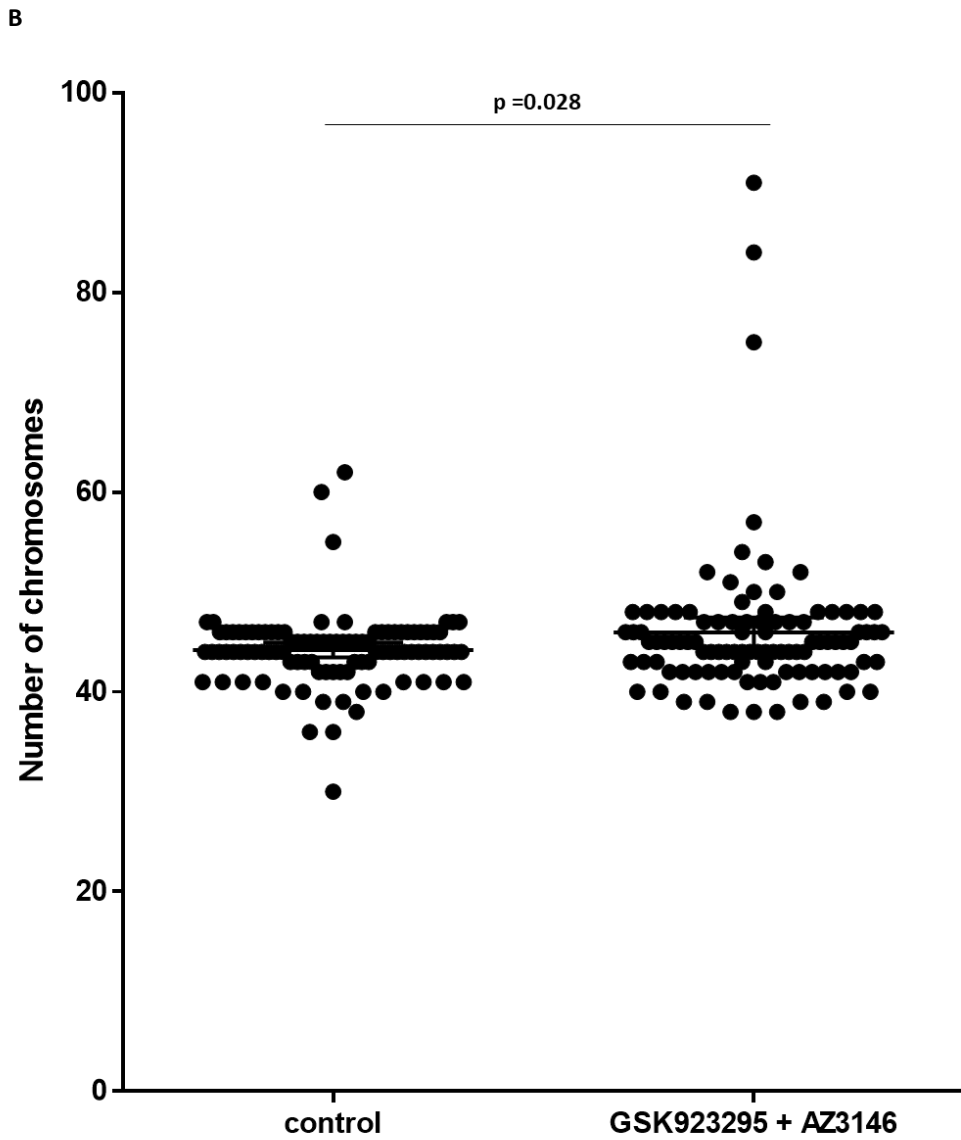


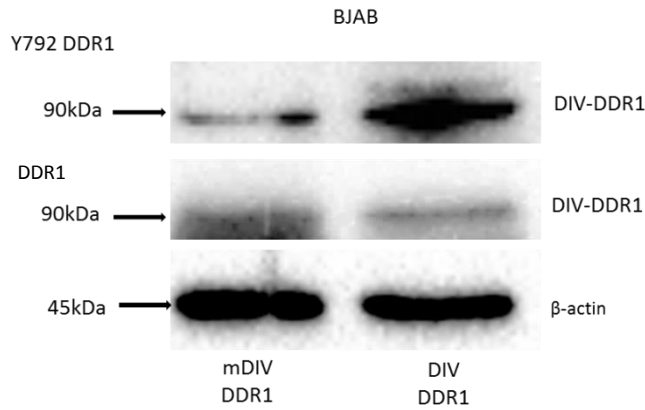
Figure 3.26B Aneuploidy in DG75 cells after CENPE/MPS1 kinase inhibition, as measured by chromosome number.

DG75 cells were treated with 50nM of GSK923295 for 4 hours, followed by 2 μ M of AZ3146 for 2 hours. Metaphase spreads were stained after 24h and the number of chromosomes counted in 100 cells. Students T test was used to compare the mean of treated and controls cells. Result is based on a single experiment.

To provide further confirmation of these observations I adopted a different strategy, this time transfecting BJAB and DG75 cells with a constitutively active DDR1 (DIV) or mutant control (mDIV) (kind gift of [REDACTED])

I confirmed expression of these constructs by immunoblotting using the phospho-DDR1 specific antibody (Y792; Cell Signaling). I observed strong activation of DDR1 in BJAB cells transfected with DIV-DDR1 plasmid, compared with mDIV-DDR1 transfected controls, which shared only lower levels of DDR1 activation (Figure 3.27A). Immunofluorescence staining of cells transfected with DIV-DDR1 DG75 cells confirmed successful transfection (Figure 3.27B).

A



B

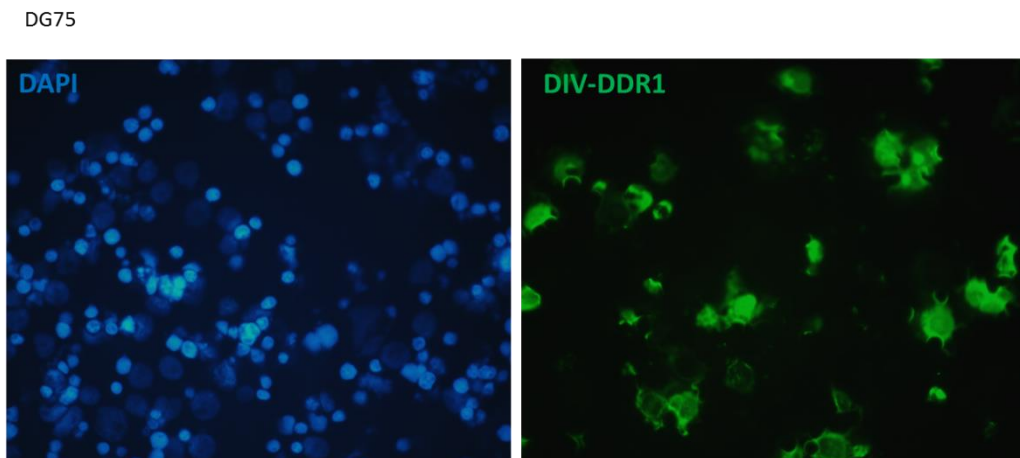


Figure 3.27 Validation of constitutively active DDR1 (DIV) plasmid in BJAB and DG75 cell line.

A) Immunoblotting confirming DIV-DDR1 expression and activation (Y791 phospho-DDR1 antibodies) in DIV-DDR1 expressing BJAB cells, in comparison to its mutant control (mDIV) (MW of protein 90kDa). Equal loading of the protein is shown using β -actin antibody (MW of protein 45kDa). Data from a single experiment. B) Immunofluorescent staining with rabbit monoclonal DDR1 (D1G6) XP[®] antibody (Cell Signaling), shows DDR1 staining in DG75 cell line, transfected with DIV-DDR1. Data shown are representative of two independent experiments.

To test if constitutively active DDR1 could induce aneuploidy, I transfected DG75 cells with the constitutively active (DIV) and non-active DDR1 mutant (mDIV) constructs. Cells were incubated for 24h to allow expression of each receptor, followed by 9 or 29h of incubation. Cells were then harvested for analysis of metaphases. I first tested if any effect could be observed without adding MPS1 inhibitor.

I first analysed cell size, again classifying cells into three groups as before. Compared to untreated cells, DG75 cells transfected with the constitutively active DDR1 (DIV) showed an increase in the percentage of hyperploid cells at both time points. Thus, after 9h, there was a noticeable increase in the percentage of hyperploid (>2N) cells which increased from 18.18% in the control un-transfected (DDR1-negative) cells to 50.87% in DG75 cells transfected with the constitutively active DDR1. The percentage of hyperploid cells was also increased in DG75 cells transfected with mutant DDR1 (mDIV). This is consistent with the lower levels of DDR1 activation previously observed in these cells (Figure 3.23B). After 29h of incubation, the percentage of hyperploid (>2N) cells increased from 32.27% in control cells and 23.18% in mDIV transfected cells to 59.09% in DG75 cells with constitutively active DDR1 (Figure 3.28A). As expected, I observed an accompanying decrease in the percentage of normal (2N) cells in cells expressing constitutively active DDR1 compared to those expressing either no DDR1 or the mutant DDR1 (Figure 3.28A).

A

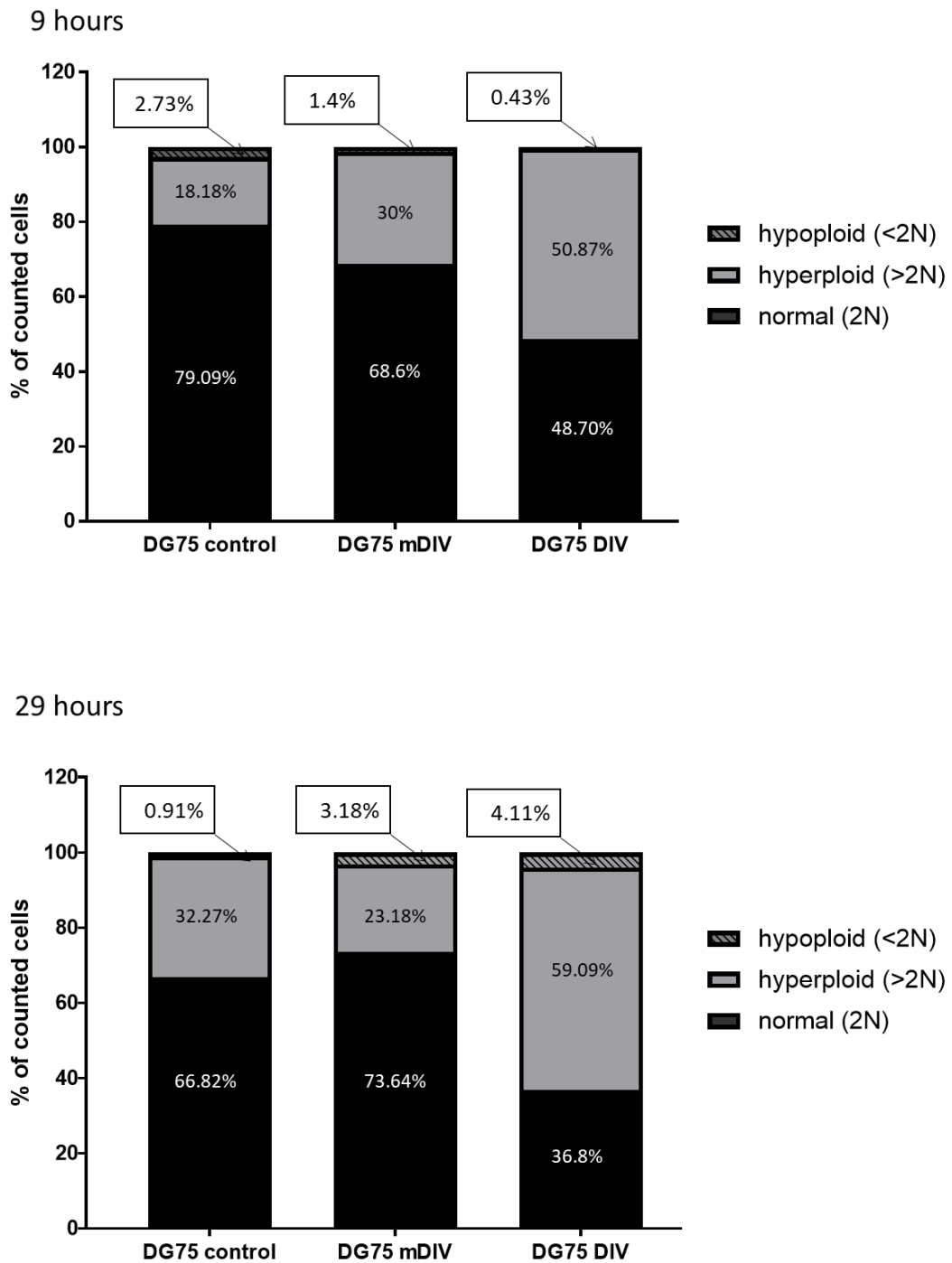


Figure 3.28A Increased detection of hyperploidy in DG75 cells expressing a constitutively active DDR1, as measured by cell size.

DG75 cells were either untreated or transfected with constitutively active DDR1 (DIV) or mutant DDR1 (mDIV) and incubated for 24h. After a further 9h (top graph) and 29h (bottom graph) metaphase spreads were stained and cell size estimated in 225 cells were analysed. Graphs shows percentages of normal (2N) (black), hyperploid (>2N) (grey) and hypoploid (<2N) (grey patterned) cells. Results are based on a single experiment.

Next, I counted the number of chromosomes in 100 control, mDIV and DIV transfected cells at both time points. This analysis revealed an increase in chromosome number in cells transfected with constitutively active DDR1 (DIV) at both time points, when compared to non-transfected and mDIV transfected control cells. This effect was particularly marked and highly significant at the 29h time-point ($p=6.56 \times 10^{-10}$, and $p=1.35 \times 10^{-15}$). At the 9h time point a significant difference was only apparent in DG75 cells transfected with constitutively active DDR1 compared to those transfected with the mutant DDR1 ($p=0.0176$).

Taken together, these results provide strong evidence that DDR1 activation is alone able to induce aneuploidy in DG75 cells (Figure 3.28B).

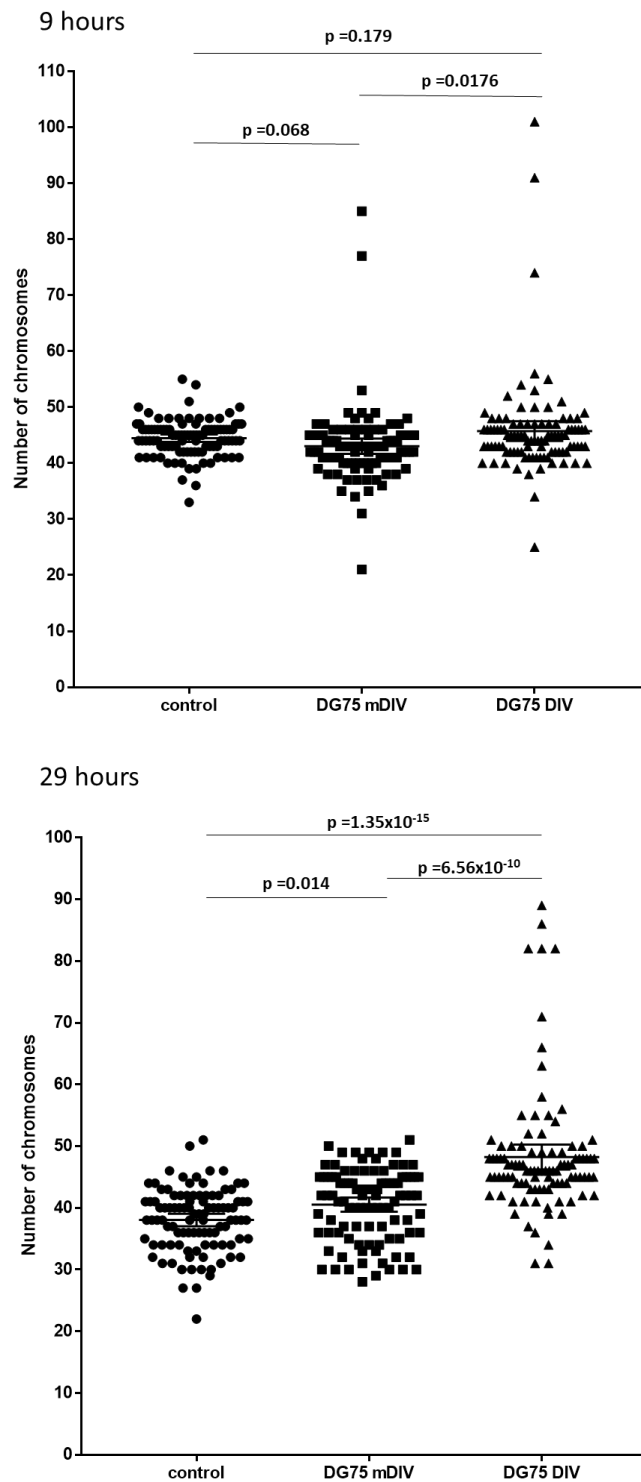
B

Figure 3.28B: Increased detection of hyperploidy in DG75 cells expressing a constitutively active DDR1, as measured by chromosome number

DG75 cells were either untreated or transfected with constitutively active DDR1 (DIV) or mutant DDR1 (mDIV) and incubated for 24h. After a further 9h (top graph) and 29h (bottom graph) metaphase spreads were stained and chromosome number measures in 100 control, mDIV and DIV transfected cells. Results show significant increase in number of chromosomes in DG75 transfected with constitutively active DDR1 (DIV), in comparison to mutant (mDIV) and non-transfected control at both time points. Student's T test was used to compare means. Results are based on a single experiment.

CHAPTER FOUR

Results part II

POTENTIAL THERAPEUTIC REVERSAL OF DDR1

ACTIVATION USING DDR1 INHIBITORS.

4. Potential therapeutic reversal of DDR1 activation using specific DDR1 inhibitors

4.1 Blocking the phosphorylation of DDR1 receptor by small molecular inhibitors

I used three published inhibitors, two: 7rh (7-4104) and 7rj (7-4109) were a gift of Dr Ke Ding, Jinan University, China and their specificity for DDR1 was already described in Gao et al. (Gao et al., 2013). The third DDR1 inhibitor - DDR1-IN-1 di-hydrochloride (R&D Systems), is the only small molecule inhibitor of DDR1 that is commercially available (Kim et al., 2014).

BJAB cells were transfected with DDR1a and serum starved cells for 2 hours, then treated for 1 h with collagen and DDR1 inhibitor. Based on previous publications, I chose a range of concentrations for each inhibitor. The inhibition of DDR1 activation, in comparison to untreated and collagen only treated control cells, was then measured by immunoblotting using specific phospho-DDR1 (Tyr792) antibody. All three inhibitors decreased DDR1 phosphorylation in a dose dependent manner. Successful inhibition, proved by weaker band in comparison to collagen control, was already noticed after addition of 0.5 μ M of 7rh, 7rj and DDR1-IN-1 inhibitor (Figure 4.1). Effectiveness and specificity of those inhibitors was confirmed by trypan blue toxicity assay, which identified 0.5 μ M concentration as non-toxic for BJAB cells, after 1, 2 and 3h of stimulation with 7rh (Figure 4.2), 7rj (Figure 4.3) and DDR1-IN-1 inhibitors (Figure 4.4).

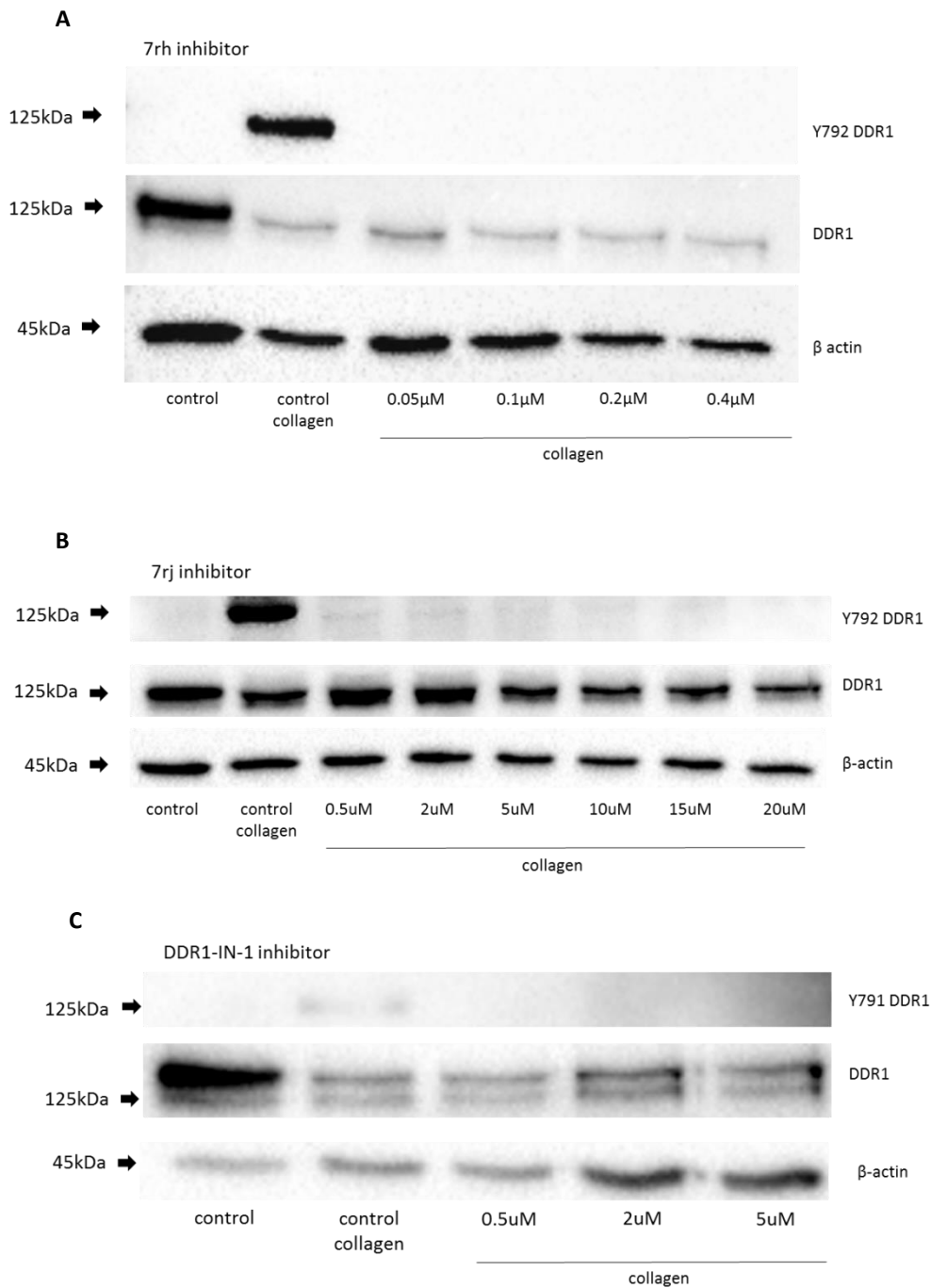


Figure 4.1 Inhibition of DDR1 activation by 7rh, 7rj and DDR1-IN-1 in BJAB cells transfected with DDR1a, after collagen stimulation.

Immunoblotting results of DDR1 expression and inhibition of receptor phosphorylation after blocking DDR1 by 7rh inhibitor (A), 7rj inhibitor (B) and DDR1-IN-1 inhibitor (C) in BJAB cell lines, transfected with DDR1a. Treatment of activated by collagen DDR1 with all tested concentrations of inhibitors resulted with reduction of its activation, when compared to collagen stimulated control. β-actin confirmed equal loading of the sample. Data shown are representative of three independent experiments.

7rh inhibitor

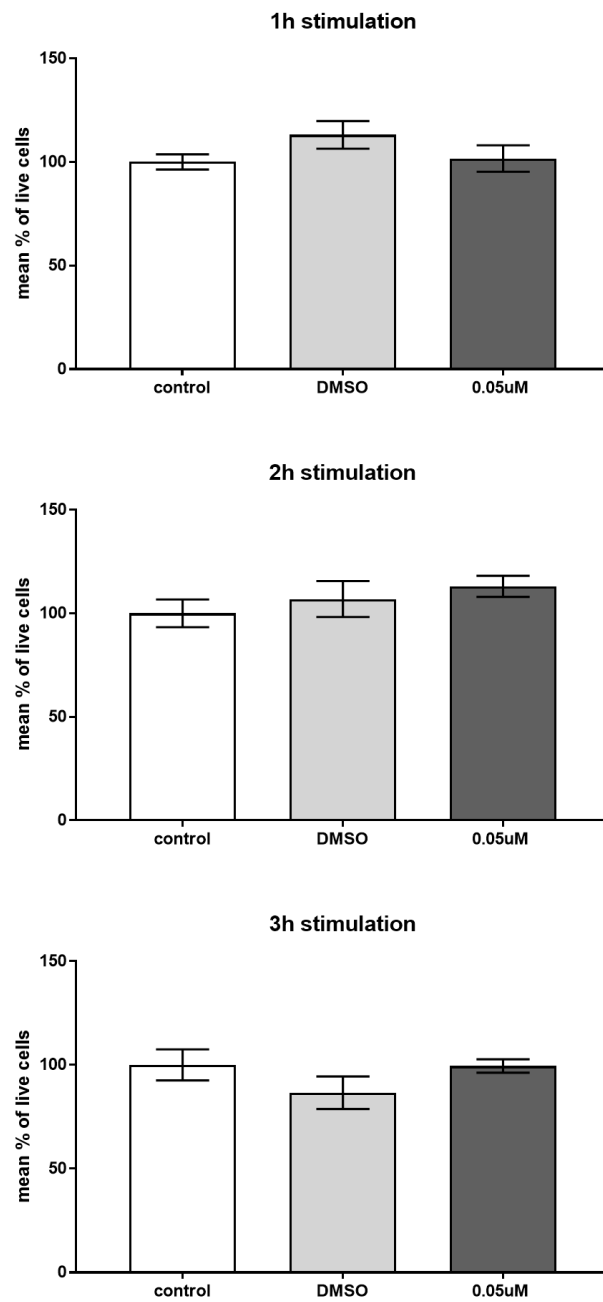


Figure 4.2 Toxicity assay with trypan blue on DDR1a transfected BJAB cell line, treated with 7rh DDR1 inhibitor.

BJAB cell line transfected with DDR1a, were treated with 0.05 μ M 7rh inhibitor for 1, 2 and 3 hours. Harvested cells were counted in haemocytometer under microscope with bright field, using 0.4% Trypan Blue solution. Mean percentage of life cells is presented on graphs. Non-treated cells and cells with DMSO was used as a control for the test. Data shown are mean percentage of three independent experiments.

7rj inhibitor

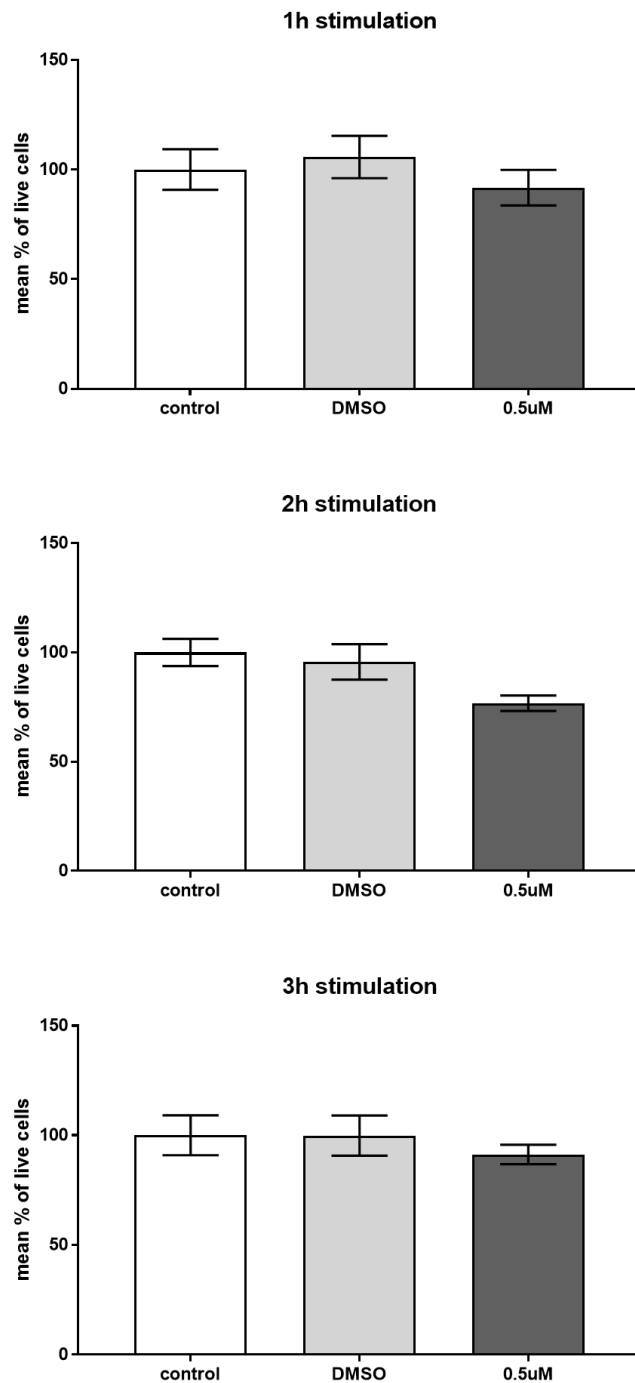


Figure 4.3 Toxicity assay with trypan blue on DDR1a transfected BJAB cell line, treated with 7rj DDR1 inhibitor.

BJAB cell line transfected with DDR1a, were treated with 0.5µM 7rj inhibitor for 1, 2 and 3 hours. Harvested cells were counted in haemocytometer under microscope with bright field, using 0.4% Trypan Blue solution. Mean percentage of live cells is presented on graphs. Non-treated cells and cells with DMSO was used as a control for the test. Data shown are mean percentage of three independent experiments.

DDR1-IN-1 inhibitor

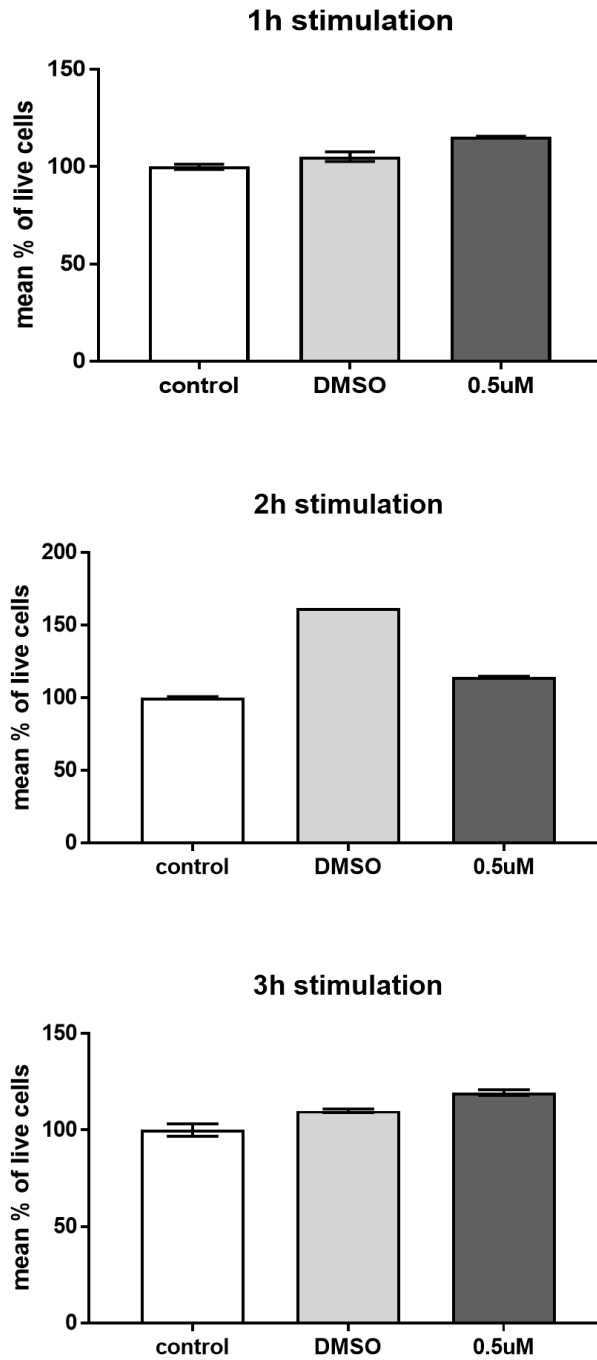


Figure 4.4 Toxicity assay with trypan blue on DDR1a transfected BJAB cell line, treated with DDR1-IN-1 DDR1 inhibitor.

BJAB cell line transfected with DDR1a, were treated with 0.5 μ M DDR1-IN-1 inhibitor for 1, 2 and 3 hours. Harvested cells were counted in haemocytometer under microscope with bright field, using 0.4% Trypan Blue solution. Mean percentage of life cells is presented on graphs. Non-treated cells and cells with DMSO was used as a control for the test. Data shown are mean percentage of two independent experiments.

4.2 Establishing an in vivo model to test DDR1 inhibitors

With a view to the future testing of these inhibitors in vivo, I next wanted to establish suitable animal models. These experiments were performed with the help of [REDACTED]

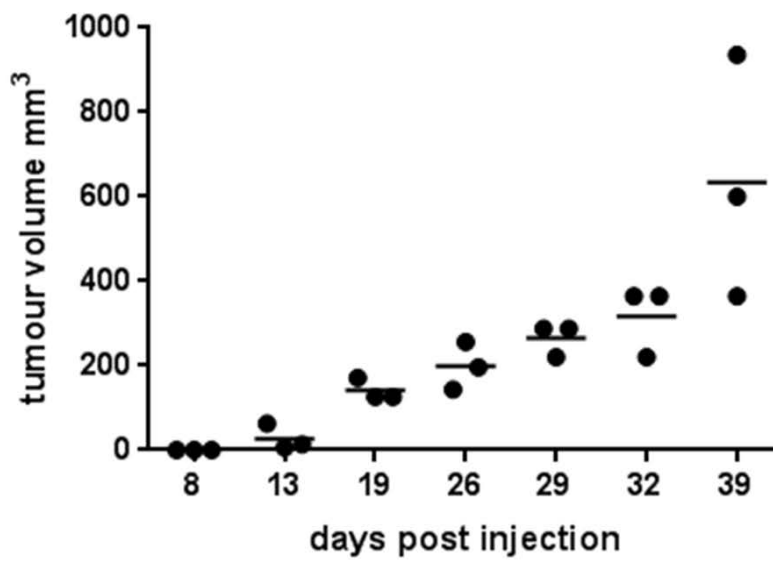
4.2.1 Tumour growth of L591 and BJAB xenograft

First I wanted to establish the baseline growth kinetics of the transduced cell lines when grown in immunodeficient mice. L591 and BJAB cells were injected subcutaneously in the right flank of 3 Immunodeficient NSGTM mice per cell line. The growth of the tumour was monitored weekly starting from 8 days after injection (Figure 4.5). Tumours were harvested after 39 days. Cells were isolated from tumours and tested by flow cytometry and some tissue fixed for immunohistochemistry.

4.2.2 DDR1 expression in L591 xenografts

I used flow cytometry to measure human DDR1 expression in the xenograft tumour. This revealed that 4.43% of CD30 positive tumour cells within the single mouse L591 xenograft studied expressed DDR1, compared to 23.3% in the cell line grown in vitro (Figure 4.6). Unfortunately there was not enough isolated from tumour BJAB cells to test it by flow cytometry.

L591 xenograft in NSG mouse; SC injection



BJAB xenograft in NSG mouse; SC injection

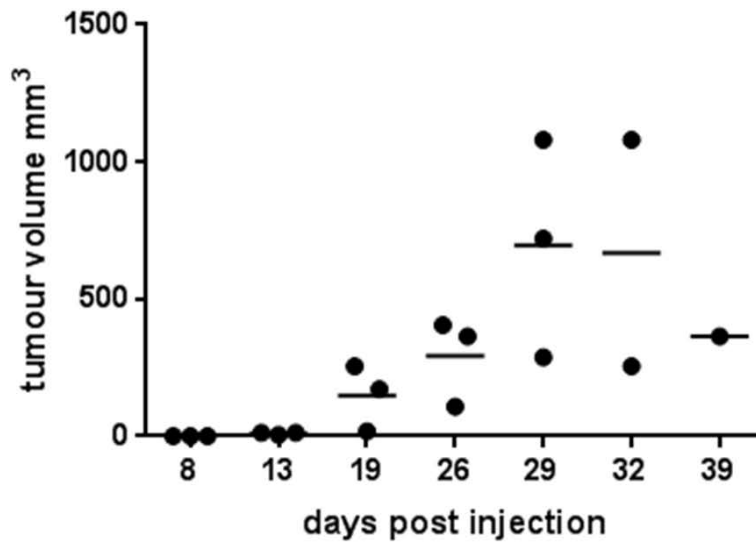
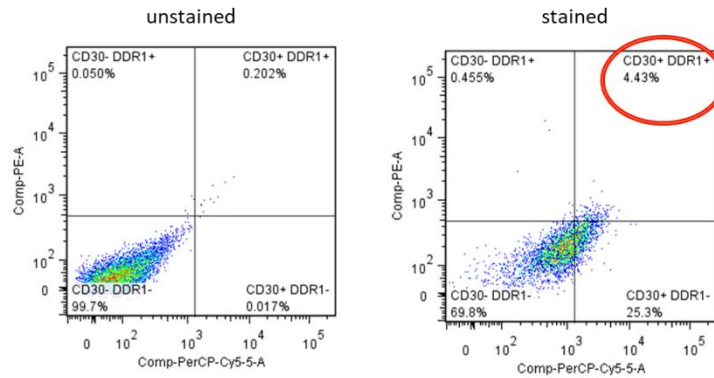
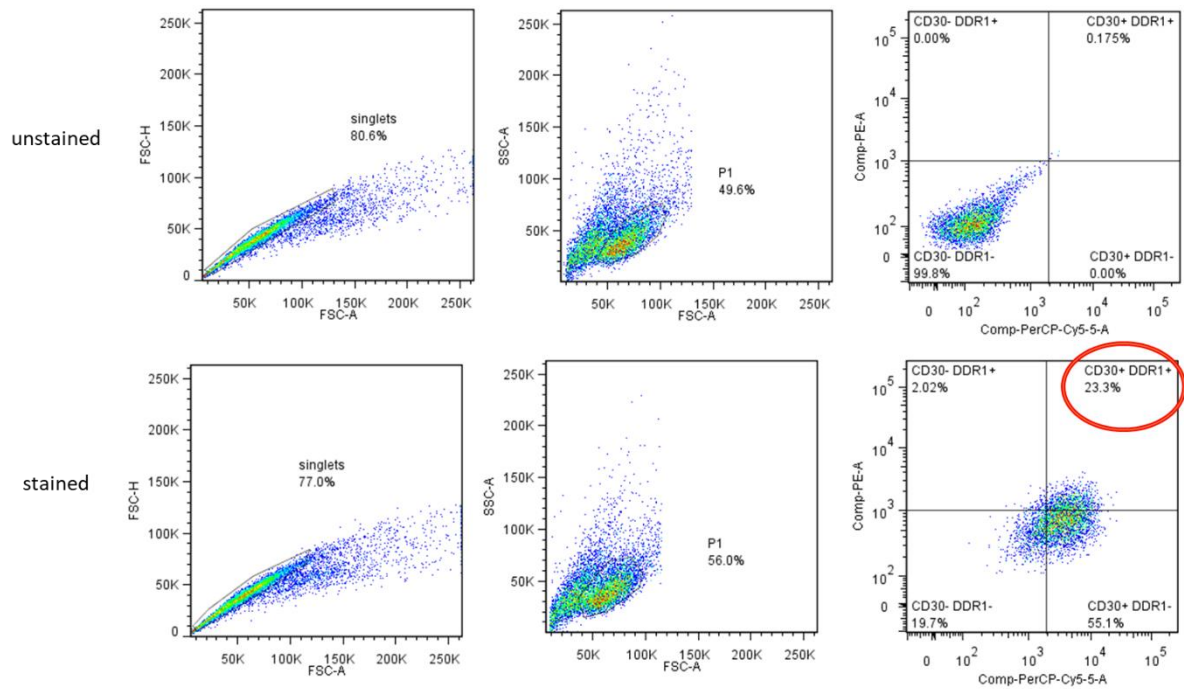


Figure 4.5 Tumour growth in L591 and BJAB mice xenograft.

A) L591 and B) BJAB tumour growth (mm³) in xenograft model. Tumour growth was monitored weekly starting from day 8 after cells injection subcutaneously in the right flank in 3 mice per cell line.

A**L591 mouse xenograft****B****L591 cell line****Figure 4.6 Human DDR1 expression in L591 xenograft model.**

A) Cells isolated from L591 tumour xenograft, after 39 days from subcutaneously injection of L591 cell line into mouse, were stained with CD30 (marker for HL tumour cells) and human DDR1, and tested by flow cytometry. 4.43% of live, CD30/DDR1 positive cells were detected in L591 xenograft (right panel) and B) 23.3% of live, double positive cells were found in L591 cell line control (bottom right panel). Percentage of double positive cells is marked by red circle. Top panels are presenting the unstained control.

4.3 Collagen expression in mouse tumours

Having confirmed the expression of human DDR1 in the mouse L591 xenograft I next, tested BJAB, OCI-LY3 and L591 xenograft sections for the presence of collagen, using van Gieson staining. These results revealed expression of collagen fibres in tumour microenvironment (Figure 4.7).

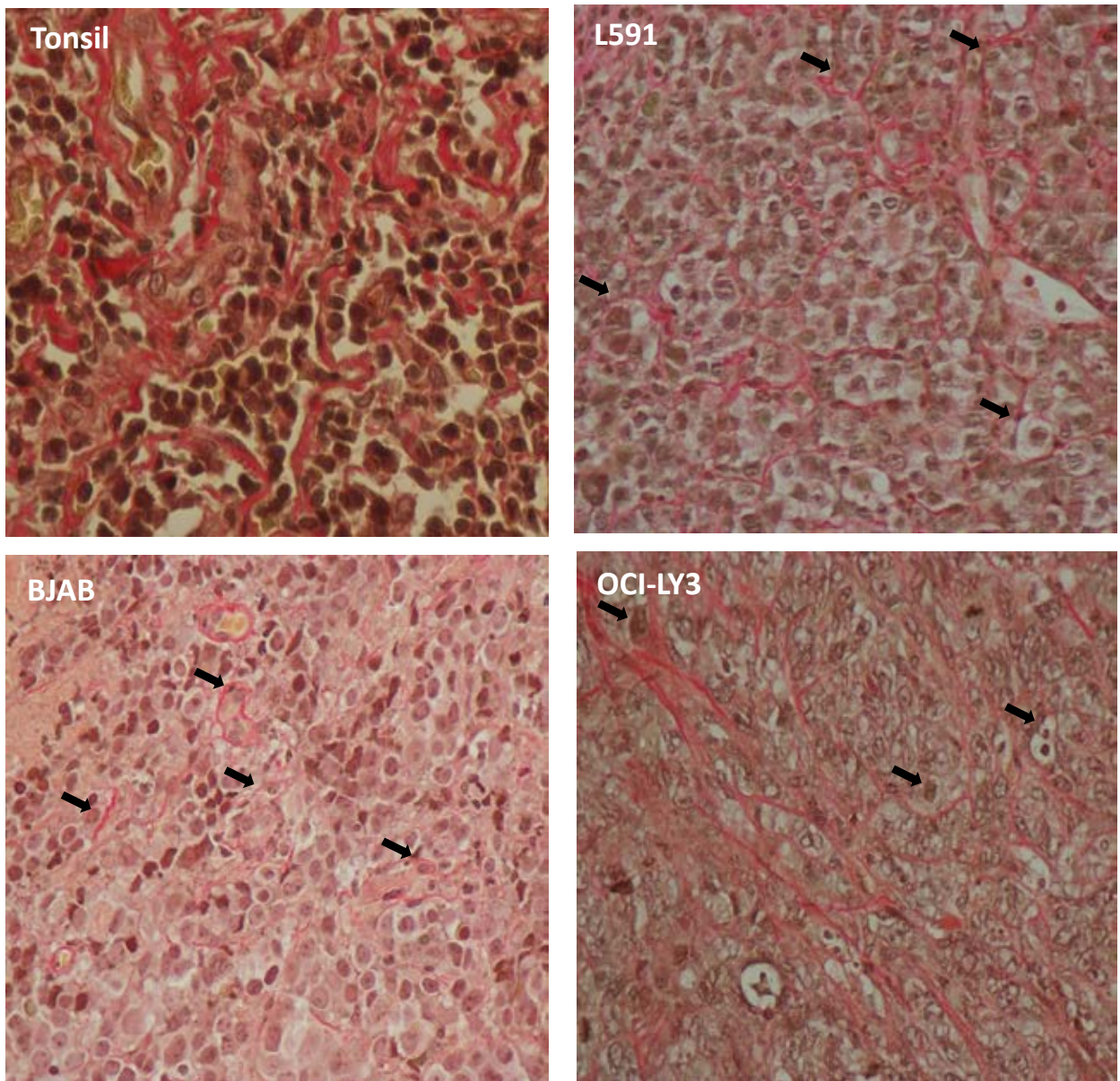




Figure 4.7 Van Gieson staining showing collagen expression in mouse xenograft models.

Van Gieson staining on L591, BJAB and OCI-LY3 xenograft revealed expression of collagen fibres (pink fibres) in tumour environment. Collagen fibres in close association with tumour cells (marked by arrows) were noticed in all tested xenografts. Tonsil staining is enclosed as a positive control.

4.4 DDR1 and collagen expression in A20 xenograft

While looking for a good mouse model for studying DDR1 inhibitors, I also tested well known mouse lymphoma cell-derived A20 xenograft for the expression of DDR1.

I first, tested A20 cell line for the expression of DDR1 by immunoblotting. This result showed undetectable level of DDR1 expression in A20 cell line, in comparison to L591 HL cell line control (Figure 4.8).

I next, investigated collagen expression in A20 xenograft ( ) by Van Gieson staining. Those results revealed presence of collagen in tumour microenvironment (Figure 4.9).

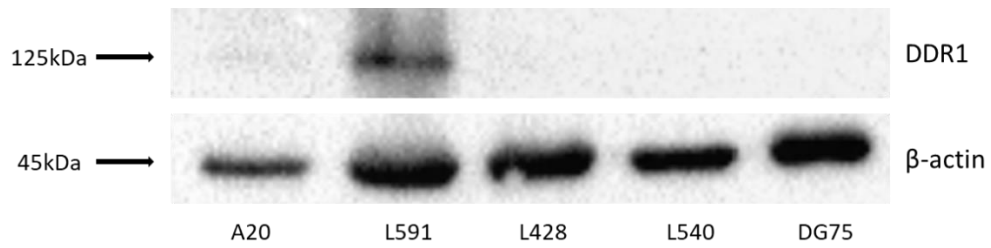


Figure 4.8 DDR1 expression in A20 cell line.

Immunoblotting results showing detectable expression level of DDR1 protein in A20 cell line, which is higher than in GC B cells control, and lower than in two tested HL cell lines (MW=125kDa). β-actin confirmed equal loading of the sample. Data shown are representative of three independent experiments.

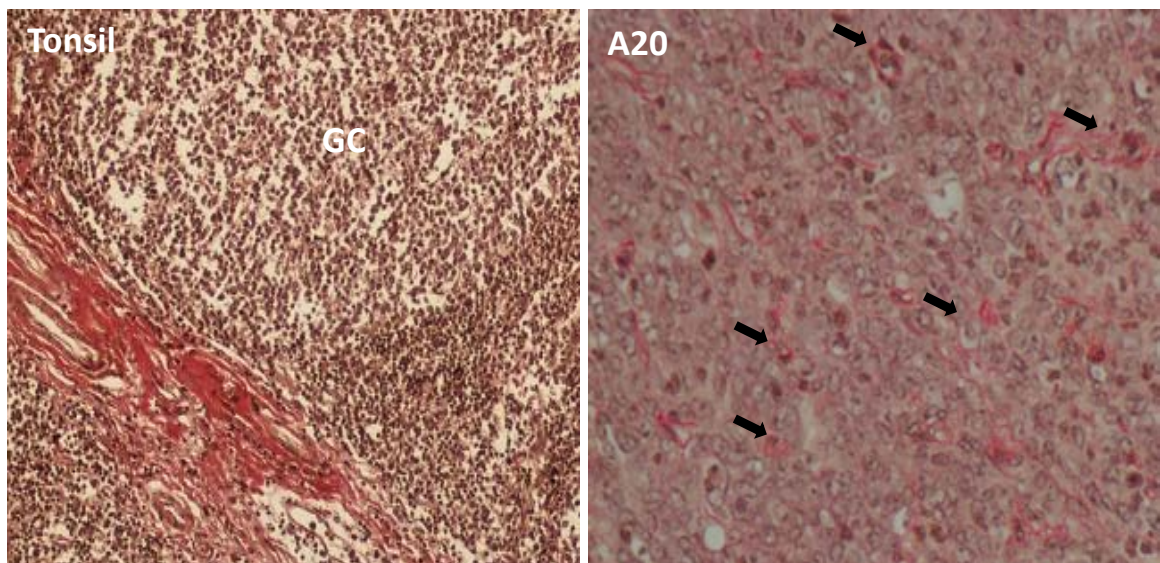


Figure 4.9. Van Gieson staining showing collagen expression in A20 xenograft.

Van Gieson staining on A20 xenograft revealed expression of collagen fibers in tumour environment. Tonsil staining was enclosed as a positive control.

CHAPTER FIVE

DISCUSSION AND FUTURE PERSPECTIVES

Discussion and future perspectives

In this thesis I have explored the contribution of the collagen receptor DDR1 to the pathogenesis of diffuse large B cell lymphoma (DLBCL). To date there has been only one study that has shown the role for DDR1 in lymphoma; Cader et al., demonstrated the overexpression of DDR1 in Hodgkin lymphoma and showed that collagen ligation of DDR1 overexpressing lymphoma cell lines promoted their survival and protected them from etoposide induced death (Cader et al., 2013).

In this thesis, I have shown that DDR1 is overexpressed also in a subset of DLBCL. This subset includes cases of GCB and ABC subtype indicating that DDR1 likely contributes to both major subtypes of DLBCL. This observation was confirmed by both qRT-PCR and immunohistochemistry on separate cohorts on patients. Furthermore, I found that all DDR1 positive cases also showed deposition of collagen type VI, in close proximity to DDR1 expressing tumour cells. I have not directly addressed the mechanism through which DDR1 is overexpressed. Previous studies have shown that several inflammatory mediators, including tumour necrosis factor α (TNF- α), interleukin 1 β (IL-1 β), granulocyte-macrophage colony-stimulating factor (GM-CSF) and lipopolysaccharides (LPS), can also increase the expression of DDR1 in leukocytes (Kamohara et al., 2001). It was also proposed that collagen I can also induce expression of DDR1 by the integrin-independent activation of DDR2 in lung fibroblasts (primary normal human lung fibroblasts; NHLF) (Ruiz and Jarai, 2011). It was shown that recruitment of phospho-JAK2 to DDR2 and activation of ERK1/2 is required for this process (Ruiz and Jarai, 2011).

A critical finding in this thesis was the observation that the overexpression of DDR1 in DLBCL was associated with aneuploidy. For example, I observed a significant overlap between genes regulated by DDR1 with three separate signatures of aneuploidy and with two gene sets representing mitotic spindle and mitotic spindle checkpoint genes, respectively. I also observed a significant positive correlation between DDR1 overexpression and total autosomal aneuploidy as measured by the analysis of copy number data from primary DLBCL. For several reasons these observations are potentially important. First, there is a growing literature linking chronic inflammation to lymphoma development. For example there is a well-established link between Burkitt lymphoma and the polyclonal stimulation of B cells caused by either malaria, HIV, or both (Moss et al., 1983, Whittle et al., 1984, Petersen et al., 1985, Burkes et al., 1986). More recently, a relationship between chronic inflammation and DLBCL has been firmly established. Indeed, DLBCL associated with chronic inflammation is an entity recognised by the WHO 2016 classification (Swarlow et al., 2016). Although this association is known, the mechanisms responsible are incompletely understood.

Several publications have suggested that elevated DDR1 expression in immune cells may be important in the context of its role in immune response and the development of several diseases including cancer. For example, DDR1 expression was shown to be higher in leukocytes in human renal tumour infiltrate, in comparison to normal cells (Kamohara et al., 2001); and on activated T-cells (Chetoui et al., 2011, Hachehouche et al., 2010). Moreover, DDR1a was identified as the major isoform expressed in leukocytes in renal tumour infiltrate (Kamohara et al., 2001) and that DDR1 is responsible for migration of THP-1 and T cells in three-dimensional (3D) collagen matrix (Kamohara et al., 2001;

Hachehouche et al., 2010). Previous studies have also shown that DDR1, through interaction with collagen of ECM mediates leukocyte and macrophage migration towards the site of inflammation, and therefore DDR1 was also connected with the development of several inflammatory diseases (such as fibrosis and atherosclerosis) and with cancer invasiveness (Franco et al., 2009, Franco et al., 2010, Avivi-Green et al., 2006, Kamohara et al., 2001, Leitinger, 2014).

Based on current knowledge about the regulation of DDR1 expression, its function observed in cells connected with the immune response (such as leukocytes and macrophages), and on my observations that overexpression of DDR1 is inversely related to expression of CENPE, which induces aneuploidy in vitro; I am proposing the hypothesis that my findings also present a novel mechanism which could underpin the contribution of chronic inflammation to lymphoma development. However, this proposition would have to be confirmed experimentally, by direct analysis of DDR1 and CENPE expression in immune cells in DLBCL.

In this thesis, the downregulation of CENPE by DDR1 was initially shown in primary GC B cells. This model has been used in previous reports by our group to explore the impact of viral and cellular genes on the early stages of lymphoma development. This model proved to be useful in this thesis, providing a unique opportunity to explore the impact of collagen activation of DDR1 in a normal B cell background. The RNAseq analysis of the transcriptional changes that follow the activation of DDR1 in these cells provided a broad picture of the potentially pathogenic effects of DDR1 in B cell lymphomas. For example I observed that DDR1 altered the expression of genes associated with cell proliferation,

protection from apoptosis and cell migration, all of which were previously established functions of DDR1 (reviewed by: Valiathan et al., 2012, Leitinger et al., 2011, Lemmon and Schlessinger, 2010). However, this GC B cell model is limited insofar as I was only able to observe the effect of DDR1 during a short time window following transfection and the low numbers of cells that are obtained from this experiment make it difficult to examine protein expression of downstream targets.

Assessment of the impact of the DDR1 on aneuploidy in vitro required the development of a new model. To do this, I took advantage of an existing model that has been reported on HeLa cells, in which chromosome miss-segregation is first induced by exposure to a CENPE inhibitor. This is then followed by the inactivation of mitotic spindle checkpoint by an inhibitor of the MPS1 kinase. I was able to reproduce the effects of these inhibitors in HeLa cells before going to show that constitutive activation of DDR1 was sufficient to induce aneuploidy in DG75 cells, which I used as a karyotypically stable B cell lymphoma line. However, a preferable model would be one in which the long-term effects of DDR1 could be monitored in vitro in untransformed B cells. Thus, one could envision a model in which GC B cells isolated from human tonsils by CD10 magnetic Dynabeads are cultured in soluble trimeric human recombinant megaCD40L and IL-4, and maintained over several weeks as we have described (Smith et al., 2013). These cells could then be subject to the CENPE and MPS1 kinase inhibitors used in this thesis

Chromosomal abnormalities were found to appear in almost all patients with non-Hodgkin lymphoma. Aneuploidy and chromosomal instability (CIN) was also previously described in DLBCL. It was shown that, in almost all (70-90% of cases in different reports)

diffuse large B cell lymphoma cases, gains or losses of whole chromosomes can be found (Bea et al., 2005, Johansson et al., 1995, Bloomfield et al., 1983, Kramer et al., 2003, Bakhoum et al., 2011b); and CIN is postulated to be important for the progression and aggressiveness of this tumour (Bakhoum et al., 2011). There is evidence showing that chromosomal instability contributes to a poor prognosis in DLBCL patients. DLBCL is reported to be heterogeneously aneuploidy and CIN seems to play an important role in tumour aggressiveness and evolution (Kramer et al., 2003, Bernasconi et al., 2008, Tibiletti et al., 2007, Tzankov et al., 2006). For example, aggressive DLBCLs were carrying centrosome aberrations in 41.8% of tested cases in comparison to 25.5% in more indolent lymphomas, such as follicular lymphoma (FL); and this finding correlated with the higher proliferation index in DLBCL (Kramer et al., 2003). Bakhoum et al. investigated CIN in 54 DLBCL patient samples by scoring chromosome segregation defects (lagging chromosomes or chromatin bridges) in anaphase and correlated the results with clinical data. Their analysis pointed to a decrease in overall survival, and increase in tumour invasiveness and relapse after treatment in patients who carried an increased frequency of chromosomal mis-segregation (Bakhoum et al., 2011a). Fluorescent in situ analysis (FISH) of DLBCL cases showed gain of chromosomes 3, 12, 18 and X (Bernasconi et al., 2008). Interestingly, these chromosomal aberrations appear to differ depending on the DLBCL subgroup. ABC-DLBCL more frequently had a gain of chromosome 3, whereas GCB type of DLBCL gained more chromosome 12. Gain of chromosome 3 in DLBCL was found to be correlated with shorter survival in these patients (Bea et al., 2005). Also deregulation of cyclin E, a critical regulator of the cell cycle, was shown to be able to

induce CIN and was connected with a poor prognosis in some neoplastic diseases including DLBCL (Saez et al., 2004, Ferreri et al., 2001, Tzankov et al., 2006).

Recent studies have highlighted the possibility of specific targeting aneuploidy as a therapeutic option. Patients with aneuploid tumours resistant to existing therapies could benefit from alternative treatments. Two approaches can be envisioned:

First, aneuploid cells that emerge following inactivation of the SAC can be recognised and eliminated by the immune system (Lopez-Soto et al., 2017). Thus, hyperploid malignant cells over-express ligands for NKG2D and DNAM1 which stimulate NK cell cytotoxicity (Lopez-Soto et al., 2015). Moreover, aneuploid cells display a pro-inflammatory senescence-associated secretory phenotype (SASP) (Lopez-Soto et al., 2015, Santaguida et al., 2017) and over-express genes regulated by the cGMP-AMP (cGAMP) synthase (cGAS)-stimulator of interferon (IFN) genes (STING) pathway (Mackenzie et al., 2017). Aneuploid cells can also be recognised by adaptive immune cells. Thus, tumours generated from hyperploid cells are increased in mice depleted of CD4⁺ or CD8⁺ T lymphocytes (Senovilla et al., 2012). Hyperploid cancer cells also show increased levels of ER stress, resulting in over-expression of calreticulin, an ER chaperone required for rejection of hyperploid tumours by adaptive immunity (Senovilla et al., 2012).

Second, aneuploid cells are characterised by energy and proteotoxic stress that increases their susceptibility to apoptosis (Milan et al., 2014). As a result aneuploid cells are more sensitive to specific small molecule compounds, such as AICAR, which allosterically activates AMP-activated protein kinase (AMPK) thereby mimicking energy stress, and 17-

AAG, which inhibits Hsp90, a chaperone required for protein folding, activation and assembly (Tang et al., 2011).

At the present moment it is difficult to envisage a role for DDR1 inhibitors in the therapeutic targeting of aneuploidy in transformed cells, since presumably the fundamental defects that lead to the development of aneuploidy have already occurred. However, blocking DDR1 activities in tumours might be expected to lead to therapeutic benefits as a result of the downregulation of cell proliferation, protection from apoptosis and cell migration. I showed that small molecule inhibitors of DDR1 are effective in blocking the phosphorylation of DDR1 in B lymphoma lines, which is in accordance with previous studies which showed that these inhibitors can block DDR1 phosphorylation in cell lines derived from bone, colon, breast, lung and uterine cancers (Kim et al., 2013: U2OS, HCT-116, T47D, A549, H1975, SkBr3, SW480, SNU-1040, EJ) (Gao et al., 2013: A549, NCI-H23, NCI-H460, MDA-MB-435S, MCF-7, T47D, HCT116, K562). These inhibitors did not cause toxicity in lymphoma cells. However, clearly more work is required to establish their effects on cellular phenotypes both in vitro and in vivo. In this latter respect I made some progress towards the establishment of relevant animal models in which these inhibitors could be tested. This included an initial assessment of the expression of collagen in 3 different xenografts of DLBCL. These in vivo models will also provide an opportunity to analyse in vivo, the effects of DDR1 on aneuploidy, as well as the potential therapeutic blockade of aneuploidy described above.

The use of DDR1 targeted therapies could be extended to the use of monoclonal antibodies which could block the interaction between DDR1 and collagen, and thereby

prevent receptor activation. Since previously published in vitro studies indicate that the ligation of DDR1 by collagen protects lymphoma cells from apoptosis induced by chemotherapy (Cader et al., 2013), therapeutic blockade of the collagen-DDR1 interaction would be expected to sensitise lymphoma cells to apoptosis induced by chemotherapy. It is well established that ligand-independent activation of receptor tyrosine kinases can occur through cross talk with other receptors and that this is important for normal tissue homeostasis (Carafoli et al., 2009). Emerging evidence suggests that this is also the case for DDR1 (Favelyukis et al., 2001, Canning et al., 2014). Furthermore, a body of evidence suggests that the collagen-independent interaction of DDR1 with other molecules such as E-cadherin regulates normal epithelial functions (Till et al., 2002, Bertrand et al., 2012). Monoclonal antibodies that sterically interfere with the structure of DDR1 may well also affect the normal collagen-independent functions of DDR1 potentially leading to unwanted toxicities. Importantly, disrupting this interaction using antibodies against the collagen binding site of DDR1 would also have no effect on the other functions of collagen that depend on its interaction with different collagen receptors.

Although I have demonstrated the transcriptional consequences of DDR1 activation in B cells, I did not study the signalling pathways activated by DDR1 in these cells. Previous studies have shown that DDR1 signalling can be mediated by several pathways, including MAPK, ERK, PI3K/Akt, NF κ B, Notch1 and STAT, in a cell-type dependent manner (reviewed by: (Leitinger, 2014, Fu et al., 2013)). This is in interest given that constitutive activation of several of these pathways, e.g. PI3K/Akt (for GCB DLBCL subtype) (Pfeifer et al., 2013) and NF- κ B and JAK/STAT (for ABC DLBCL subtype) (Davies et al., 2010, Compagno et al., 2009), was reported in DLBCL. However, the precise mechanisms through which DDR1 could

influence the activation of these pathways are not known. For the future, it will be important to investigate the signalling pathways activated by DDR1 in DLBCL. This could be done in several ways. First, transcription factor activation could be analysed for example using the PathDetect Trans-reporting System (Agilent Technologies) (Cismowski et al., 2000)(Rechfeld et al., 2014) in DDR1 transfected GC B cells. This system is able to detect if a gene of interest is involved in signal transduction, and also which step of the pathway is involved; Moreover, the ontology analysis (GO) of the genes positively correlated with DDR1 expression in DLBCL pointed at wound healing, regulation of apoptosis, cell proliferation, migration and angiogenesis; functions known to be mediated by for example, the MAPK/ERK and PI3K/Akt pathways.

Future plans - summary

I outline below several immediate and short term objectives for the extension of this work:

- DDR1 and collagen contribution to the pathogenesis of DLBCL
 - DDR1 activation in GC B cells and analysis of the activation of transcription factors by PathDetect Trans-reporting System.
 - In silico analysis of the GC B cell RNAseq data in context of the activated signalling pathways.
- The potential therapeutic use of DDR1 inhibitors
 - Create stable BJAB cell line expressing constitutively active DDR1
 - Mouse xenograft with stable DDR1⁺ BJAB cell line
 - Treatment of animals with DDR1 inhibitors; observation of tumour growth
 - Organoids grown on collagen matrix and treated with DDR1 inhibitors—an alternative model
 - Analysis of the signalling pathways activated by DDR1 in the presence of DDR1 inhibitors in cell lines or in the mouse model, with a focus on the functional effects of DDR1 inhibition
- Confirmation of the DDR1 input towards an aneuploidy signature of DLBCL
 - Repeat activated DDR1 plasmid (DDR1-DIV) transfection in DG75 cells; confirmation of observed changes in chromosome number in cells (replication of experiment presented in this thesis)

- Activated DDR1 transfection (DDR1-DIV) in BJAB cell line; chromosome count
- BJAB xenograft in mouse; analysis of aneuploidy signature in cells (ditto)

Longer term objectives

- More studies on DDR1 in DLBCL – understanding the cell signalling and agents which are driving this process
- Development of specific antibodies detecting phosphorylation of the receptor at different residues

APPENDICES

Appendix 1. Data from published dataset (Brune et al., 2008) used for investigation of DDR1 expression in primary DLBCL in comparison to normal GCB cells.

GEO_id	Cell type	DDR1 exp
GSM312870	Naive B cells 1	37,41
GSM312872	Naive B cells 2	43,62
GSM312874	Naive B cells 3	25,94
GSM312875	Naive B cells 4	50,08
GSM312876	Naive B cells 5	26,31
GSM312877	Memory B cells 1	43,23
GSM312879	Memory B cells 2	27,55
GSM312882	Memory B cells 3	40,27
GSM312883	Memory B cells 4	27,21
GSM312886	Memory B cells 5	43,25
GSM312887	Centrocytes 1	11,07
GSM312890	Centrocytes 2	21,44
GSM312893	Centrocytes 3	20,67
GSM312894	Centrocytes 4	29,26
GSM312895	Centrocytes 5	33,46
GSM312937	Centroblasts 1	19,26
GSM312938	Centroblasts 2	25,83
GSM312939	Centroblasts 3	24,49
GSM312940	Centroblasts 4	26,57
GSM312941	Centroblasts 5	27,31
GSM312942	Plasma cells 1	28,44
GSM312943	Plasma cells 2	24,33
GSM312944	Plasma cells 3	28,79
GSM312945	Plasma cells 4	30,89
GSM312946	Plasma cells 5	32,2
GSM312858	DLBCL 1	27,76
GSM312859	DLBCL 2	28,65
GSM312860	DLBCL 3	37,86
GSM312861	DLBCL 4	52,35
GSM312862	DLBCL 5	19,15
GSM312863	DLBCL 6	71,42
GSM312864	DLBCL 7	42,55
GSM312865	DLBCL 8	22,17
GSM312867	DLBCL 9	47,47
GSM312868	DLBCL 10	33,7
GSM312869	DLBCL 11	26,49

Appendix 2. Data from published dataset (Morin et al., 2013) used for investigation of DDR1 expression in primary DLBCL in comparison to normal GCB cells.

Sample type	DDR1 expression [cpm]	Sample type	DDR1 expression [cpm]
ABC-DLBCL 1	4,00	GCB-DLBCL 14	1,82
ABC-DLBCL 2	4,16	GCB-DLBCL 15	9,51
ABC-DLBCL 3	4.07	GCB-DLBCL 16	6,71
ABC-DLBCL 4	7.95	GCB-DLBCL 17	17,23
ABC-DLBCL 5	4.73	GCB-DLBCL 18	21,68
ABC-DLBCL 6	0.95	GCB-DLBCL 19	6,56
ABC-DLBCL 7	2.15	GCB-DLBCL 20	9,98
ABC-DLBCL 8	5.13	GCB-DLBCL 21	12,60
ABC-DLBCL 9	3.50	GCB-DLBCL 22	2,14
ABC-DLBCL 10	0.2	GCB-DLBCL 23	52,36
ABC-DLBCL 11	53,98	GCB-DLBCL 24	16,59
ABC-DLBCL 12	3.54	GCB-DLBCL 25	46,72
ABC-DLBCL 13	24.63	GCB-DLBCL 26	4,30
ABC-DLBCL 14	2.83	GCB-DLBCL 27	13,71
ABC-DLBCL 15	1.96	GCB-DLBCL 28	4,15
ABC-DLBCL 16	3.90	GCB-DLBCL 29	2,76
ABC-DLBCL 17	0.65	GCB-DLBCL 30	1,47
ABC-DLBCL 18	3.22	GCB-DLBCL 31	6,52
ABC-DLBCL 19	2.02	GCB-DLBCL 32	36,14
ABC-DLBCL 20	5.45	GCB-DLBCL 33	7,33
ABC-DLBCL 21	9.03	GCB-DLBCL 34	10,00
ABC-DLBCL 22	28,53	GCB-DLBCL 35	9,94
ABC-DLBCL 23	4,19	GCB-DLBCL 36	8,01
ABC-DLBCL 24	5,64	GCB-DLBCL 37	7,28
ABC-DLBCL 25	2,18	GCB-DLBCL 38	5,19
ABC-DLBCL 26	3,71	GCB-DLBCL 39	38,58
ABC-DLBCL 27	14,08	GCB-DLBCL 40	122,53
ABC-DLBCL 28	5,16	GCB-DLBCL 41	0,94
ABC-DLBCL 29	3,61	GCB-DLBCL 42	13,40
ABC-DLBCL 30	12,85	GCB-DLBCL 43	4,91
ABC-DLBCL 31	12,66	GCB-DLBCL 44	7,30
ABC-DLBCL 32	3,03	GCB-DLBCL 45	5,71
GCB-DLBCL 1	7,52	GCB-DLBCL 46	101,28
GCB-DLBCL 2	3,55	GCB-DLBCL 47	8,26
GCB-DLBCL 3	7,68	GCB-DLBCL 48	4,66
GCB-DLBCL 4	6,97	GCB-DLBCL 49	12,50
GCB-DLBCL 5	51,42	GCB-DLBCL 50	1,40
GCB-DLBCL 6	4,48	GCB-DLBCL 51	56,84
GCB-DLBCL 7	7,38	GCB-DLBCL 52	3,66
GCB-DLBCL 8	16,02	GCB-DLBCL 53	47,72
GCB-DLBCL 9	5,12	GCB-DLBCL 54	8,19
GCB-DLBCL 10	1,91	Normal GC B cell 1	19,82
GCB-DLBCL 11	19,11	Normal GC B cell 2	13,47
GCB-DLBCL 12	7,63	Normal GC B cell 3	15,75
GCB-DLBCL 13	1,78	Normal GC B cell 4	8,89

Appendix 3. Data from published dataset (Lenz et al., 2008) used for investigation of DDR1 expression in primary DLBCL. Database present expression of DDR1 in 167 DLBCL ABC type and 183 GCB type samples.

Sample type	DDR1 expression [RMA linear]
ABC-DLBCL 1	102,62
ABC-DLBCL 2	81,87
ABC-DLBCL 3	44,76
ABC-DLBCL 4	98,66
ABC-DLBCL 5	51,41
ABC-DLBCL 6	53,63
ABC-DLBCL 7	121,51
ABC-DLBCL 8	81,90
ABC-DLBCL 9	65,93
ABC-DLBCL 10	60,41
ABC-DLBCL 11	124,70
ABC-DLBCL 12	56,07
ABC-DLBCL 13	78,83
ABC-DLBCL 14	57,07
ABC-DLBCL 15	70,47
ABC-DLBCL 16	119,88
ABC-DLBCL 17	87,88
ABC-DLBCL 18	62,78
ABC-DLBCL 19	55,18
ABC-DLBCL 20	80,98
ABC-DLBCL 21	103,05
ABC-DLBCL 22	68,44
ABC-DLBCL 23	84,93
ABC-DLBCL 24	47,30
ABC-DLBCL 25	52,05
ABC-DLBCL 26	163,06
ABC-DLBCL 27	71,61
ABC-DLBCL 28	66,17
ABC-DLBCL 29	84,90
ABC-DLBCL 30	90,91
ABC-DLBCL 31	57,07
ABC-DLBCL 32	80,50
ABC-DLBCL 33	54,61
ABC-DLBCL 34	80,93
ABC-DLBCL 35	51,35
ABC-DLBCL 36	72,13

Sample type	DDR1 expression [RMA linear]
ABC-DLBCL 37	96,77
ABC-DLBCL 38	97,16
ABC-DLBCL 39	77,07
ABC-DLBCL 40	40,50
ABC-DLBCL 41	118,73
ABC-DLBCL 42	95,87
ABC-DLBCL 43	51,87
ABC-DLBCL 44	72,21
ABC-DLBCL 45	95,74
ABC-DLBCL 46	113,67
ABC-DLBCL 47	101,84
ABC-DLBCL 48	63,66
ABC-DLBCL 49	89,97
ABC-DLBCL 50	90,55
ABC-DLBCL 51	76,63
ABC-DLBCL 52	87,07
ABC-DLBCL 53	54,88
ABC-DLBCL 54	41,42
ABC-DLBCL 55	62,57
ABC-DLBCL 56	49,10
ABC-DLBCL 57	63,72
ABC-DLBCL 58	94,75
ABC-DLBCL 59	64,25
ABC-DLBCL 60	68,04
ABC-DLBCL 61	90,82
ABC-DLBCL 62	87,61
ABC-DLBCL 63	87,82
ABC-DLBCL 64	55,26
ABC-DLBCL 65	128,39
ABC-DLBCL 66	68,15
ABC-DLBCL 67	38,15
ABC-DLBCL 68	61,87
ABC-DLBCL 69	93,18
ABC-DLBCL 70	69,86
ABC-DLBCL 71	79,06
ABC-DLBCL 72	60,21

Sample type	DDR1 expression [RMA linear]
ABC-DLBCL 73	62,00
ABC-DLBCL 74	95,89
ABC-DLBCL 75	80,25
ABC-DLBCL 76	103,26
ABC-DLBCL 77	81,98
ABC-DLBCL 78	115,82
ABC-DLBCL 79	93,18
ABC-DLBCL 80	76,17
ABC-DLBCL 81	127,01
ABC-DLBCL 82	83,96
ABC-DLBCL 83	71,97
ABC-DLBCL 84	86,13
ABC-DLBCL 85	95,06
ABC-DLBCL 86	63,40
ABC-DLBCL 87	68,08
ABC-DLBCL 88	75,28
ABC-DLBCL 89	45,64
ABC-DLBCL 90	94,18
ABC-DLBCL 91	131,61
ABC-DLBCL 92	53,65
ABC-DLBCL 93	80,10
ABC-DLBCL 94	101,19
ABC-DLBCL 95	86,37
ABC-DLBCL 96	125,66
ABC-DLBCL 97	158,12
ABC-DLBCL 98	75,61
ABC-DLBCL 99	90,53
ABC-DLBCL 100	172,21
ABC-DLBCL 101	169,32
ABC-DLBCL 102	155,03
ABC-DLBCL 103	112,88
ABC-DLBCL 104	148,31
ABC-DLBCL 105	117,30
ABC-DLBCL 106	94,86
ABC-DLBCL 107	103,39
ABC-DLBCL 108	129,97

Sample type	DDR1 expression [RMA linear]
ABC-DLBCL 109	108,14
ABC-DLBCL 110	106,85
ABC-DLBCL 111	87,48
ABC-DLBCL 112	81,12
ABC-DLBCL 113	57,44
ABC-DLBCL 114	76,54
ABC-DLBCL 115	82,44
ABC-DLBCL 116	144,50
ABC-DLBCL 117	81,89
ABC-DLBCL 118	66,87
ABC-DLBCL 119	110,69
ABC-DLBCL 120	69,56
ABC-DLBCL 121	94,33
ABC-DLBCL 122	57,68
ABC-DLBCL 123	97,69
ABC-DLBCL 124	115,98
ABC-DLBCL 125	99,97
ABC-DLBCL 126	83,63
ABC-DLBCL 127	157,46
ABC-DLBCL 128	229,39
ABC-DLBCL 129	139,80
ABC-DLBCL 130	85,26
ABC-DLBCL 131	73,90
ABC-DLBCL 132	75,55
ABC-DLBCL 133	70,69
ABC-DLBCL 134	81,28
ABC-DLBCL 135	88,84
ABC-DLBCL 136	88,96
ABC-DLBCL 137	100,63
ABC-DLBCL 138	75,82
ABC-DLBCL 139	115,65
ABC-DLBCL 140	57,37
ABC-DLBCL 141	81,54
ABC-DLBCL 142	124,84
ABC-DLBCL 143	63,41
ABC-DLBCL 144	85,94
ABC-DLBCL 145	97,89
ABC-DLBCL 146	90,11
ABC-DLBCL 147	221,94
ABC-DLBCL 148	77,80
ABC-DLBCL 149	102,22

Sample type	DDR1 expression [RMA linear]
ABC-DLBCL 150	74,09
ABC-DLBCL 151	114,54
ABC-DLBCL 152	159,00
ABC-DLBCL 153	83,45
ABC-DLBCL 154	83,70
ABC-DLBCL 155	82,14
ABC-DLBCL 156	71,54
ABC-DLBCL 157	90,31
ABC-DLBCL 158	138,70
ABC-DLBCL 159	86,75
ABC-DLBCL 160	124,56
ABC-DLBCL 161	77,12
ABC-DLBCL 162	148,07
ABC-DLBCL 163	147,19
ABC-DLBCL 164	229,55
ABC-DLBCL 165	120,39
ABC-DLBCL 166	106,44
ABC-DLBCL 167	70,27
GCB-DLBCL 1	120,24
GCB-DLBCL 2	104,25
GCB-DLBCL 3	68,29
GCB-DLBCL 4	88,54
GCB-DLBCL 5	139,15
GCB-DLBCL 6	106,72
GCB-DLBCL 7	73,69
GCB-DLBCL 8	93,47
GCB-DLBCL 9	51,27
GCB-DLBCL 10	91,66
GCB-DLBCL 11	105,60
GCB-DLBCL 12	98,24
GCB-DLBCL 13	66,96
GCB-DLBCL 14	75,86
GCB-DLBCL 15	85,44
GCB-DLBCL 16	123,35
GCB-DLBCL 17	51,92
GCB-DLBCL 18	127,00
GCB-DLBCL 19	125,28
GCB-DLBCL 20	58,21
GCB-DLBCL 21	163,67
GCB-DLBCL 22	139,47
GCB-DLBCL 23	59,62

Sample type	DDR1 expression [RMA linear]
GCB-DLBCL 24	104,86
GCB-DLBCL 25	78,88
GCB-DLBCL 26	70,68
GCB-DLBCL 27	62,82
GCB-DLBCL 28	164,41
GCB-DLBCL 29	116,78
GCB-DLBCL 30	85,78
GCB-DLBCL 31	72,59
GCB-DLBCL 32	77,32
GCB-DLBCL 33	73,36
GCB-DLBCL 34	75,46
GCB-DLBCL 35	105,10
GCB-DLBCL 36	120,59
GCB-DLBCL 37	63,57
GCB-DLBCL 38	131,40
GCB-DLBCL 39	67,43
GCB-DLBCL 40	100,08
GCB-DLBCL 41	95,85
GCB-DLBCL 42	65,64
GCB-DLBCL 43	96,81
GCB-DLBCL 44	115,93
GCB-DLBCL 45	66,35
GCB-DLBCL 46	65,42
GCB-DLBCL 47	108,68
GCB-DLBCL 48	103,19
GCB-DLBCL 49	66,92
GCB-DLBCL 50	111,98
GCB-DLBCL 51	85,67
GCB-DLBCL 52	105,66
GCB-DLBCL 53	100,47
GCB-DLBCL 54	93,49
GCB-DLBCL 55	66,38
GCB-DLBCL 56	120,38
GCB-DLBCL 57	143,44
GCB-DLBCL 58	111,10
GCB-DLBCL 59	81,29
GCB-DLBCL 60	70,29
GCB-DLBCL 61	72,10
GCB-DLBCL 62	130,64
GCB-DLBCL 63	172,62
GCB-DLBCL 64	104,84

Sample type	DDR1 expression [RMA linear]
GCB-DLBCL 65	102,83
GCB-DLBCL 66	82,05
GCB-DLBCL 67	136,21
GCB-DLBCL 68	176,49
GCB-DLBCL 69	94,21
GCB-DLBCL 70	169,41
GCB-DLBCL 71	215,97
GCB-DLBCL 72	83,96
GCB-DLBCL 73	65,68
GCB-DLBCL 74	69,63
GCB-DLBCL 75	101,80
GCB-DLBCL 76	79,86
GCB-DLBCL 77	64,12
GCB-DLBCL 78	85,12
GCB-DLBCL 79	109,69
GCB-DLBCL 80	74,11
GCB-DLBCL 81	78,77
GCB-DLBCL 82	120,86
GCB-DLBCL 83	106,70
GCB-DLBCL 84	147,35
GCB-DLBCL 85	167,67
GCB-DLBCL 86	195,17
GCB-DLBCL 87	50,75
GCB-DLBCL 88	122,34
GCB-DLBCL 89	120,69
GCB-DLBCL 90	86,77
GCB-DLBCL 91	104,21
GCB-DLBCL 92	79,46
GCB-DLBCL 93	169,49
GCB-DLBCL 94	102,01
GCB-DLBCL 95	73,45
GCB-DLBCL 96	123,50
GCB-DLBCL 97	113,74
GCB-DLBCL 98	81,17
GCB-DLBCL 99	135,55
GCB-DLBCL 100	103,68
GCB-DLBCL 101	59,44
GCB-DLBCL 102	70,94
GCB-DLBCL 103	99,42
GCB-DLBCL 104	133,39
GCB-DLBCL 105	115,73

Sample type	DDR1 expression [RMA linear]
GCB-DLBCL 106	182,46
GCB-DLBCL 107	63,38
GCB-DLBCL 108	106,71
GCB-DLBCL 109	141,24
GCB-DLBCL 110	242,09
GCB-DLBCL 111	143,44
GCB-DLBCL 112	82,03
GCB-DLBCL 113	147,07
GCB-DLBCL 114	132,74
GCB-DLBCL 115	94,01
GCB-DLBCL 116	122,61
GCB-DLBCL 117	82,53
GCB-DLBCL 118	80,76
GCB-DLBCL 119	92,64
GCB-DLBCL 120	114,85
GCB-DLBCL 121	92,71
GCB-DLBCL 122	110,49
GCB-DLBCL 123	115,88
GCB-DLBCL 124	131,88
GCB-DLBCL 125	174,08
GCB-DLBCL 126	106,23
GCB-DLBCL 127	106,57
GCB-DLBCL 128	105,24
GCB-DLBCL 129	432,21
GCB-DLBCL 130	154,03
GCB-DLBCL 131	92,21
GCB-DLBCL 132	173,03
GCB-DLBCL 133	90,75
GCB-DLBCL 134	201,66
GCB-DLBCL 135	168,89
GCB-DLBCL 136	68,51
GCB-DLBCL 137	111,85
GCB-DLBCL 138	91,95
GCB-DLBCL 139	91,90
GCB-DLBCL 140	88,72
GCB-DLBCL 141	117,13
GCB-DLBCL 142	185,38
GCB-DLBCL 143	122,52
GCB-DLBCL 144	115,99
GCB-DLBCL 145	110,35
GCB-DLBCL 146	83,24

Sample type	DDR1 expression [RMA linear]
GCB-DLBCL 147	119,06
GCB-DLBCL 148	97,24
GCB-DLBCL 149	102,06
GCB-DLBCL 150	92,56
GCB-DLBCL 151	87,22
GCB-DLBCL 152	77,41
GCB-DLBCL 153	133,53
GCB-DLBCL 154	75,60
GCB-DLBCL 155	104,22
GCB-DLBCL 156	102,50
GCB-DLBCL 157	161,63
GCB-DLBCL 158	545,81
GCB-DLBCL 159	86,93
GCB-DLBCL 160	101,86
GCB-DLBCL 161	563,08
GCB-DLBCL 162	55,10
GCB-DLBCL 163	96,41
GCB-DLBCL 164	82,01
GCB-DLBCL 165	110,44
GCB-DLBCL 166	109,90
GCB-DLBCL 167	81,56
GCB-DLBCL 168	83,07
GCB-DLBCL 169	78,43
GCB-DLBCL 170	105,74
GCB-DLBCL 171	98,95
GCB-DLBCL 172	69,53
GCB-DLBCL 173	74,93
GCB-DLBCL 174	123,23
GCB-DLBCL 175	151,00
GCB-DLBCL 176	92,19
GCB-DLBCL 177	76,62
GCB-DLBCL 178	89,16
GCB-DLBCL 179	128,94
GCB-DLBCL 180	76,33
GCB-DLBCL 181	218,18
GCB-DLBCL 182	169,89
GCB-DLBCL 183	64,04

Appendix 4. DDR1 expression in 50 samples from a series of tumour biopsies of DLBCL patients and 3 GC B cells samples, obtained by Fluidigm®48.48 Fast Real Time PCR analysis.

	Sample	Relative expression of DDR1
GC B cells	GCB 1	2,470647
	GCB 2	1,239899
	GCB 3	0,882194
DLBCL	8	956,5984
	26	264,5807
	1	19,05468
	17B	16,85453
	7B	11,50662
	9B	10,70792
	10B	7,98521
	30B	5,447077
	7	4,457224
	23	4,281078
	12B	3,636998
	13	3,516518
	5	2,767029
	19	2,718059
	26B	2,525352
	6	2,474068
	15	2,320874
	3B	2,268519
	5B	2,268519
	25B	2,214993
	22	1,676158
	27B	1,573339
24	1,570151	
14	1,459154	

	Sample	Relative expression of DDR1
DLBCL	20B	1,355245
	3	1,22243
	18	1,179488
	14B	1,148293
	9	0,958022
	19B	0,942199
	4B	0,738605
	2	0,722606
	18B	0,549832
	16	0,503887
	10	0,494023
	4	0,424183
	20	0,14693
	24B	0,023967
	11	0
	12	0
	17	0
	21	0
	25	0
	13B	0
	1B	0
	21B	0
	22B	0
28B	0	
2B	0	
8B	0	

Appendix 5. List of collagen genes (source: <http://www.genenames.org/genefamilies/COLLAGEN>).

Name of collagen gene
COL1A1
COL1A2
COL2A1
COL3A1
COL4A1
COL4A2
COL4A3
COL4A4
COL4A5
COL4A6
COL5A1
COL5A2
COL5A3
COL6A1
COL6A2
COL6A3
COL6A4P1
COL6A4P2
COL6A5
COL6A6
COL7A1
COL8A1
COL8A2

COL9A1
COL9A2
COL9A3
COL10A1
COL11A1
COL11A2
COL12A1
COL13A1
COL14A1
COL15A1
COL16A1
COL17A1
COL18A1
COL19A1
COL20A1
COL21A1
COL22A1
COL23A1
COL24A1
COL25A1
COL26A1
COL27A1
COL28A1

Appendix 6A. TRI70 aneuploidy genes signature, which contains 20 genes positively correlated with aneuploidy and 50 genes negatively correlated with aneuploidy.

Positively correlated with aneuploidy
ANXA7
ATG7
BDNF
CDKN2B
CHFR
CNDP2
ENO3
F3
GIPC2
GJB5
HSPB7
IMPACT
P2RY14
PCDH7
PKD1
PLCG2
SNCA
SNCG
TMEM140
TMEM40
Negatively correlated with aneuploidy
AURKA
BCL11B
BIRC5
BLMH
BRD8
BUB1B
CCNA2
CDC5L
CDK1
CENPE
CENPN
CTH
DLGAP5
HMGB2
IDH2
ISOC1

KIAA0101
KIF22
LIG1
LSM2
MCM2
MCM5
MCM7
MYBL2
NASP
NCAPD2
NCAPH
NMI
NUDT21
PCNA
PIGO
PLK1
PLK4
POLD2
RACGAP1
RAD51
RFC2
RFC3
RFC5
RPA2
SMAD4
SMC4
SSRP1
TAB2
TCOF1
TIMELESS
TIPIN
TOP2A
UBE2C
USP1

Appendix 6B. 70 genes from HET70 aneuploidy gene signature.

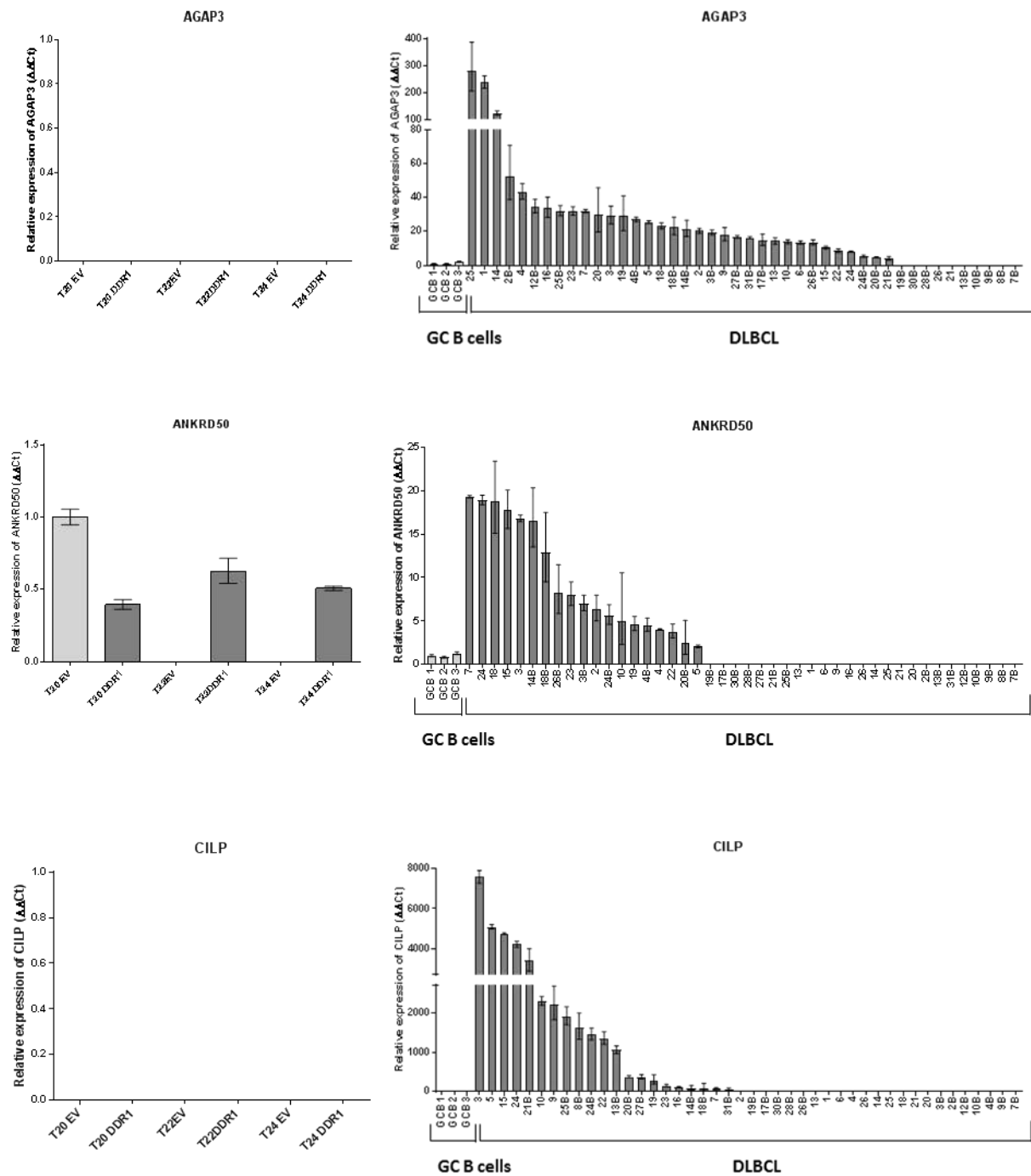
AHCYL1
AKT3
ANO10
ANTXR1
ATP6V0E1
ATXN1
B4GALT2
BASP1
BHLHE40
BLVRA
CALU
CAP1
CAST
CAV1
CLIC4
CTSL
CYB5R3
ELOVL1
EMP3
FKBP14
FN1
FST
GNA12
GOLT1B
HECTD3
HEG1
HOMER3
IGFBP3
IL6ST
ITCH
P3H1
P3H2
LEPROT
LGALS1
LIMA1
LPP

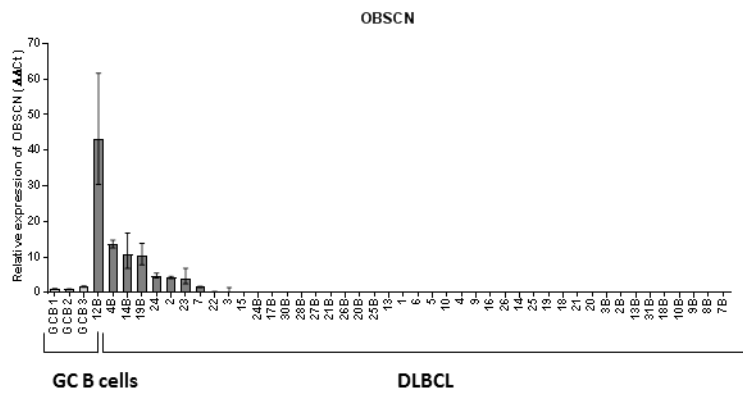
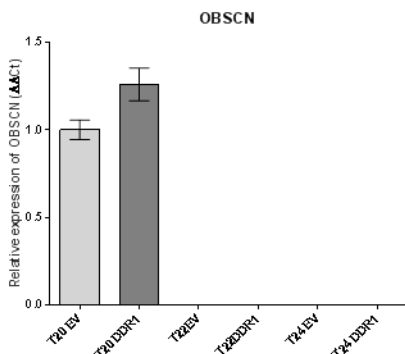
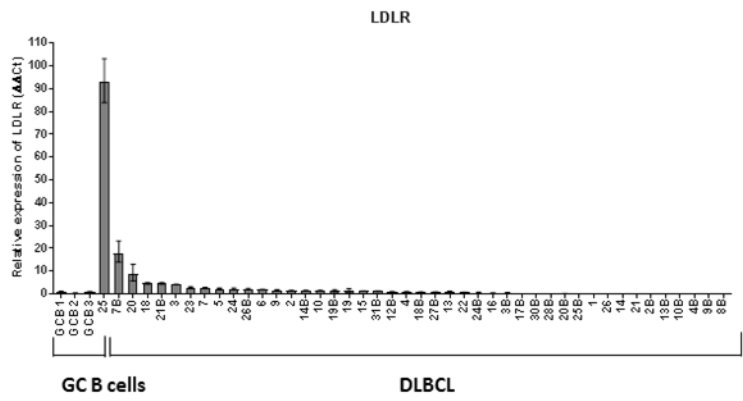
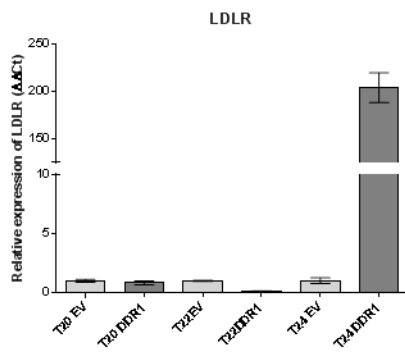
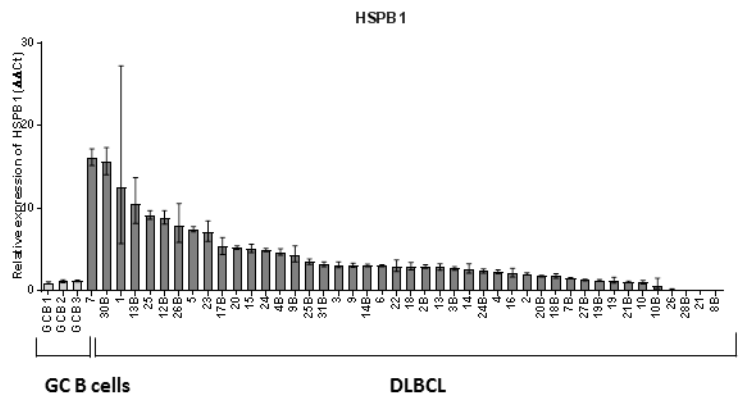
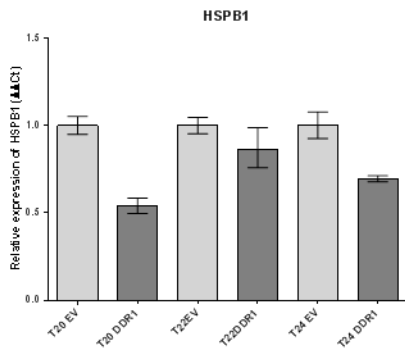
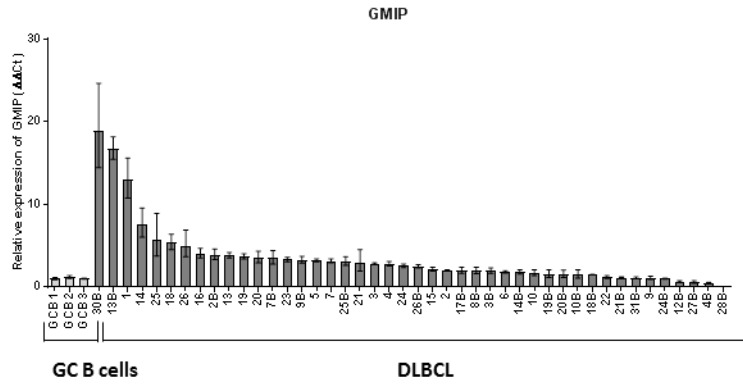
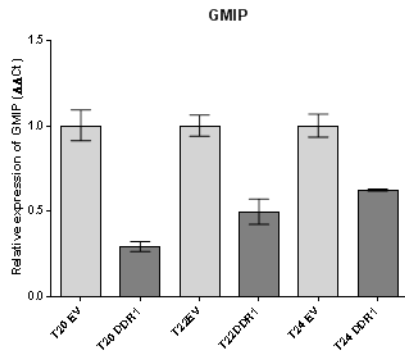
MED8
MMP2
MUL1
MYO10
NAGK
NR1D2
NRIP3
P4HA2
PKIG
PLOD2
PMP22
POFUT2
POMGNT1
PRKAR2A
AGER
RHOC
RRAGC
SEC22B
SERPINB8
SPAG9
SQSTM1
TIMP2
EMC3
TRIM16
TRIO
TUBB2A
VEGFC
VIM
WASL
YIPF5
YKT6
ZBTB38
ZCCHC24
ZMPSTE24

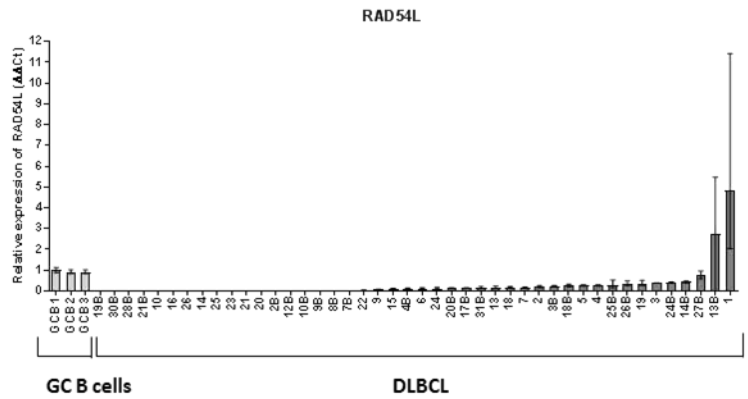
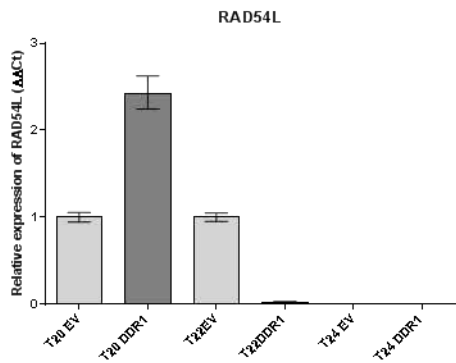
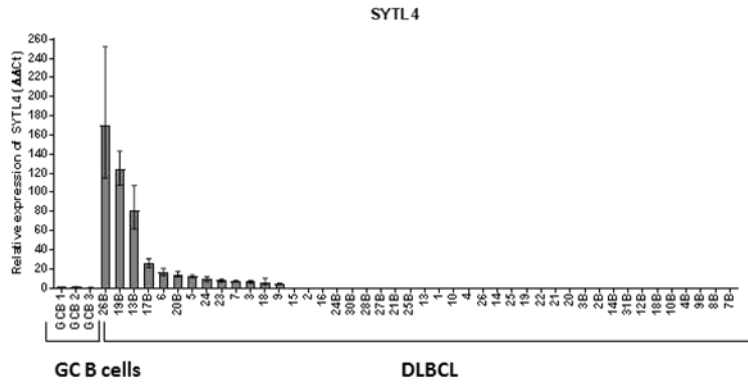
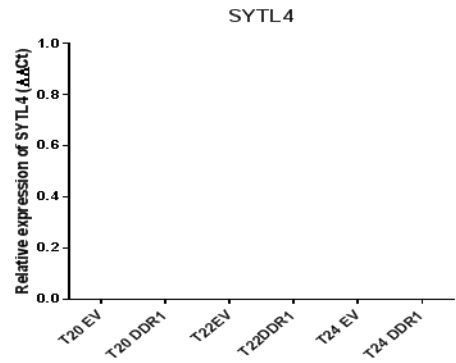
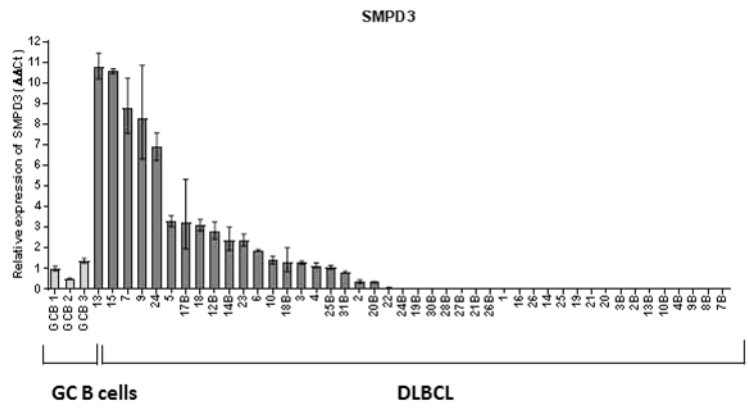
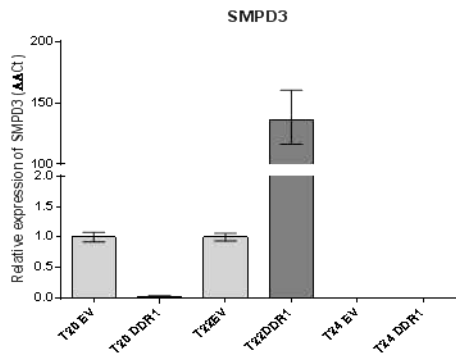
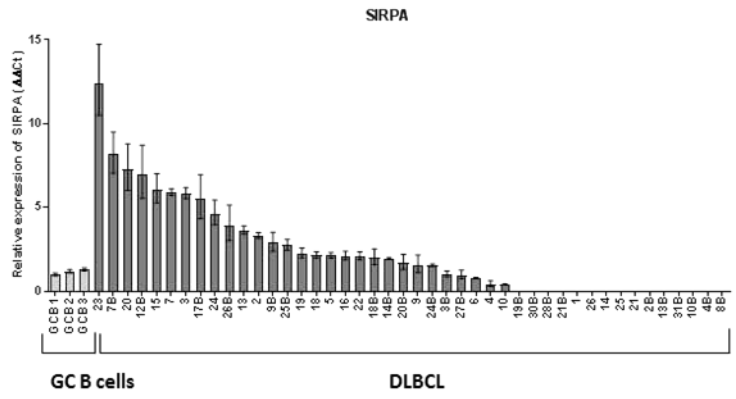
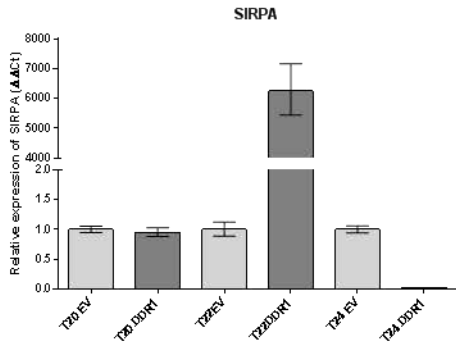
Appendix 7. Quality check for GC B cells transfected with DDR1 and EV as a control, stimulated with collagen for 4 and 8 hours. Data from one tonsil.

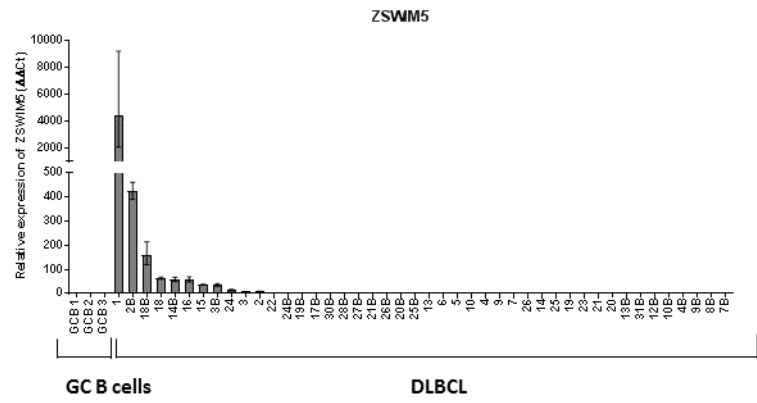
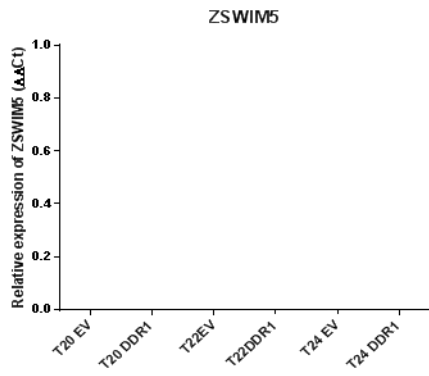
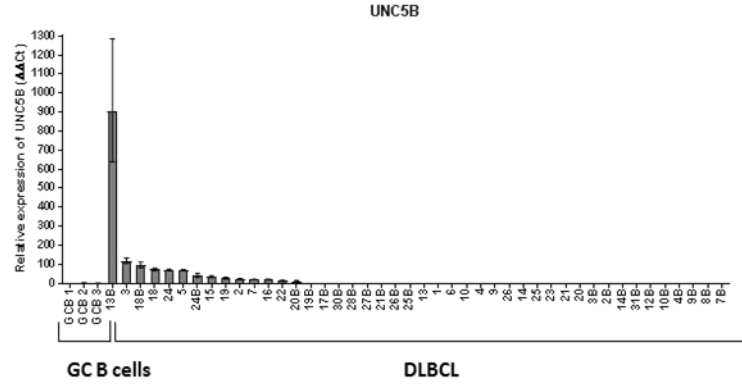
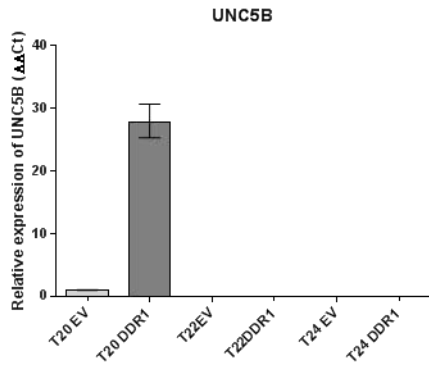
Time of stimulation	Sample	RNA concentration [pg/μl]	RIN
4 HOURS	EV + collagen	50	8.20
	DDR1 + collagen	322	7.80
8 HOURS	EV + collagen	91	2.90
	DDR1 + collagen	588	N/A

Appendix 8. DDR1 target genes not validated in GCB cells transfected with DDR1 or EV (left), and its expression in primary DLBCL (right).









References

- ABDULHUSSEIN, R., MCFADDEN, C., FUENTES-PRIOR, P. & VOGEL, W. F. 2004. Exploring the collagen-binding site of the DDR1 tyrosine kinase receptor. *Journal of Biological Chemistry*, 279, 31462-31470.
- ABRIEU, A., KAHANA, J. A., WOOD, K. W. & CLEVELAND, D. W. 2000. CENP-E as an essential component of the mitotic checkpoint in vitro. *Molecular Biology of the Cell*, 11, 447A-447A.
- ABRIEU, A., MAGNAGHI-JAULIN, L., KAHANA, J. A., PETER, M., CASTRO, A., VIGNERON, S., LORCA, T., CLEVELAND, D. W. & LABBE, J. C. 2001. Mps1 is a kinetochore-associated kinase essential for the vertebrate mitotic checkpoint. *Cell*, 106, 83-93.
- AFONSO, P. V., MCCANN, C. P., KAPNICK, S. M. & PARENT, C. A. 2013. Discoidin domain receptor 2 regulates neutrophil chemotaxis in 3D collagen matrices. *Blood*, 121, 1644-50.
- AGARWAL, R., GONZALEZ-ANGULO, A.-M., MYHRE, S., CAREY, M., LEE, J.-S., OVERGAARD, J., ALSNER, J., STEMKE-HALE, K., LLUCH, A., NEVE, R. M., KUO, W. L., SORLIE, T., SAHIN, A., VALERO, V., KEYOMARSI, K., GRAY, J. W., BORRESEN-DALE, A.-L., MILLS, G. B. & HENNESSY, B. T. 2009. Integrative Analysis of Cyclin Protein Levels Identifies Cyclin B1 as a Classifier and Predictor of Outcomes in Breast Cancer. *Clinical Cancer Research*, 15, 3654-3662.
- ALIZADEH, A. A., EISEN, M. B., DAVIS, R. E., MA, C., LOSSOS, I. S., ROSENWALD, A., BOLDRICK, J. C., SABET, H., TRAN, T., YU, X., POWELL, J. I., YANG, L., MARTI, G. E., MOORE, T., HUDSON, J., JR., LU, L., LEWIS, D. B., TIBSHIRANI, R., SHERLOCK, G., CHAN, W. C., GREINER, T. C., WEISENBURGER, D. D., ARMITAGE, J. O., WARNKE, R., LEVY, R., WILSON, W., GREVER, M. R., BYRD, J. C., BOTSTEIN, D., BROWN, P. O. & STAUDT, L. M. 2000. Distinct types of diffuse large B-cell lymphoma identified by gene expression profiling. *Nature*, 403, 503-11.
- ALVES, F., SAUPE, S., LEDWON, M., SCHAUB, F., HIDDEMANN, W. & VOGEL, W. F. 2001. Identification of two novel, kinase-deficient variants of discoidin domain receptor 1: differential expression in human colon cancer cell lines. *FASEB J*, 15, 1321-3.
- ALVES, F., VOGEL, W., MOSSIE, K., MILLAUER, B., HOFER, H. & ULLRICH, A. 1995. Distinct structural characteristics of discoidin I subfamily receptor tyrosine kinases and complementary expression in human cancer. *Oncogene*, 10, 609-18.
- AMINI, R. M., BERGLUND, M., ROSENQUIST, R., VON HEIDEMAN, A., LAGERCRANTZ, S., THUNBERG, U., BERGH, J., SUNDSTROM, C., GLIMELIUS, B. & ENBLAD, G. 2002. A novel B-cell line (U-2932) established from a patient with diffuse large B-cell lymphoma following Hodgkin lymphoma. *Leukemia & Lymphoma*, 43, 2179-2189.
- ARKIN, I. T. 2002. Structural aspects of oligomerization taking place between the transmembrane alpha-helices of bitopic membrane proteins. *Biochimica Et Biophysica Acta-Biomembranes*, 1565, 347-363.
- ASSENT, D., BOURGOT, I., HENNUY, B., GEURTS, P., NOEL, A., FOIDART, J. M. & MAQUOI, E. 2015. A membrane-type-1 matrix metalloproteinase (MT1-MMP)-discoidin domain receptor 1 axis regulates collagen-induced apoptosis in breast cancer cells. *PLoS One*, 10, e0116006.

- AVILES, A., DELGADO, S., NAMBO, M. J., ALATRISTE, S. & DIAZMAQUEO, J. C. 1994. ADJUVANT RADIOTHERAPY TO SITES OF PREVIOUS BULKY DISEASE IN PATIENTS STAGE-IV DIFFUSE LARGE-CELL LYMPHOMA. *International Journal of Radiation Oncology Biology Physics*, 30, 799-803.
- AVILES, A., NERI, N., DELGADO, S., PEREZ, F., NAMBO, M. J., CLETO, S., TALAVERA, A. & HUERTA-GUZMAN, J. 2005. Residual disease after chemotherapy in aggressive malignant lymphoma. *Medical Oncology*, 22, 383-387.
- AVIVI-GREEN, C., SINGAL, M. & VOGEL, W. F. 2006. Discoidin domain receptor 1-deficient mice are resistant to bleomycin-induced lung fibrosis. *Am J Respir Crit Care Med*, 174, 420-7.
- BABU, J. R., JEGANATHAN, K. B., BAKER, D. J., WU, X. S., KANG-DECKER, N. & VAN DEURSEN, J. M. 2003. Rae1 is an essential mitotic checkpoint regulator that cooperates with Bub3 to prevent chromosome missegregation. *Journal of Cell Biology*, 160, 341-353.
- BAKHOUM, S. F., DANILOVA, O. V., KAUR, P., LEVY, N. B. & COMPTON, D. A. 2011a. Chromosomal instability substantiates poor prognosis in patients with diffuse large B-cell lymphoma. *Clin Cancer Res*, 17, 7704-11.
- BAKHOUM, S. F., DANILOVA, O. V., KAUR, P., LEVY, N. B. & COMPTON, D. A. 2011b. Chromosomal Instability Substantiates Poor Prognosis in Patients with Diffuse Large B-cell Lymphoma. *Clinical Cancer Research*, 17, 7704-7711.
- BALAMUTH, N. J., WOOD, A., WANG, Q., JAGANNATHAN, J., MAYES, P., ZHANG, Z., CHEN, Z., RAPPAPORT, E., COURTRIGHT, J., PAWEL, B., WEBER, B., WOOSTER, R., SEKYERE, E. O., MARSHALL, G. M. & MARIS, J. M. 2010. Serial Transcriptome Analysis and Cross-Species Integration Identifies Centromere-Associated Protein E as a Novel Neuroblastoma Target. *Cancer Research*, 70, 2749-2758.
- BARGAL, R., CORMIER-DAIRE, V., BEN-NERIAH, Z., LE MERRER, M., SOSNA, J., MELKI, J., ZANGEN, D. H., SMITHSON, S. F., BOROCHOWITZ, Z., BELOSTOTSKY, R. & RAAS-ROTHSCHILD, A. 2009. Mutations in DDR2 Gene Cause SMED with Short Limbs and Abnormal Calcifications. *American Journal of Human Genetics*, 84, 80-84.
- BARISIONE, G., FABBI, M., CUTRONA, G., DE CECCO, L., ZUPO, S., LEITINGER, B., GENTILE, M., MANZONI, M., NERI, A., MORABITO, F., FERRARINI, M. & FERRINI, S. 2017. Heterogeneous expression of the collagen receptor DDR1 in chronic lymphocytic leukaemia and correlation with progression. *Blood Cancer J*, 7.
- BARKER, K. T., MARTINDALE, J. E., MITCHELL, P. J., KAMALATI, T., PAGE, M. J., PHIPPARD, D. J., DALE, T. C., GUSTERSON, B. A. & CROMPTON, M. R. 1995. EXPRESSION PATTERNS OF THE NOVEL RECEPTOR-LIKE TYROSINE KINASE, DDR, IN HUMAN BREAST-TUMORS. *Oncogene*, 10, 569-575.
- BARRANS, S., CROUCH, S., SMITH, A., TURNER, K., OWEN, R., PATMORE, R., ROMAN, E. & JACK, A. 2010. Rearrangement of MYC Is Associated With Poor Prognosis in Patients With Diffuse Large B-Cell Lymphoma Treated in the Era of Rituximab. *Journal of Clinical Oncology*, 28, 3360-3365.
- BASSO, K. & DALLA-FAVERA, R. 2012. Roles of BCL6 in normal and transformed germinal center B cells. *Immunol Rev*, 247, 172-83.
- BEA, S., ZETTL, A., WRIGHT, G., SALAVERRIA, I., JEHN, P., MORENO, V., BUREK, C., OTT, G., PUIG, X., YANG, L., LOPEZ-GUILLERMO, A., CHAN, W. C., GREINER, T. C.,

- WEISENBURGER, D. D., ARMITAGE, J. O., GASCOYNE, R. D., CONNORS, J. M., GROGAN, T. M., BRAZIEL, R., FISHER, R. I., SMELAND, E. B., KVALOY, S., HOLTE, H., DELABIE, J., SIMON, R., POWELL, J., WILSON, W. H., JAFFE, E. S., MONTSERRAT, E., MULLER-HERMELINK, H. K., STAUDT, L. M., CAMPO, E. & ROSENWALD, A. 2005. Diffuse large B-cell lymphoma subgroups have distinct genetic profiles that influence tumor biology and improve gene-expression-based survival prediction. *Blood*, 106, 3183-90.
- BECKWITH, M., LONGO, D. L., OCONNELL, C. D., MORATZ, C. M. & URBA, W. J. 1990. PHORBOL ESTER-INDUCED, CELL-CYCLE-SPECIFIC, GROWTH-INHIBITION OF HUMAN B-LYMPHOMA CELL-LINES. *Journal of the National Cancer Institute*, 82, 501-509.
- BEGUELIN, W., POPOVIC, R., TEATER, M., JIANG, Y., BUNTING, K. L., ROSEN, M., SHEN, H., YANG, S. N., WANG, L., EZPONDA, T., MARTINEZ-GARCIA, E., ZHANG, H., ZHENG, Y., VERMA, S. K., MCCABE, M. T., OTT, H. M., VAN ALLER, G. S., KRUGER, R. G., LIU, Y., MCHUGH, C. F., SCOTT, D. W., CHUNG, Y. R., KELLEHER, N., SHAKNOVICH, R., CREASY, C. L., GASCOYNE, R. D., WONG, K.-K., CERCHIETTI, L., LEVINE, R. L., ABDELWAHAB, O., LICHT, J. D., ELEMENTO, O. & MELNICK, A. M. 2013. EZH2 Is Required for Germinal Center Formation and Somatic EZH2 Mutations Promote Lymphoid Transformation. *Cancer Cell*, 23, 677-692.
- BENBASSAT, H., GOLDBLUM, N., MITRANI, S., GOLDBLUM, T., YOFFEY, J. M., COHEN, M. M., BENTWICH, Z., RAMOT, B., KLEIN, E. & KLEIN, G. 1977. ESTABLISHMENT IN CONTINUOUS CULTURE OF A NEW TYPE OF LYMPHOCYTE FROM A BURKITT-LIKE MALIGNANT-LYMPHOMA (LINE DG-75). *International Journal of Cancer*, 19, 27-33.
- BENBASSAT, H., POLLIACK, A., SHLOMAI, Z., KOHN, G., HADAR, R., RABINOWITZ, R., LEIZEROWITZ, R., MATUTES, E., BUCHIER, V., BROKSIMONI, F., OKON, E., LIVNI, N. & SCHLESINGER, M. 1992. FARAGE, A NOVEL EARLY B-CELL LYMPHOMA CELL-LINE WITH TRISOMY 11. *Leukemia & Lymphoma*, 6, 513-521.
- BENNASROUNE, A., GARDIN, A., AUNIS, D., CREMEL, G. & HUBERT, P. 2004. Tyrosine kinase receptors as attractive targets of cancer therapy. *Critical Reviews in Oncology Hematology*, 50, 23-38.
- BENNETT, A., BECHI, B., TIGHE, A., THOMPSON, S., PROCTER, D. J. & TAYLOR, S. S. 2015. Cenp-E inhibitor GSK923295: Novel synthetic route and use as a tool to generate aneuploidy. *Oncotarget*, 6, 20921-20932.
- BERNASCONI, B., KARAMITOPOLOU-DIAMANTIIS, E., TORNILLO, L., LUGLI, A., DI VIZIO, D., DIRNHOFER, S., WENGMANN, S., GLATZ-KRIEGER, K., FEND, F., CAPELLA, C., INSABATO, L. & TERRACCIANO, L. M. 2008. Chromosomal instability in gastric mucosa-associated lymphoid tissue lymphomas: a fluorescent in situ hybridization study using a tissue microarray approach. *Human Pathology*, 39, 536-542.
- BERTRAND, T., KOTHE, M., LIU, J., DUPUY, A., RAK, A., BERNE, P. F., DAVIS, S., GLADYSHEVA, T., VALTRE, C., CRENNE, J. Y. & MATHIEU, M. 2012. The Crystal Structures of TrkA and TrkB Suggest Key Regions for Achieving Selective Inhibition. *Journal of Molecular Biology*, 423, 439-453.
- BHATT, R. S., TOMODA, T., FANG, Y. & HATTEN, M. E. 2000. Discoidin domain receptor 1 functions in axon extension of cerebellar granule neurons. *Genes Dev*, 14, 2216-28.

- BLOOMFIELD, C. D., ARTHUR, D. C., FRIZZERA, G., LEVINE, E. G., PETERSON, B. A. & GAJLPECZALSKA, K. J. 1983. NONRANDOM CHROMOSOME-ABNORMALITIES IN LYMPHOMA. *Cancer Research*, 43, 2975-2984.
- BLUME-JENSEN, P. & HUNTER, T. 2001. Oncogenic kinase signalling. *Nature*, 411, 355-365.
- BOLSTAD, B. M., IRIZARRY, R. A., ASTRAND, M. & SPEED, T. P. 2003. A comparison of normalization methods for high density oligonucleotide array data based on variance and bias. *Bioinformatics*, 19, 185-193.
- BOROCHOWITZ, Z., LANGER, L. O., GRUBER, H. E., LACHMAN, R., KATZNELSON, M. B. M. & RIMOIN, D. L. 1993. SPONDYLOMETAEPHYPHYSEAL DYSPLASIA (SMED), SHORT LIMB-HAND TYPE - A CONGENITAL FAMILIAL SKELETAL DYSPLASIA WITH DISTINCTIVE FEATURES AND HISTOPATHOLOGY. *American Journal of Medical Genetics*, 45, 320-326.
- BORZA, C. M. & POZZI, A. 2014. Discoidin domain receptors in disease. *Matrix Biol*, 34, 185-92.
- BOVERI, T. 1902. Über mehrpolige Mitosen als Mittel zur analyse des zelikerns. *Verh. D. phys. Med Ges. Wurzburg N.F.*, 35, 67-90.
- BROMANN, P. A., KORKAYA, H. & COURTNEIDGE, S. A. 2004. The interplay between Src family kinases and receptor tyrosine kinases. *Oncogene*, 23, 7957-7968.
- BRUNE, V., TIACCI, E., PFEIL, I., DORING, C., ECKERLE, S., VAN NOESEL, C. J., KLAPPER, W., FALINI, B., VON HEYDEBRECK, A., METZLER, D., BRAUNINGER, A., HANSMANN, M. L. & KUPPERS, R. 2008. Origin and pathogenesis of nodular lymphocyte-predominant Hodgkin lymphoma as revealed by global gene expression analysis. *J Exp Med*, 205, 2251-68.
- BUNZ, F., FAUTH, C., SPEICHER, M. R., DUTRIAUX, A., SEDIVY, J. M., KINZLER, K. W., VOGELSTEIN, B. & LENGAUER, C. 2002. Targeted inactivation of p53 in human cells does not result in aneuploidy. *Cancer Research*, 62, 1129-1133.
- BURKES, R. L., MEYER, P. R., GILL, P. S., PARKER, J. W., RASHEED, S. & LEVINE, A. M. 1986. Rectal lymphoma in homosexual men. *Arch Intern Med*, 146, 913-5.
- CADER, F. Z., VOCKERODT, M., BOSE, S., NAGY, E., BRUNDLER, M. A., KEARNS, P. & MURRAY, P. G. 2013. The EBV oncogene LMP1 protects lymphoma cells from cell death through the collagen-mediated activation of DDR1. *Blood*, 122, 4237-45.
- CAGANOVA, M., CARRISI, C., VARANO, G., MAINOLDI, F., ZANARDI, F., GERMAIN, P. L., GEORGE, L., ALBERGHINI, F., FERRARINI, L., TALUKDER, A. K., PONZONI, M., TESTA, G., NOJIMA, T., DOGLIONI, C., KITAMURA, D., TOELLNER, K. M., SU, I. H. & CASOLA, S. 2013. Germinal center dysregulation by histone methyltransferase EZH2 promotes lymphomagenesis. *Journal of Clinical Investigation*, 123, 5009-5022.
- CAHILL, D. P., LENGAUER, C., YU, J., RIGGINS, G. J., WILLSON, J. K. V., MARKOWITZ, S. D., KINZLER, K. W. & VOGELSTEIN, B. 1998. Mutations of mitotic checkpoint genes in human cancers. *Nature*, 392, 300-303.
- CANNING, P., TAN, L., CHU, K., LEE, S. W., GRAY, N. S. & BULLOCK, A. N. 2014. Structural Mechanisms Determining Inhibition of the Collagen Receptor DDR1 by Selective and Multi-Targeted Type II Kinase Inhibitors. *Journal of Molecular Biology*, 426, 2457-2470.

- CARAFOLI, F., BIHAN, D., STATHOPOULOS, S., KONITSIOTIS, A. D., KVANSAKUL, M., FARNDAL, R. W., LEITINGER, B. & HOHENESTER, E. 2009. Crystallographic insight into collagen recognition by discoidin domain receptor 2. *Structure*, 17, 1573-81.
- CARAFOLI, F., MAYER, M. C., SHIRAIISHI, K., PECHEVA, M. A., CHAN, L. Y., NAN, R., LEITINGER, B. & HOHENESTER, E. 2012. Structure of the discoidin domain receptor 1 extracellular region bound to an inhibitory Fab fragment reveals features important for signaling. *Structure*, 20, 688-97.
- CARE, M. A., WESTHEAD, D. R. & TOOZE, R. M. 2015. Gene expression meta-analysis reveals immune response convergence on the IFN gamma-STAT1-IRF1 axis and adaptive immune resistance mechanisms in lymphoma. *Genome Medicine*, 7.
- CARGNELLO, M. & ROUX, P. P. 2011. Activation and Function of the MAPKs and Their Substrates, the MAPK-Activated Protein Kinases. *Microbiology and Molecular Biology Reviews*, 75, 50-83.
- CASTRO-SANCHEZ, L., SOTO-GUZMAN, A., NAVARRO-TITO, N., MARTINEZ-OROZCO, R. & SALAZAR, E. P. 2010. Native type IV collagen induces cell migration through a CD9 and DDR1-dependent pathway in MDA-MB-231 breast cancer cells. *Eur J Cell Biol*, 89, 843-52.
- CHALLA-MALLADI, M., LIEU, Y. K., CALIFANO, O., HOLMES, A. B., BHAGAT, G., MURTY, V. V., DOMINGUEZ-SOLA, D., PASQUALUCCI, L. & DALLA-FAVERA, R. 2011. Combined genetic inactivation of beta2-Microglobulin and CD58 reveals frequent escape from immune recognition in diffuse large B cell lymphoma. *Cancer Cell*, 20, 728-40.
- CHAN, G. K. T., JABLONSKI, S. A., STARR, D. A., GOLDBERG, M. L. & YEN, T. J. 2000. Human Zw10 and ROD are mitotic checkpoint proteins that bind to kinetochores. *Nature Cell Biology*, 2, 944-947.
- CHAN, G. K. T., JABLONSKI, S. A., SUDAKIN, V., HITTLE, J. C. & YEN, T. J. 1999. Human BUB1 is a mitotic checkpoint kinase that monitors CENP-E functions at kinetochores and binds the cyclosome/APC. *Journal of Cell Biology*, 146, 941-954.
- CHEN, R. H., BRADY, D. M., SMITH, D., MURRAY, A. W. & HARDWICK, K. G. 1999. The spindle checkpoint of budding yeast depends on a tight complex between the Mad1 and Mad2 proteins. *Molecular Biology of the Cell*, 10, 2607-2618.
- CHETOUI, N., EL AZREQ, M. A., BOISVERT, M., BERGERON, M. E. & AOUDJIT, F. 2011. Discoidin domain receptor 1 expression in activated T cells is regulated by the ERK MAP kinase signaling pathway. *J Cell Biochem*, 112, 3666-74.
- CHIARETTI, S., LI, X. C., GENTLEMAN, R., VITALE, A., WANG, K. S., MANDELLI, F., FOA, R. & RITZ, J. 2005. Gene expression profiles of B-lineage adult acute lymphocytic leukemia reveal genetic patterns that identify lineage derivation and distinct mechanisms of transformation. *Clinical Cancer Research*, 11, 7209-7219.
- CHUN, A. C. S. & JIN, D. Y. 2003. Transcriptional regulation of mitotic checkpoint gene MAD1 by p53. *Journal of Biological Chemistry*, 278, 37439-37450.
- CHUNG, V., HEATH, E. I., SCHELMAN, W. R., JOHNSON, B. M., KIRBY, L. C., LYNCH, K. M., BOTBYL, J. D., LAMPKIN, T. A. & HOLEN, K. D. 2012. First-time-in-human study of GSK923295, a novel antimetabolic inhibitor of centromere-associated protein E (CENP-E), in patients with refractory cancer. *Cancer Chemotherapy and Pharmacology*, 69, 733-741.

- CIMINI, D., HOWELL, B., MADDOX, P., KHODJAKOV, A., DEGRASSI, F. & SALMON, E. D. 2001. Merotelic kinetochore orientation is a major mechanism of aneuploidy in mitotic mammalian tissue cells. *Journal of Cell Biology*, 153, 517-527.
- CLEVELAND, D. W., MAO, Y. H. & SULLIVAN, K. F. 2003. Centromeres and kinetochores: From epigenetics to mitotic checkpoint signaling. *Cell*, 112, 407-421.
- COBALEDA, C., SCHEBESTA, A., DELOGU, A. & BUSSLINGER, M. 2007. Pax5: the guardian of B cell identity and function. *Nature Immunology*, 8, 463-470.
- COIFFIER, B., GISSELBRECHT, C., VOSE, J. M., TILLY, H., HERBRECHT, R., BOSLY, A. & ARMITAGE, J. O. 1991. Prognostic factors in aggressive malignant lymphomas: description and validation of a prognostic index that could identify patients requiring a more intensive therapy. The Groupe d'Etudes des Lymphomes Agressifs. *J Clin Oncol*, 9, 211-9.
- COIFFIER, B., LEPAGE, E., BRIERE, J., HERBRECHT, R., TILLY, H., BOUABDALLAH, R., MOREL, P., VAN DEN NESTE, E., SALLES, G., GAULARD, P., REYES, F., LEDERLIN, P. & GISSELBRECHT, C. 2002. CHOP chemotherapy plus rituximab compared with CHOP alone in elderly patients with diffuse large-B-cell lymphoma. *N Engl J Med*, 346, 235-42.
- COIFFIER, B., THIEBLEMONT, C., VAN DEN NESTE, E., LEPEU, G., PLANTIER, I., CASTAIGNE, S., LEFORT, S., MARIT, G., MACRO, M., SEBBAN, C., BELHADJ, K., BORDESSOULE, D., FERME, C. & TILLY, H. 2010. Long-term outcome of patients in the LNH-98.5 trial, the first randomized study comparing rituximab-CHOP to standard CHOP chemotherapy in DLBCL patients: a study by the Groupe d'Etudes des Lymphomes de l'Adulte. *Blood*, 116, 2040-5.
- COLAS, E., PEREZ, C., CABRERA, S., PEDROLA, N., MONGE, M., CASTELLVI, J., EYZAGUIRRE, F., GREGORIO, J., RUIZ, A., LLAURADO, M., RIGAU, M., GARCIA, M., ERTEKIN, T., MONTES, M., LOPEZ-LOPEZ, R., CARRERAS, R., XERCAVINS, J., ORTEGA, A., MAES, T., ROSELL, E., DOLL, A., ABAL, M., REVENTOS, J. & GIL-MORENO, A. 2011. Molecular markers of endometrial carcinoma detected in uterine aspirates. *International Journal of Cancer*, 129, 2435-2444.
- COMPAGNO, M., LIM, W. K., GRUNN, A., NANDULA, S. V., BRAHMACHARY, M., SHEN, Q., BERTONI, F., PONZONI, M., SCANDURRA, M., CALIFANO, A., BHAGAT, G., CHADBURN, A., DALLA-FAVERA, R. & PASQUALUCCI, L. 2009. Mutations of multiple genes cause deregulation of NF-kappaB in diffuse large B-cell lymphoma. *Nature*, 459, 717-21.
- COOPER, M. D. & ALDER, M. N. 2006. The evolution of adaptive immune systems. *Cell*, 124, 815-822.
- COUVELARD, A., HU, J., STEERS, G., O'TOOLE, D., SAUVANET, A., BELGHITI, J., BEDOSSA, P., GATTER, K., RUSZNIEWSKI, P. & PEZZELLA, F. 2006. Identification of potential therapeutic targets by gene-expression profiling in pancreatic endocrine tumors. *Gastroenterology*, 131, 1597-1610.
- CSEH, B., DOMA, E. & BACCARINI, M. 2014. "RAF" neighborhood: Protein-protein interaction in the Raf/Mek/Erk pathway. *Febs Letters*, 588, 2398-2406.
- CURAT, C. A. & VOGEL, W. F. 2002. Discoidin domain receptor 1 controls growth and adhesion of mesangial cells. *J Am Soc Nephrol*, 13, 2648-56.

- DAI, W., WANG, Q., LIU, T., SWAMY, M. & RAO, C. 2004. Slippage of mitotic arrest and enhanced tumor development in mice with BUBR1 haploinsufficiency. *Proceedings of the American Association for Cancer Research Annual Meeting*, 45, 911-911.
- DAR, A. A., GOFF, L. W., MAJID, S., BERLIN, J. & EL-RIFAI, W. 2010. Aurora Kinase Inhibitors - Rising Stars in Cancer Therapeutics? *Molecular Cancer Therapeutics*, 9, 268-278.
- DAS, S., ONGUSAHA, P. P., YANG, Y. S., PARK, J. M., AARONSON, S. A. & LEE, S. W. 2006. Discoidin domain receptor 1 receptor tyrosine kinase induces cyclooxygenase-2 and promotes chemoresistance through nuclear factor-kappaB pathway activation. *Cancer Res*, 66, 8123-30.
- DAVIDS, M. S., SEYMOUR, J. F., GERECITANO, J. F., KAHL, B. S., PAGEL, J. M., WIERDA, W. G., ANDERSON, M. A., RUDERSDORF, N., GRESSICK, L. A., MONTALVO, N. P., YANG, J., ZHU, M., DUNBAR, M., CERRI, E., ENSCHEDE, S. H., HUMERICKHOUSE, R. & ROBERTS, A. W. 2014. Phase I study of ABT-199 (GDC-0199) in patients with relapsed/refractory (R/R) non-Hodgkin lymphoma (NHL): Responses observed in diffuse large B-cell (DLBCL) and follicular lymphoma (FL) at higher cohort doses. *Journal of Clinical Oncology*, 32.
- DAVIES, H., HUNTER, C., SMITH, R., STEPHENS, P., GREENMAN, C., BIGNELL, G., TEAGUE, B., BUTLER, A., EDKINS, S., STEVENS, C., PARKER, A., O'MEARA, S., AVIS, T., BARTHORPE, S., BRACKENBURY, L., BUCK, G., CLEMENTS, B., COLE, J., DICKS, E., EDWARDS, K., FORBES, S., GORTON, M., GRAY, K., HALLIDAY, K., HARRISON, R., HILLS, K., HINTON, J., JONES, D., KOSMIDOU, V., LAMAN, R., LUGG, R., MENZIES, A., PERRY, J., PETTY, R., RAINE, K., SHEPHERD, R., SMALL, A., SOLOMON, H., STEPHENS, Y., TOFTS, C., VARIAN, J., WEBB, A., WEST, S., WIDAA, S., YATES, A., BRASSEUR, F., COOPER, C. S., FLANAGAN, A. M., GREEN, A., KNOWLES, M., LEUNG, S. Y., LOOIJENGA, L. H. J., MALKOWICZ, B., PIEROTTI, M. A., TEH, B. T., YUEN, S. T., LAKHANI, S. R., EASTON, D. F., WEBER, B. L., GOLDSTRAW, P., NICHOLSON, A. G., WOOSTER, R., STRATTON, M. R. & FUTREAL, P. A. 2005. Somatic mutations of the protein kinase gene family in human lung cancer. *Cancer Research*, 65, 7591-7595.
- DAVIES, M. L., XU, S., LYONS-WEILER, J., ROSENDORFF, A., WEBBER, S. A., WASIL, L. R., METES, D. & ROWE, D. T. 2010. Cellular factors associated with latency and spontaneous Epstein-Barr virus reactivation in B-lymphoblastoid cell lines. *Virology*, 400, 53-67.
- DAVIS, R. E., BROWN, K. D., SIEBENLIST, U. & STAUDT, L. M. 2001. Constitutive nuclear factor kappa B activity is required for survival of activated B cell-like diffuse large B cell lymphoma cells. *Journal of Experimental Medicine*, 194, 1861-1874.
- DAVIS, R. E., NGO, V. N., LENZ, G., TOLAR, P., YOUNG, R. M., ROMESSER, P. B., KOHLHAMMER, H., LAMY, L., ZHAO, H., YANG, Y., XU, W., SHAFFER, A. L., WRIGHT, G., XIAO, W., POWELL, J., JIANG, J. K., THOMAS, C. J., ROSENWALD, A., OTT, G., MULLER-HERMELINK, H. K., GASCOYNE, R. D., CONNORS, J. M., JOHNSON, N. A., RIMSZA, L. M., CAMPO, E., JAFFE, E. S., WILSON, W. H., DELABIE, J., SMELAND, E. B., FISHER, R. I., BRAZIEL, R. M., TUBBS, R. R., COOK, J. R., WEISENBURGER, D. D., CHAN, W. C., PIERCE, S. K. & STAUDT, L. M. 2010. Chronic active B-cell-receptor signalling in diffuse large B-cell lymphoma. *Nature*, 463, 88-92.
- DAY, E., WATERS, B., SPIEGEL, K., ALNADAF, T., MANLEY, P. W., BUCHDUNGER, E., WALKER, C. & JARAI, G. 2008. Inhibition of collagen-induced discoidin domain

- receptor 1 and 2 activation by imatinib, nilotinib and dasatinib. *Eur J Pharmacol*, 599, 44-53.
- DE JONG, D., ROSENWALD, A., CHHANABHAI, M., GAULARD, P., KLAPPER, W., LEE, A., SANDER, B., THORNS, C., CAMPO, E., MOLINA, T., NORTON, A., HAGENBEEK, A., HORNING, S., LISTER, A., RAEMAEEKERS, J., GASCOYNE, R. D., SALLES, G. & WELLER, E. 2007. Immunohistochemical prognostic markers in diffuse large B-cell lymphoma: validation of tissue microarray as a prerequisite for broad clinical applications--a study from the Lunenburg Lymphoma Biomarker Consortium. *J Clin Oncol*, 25, 805-12.
- DENG, C. X. 2002. Roles of BRCA1 in centrosome duplication. *Oncogene*, 21, 6222-6227.
- DENNIS, G., JR., SHERMAN, B. T., HOSACK, D. A., YANG, J., GAO, W., LANE, H. C. & LEMPICKI, R. A. 2003. DAVID: Database for Annotation, Visualization, and Integrated Discovery. *Genome biology*, 4, P3-P3.
- DIEHL, V., KIRCHNER, H. H., BURRICHTER, H., STEIN, H., FONATSCH, C., GERDES, J., SCHAADT, M., HEIT, W., UCHANSKAZIEGLER, B., ZIEGLER, A., HEINTZ, F. & SUENO, K. 1982. CHARACTERISTICS OF HODGKINS-DISEASE DERIVED CELL-LINES. *Cancer Treatment Reports*, 66, 615-632.
- DIEHL, V., KIRCHNER, H. H., SCHAADT, M., FONATSCH, C., STEIN, H., GERDES, J. & BOIE, C. 1981. HODGKINS-DISEASE - ESTABLISHMENT AND CHARACTERIZATION OF 4 INVITRO-CELL LINES. *Journal of Cancer Research and Clinical Oncology*, 101, 111-124.
- DIMARCO, E., CUTULI, N., GUERRA, L., CANCEDDA, R. & DELUCA, M. 1993. MOLECULAR-CLONING OF TRKE, A NOVEL TRK-RELATED PUTATIVE TYROSINE KINASE RECEPTOR ISOLATED FROM NORMAL HUMAN KERATINOCYTES AND WIDELY EXPRESSED BY NORMAL HUMAN TISSUES. *Journal of Biological Chemistry*, 268, 24290-24295.
- DING, L., GETZ, G., WHEELER, D. A., MARDIS, E. R., MCLELLAN, M. D., CIBULSKIS, K., SOUGNEZ, C., GREULICH, H., MUZNY, D. M., MORGAN, M. B., FULTON, L., FULTON, R. S., ZHANG, Q. Y., WENDL, M. C., LAWRENCE, M. S., LARSON, D. E., CHEN, K., DOOLING, D. J., SABO, A., HAWES, A. C., SHEN, H., JHANGIANI, S. N., LEWIS, L. R., HALL, O., ZHU, Y. M., MATHEW, T., REN, Y. R., YAO, J. Q., SCHERER, S. E., CLERC, K., METCALF, G. A., NG, B., MILOSAVLJEVIC, A., GONZALEZ-GARAY, M. L., OSBORNE, J. R., MEYER, R., SHI, X. Q., TANG, Y. Z., KOBOLDT, D. C., LIN, L., ABBOTT, R., MINER, T. L., POHL, C., FEWELL, G., HAIPEK, C., SCHMIDT, H., DUNFORD-SHORE, B. H., KRAJA, A., CROSBY, S. D., SAWYER, C. S., VICKERY, T., SANDER, S., ROBINSON, J., WINCKLER, W., BALDWIN, J., CHIRIEAC, L. R., DUTT, A., FENNELL, T., HANNA, M., JOHNSON, B. E., ONOFRIO, R. C., THOMAS, R. K., TONON, G., WEIR, B. A., ZHAO, X. J., ZIAUGRA, L., ZODY, M. C., GIORDANO, T., ORRINGER, M. B., ROTH, J. A., SPITZ, M. R., WISTUBA, II, OZENBERGER, B., GOOD, P. J., CHANG, A. C., BEER, D. G., WATSON, M. A., LADANYI, M., BRODERICK, S., YOSHIZAWA, A., TRAVIS, W. D., PAO, W., PROVINCE, M. A., WEINSTOCK, G. M., VARMUS, H. E., GABRIEL, S. B., LANDER, E. S., GIBBS, R. A., MEYERSON, M. & WILSON, R. K. 2008. Somatic mutations affect key pathways in lung adenocarcinoma. *Nature*, 455, 1069-1075.
- DOLL, D. C. & RINGENBERG, Q. S. 1989. Lymphomas associated with HIV infection. *Seminars in oncology nursing*, 5, 255-62.

- DORTH, J. A., PROSNITZ, L. R., BROADWATER, G., DIEHL, L. F., BEAVEN, A. W., COLEMAN, R. E. & KELSEY, C. R. 2012. Impact of Consolidation Radiation Therapy in Stage III-IV Diffuse Large B-cell Lymphoma With Negative Post-Chemotherapy Radiologic Imaging. *International Journal of Radiation Oncology Biology Physics*, 84, 762-767.
- DUERRBAUM, M., KUZNETSOVA, A. Y., PASSERINI, V., STINGELE, S., STOEHR, G. & STORCHOVA, Z. 2014. Unique features of the transcriptional response to model aneuploidy in human cells. *Bmc Genomics*, 15.
- DUESBERG, P., RASNICK, D., LI, R. H., WINTERS, L., RAUSCH, C. & HEHLMANN, R. 1999. How aneuploidy may cause cancer and genetic instability. *Anticancer Research*, 19, 4887-4906.
- DUNLEAVY, K., PITTALUGA, S., CZUCZMAN, M. S., DAVE, S. S., WRIGHT, G., GRANT, N., SHOVLIN, M., JAFFE, E. S., JANIK, J. E., STAUDT, L. M. & WILSON, W. H. 2009. Differential efficacy of bortezomib plus chemotherapy within molecular subtypes of diffuse large B-cell lymphoma. *Blood*, 113, 6069-6076.
- DYER, M. J., FISCHER, P., NACHEVA, E., LABASTIDE, W. & KARPAS, A. 1990. A new human B-cell non-Hodgkin's lymphoma cell line (Karpas 422) exhibiting both t (14;18) and t(4;11) chromosomal translocations. *Blood*, 75, 709-14.
- EGLIN, R. M. & REISINE, T. 2009. The Current Status of Drug Discovery Against the Human Kinome. *Assay and Drug Development Technologies*, 7, 22-43.
- EPSTEIN, A. L., LEVY, R., KIM, H., HENLE, W., HENLE, G. & KAPLAN, H. S. 1978. BIOLOGY OF HUMAN MALIGNANT-LYMPHOMAS .4. FUNCTIONAL CHARACTERIZATION OF 10 DIFFUSE HISTIOCYTIC LYMPHOMA CELL LINES. *Cancer*, 42, 2379-2391.
- FAESEN, A. C., THANASOULA, M., MAFFINI, S., BREIT, C., MUELLER, F., VAN GERWEN, S., BANGE, T. & MUSACCHIO, A. 2017. Basis of catalytic assembly of the mitotic checkpoint complex. *Nature*, 542, 498+.
- FAVELYUKIS, S., TILL, J. H., HUBBARD, S. R. & MILLER, W. T. 2001. Structure and autoregulation of the insulin-like growth factor 1 receptor kinase. *Nature Structural Biology*, 8, 1058-1063.
- FAVREAU, A. J., CROSS, E. L. & SATHYANARAYANA, P. 2012. miR-199b-5p directly targets PODXL and DDR1 and decreased levels of miR-199b-5p correlate with elevated expressions of PODXL and DDR1 in acute myeloid leukemia. *Am J Hematol*, 87, 442-446.
- FEARON, E. R. & VOGELSTEIN, B. 1990. A GENETIC MODEL FOR COLORECTAL TUMORIGENESIS. *Cell*, 61, 759-767.
- FERRERI, A. J. M., PONZONI, M., PRUNERI, G., FRESCHI, M., ROSSI, R., DELL'ORO, S., BALDINI, L., BUFFA, R., CARBONI, N., VILLA, E. & VIALE, G. 2001. Immunoreactivity for p27(kip1) and cyclin E is an independent predictor of survival in primary gastric non-Hodgkin's lymphoma. *International Journal of Cancer*, 94, 599-604.
- FERRI, N., CARRAGHER, N. O. & RAINES, E. W. 2004. Role of discoidin domain receptors 1 and 2 in human smooth muscle cell-mediated collagen remodeling - Potential implications in atherosclerosis and lymphangioliomyomatosis. *American Journal of Pathology*, 164, 1575-1585.
- FISHER, E. & SCAMBLER, P. 1994. HUMAN HAPLOINSUFFICIENCY - ONE FOR SORROW, 2 FOR JOY. *Nature Genetics*, 7, 5-7.

- FLAMANT, M., PLACIER, S., RODENAS, A., CURAT, C. A., VOGEL, W. F., CHATZIANTONIOU, C. & DUSSAULE, J. C. 2006. Discoidin domain receptor 1 null mice are protected against hypertension-induced renal disease. *J Am Soc Nephrol*, 17, 3374-81.
- FORD, C. E., LAU, S. K., ZHU, C. Q., ANDERSSON, T., TSAO, M. S. & VOGEL, W. F. 2007. Expression and mutation analysis of the discoidin domain receptors 1 and 2 in non-small cell lung carcinoma. *Br J Cancer*, 96, 808-14.
- FRANCO, C., AHMAD, P. J., HOU, G., WONG, E. & BENDECK, M. P. 2010. Increased cell and matrix accumulation during atherogenesis in mice with vessel wall-specific deletion of discoidin domain receptor 1. *Circ Res*, 106, 1775-83.
- FRANCO, C., BRITTO, K., WONG, E., HOU, G., ZHU, S. N., CHEN, M., CYBULSKY, M. I. & BENDECK, M. P. 2009. Discoidin domain receptor 1 on bone marrow-derived cells promotes macrophage accumulation during atherogenesis. *Circ Res*, 105, 1141-8.
- FRANCO, C., HOU, G., AHMAD, P. J., FU, E. Y., KOH, L., VOGEL, W. F. & BENDECK, M. P. 2008. Discoidin domain receptor 1 (ddr1) deletion decreases atherosclerosis by accelerating matrix accumulation and reducing inflammation in low-density lipoprotein receptor-deficient mice. *Circ Res*, 102, 1202-11.
- FRIEDBERG, J. W. 2011. Relapsed/Refractory Diffuse Large B-Cell Lymphoma. *Hematology-American Society Hematology Education Program*, 498-505.
- FRIEDBERG, J. W. & FISHER, R. I. 2008. Diffuse Large B-Cell Lymphoma. *Hematology-Oncology Clinics of North America*, 22, 941-+.
- FRIEDBERG, J. W., SHARMAN, J., SWEETENHAM, J., JOHNSTON, P. B., VOSE, J. M., LACASCE, A., SCHAEFER-CUTILLO, J., DE VOS, S., SINHA, R., LEONARD, J. P., CRIFE, L. D., GREGORY, S. A., STERBA, M. P., LOWE, A. M., LEVY, R. & SHIPP, M. A. 2010. Inhibition of Syk with fostamatinib disodium has significant clinical activity in non-Hodgkin lymphoma and chronic lymphocytic leukemia. *Blood*, 115, 2578-85.
- FU, H. L., VALIATHAN, R. R., ARKWRIGHT, R., SOHAIL, A., MIHAI, C., KUMARASIRI, M., MAHASANAN, K. V., MOBASHERY, S., HUANG, P., AGARWAL, G. & FRIDMAN, R. 2013. Discoidin domain receptors: unique receptor tyrosine kinases in collagen-mediated signaling. *J Biol Chem*, 288, 7430-7.
- FUKASAWA, K., CHOI, T., KURIYAMA, R., RULONG, S. & VANDEVOUDE, G. F. 1996. Abnormal centrosome amplification in the absence of p53. *Science*, 271, 1744-1747.
- GAO, H., CHAKRABORTY, G., ZHANG, Z., AKALAY, I., GADIYA, M., GAO, Y., SINHA, S., HU, J., JIANG, C., AKRAM, M., BROGI, E., LEITINGER, B. & GIANCOTTI, F. G. 2016. Multi-organ Site Metastatic Reactivation Mediated by Non-canonical Discoidin Domain Receptor 1 Signaling. *Cell*, 166, 47-62.
- GAO, M., DUAN, L., LUO, J., ZHANG, L., LU, X., ZHANG, Y., ZHANG, Z., TU, Z., XU, Y., REN, X. & DING, K. 2013. Discovery and optimization of 3-(2-(Pyrazolo[1,5-a]pyrimidin-6-yl)ethynyl)benzamides as novel selective and orally bioavailable discoidin domain receptor 1 (DDR1) inhibitors. *J Med Chem*, 56, 3281-95.
- GASSMANN, R., CARVALHO, A., HENZING, A. J., RUCHAUD, S., HUDSON, D. E., HONDA, R., NIGG, E. A., GERLOFF, D. L. & EARNSHAW, W. C. 2004. Borealin: a novel chromosomal passenger required for stability of the bipolar mitotic spindle. *Journal of Cell Biology*, 166, 179-191.

- GATTER, K. C., DELSOL, G., WARNKE, R. A., PEZZELLA, F., GATTER, K. C., DELSOL, G., WARNKE, R. A. & PEZZELLA, F. 2012. *Diffuse Large B-cell Lymphoma*.
- GEMMA, A., SEIKE, M., SEIKE, Y., UEMATSU, K., HIBINO, S., KURIMOTO, F., YOSHIMURA, A., SHIBUYA, M., HARRIS, C. C. & KUDOH, S. 2000. Somatic mutation of the hBUB1 mitotic checkpoint gene in primary lung cancer. *Genes Chromosomes & Cancer*, 29, 213-218.
- GHOSH, S., ASHCRAFT, K., JAHID, M. J., APRIL, C., GHAJAR, C. M., RUAN, J. H., WANG, H., FOSTER, M., HUGHES, D. C., RAMIREZ, A. G., HUANG, T., FAN, J. B., HU, Y. F. & LI, R. 2013. Regulation of adipose oestrogen output by mechanical stress. *Nature Communications*, 4.
- GREEN, T. M., YOUNG, K. H., VISCO, C., XU-MONETTE, Z. Y., ORAZI, A., GO, R. S., NIELSEN, O., GADEBERG, O. V., MOURITS-ANDERSEN, T., FREDERIKSEN, M., PEDERSEN, L. M. & MOLLER, M. B. 2012. Immunohistochemical Double-Hit Score Is a Strong Predictor of Outcome in Patients With Diffuse Large B-Cell Lymphoma Treated With Rituximab Plus Cyclophosphamide, Doxorubicin, Vincristine, and Prednisone. *Journal of Clinical Oncology*, 30, 3460-3467.
- GROSS, O., GIRGERT, R., BEIROWSKI, B., KRETZLER, M., KANG, H. G., KRUEGEL, J., MIOSGE, N., BUSSE, A. C., SEGERER, S., VOGEL, W. F., MULLER, G. A. & WEBER, M. 2010. Loss of collagen-receptor DDR1 delays renal fibrosis in hereditary type IV collagen disease. *Matrix Biology*, 29, 346-356.
- GU, T.-L., DENG, X., HUANG, F., TUCKER, M., CROSBY, K., RIMKUNAS, V., WANG, Y., DENG, G., ZHU, L., TAN, Z., HU, Y., WU, C., NARDONE, J., MACNEILL, J., REN, J., REEVES, C., INNOCENTI, G., NORRIS, B., YUAN, J., YU, J., HAACK, H., SHEN, B., PENG, C., LI, H., ZHOU, X., LIU, X., RUSH, J. & COMB, M. J. 2011. Survey of Tyrosine Kinase Signaling Reveals ROS Kinase Fusions in Human Cholangiocarcinoma. *Plos One*, 6.
- HABERMANN, T. M., WELLER, E. A., MORRISON, V. A., GASCOYNE, R. D., CASSILETH, P. A., COHN, J. B., DAKHIL, S. R., WODA, B., FISHER, R. I., PETERSON, B. A. & HORNING, S. J. 2006. Rituximab-CHOP versus CHOP alone or with maintenance rituximab in older patients with diffuse large B-cell lymphoma. *J Clin Oncol*, 24, 3121-7.
- HACHEHOUCHE, L. N., CHETOUI, N. & AOU DJIT, F. 2010. Implication of discoidin domain receptor 1 in T cell migration in three-dimensional collagen. *Mol Immunol*, 47, 1866-9.
- HAMMERMAN, P. S., SOS, M. L., RAMOS, A. H., XU, C. X., DUTT, A., ZHOU, W. J., BRACE, L. E., WOODS, B. A., LIN, W. C., ZHANG, J. M., DENG, X. M., LIM, S. M., HEYNCK, S., PEIFER, M., SIMARD, J. R., LAWRENCE, M. S., ONOFRIO, R. C., SALVESEN, H. B., SEIDEL, D., ZANDER, T., HEUCKMANN, J. M., SOLTERMANN, A., MOCH, H., KOKER, M., LEENDERS, F., GABLER, F., QUERINGS, S., ANSEN, S., BRAMBILLA, E., BRAMBILLA, C., LORIMIER, P., BRUSTUGUN, O. T., HELLAND, A., PETERSEN, I., CLEMENT, J. H., GROEN, H., TIMENS, W., SIETSMA, H., STOELBEN, E., WOLF, J., BEER, D. G., TSAO, M. S., HANNA, M., HATTON, C., ECK, M. J., JANNE, P. A., JOHNSON, B. E., WINCKLER, W., GREULICH, H., BASS, A. J., CHO, J. H., RAUH, D., GRAY, N. S., WONG, K. K., HAURA, E. B., THOMAS, R. K. & MEYERSON, M. 2011. Mutations in the DDR2 Kinase Gene identify a Novel therapeutic target in squamous cell lung cancer. *Cancer Discovery*, 1, 78-89.

- HANKS, S. K., QUINN, A. M. & HUNTER, T. 1988. THE PROTEIN-KINASE FAMILY - CONSERVED FEATURES AND DEDUCED PHYLOGENY OF THE CATALYTIC DOMAINS. *Science*, 241, 42-52.
- HANS, C. P., WEISENBURGER, D. D., GREINER, T. C., GASCOYNE, R. D., DELABIE, J., OTT, G., MULLER-HERMELINK, H. K., CAMPO, E., BRAZIEL, R. M., JAFFE, E. S., PAN, Z., FARINHA, P., SMITH, L. M., FALINI, B., BANHAM, A. H., ROSENWALD, A., STAUDT, L. M., CONNORS, J. M., ARMITAGE, J. O. & CHAN, W. C. 2004. Confirmation of the molecular classification of diffuse large B-cell lymphoma by immunohistochemistry using a tissue microarray. *Blood*, 103, 275-82.
- HARRIS, N. L., SWERDLOW, S., CAMPO, E., JAFFE, E. S., STEIN, H., PILERI, S., THIELE, J. & VARDIMAN, J. 2008. The World Health Organization (WHO) classification of lymphoid neoplasms: What's new? *Annals of Oncology*, 19, 119-119.
- HARTWELL, L., DUTCHER, S., WOOD, J. & GARVIK, B. 1982. The fidelity of mitotic chromosome reproduction in *Saccharomyces cerevisiae*. *Rec. Adv. Yeast Molecular Biology*, 1, 28-23.
- HASLE, H., CLEMMENSEN, I. H. & MIKKELSEN, M. 2000. Risks of leukaemia and solid tumours in individuals with Down's syndrome. *Lancet*, 355, 165-169.
- HEINZELMANN-SCHWARZ, V. A., GARDINER-GARDEN, M., HENSHALL, S. M., SCURRY, J., SCOLYER, R. A., DAVIES, M. J., HEINZELMANN, M., KALISH, L. H., BALI, A., KENCH, J. G., EDWARDS, L. S., VANDEN BERGH, P. M., HACKER, N. F., SUTHERLAND, R. L. & O'BRIEN, P. M. 2004. Overexpression of the cell adhesion molecules DDR1, claudin 3, and Ep-CAM in metaplastic ovarian epithelium and ovarian cancer. *Clinical Cancer Research*, 10, 4427-4436.
- HELD, G., MURAWSKI, N., ZIEPERT, M., FLECKENSTEIN, J., POESCHEL, V., ZWICK, C., BITTENBRING, J., HAENEL, M., WILHELM, S., SCHUBERT, J., SCHMITZ, N., LOEFFLER, M., RUEBE, C. & PFREUNDSCHUH, M. 2014. Role of Radiotherapy to Bulky Disease in Elderly Patients With Aggressive B-Cell Lymphoma. *Journal of Clinical Oncology*, 32, 1112-+.
- HEMPEN, P. M., KURPAD, H., CALHOUN, E. S., ABRAHAM, S. & KERN, S. E. 2003. A double missense variation of the BUB1 gene and a defective mitotic spindle checkpoint in the pancreatic cancer cell line Hs766T. *Human mutation*, 21, 445-445.
- HERNANDO, E., ORLOW, I., LIBERAL, V., NOHALES, G., BENEZRA, R. & CORDON-CARDO, C. 2001. Molecular analyses of the mitotic checkpoint components hsMAD2, hBUB1 and hBUB3 in human cancer. *International Journal of Cancer*, 95, 223-227.
- HEWITT, L., TIGHE, A., SANTAGUIDA, S., WHITE, A. M., JONES, C. D., MUSACCHIO, A., GREEN, S. & TAYLOR, S. S. 2010. Sustained Mps1 activity is required in mitosis to recruit O-Mad2 to the Mad1-C-Mad2 core complex. *Journal of Cell Biology*, 190, 25-34.
- HIROKAWA, N., NIWA, S. & TANAKA, Y. 2010. Molecular Motors in Neurons: Transport Mechanisms and Roles in Brain Function, Development, and Disease. *Neuron*, 68, 610-638.
- HITZ, F., CONNORS, J. M., GASCOYNE, R. D., HOSKINS, P., MOCCIA, A., SAVAGE, K. J., SEHN, L. H., SHENKIER, T., VILLA, D. & KLASA, R. 2015. Outcome of patients with primary refractory diffuse large B cell lymphoma after R-CHOP treatment. *Ann Hematol*, 94, 1839-43.

- HOELLER, S., TZANKOV, A., PILERI, S. A., WENT, P. & DIRNHOFER, S. 2010. Epstein-Barr virus-positive diffuse large B-cell lymphoma in elderly patients is rare in Western populations. *Hum Pathol*, 41, 352-7.
- HOU, G., VOGEL, W. & BENDECK, M. P. 2001. The discoidin domain receptor tyrosine kinase DDR1 in arterial wound repair. *J Clin Invest*, 107, 727-35.
- HU, S., XU-MONETTE, Z. Y., TZANKOV, A., GREEN, T., WU, L., BALASUBRAMANYAM, A., LIU, W. M., VISCO, C., LI, Y., MIRANDA, R. N., MONTES-MORENO, S., DYBKAER, K., CHIU, A., ORAZI, A., ZU, Y., BHAGAT, G., RICHARDS, K. L., HSI, E. D., CHOI, W. W., ZHAO, X., VAN KRIEKEN, J. H., HUANG, Q., HUH, J., AI, W., PONZONI, M., FERRERI, A. J., ZHOU, F., SLACK, G. W., GASCOYNE, R. D., TU, M., VARIAKOJIS, D., CHEN, W., GO, R. S., PIRIS, M. A., MOLLER, M. B., MEDEIROS, L. J. & YOUNG, K. H. 2013. MYC/BCL2 protein coexpression contributes to the inferior survival of activated B-cell subtype of diffuse large B-cell lymphoma and demonstrates high-risk gene expression signatures: a report from The International DLBCL Rituximab-CHOP Consortium Program. *Blood*, 121, 4021-31; quiz 4250.
- HUBBARD, S. R. 1997. Crystal structure of the activated insulin receptor tyrosine kinase in complex with peptide substrate and ATP analog. *Embo Journal*, 16, 5572-5581.
- HUBBARD, S. R. & TILL, J. H. 2000. Protein tyrosine kinase structure and function. *Annual Review of Biochemistry*, 69, 373-398.
- HUNTER, T. 1998. The Croonian Lecture 1997. The phosphorylation of proteins on tyrosine: Its role in cell growth and disease. *Philosophical Transactions of the Royal Society of London Series B-Biological Sciences*, 353, 583-605.
- HWANG, L. H., LAU, L. F., SMITH, D. L., MISTROT, C. A., HARDWICK, K. G., HWANG, E. S., AMON, A. & MURRAY, A. W. 1998. Budding yeast Cdc20: A target of the spindle checkpoint. *Science*, 279, 1041-1044.
- IMAI, Y., SHIRATORI, Y., KATO, N., INOUE, T. & OMATA, M. 1999. Mutational inactivation of mitotic checkpoint genes, hsMAD2 and hBUB1, is rare in sporadic digestive tract cancers. *Japanese Journal of Cancer Research*, 90, 837-840.
- INTERNATIONAL NON-HODGKIN'S LYMPHOMA PROGNOSTIC FACTORS, P. 1993. A predictive model for aggressive non-Hodgkin's lymphoma. *New England Journal of Medicine*, 329, 987-994.
- IQBAL, J., MEYER, P. N., SMITH, L. M., JOHNSON, N. A., VOSE, J. M., GREINER, T. C., CONNORS, J. M., STAUDT, L. M., RIMSZA, L., JAFFE, E., ROSENWALD, A., OTT, G., DELABIE, J., CAMPO, E., BRAZIEL, R. M., COOK, J. R., TUBBS, R. R., GASCOYNE, R. D., ARMITAGE, J. O., WEISENBURGER, D. D. & CHAN, W. C. 2011. BCL2 predicts survival in germinal center B-cell-like diffuse large B-cell lymphoma treated with CHOP-like therapy and rituximab. *Clin Cancer Res*, 17, 7785-95.
- IRIZARRY, R. A., BOLSTAD, B. M., COLLIN, F., COPE, L. M., HOBBS, B. & SPEED, T. P. 2003. Summaries of affymetrix GeneChip probe level data. *Nucleic Acids Research*, 31.
- IWANAGA, Y. & JEANG, K. T. 2002. Expression of mitotic spindle checkpoint protein hsMAD1 correlates with cellular proliferation and is activated by a gain-of-function p53 mutant. *Cancer Research*, 62, 2618-2624.
- JAGLAL, M. V., PEKER, D., TAO, J. & CULTRERA, J. L. 2012. Double and Triple Hit Diffuse Large B Cell Lymphomas and First Line Therapy. *Blood*, 120.

- JALLEPALLI, P. V., WAIZENEGGER, I. C., BUNZ, F., LANGER, S., SPEICHER, M. R., PETERS, J. M., KINZLER, K. W., VOGELSTEIN, B. & LENGAUER, C. 2001. Securin is required for chromosomal stability in human cells. *Cell*, 105, 445-457.
- JANSSON, M. & ANDERSSON, T. 2001. Repression of Wnt-5a impairs DDR1 phosphorylation and modifies adhesion and migration of mammary cells. *Journal of Cell Science*, 114, 2043-2053.
- JEDRZEJCZAK, W. W. 2015. Diffuse large B-cell lymphoma: R-CHOP forever? *Polskie Archiwum Medycyny Wewnetrznej-Polish Archives of Internal Medicine*, 125, 713-714.
- JEITANY, M., LEROY, C., TOSTI, P., LAFITTE, M., LE GUET, J., SIMON, V., BONENFANT, D., ROBERT, B., GRILLET, F., MOLLEVI, C., EL MESSAOUDI, S., OTANDAULT, A., CANTEREL-THOUENNON, L., BUSSON, M., THIERRY, A. R., MARTINEAU, P., PANNEQUIN, J., ROCHE, S. & SIRVENT, A. 2018. Inhibition of DDR1-BCR signalling by nilotinib as a new therapeutic strategy for metastatic colorectal cancer. *Embo Molecular Medicine*, 10.
- JIN, D. Y., SPENCER, F. & JEANG, K. T. 1998. Human T cell leukemia virus type 1 oncoprotein tax targets the human mitotic checkpoint protein MAD1. *Cell*, 93, 81-91.
- JING, H., SONG, J. & ZHENG, J. 2018. Discoidin domain receptor 1: New star in cancer-targeted therapy and its complex role in breast carcinoma. *Oncology letters*, 15, 3403-3408.
- JOHANSSON, B., MERTENS, F. & MITELMAN, F. 1995. CYTOGENETIC EVOLUTION PATTERNS IN NON-HODGKINS-LYMPHOMA. *Blood*, 86, 3905-3914.
- JOHNSON, J. D., EDMAN, J. C. & RUTTER, W. J. 1993. A receptor tyrosine kinase found in breast carcinoma cells has an extracellular discoidin I-like domain. *Proc Natl Acad Sci U S A*, 90, 10891.
- JOHNSON, N. A., SLACK, G. W., SAVAGE, K. J., CONNORS, J. M., BEN-NERIAH, S., ROGIC, S., SCOTT, D. W., TAN, K. L., STEIDL, C., SEHN, L. H., CHAN, W. C., IQBAL, J., MEYER, P. N., LENZ, G., WRIGHT, G., RIMSZA, L. M., VALENTINO, C., BRUNHOEBER, P., GROGAN, T. M., BRAZIEL, R. M., COOK, J. R., TUBBS, R. R., WEISENBURGER, D. D., CAMPO, E., ROSENWALD, A., OTT, G., DELABIE, J., HOLCROFT, C., JAFFE, E. S., STAUDT, L. M. & GASCOYNE, R. D. 2012. Concurrent expression of MYC and BCL2 in diffuse large B-cell lymphoma treated with rituximab plus cyclophosphamide, doxorubicin, vincristine, and prednisone. *J Clin Oncol*, 30, 3452-9.
- JORDAN, M. A. & WILSON, L. 2004. Microtubules as a target for anticancer drugs. *Nature Reviews Cancer*, 4, 253-265.
- JUIN, A., DI MARTINO, J., LEITINGER, B., HENRIET, E., GARY, A. S., PAYSAN, L., BOMO, J., BAFFET, G., GAUTHIER-ROUVIERE, C., ROSENBAUM, J., MOREAU, V. & SALTEL, F. 2014. Discoidin domain receptor 1 controls linear invadosome formation via a Cdc42-Tuba pathway. *J Cell Biol*, 207, 517-33.
- KADLER, K. E., BALDOCK, C., BELLA, J. & BOOT-HANDFORD, R. P. 2007. Collagens at a glance. *Journal of Cell Science*, 120, 1955-1958.
- KAMESAKI, H., FUKUHARA, S., TATSUMI, E., UCHINO, H., YAMABE, H., MIWA, H., SHIRAKAWA, S., HATANAKA, M. & HONJO, T. 1986. CYTOCHEMICAL,

- IMMUNOLOGICAL, CHROMOSOMAL, AND MOLECULAR GENETIC-ANALYSIS OF A NOVEL CELL-LINE DERIVED FROM HODGKINS-DISEASE. *Blood*, 68, 285-292.
- KAMOHARA, H., YAMASHIRO, S., GALLIGAN, C. & YOSHIMURA, T. 2001. Discoidin domain receptor 1 isoform-a (DDR1alpha) promotes migration of leukocytes in three-dimensional collagen lattices. *FASEB J*, 15, 2724-6.
- KANZLER, H., HANSMANN, M. L., KAPP, U., WOLF, J., DIEHL, V., RAJEWSKY, K. & KUPPERS, R. 1996. Molecular single cell analysis demonstrates the derivation of a peripheral blood-derived cell line (L1236) from the Hodgkin Reed-Sternberg cells of a Hodgkin's lymphoma patient. *Blood*, 87, 3429-3436.
- KATO, M., SANADA, M., KATO, I., SATO, Y., TAKITA, J., TAKEUCHI, K., NIWA, A., CHEN, Y., NAKAZAKI, K., NOMOTO, J., ASAKURA, Y., MUTO, S., TAMURA, A., IIO, M., AKATSUKA, Y., HAYASHI, Y., MORI, H., IGARASHI, T., KUOKAWA, M., CHIBA, S., MORI, S., ISHIKAWA, Y., OKAMOTO, K., TOBINAI, K., NAKAGAMA, H., NAKAHATA, T., YOSHINO, T., KOBAYASHI, Y. & OGAWA, S. 2009. Frequent inactivation of A20 in B-cell lymphomas. *Nature*, 459, 712-U118.
- KAWAI, I., MATSUMURA, H., FUJII, W., NAITO, K., KUSAKABE, K., KISO, Y. & KANO, K. 2014. Discoidin domain receptor 2 (DDR2) regulates body size and fat metabolism in mice. *Transgenic Res*, 23, 165-75.
- KERROCH, M., GUERROT, D., VANDERMEERSCH, S., PLACIER, S., MESNARD, L., JOUANNEAU, C., RONDEAU, E., RONCO, P., BOFFA, J. J., CHATZIANTONIOU, C. & DUSSAULE, J. C. 2012. Genetic inhibition of discoidin domain receptor 1 protects mice against crescentic glomerulonephritis. *FASEB J*, 26, 4079-91.
- KEWALRAMANI, T., ZELENETZ, A. D., NIMER, S. D., PORTLOCK, C., STRAUS, D., NOY, A., O'CONNOR, O., FILIPPA, D. A., TERUYA-FELDSTEIN, J., GENCARELLI, A., QIN, J., WAXMAN, A., YAHALOM, J. & MOSKOWITZ, C. H. 2004. Rituximab and ICE as second-line therapy before autologous stem cell transplantation for relapsed or primary refractory diffuse large B-cell lymphoma. *Blood*, 103, 3684-3688.
- KIM, H. G., HWANG, S. Y., AARONSON, S. A., MANDINOVA, A. & LEE, S. W. 2011. DDR1 Receptor Tyrosine Kinase Promotes Prosurvival Pathway through Notch1 Activation. *Journal of Biological Chemistry*, 286, 17672-17681.
- KIM, H. G., TAN, L., WEISBERG, E. L., LIU, F. Y., CANNING, P., CHOI, H. G., EZELL, S., ZHAO, Z., WU, H., WANG, J. H., MANDINOVA, A., BULLOCK, A. N., LIU, Q. S., LEE, S. W. & GRAY, N. S. 2014. Discovery of a Potent and Selective DDR1 Receptor Tyrosine Kinase Inhibitor (vol 8, pg 2145, 2013). *Acs Chemical Biology*, 9, 840-840.
- KIM, K. J., KANELLOPOULOS-LANGEVIN, C., MERWIN, R. M., SACHS, D. H. & ASOFSKY, R. 1979. ESTABLISHMENT AND CHARACTERIZATION OF BALB-C LYMPHOMA LINES WITH B-CELL PROPERTIES. *Journal of Immunology*, 122, 549-554.
- KLEIN, G., LINDAHL, T., JONDAL, M., LEIBOLD, W., MENEZES, J., NILSSON, K. & SUNDSTROM, C. 1974. Continuous lymphoid cell lines with characteristics of B cells (bone-marrow-derived), lacking the Epstein-Barr virus genome and derived from three human lymphomas. *Proc Natl Acad Sci U S A*, 71, 3283-6.
- KLEIN, U., CASOLA, S., CATTORETTI, G., SHEN, Q., LIA, M., MO, T., LUDWIG, T., RAJEWSKY, K. & DALLA-FAVERA, R. 2006. Transcription factor IRF4 controls plasma cell differentiation and class-switch recombination. *Nat Immunol*, 7, 773-82.

- KNUDSON, A. G. 2001. Two genetic hits (more or less) to cancer. *Nature Reviews Cancer*, 1, 157-162.
- KOH, M., WOO, Y., VALIATHAN, R. R., JUNG, H. Y., PARK, S. Y., KIM, Y. N., KIM, H. R., FRIDMAN, R. & MOON, A. 2015. Discoidin domain receptor 1 is a novel transcriptional target of ZEB1 in breast epithelial cells undergoing H-Ras-induced epithelial to mesenchymal transition. *Int J Cancer*, 136, E508-20.
- KOO, D. H. H., MCFADDEN, C., HUANG, Y., ABDULHUSSEIN, R., FRIESE-HAMIM, M. & VOGEL, W. F. 2006. Pinpointing phosphotyrosine-dependent interactions downstream of the collagen receptor DDR1. *Febs Letters*, 580, 15-22.
- KOPS, G., WEAVER, B. A. A. & CLEVELAND, D. W. 2005. On the road to cancer: Aneuploidy and the mitotic checkpoint. *Nature Reviews Cancer*, 5, 773-785.
- KOTHIWALE, S., BORZA, C. M., LOWE, E. W., JR., POZZI, A. & MEILER, J. 2015. Discoidin domain receptor 1 (DDR1) kinase as target for structure-based drug discovery. *Drug Discov Today*, 20, 255-61.
- KRAMER, A., SCHWEIZER, S., NEBEN, K., GIESECKE, C., KALLA, J., KATZENBERGER, T., BENNER, A., MULLER-HERMELINK, H. K., HO, A. D. & OTT, G. 2003. Centrosome aberrations as a possible mechanism for chromosomal instability in non-Hodgkin's lymphoma. *Leukemia*, 17, 2207-13.
- KUNG, P.-P., MARTINEZ, R., ZHU, Z., ZAGER, M., BLASINA, A., RYMER, I., HALLIN, J., XU, M., CARROLL, C., CHIONIS, J., WELLS, P., KOZMINSKI, K., FAN, J., GUICHERIT, O., HUANG, B., CUI, M., LIU, C., HUANG, Z., SISTLA, A., YANG, J. & MURRAY, B. W. 2014. Chemogenetic Evaluation of the Mitotic Kinesin CENP-E Reveals a Critical Role in Triple-Negative Breast Cancer. *Molecular Cancer Therapeutics*, 13, 2104-2115.
- L'HOTE C, G., THOMAS, P. H. & GANESAN, T. S. 2002. Functional analysis of discoidin domain receptor 1: effect of adhesion on DDR1 phosphorylation. *FASEB J*, 16, 234-6.
- LABRADOR, J. P., AZCOITIA, V., TUCKERMANN, J., LIN, C., OLASO, E., MANES, S., BRUCKNER, K., GOERGEN, J. L., LEMKE, G., YANCOPOULOS, G., ANGEL, P., MARTINEZ, C. & KLEIN, R. 2001. The collagen receptor DDR2 regulates proliferation and its elimination leads to dwarfism. *Embo Reports*, 2, 446-452.
- LAI, C. & LEMKE, G. 1994. STRUCTURE AND EXPRESSION OF THE TYRO-10 RECEPTOR TYROSINE KINASE. *Oncogene*, 9, 877-883.
- LEBIEN, T. W. & TEDDER, T. F. 2008. B lymphocytes: how they develop and function. *Blood*, 112, 1570-1580.
- LEITINGER, B. 2003. Molecular analysis of collagen binding by the human discoidin domain receptors, DDR1 and DDR2. Identification of collagen binding sites in DDR2. *J Biol Chem*, 278, 16761-9.
- LEITINGER, B. 2011. Transmembrane Collagen Receptors. In: SCHEKMAN, R., GOLDSTEIN, L. & LEHMANN, R. (eds.) *Annual Review of Cell and Developmental Biology*, Vol 27.
- LEITINGER, B. 2014. Discoidin domain receptor functions in physiological and pathological conditions. *Int Rev Cell Mol Biol*, 310, 39-87.
- LEMEER, S., BLUWSTEIN, A., WU, Z., LEBERFINGER, J., MUELLER, K., KRAMER, K. & KUSTER, B. 2012. Phosphotyrosine mediated protein interactions of the discoidin domain receptor 1. *Journal of Proteomics*, 75, 3465-3477.

- LEMMON, M. A. & SCHLESSINGER, J. 2010. Cell Signaling by Receptor Tyrosine Kinases. *Cell*, 141, 1117-1134.
- LENGAUER, C., KINZLER, K. W. & VOGELSTEIN, B. 1997. Genetic instability in colorectal cancers. *Nature*, 386, 623-627.
- LENZ, G., DAVIS, R. E., NGO, V. N., LAM, L., GEORGE, T. C., WRIGHT, G. W., DAVE, S. S., ZHAO, H., XU, W., ROSENWALD, A., OTT, G., MULLER-HERMELINK, H. K., GASCOYNE, R. D., CONNORS, J. M., RIMSZA, L. M., CAMPO, E., JAFFE, E. S., DELABIE, J., SMELAND, E. B., FISHER, R. I., CHAN, W. C. & STAUDT, L. M. 2008a. Oncogenic CARD11 mutations in human diffuse large B cell lymphoma. *Science*, 319, 1676-9.
- LENZ, G. & STAUDT, L. M. 2010a. Aggressive lymphomas. *N Engl J Med*, 362, 1417-29.
- LENZ, G. & STAUDT, L. M. 2010b. Mechanisms of Disease: Aggressive Lymphomas. *New England Journal of Medicine*, 362, 1417-1429.
- LENZ, G., WRIGHT, G., DAVE, S. S., XIAO, W., POWELL, J., ZHAO, H., XU, W., TAN, B., GOLDSCHMIDT, N., IQBAL, J., VOSE, J., BAST, M., FU, K., WEISENBURGER, D. D., GREINER, T. C., ARMITAGE, J. O., KYLE, A., MAY, L., GASCOYNE, R. D., CONNORS, J. M., TROEN, G., HOLTE, H., KVALOY, S., DIERICKX, D., VERHOEF, G., DELABIE, J., SMELAND, E. B., JARES, P., MARTINEZ, A., LOPEZ-GUILLERMO, A., MONTSERRAT, E., CAMPO, E., BRAZIEL, R. M., MILLER, T. P., RIMSZA, L. M., COOK, J. R., POHLMAN, B., SWEETENHAM, J., TUBBS, R. R., FISHER, R. I., HARTMANN, E., ROSENWALD, A., OTT, G., MULLER-HERMELINK, H. K., WRENCH, D., LISTER, T. A., JAFFE, E. S., WILSON, W. H., CHAN, W. C. & STAUDT, L. M. 2008b. Stromal gene signatures in large-B-cell lymphomas. *N Engl J Med*, 359, 2313-23.
- LENZ, G., WRIGHT, G. W., EMRE, N. C., KOHLHAMMER, H., DAVE, S. S., DAVIS, R. E., CARTY, S., LAM, L. T., SHAFFER, A. L., XIAO, W., POWELL, J., ROSENWALD, A., OTT, G., MULLER-HERMELINK, H. K., GASCOYNE, R. D., CONNORS, J. M., CAMPO, E., JAFFE, E. S., DELABIE, J., SMELAND, E. B., RIMSZA, L. M., FISHER, R. I., WEISENBURGER, D. D., CHAN, W. C. & STAUDT, L. M. 2008c. Molecular subtypes of diffuse large B-cell lymphoma arise by distinct genetic pathways. *Proc Natl Acad Sci U S A*, 105, 13520-5.
- LI, Y. & BENEZRA, R. 1996. Identification of a human mitotic checkpoint gene: HSMAD2. *Molecular Biology of the Cell*, 7, 2065-2065.
- LIAO, Y., SMYTH, G. K. & SHI, W. 2013. The Subread aligner: fast, accurate and scalable read mapping by seed-and-vote. *Nucleic Acids Research*, 41.
- LITAM, P., SWAN, F., CABANILLAS, F., TUCKER, S. L., MCLAUGHLIN, P., HAGEMEISTER, F. B., RODRIGUEZ, M. A. & VELASQUEZ, W. S. 1991. PROGNOSTIC VALUE OF SERUM BETA-2 MICROGLOBULIN IN LOW-GRADE LYMPHOMA. *Annals of Internal Medicine*, 114, 855-860.
- LIU, B., LUO, H., WU, G., LIU, J., PAN, J. & LIU, Z. 2015. Low expression of spindle checkpoint protein, Cenp-E, causes numerical chromosomal abnormalities in HepG-2 human hepatoma cells. *Oncology Letters*, 10, 2699-2704.
- LIVAK, K. J. & SCHMITTGEN, T. D. 2001. Analysis of relative gene expression data using real-time quantitative PCR and the 2(T)(-Delta Delta C) method. *Methods*, 25, 402-408.

- LO COCO, F., YE, B. H., LISTA, F., CORRADINI, P., OFFIT, K., KNOWLES, D. M., CHAGANTI, R. S. & DALLA-FAVERA, R. 1994. Rearrangements of the BCL6 gene in diffuse large cell non-Hodgkin's lymphoma. *Blood*, 83, 1757-9.
- LOPEZ-SOTO, A., GONZALEZ, S., LOPEZ-LARREA, C. & KROEMER, G. 2017. Immunosurveillance of Malignant Cells with Complex Karyotypes. *Trends in Cell Biology*, 27, 880-884.
- LOPEZ-SOTO, A., HUERGO-ZAPICO, L., ACEBES-HUERTA, A., VILLA-ALVAREZ, M. & GONZALEZ, S. 2015. NKG2D signaling in cancer immunosurveillance. *International Journal of Cancer*, 136, 1741-1750.
- LORIAUX, M. M., LEVINE, R. L., TYNER, J. W., FROEHLING, S., SCHOLL, C., STOFFREGEN, E. P., WERNIG, G., ERICKSON, H., EIDE, C. A., BERGER, R., BERNARD, O. A., GRIFFIN, J. D., STONE, R. M., LEE, B., MEYERSON, M., HEINRICH, M. C., DEININGER, M. W., GILLILAND, D. G. & DRUKER, B. J. 2008. High-throughput sequence analysis of the tyrosine kinome in acute myeloid leukemia. *Blood*, 111, 4788-4796.
- LOSSOS, I. S., CZERWINSKI, D. K., ALIZADEH, A. A., WECHSER, M. A., TIBSHIRANI, R., BOTSTEIN, D. & LEVY, R. 2004. Prediction of survival in diffuse large-B-cell lymphoma based on the expression of six genes. *N Engl J Med*, 350, 1828-37.
- LU, K. K., TRCKA, D. & BENDECK, M. P. 2011. Collagen stimulates discoidin domain receptor 1-mediated migration of smooth muscle cells through Src. *Cardiovasc Pathol*, 20, 71-6.
- MACKENZIE, K. J., CARROLL, P., MARTIN, C.-A., MURINA, O., FLUTEAU, A., IMPSON, D. J. S., OLOVA, N., SUTCLIFFE, H., RAINGER, J. K., LEITCH, A., OSBORN, R. T., WHEELER, A. P., NOWOTNY, M., GILBERT, N., CHANDRA, T., REIJNS, M. A. M. & JACKSON, A. P. 2017. cGAS surveillance of micronuclei links genome instability to innate immunity. *Nature*, 548, 461-+.
- MAEYAMA, M., KOGA, H., SELVENDIRAN, K., YANAGIMOTO, C., HANADA, S., TANIGUCHI, E., KAWAGUCHI, T., HARADA, M., UENO, T. & SATA, M. 2008. Switching in Discoid Domain Receptor Expressions in SLUG-induced Epithelial-Mesenchymal Transition. *Cancer*, 113, 2823-2831.
- MALUMBRES, M. & BARBACID, M. 2009. Cell cycle, CDKs and cancer: a changing paradigm. *Nature Reviews Cancer*, 9, 153-166.
- MANNING, G., WHYTE, D. B., MARTINEZ, R., HUNTER, T. & SUDARSANAM, S. 2002. The protein kinase complement of the human genome. *Science*, 298, 1912-+.
- MAO, Y. H., ABRIEU, A. & CLEVELAND, D. W. 2003. Activating and silencing the mitotic checkpoint through CENP-E-dependent activation/inactivation of BubR1. *Cell*, 114, 87-98.
- MARTELLI, M., FERRERI, A. J. M., AGOSTINELLI, C., DI ROCCO, A., PFREUNDSCHUH, M. & PILERI, S. A. 2013. Diffuse large B-cell lymphoma. *Critical Reviews in Oncology Hematology*, 87, 146-171.
- MATTISON, C. P., OLD, W. M., STEINER, E., HUNEYCUTT, B. J., RESING, K. A., AHN, N. G. & WINEY, M. 2007. Mps1 activation loop autophosphorylation enhances kinase activity. *Journal of Biological Chemistry*, 282, 30553-30561.
- MELCHERS, F. 2005. Opinion - The pre-B-cell receptor: selector of fitting immunoglobulin heavy chains for the B-cell repertoire. *Nature Reviews Immunology*, 5, 578-584.

- MENGUY, S., FRISON, E., PROCHAZKOVA-CARLOTTI, M., DALLE, S., DEREURE, O., BOULINGUEZ, S., DALAC, S., MACHET, L., RAM-WOLFF, C., VERNEUIL, L., GROS, A., VERGIER, B., BEYLOT-BARRY, M., MERLIO, J.-P. & PHAM-LEDARD, A. 2018. Double-hit or dual expression of MYC and BCL2 in primary cutaneous large B-cell lymphomas. *Modern pathology : an official journal of the United States and Canadian Academy of Pathology, Inc.*
- MEYER, P. N., FU, K., GREINER, T. C., SMITH, L. M., DELABIE, J., GASCOYNE, R. D., OTT, G., ROSENWALD, A., BRAZIEL, R. M., CAMPO, E., VOSE, J. M., LENZ, G., STAUDT, L. M., CHAN, W. C. & WEISENBURGER, D. D. 2011. Immunohistochemical methods for predicting cell of origin and survival in patients with diffuse large B-cell lymphoma treated with rituximab. *J Clin Oncol*, 29, 200-7.
- MICHEL, L. S., LIBERAL, V., CHATTERJEE, A., KIRCHWEGGER, R., PASCHE, B., GERALD, W., DOBLES, M., SORGER, P. K., MURTY, V. & BENEZRA, R. 2001. MAD2 haplo-insufficiency causes premature anaphase and chromosome instability in mammalian cells. *Nature*, 409, 355-359.
- MIHAI, C., CHOTANI, M., ELTON, T. S. & AGARWAL, G. 2009. Mapping of DDR1 Distribution and Oligomerization on the Cell Surface by FRET Microscopy. *Journal of Molecular Biology*, 385, 432-445.
- MILAN, M., CLEMENTE-RUIZ, M., DEKANTY, A. & MUZZOPAPPA, M. 2014. Aneuploidy and tumorigenesis in *Drosophila*. *Seminars in Cell & Developmental Biology*, 28, 110-115.
- MILLER, T. P., DAHLBERG, S., CASSADY, J. R., ADELSTEIN, D. J., SPIER, C. M., GROGAN, T. M., LEBLANC, M., CARLIN, S., CHASE, E. & FISHER, R. I. 1998. Chemotherapy alone compared with chemotherapy plus radiotherapy for localized intermediate-and high-grade non-Hodgkin's lymphoma. *New England Journal of Medicine*, 339, 21-26.
- MINSHULL, J., SUN, H., TONKS, N. K. & MURRAY, A. W. 1994. A MAP KINASE-DEPENDENT SPINDLE ASSEMBLY CHECKPOINT IN XENOPUS EGG EXTRACTS. *Cell*, 79, 475-486.
- MITCHISON, T. J. 1988. MICROTUBULE DYNAMICS AND KINETOCHORE FUNCTION IN MITOSIS. *Annual Review of Cell Biology*, 4, 527-549.
- MORIKI, T., MARUYAMA, H. & MARUYAMA, I. N. 2001. Activation of preformed EGF receptor dimers by ligand-induced rotation of the transmembrane domain. *Journal of Molecular Biology*, 311, 1011-1026.
- MORIN, R. D., JOHNSON, N. A., SEVERSON, T. M., MUNGALL, A. J., AN, J., GOYA, R., PAUL, J. E., BOYLE, M., WOOLCOCK, B. W., KUCHENBAUER, F., YAP, D., HUMPHRIES, R. K., GRIFFITH, O. L., SHAH, S., ZHU, H., KIMBARA, M., SHASHKIN, P., CHARLOT, J. F., TCHERPAKOV, M., CORBETT, R., TAM, A., VARHOL, R., SMAILUS, D., MOKSA, M., ZHAO, Y., DELANEY, A., QIAN, H., BIROL, I., SCHEIN, J., MOORE, R., HOLT, R., HORSMAN, D. E., CONNORS, J. M., JONES, S., APARICIO, S., HIRST, M., GASCOYNE, R. D. & MARRA, M. A. 2010. Somatic mutations altering EZH2 (Tyr641) in follicular and diffuse large B-cell lymphomas of germinal-center origin. *Nat Genet*, 42, 181-5.
- MORIN, R. D., MENDEZ-LAGO, M., MUNGALL, A. J., GOYA, R., MUNGALL, K. L., CORBETT, R. D., JOHNSON, N. A., SEVERSON, T. M., CHIU, R., FIELD, M., JACKMAN, S., KRZYWINSKI, M., SCOTT, D. W., TRINH, D. L., TAMURA-WELLS, J., LI, S., FIRME, M.

- R., ROGIC, S., GRIFFITH, M., CHAN, S., YAKOVENKO, O., MEYER, I. M., ZHAO, E. Y., SMAILUS, D., MOKSA, M., CHITTARANJAN, S., RIMSZA, L., BROOKS-WILSON, A., SPINELLI, J. J., BEN-NERIAH, S., MEISSNER, B., WOOLCOCK, B., BOYLE, M., MCDONALD, H., TAM, A., ZHAO, Y., DELANEY, A., ZENG, T., TSE, K., BUTTERFIELD, Y., BIROL, I., HOLT, R., SCHEIN, J., HORSMAN, D. E., MOORE, R., JONES, S. J., CONNORS, J. M., HIRST, M., GASCOYNE, R. D. & MARRA, M. A. 2011. Frequent mutation of histone-modifying genes in non-Hodgkin lymphoma. *Nature*, 476, 298-303.
- MOSS, D. J., BURROWS, S. R., CASTELINO, D. J., KANE, R. G., POPE, J. H., RICKINSON, A. B., ALPERS, M. P. & HEYWOOD, P. F. 1983. A comparison of Epstein-Barr virus-specific T-cell immunity in malaria-endemic and -nonendemic regions of Papua New Guinea. *Int J Cancer*, 31, 727-32.
- MURAMATSU, M., KINOSHITA, K., FAGARASAN, S., YAMADA, S., SHINKAI, Y. & HONJO, T. 2000. Class switch recombination and hypermutation require activation-induced cytidine deaminase (AID), a potential RNA editing enzyme. *Cell*, 102, 553-563.
- MURRAY, C. W., BERDINI, V., BUCK, I. M., CARR, M. E., CLEASBY, A., COYLE, J. E., CURRY, J. E., DAY, J. E. H., DAY, P. J., HEARN, K., IQBAL, A., LEE, L. Y. W., MARTINS, V., MORTENSON, P. N., MUNCK, J. M., PAGE, L. W., PATEL, S., ROOMANS, S., SMITH, K., TAMANINI, E. & SAXTY, G. 2015. Fragment-Based Discovery of Potent and Selective DDR1/2 Inhibitors. *Acs Medicinal Chemistry Letters*, 6, 798-803.
- NAKAMURA, N., IKOMA, Y., SHIBATA, Y., MATSUMOTO, T., NINOMIYA, S., KITAGAWA, J., SHIMIZU, M., HARA, T. & TSURUMI, H. 2016. Benefit of Consolidative Radiotherapy in Patients with Limited Stage Diffuse Large B-Cell Lymphoma in the Rituximab Era. *Blood*, 128.
- NEUHAUS, B., BUHREN, S., BOCK, B., ALVES, F., VOGEL, W. F. & KIEFER, F. 2011. Migration inhibition of mammary epithelial cells by Syk is blocked in the presence of DDR1 receptors. *Cellular and Molecular Life Sciences*, 68, 3757-3770.
- NGO, V. N., YOUNG, R. M., SCHMITZ, R., JHAVAR, S., XIAO, W., LIM, K. H., KOHLHAMMER, H., XU, W., YANG, Y., ZHAO, H., SHAFFER, A. L., ROMESSER, P., WRIGHT, G., POWELL, J., ROSENWALD, A., MULLER-HERMELINK, H. K., OTT, G., GASCOYNE, R. D., CONNORS, J. M., RIMSZA, L. M., CAMPO, E., JAFFE, E. S., DELABIE, J., SMELAND, E. B., FISHER, R. I., BRAZIEL, R. M., TUBBS, R. R., COOK, J. R., WEISENBURGER, D. D., CHAN, W. C. & STAUDT, L. M. 2011. Oncogenically active MYD88 mutations in human lymphoma. *Nature*, 470, 115-9.
- NIGG, E. A. 2002. Centrosome aberrations: Cause or consequence of cancer progression? *Nature Reviews Cancer*, 2, 815-825.
- NOMOTO, S., HARUKI, N., TAKAHASHI, T., MASUDA, A., KOSHIKAWA, T., FUJII, Y. & OSADA, H. 1999. Search for in vivo somatic mutations in the mitotic checkpoint gene, hMAD1, in human lung cancers. *Oncogene*, 18, 7180-7183.
- NOORDEEN, N. A., CARAFOLI, F., HOHENESTER, E., HORTON, M. A. & LEITINGER, B. 2006. A transmembrane leucine zipper is required for activation of the dimeric receptor tyrosine kinase DDR1. *Journal of Biological Chemistry*, 281, 22744-22751.
- NOVELLI, S., BRIONES, J. & SIERRA, J. 2013. Epidemiology of lymphoid malignancies: last decade update. *Springerplus*, 2.

- NOWAK, M. A., KOMAROVA, N. L., SENGUPTA, A., JALLEPALLI, P. V., SHIH, I. M., VOGELSTEIN, B. & LENGAUER, C. 2002. The role of chromosomal instability in tumor initiation. *Proc Natl Acad Sci U S A*, 99, 16226-16231.
- NOWAKOWSKI, G. S., LAPLANT, B., HABERMANN, T. M., RIVERA, C. E., MACON, W. R., INWARDS, D. J., MICALLEF, I. N., JOHNSTON, P. B., PORRATA, L. F., ANSELL, S. M., KLEBIG, R. R., REEDER, C. B. & WITZIG, T. E. 2011. Lenalidomide can be safely combined with R-CHOP (R2CHOP) in the initial chemotherapy for aggressive B-cell lymphomas: phase I study. *Leukemia*, 25, 1877-1881.
- NOWELL, P. C. 1976. CLONAL EVOLUTION OF TUMOR-CELL POPULATIONS. *Science*, 194, 23-28.
- OHSHIMA, K., HARAOKA, S., YOSHIOKA, S., HAMASAKI, M., FUJIKI, T., SUZUMIYA, J., KAWASAKI, C., KANDA, M. & KIKUCHI, M. 2000. Mutation analysis of mitotic checkpoint genes (hBUB1 and hBUBR1) and microsatellite instability in adult T-cell leukemia/lymphoma. *Cancer Letters*, 158, 141-150.
- ONGUSAHA, P. P., KIM, J. I., FANG, L., WONG, T. W., YANCOPOULOS, G. D., AARONSON, S. A. & LEE, S. W. 2003. p53 induction and activation of DDR1 kinase counteract p53-mediated apoptosis and influence p53 regulation through a positive feedback loop. *Embo Journal*, 22, 1289-1301.
- ORR, B., GODEK, K. M. & COMPTON, D. 2015. Aneuploidy. *Current Biology*, 25, R538-R542.
- PARK, H. S., KIM, K. R., LEE, H. J., CHOI, H. N., KIM, D. K., KIM, B. T. & MOON, W. S. 2007. Overexpression of discoidin domain receptor 1 increases the migration and invasion of hepatocellular carcinoma cells in association with matrix metalloproteinase. *Oncol Rep*, 18, 1435-41.
- PASQUALUCCI, L., COMPAGNO, M., HOULDSWORTH, J., MONTI, S., GRUNN, A., NANDULA, S. V., ASTER, J. C., MURTY, V. V., SHIPP, M. A. & DALLA-FAVERA, R. 2006. Inactivation of the PRDM1/BLIMP1 gene in diffuse large B cell lymphoma. *J Exp Med*, 203, 311-7.
- PEI, L. & MELMED, S. 1997. Isolation and characterization of a pituitary tumor-transforming gene (PTTG). *Molecular Endocrinology*, 11, 433-441.
- PERCY, M. J., MYRIE, E. A., NEELEY, C. K., AZIM, J. N., ETHIER, S. P. & PETTY, E. M. 2000. Expression and mutational analyses of the human MAD2L1 gene in breast cancer. *Genes Chromosomes & Cancer*, 29, 356-362.
- PEREZ, J. L., JING, S. Q. & WONG, T. W. 1996. Identification of two isoforms of the Cak receptor kinase that are coexpressed in breast tumor cell lines. *Oncogene*, 12, 1469-1477.
- PEREZ, J. L., SHEN, X. Y., FINKERNAGEL, S., SCIORRA, L., JENKINS, N. A., GILBERT, D. J., COPELAND, N. G. & WONG, T. W. 1994. IDENTIFICATION AND CHROMOSOMAL MAPPING OF A RECEPTOR TYROSINE KINASE WITH A PUTATIVE PHOSPHOLIPID-BINDING SEQUENCE IN ITS ECTODOMAIN. *Oncogene*, 9, 211-219.
- PETERS, J. M. 2002. The anaphase-promoting complex: Proteolysis in mitosis and beyond. *Molecular Cell*, 9, 931-943.
- PETERSEN, J. M., TUBBS, R. R., SAVAGE, R. A., CALABRESE, L. C., PROFFITT, M. R., MANOLOVA, Y., MANOLOV, G., SHUMAKER, A., TATSUMI, E., MCCLAIN, K. & ET AL. 1985. Small noncleaved B cell Burkitt-like lymphoma with chromosome t(8;14)

- translocation and Epstein-Barr virus nuclear-associated antigen in a homosexual man with acquired immune deficiency syndrome. *Am J Med*, 78, 141-8.
- PFEIFER, M., GRAU, M., LENZE, D., WENZEL, S. S., WOLF, A., WOLLERT-WULF, B., DIETZE, K., NOGAI, H., STOREK, B., MADLE, H., DORKEN, B., JANZ, M., DIRNHOFER, S., LENZ, P., HUMMEL, M., TZANKOV, A. & LENZ, G. 2013. PTEN loss defines a PI3K/AKT pathway-dependent germinal center subtype of diffuse large B-cell lymphoma. *Proceedings of the National Academy of Sciences of the United States of America*, 110, 12420-12425.
- PFREUNDSCHUH, M., SCHUBERT, J., ZIEPERT, M., SCHMITS, R., MOHREN, M., LENGFELDER, E., REISER, M., NICKENIG, C., CLEMENS, M., PETER, N., BOKEMEYER, C., EIMERMACHER, H., HO, A., HOFFMANN, M., MERTELSMANN, R., TRUEMPER, L., BALLEISEN, L., LIERSCH, R., METZNER, B., HARTMANN, F., GLASS, B., POESCHEL, V., SCHMITZ, N., RUEBE, C., FELLER, A. C., LOEFFLER, M. & DSHNHL 2008. Six versus eight cycles of bi-weekly CHOP-14 with or without rituximab in elderly patients with aggressive CD20+ B-cell lymphomas: a randomised controlled trial (RICOVER-60). *Lancet Oncology*, 9, 105-116.
- PFREUNDSCHUH, M., TRUMPER, L., OSTERBORG, A., PETTENGELL, R., TRNENY, M., IMRIE, K., MA, D., GILL, D., WALEWSKI, J., ZINZANI, P. L., STAHEL, R., KVALOY, S., SHPILBERG, O., JAEGER, U., HANSEN, M., LEHTINEN, T., LOPEZ-GUILLERMO, A., CORRADO, C., SCHELIGA, A., MILPIED, N., MENDILA, M., RASHFORD, M., KUHN, E., LOEFFLER, M. & GRP, M. I. 2006. CHOP-like chemotherapy plus rituximab versus CHOP-like chemotherapy alone in young patients with good-prognosis diffuse large-B-cell lymphoma: a randomised controlled trial by the MabThera International Trial (MInT) Group. *Lancet Oncology*, 7, 379-391.
- PHAN, J., MAZLOOM, A., MEDEIROS, L. J., ZREIK, T. G., WOGAN, C., SHIHADDEH, F., RODRIGUEZ, M. A., FAYAD, L., FOWLER, N., REED, V., HORACE, P. & DABAJA, B. S. 2010. Benefit of consolidative radiation therapy in patients with diffuse large B-cell lymphoma treated with R-CHOP chemotherapy. *Journal of clinical oncology : official journal of the American Society of Clinical Oncology*, 28, 4170-6.
- PHILIP, T., GUGLIELMI, C., HAGENBEEK, A., SOMERS, R., VANDERLIE, H., BRON, D., SONNEVELD, P., GISSELBRECHT, C., CAHN, J. Y., HAROUSSEAU, J. L., COIFFIER, B., BIRON, P., MANDELLI, F. & CHAUVIN, F. 1995. AUTOLOGOUS BONE-MARROW TRANSPLANTATION AS COMPARED WITH SALVAGE CHEMOTHERAPY IN RELAPSES OF CHEMOTHERAPY-SENSITIVE NON-HODGKINS-LYMPHOMA. *New England Journal of Medicine*, 333, 1540-1545.
- PLAYFORD, M. P., BUTLER, R. J., WANG, X. C., KATSO, R. M., COOKE, I. E. & GANESAN, T. S. 1996. The genomic structure of discoidin receptor tyrosine kinase. *Genome Res*, 6, 620-7.
- PURCELL, J. W., DAVIS, J., REDDY, M., MARTIN, S., SAMAYOA, K., VO, H., THOMSEN, K., BEAN, P., KUO, W. L., ZIYAD, S., BILLIG, J., FEILER, H. S., GRAY, J. W., WOOD, K. W. & CASES, S. 2010. Activity of the Kinesin Spindle Protein Inhibitor Ispinesib (SB-715992) in Models of Breast Cancer. *Clinical Cancer Research*, 16, 566-576.
- PUTKEY, F. R., CRAMER, T., MORPHEW, M. K., SILK, A. D., JOHNSON, R. S., MCINTOSH, J. R. & CLEVELAND, D. W. 2002. Unstable kinetochore-microtubule capture and

- chromosomal instability following deletion of CENP-E. *Molecular Biology of the Cell*, 13, 175A-175A.
- QUAN, J., YAHATA, T., ADACHI, S., YOSHIHARA, K. & TANAKA, K. 2011. Identification of receptor tyrosine kinase, discoidin domain receptor 1 (DDR1), as a potential biomarker for serous ovarian cancer. *Int J Mol Sci*, 12, 971-82.
- RAJAGOPALAN, H. & LENGAUER, C. 2004. Aneuploidy and cancer. *Nature*, 432, 338-341.
- RAM, R., LORENTE, G., NIKOLICH, K., URFER, R., FOEHR, E. & NAGAVARAPU, U. 2006. Discoidin domain receptor-1a (DDR1a) promotes glioma cell invasion and adhesion in association with matrix metalloproteinase-2. *J Neurooncol*, 76, 239-48.
- RAMAN, M., CHEN, W. & COBB, M. H. 2007. Differential regulation and properties of MAPKs. *Oncogene*, 26, 3100-3112.
- RAMMAL, H., SABY, C., MAGNIEN, K., VAN-GULICK, L., GAMOTEL, P., BUACHE, E., EL BTAOURI, H., JEANNESSON, P. & MORJANI, H. 2016. Discoidin Domain Receptors: Potential Actors and Targets in Cancer. *Frontiers in Pharmacology*, 7.
- RAO, C. V., YANG, Y. M., SWAMY, M. V., LIU, T. Y., FANG, Y. Q., MAHMOOD, R., JHANWAR-UNIYAL, M. & DAI, W. 2005. Colonic tumorigenesis in BubR1(+/-) Apc(Min/+) compound mutant mice is linked to premature separation of sister chromatids and enhanced genomic instability. *Proc Natl Acad Sci U S A*, 102, 4365-4370.
- RATH, O. & KOZIELSKI, F. 2012. Kinesins and cancer. *Nature Reviews Cancer*, 12, 527-539.
- RECHFELD, F., GRUBERT, P., KIRCHMAIR, J., BOEHLER, M., HAUSER, N., HECHENBERGER, G., GARCZARCZYK, D., LAPALL, G., PREOBRAZHENSKAYALL, M., GOEKJIAN, P., LANGER, T. & HOFMANN, J. 2014. Thienoquinolines as novel disruptors of the PKCe/RACK2 protein-protein interaction. *Journal of Medicinal Chemistry*, 57, 3235-3246.
- REN, B., CAM, H., TAKAHASHI, Y., VOLKERT, T., TERRAGNI, J., YOUNG, R. A. & DYNLACHT, B. D. 2002. E2F integrates cell cycle progression with DNA repair, replication, and G(2)/M checkpoints. *Genes & Development*, 16, 245-256.
- RENNE, C., WILLENBROCK, K., KUPPERS, R., HANSMANN, M. L. & BRAUNINGER, A. 2005. Autocrine- and paracrine-activated receptor tyrosine kinases in classic Hodgkin lymphoma. *Blood*, 105, 4051-4059.
- RIEDER, C. L. 2011. Mitosis in vertebrates: the G2/M and M/A transitions and their associated checkpoints. *Chromosome Research*, 19, 291-306.
- RIEDER, C. L., SCHULTZ, A., COLE, R. & SLUDER, G. 1994. ANAPHASE ONSET IN VERTEBRATE SOMATIC-CELLS IS CONTROLLED BY A CHECKPOINT THAT MONITORS SISTER KINETOCHORE ATTACHMENT TO THE SPINDLE. *Journal of Cell Biology*, 127, 1301-1310.
- RIKOVA, K., GUO, A., ZENG, Q., POSSEMATO, A., YU, J., HAACK, H., NARDONE, J., LEE, K., REEVES, C., LI, Y., HU, Y., TAN, Z. P., STOKES, M., SULLIVAN, L., MITCHELL, J., WETZEL, R., MACNEILL, J., REN, J. M., YUAN, J., BAKALARSKI, C. E., VILLEN, J., KORNHAUSER, J. M., SMITH, B., LI, D., ZHOU, X., GYGI, S. P., GU, T. L., POLAKIEWICZ, R. D., RUSH, J. & COMB, M. J. 2007. Global survey of phosphotyrosine signaling identifies oncogenic kinases in lung cancer. *Cell*, 131, 1190-1203.
- RIX, U., RIX, L. L. R., TERKER, A. S., FERNBACH, N. V., HANTSCHHEL, O., PLANAVSKY, M., BREITWIESER, F. P., HERRMANN, H., COLINGE, J., BENNETT, K. L., AUGUSTIN, M.,

- TILL, J. H., HEINRICH, M. C., VALENT, P. & SUPERTI-FURGA, G. 2010. A comprehensive target selectivity survey of the BCR-ABL kinase inhibitor INNO-406 by kinase profiling and chemical proteomics in chronic myeloid leukemia cells. *Leukemia*, 24, 44-50.
- ROARTY, K. & SERRA, R. 2007. Wnt5a is required for proper mammary gland development and TGF-beta-mediated inhibition of ductal growth. *Development*, 134, 3929-3939.
- ROBERTS, M. E., MAGOWAN, L., HALL, I. P. & JOHNSON, S. R. 2011. Discoidin domain receptor 1 regulates bronchial epithelial repair and matrix metalloproteinase production. *Eur Respir J*, 37, 1482-93.
- ROBINSON, D. R., WU, Y. M. & LIN, S. F. 2000. The protein tyrosine kinase family of the human genome. *Oncogene*, 19, 5548-5557.
- ROBINSON, M. D., MCCARTHY, D. J. & SMYTH, G. K. 2010. edgeR: a Bioconductor package for differential expression analysis of digital gene expression data. *Bioinformatics*, 26, 139-140.
- ROSCHEWSKI, M., STAUDT, L. M. & WILSON, W. H. 2014. Diffuse large B-cell lymphoma-treatment approaches in the molecular era. *Nature Reviews Clinical Oncology*, 11, 12-23.
- ROSENBLATT, J. 2005. Spindle assembly: asters part their separate ways. *Nature Cell Biology*, 7, 219-222.
- ROSENWALD, A., WRIGHT, G., CHAN, W. C., CONNORS, J. M., CAMPO, E., FISHER, R. I., GASCOYNE, R. D., MULLER-HERMELINK, H. K., SMELAND, E. B., GILTANANE, J. M., HURT, E. M., ZHAO, H., AVERETT, L., YANG, L., WILSON, W. H., JAFFE, E. S., SIMON, R., KLAUSNER, R. D., POWELL, J., DUFFEY, P. L., LONGO, D. L., GREINER, T. C., WEISENBURGER, D. D., SANGER, W. G., DAVE, B. J., LYNCH, J. C., VOSE, J., ARMITAGE, J. O., MONTSERRAT, E., LOPEZ-GUILLERMO, A., GROGAN, T. M., MILLER, T. P., LEBLANC, M., OTT, G., KVALOY, S., DELABIE, J., HOLTE, H., KRAJCI, P., STOKKE, T. & STAUDT, L. M. 2002. The use of molecular profiling to predict survival after chemotherapy for diffuse large-B-cell lymphoma. *N Engl J Med*, 346, 1937-47.
- ROSKOSKI, R. 2012. ERK1/2 MAP kinases: Structure, function, and regulation. *Pharmacological Research*, 66, 105-143.
- RUDRA-GANGULY, N., LOWE, C., MATTIE, M., CHANG, M. S., SATPAYEV, D., VERLINSKY, A., AN, Z., HU, L., YANG, P., CHALLITA-EID, P., STOVER, D. R. & PEREIRA, D. S. 2014. Discoidin domain receptor 1 contributes to tumorigenesis through modulation of TGFBI expression. *PLoS One*, 9, e111515.
- RUIZ, P. A. & JARAI, G. 2011. Collagen I induces discoidin domain receptor (DDR) 1 expression through DDR2 and a JAK2-ERK1/2-mediated mechanism in primary human lung fibroblasts. *J Biol Chem*, 286, 12912-23.
- SAEZ, A. I., SAEZ, A. J., ARTIGA, M. J., PEREZ-ROSADO, A., CAMACHO, F. I., DIEZ, A., GARCIA, J. F., FRAGA, M., BOSCH, R., RODRIGUEZ-PINILLA, S. M., MOLLEJO, M., ROMERO, C., SANCHEZ-VERDE, L., POLLAN, M. & PIRIS, M. A. 2004. Building an outcome predictor model for diffuse large B-cell lymphoma. *American Journal of Pathology*, 164, 613-622.

- SAKAMOTO, O., SUGA, M., SUDA, T. & ANDO, M. 2001. Expression of discoidin domain receptor 1 tyrosine kinase on the human bronchial epithelium. *Eur Respir J*, 17, 969-74.
- SANCHEZ, M. P., TAPLEY, P., SAINI, S. S., HE, B., PULIDO, D. & BARBACID, M. 1994. MULTIPLE TYROSINE PROTEIN-KINASES IN RAT HIPPOCAMPAL-NEURONS - ISOLATION OF PTK-3, A RECEPTOR EXPRESSED IN PROLIFERATIVE ZONES OF THE DEVELOPING BRAIN. *Proc Natl Acad Sci U S A*, 91, 1819-1823.
- SANTAGUIDA, S., RICHARDSON, A., IYER, D. R., M'SAAD, O., ZASADIL, L., KNOUSE, K. A., WONG, Y. L., RHIND, N., DESAI, A. & AMON, A. 2017. Chromosome Mis-segregation Generates Cell-Cycle-Arrested Cells with Complex Karyotypes that Are Eliminated by the Immune System. *Developmental Cell*, 41, 638-+.
- SATGE, D., SASCO, A. J. & LACOUR, B. 2003. Are solid tumours different in children with Down's syndrome? *International Journal of Cancer*, 106, 297-298.
- SAVAGE, K. J., JOHNSON, N. A., BEN-NERIAH, S., CONNORS, J. M., SEHN, L. H., FARINHA, P., HORSMAN, D. E. & GASCOYNE, R. D. 2009. MYC gene rearrangements are associated with a poor prognosis in diffuse large B-cell lymphoma patients treated with R-CHOP chemotherapy. *Blood*, 114, 3533-7.
- SAWYERS, C. L. 2001. Research on resistance to cancer drug Gleevec. *Science*, 294, 1834-1834.
- SCHAADT, M., DIEHL, V., STEIN, H., FONATSCH, C. & KIRCHNER, H. H. 1980. 2 NEOPLASTIC CELL-LINES WITH UNIQUE FEATURES DERIVED FROM HODGKINS-DISEASE. *International Journal of Cancer*, 26, 723-731.
- SCHAADT, M., FONATSCH, C., KIRCHNER, H. & DIEHL, V. 1979. ESTABLISHMENT OF A MALIGNANT, EPSTEIN-BARR-VIRUS (EBV) NEGATIVE CELL-LINE FROM THE PLEURA EFFUSION OF A PATIENT WITH HODGKINS-DISEASE. *Blut*, 38, 185-190.
- SCHERER, W. F., SYVERTON, J. T. & GEY, G. O. 1953. STUDIES ON THE PROPAGATION INVITRO OF POLIOMYELITIS VIRUSES .4. VIRAL MULTIPLICATION IN A STABLE STRAIN OF HUMAN MALIGNANT EPITHELIAL CELLS (STRAIN HELA) DERIVED FROM AN EPIDERMOID CARCINOMA OF THE CERVIX. *Journal of Experimental Medicine*, 97, 695-&.
- SCHVARTZMAN, J. M., SOTILLO, R. & BENEZRA, R. 2010. Mitotic chromosomal instability and cancer: mouse modelling of the human disease. *Nature Reviews Cancer*, 10, 102-115.
- SCOLNICK, D. M. & HALAZONETIS, T. D. 2000. Chfr defines a mitotic stress checkpoint that delays entry into metaphase. *Nature*, 406, 430-435.
- SCOTT, D. W., WRIGHT, G. W., WILLIAMS, P. M., LIH, C. J., WALSH, W., JAFFE, E. S., ROSENWALD, A., CAMPO, E., CHAN, W. C., CONNORS, J. M., SMELAND, E. B., MOTTOK, A., BRAZIEL, R. M., OTT, G., DELABIE, J., TUBBS, R. R., COOK, J. R., WEISENBURGER, D. D., GREINER, T. C., GLINSMANN-GIBSON, B. J., FU, K., STAUDT, L. M., GASCOYNE, R. D. & RIMSZA, L. M. 2014. Determining cell-of-origin subtypes of diffuse large B-cell lymphoma using gene expression in formalin-fixed paraffin-embedded tissue. *Blood*, 123, 1214-7.
- SEGALINY, A. I., TELLEZ-GABRIEL, M., HEYMANN, M.-F. & HEYMANN, D. 2015. Receptor tyrosine kinases: Characterisation, mechanism of action and therapeutic interests for bone cancers. *Journal of Bone Oncology*, 4, 1-12.

- SEHN, L. H., BERRY, B., CHHANABHAI, M., FITZGERALD, C., GILL, K., HOSKINS, P., KLASA, R., SAVAGE, K. J., SHENKIER, T., SUTHERLAND, J., GASCOYNE, R. D. & CONNORS, J. M. 2007. The revised International Prognostic Index (R-IPI) is a better predictor of outcome than the standard IPI for patients with diffuse large B-cell lymphoma treated with R-CHOP. *Blood*, 109, 1857-61.
- SEHN, L. H., DONALDSON, J., CHHANABHAI, M., FITZGERALD, C., GILL, K., KLASA, R., MACPHERSON, N., O'REILLY, S., SPINELLI, J. J., SUTHERLAND, J., WILSON, K. S., GASCOYNE, R. D. & CONNORS, J. M. 2005. Introduction of combined CHOP plus rituximab therapy dramatically improved outcome of diffuse large B-cell lymphoma in British Columbia. *J Clin Oncol*, 23, 5027-33.
- SENOVILLA, L., VITALE, I., MARTINS, I., TAILLER, M., PAILLERET, C., MICHAUD, M., GALLUZZI, L., ADJEMIAN, S., KEPP, O., NISO-SANTANO, M., SHEN, S., MARINO, G., CRIOLLO, A., BOILEVE, A., JOB, B., LADOIRE, S., GHIRINGHELLI, F., SISTIGU, A., YAMAZAKI, T., RELLO-VARONA, S., LOCHER, C., POIRIER-COLAME, V., TALBOT, M., VALENT, A., BERARDINELLI, F., ANTOCCIA, A., CICCOSANTI, F., FIMIA, G. M., PIACENTINI, M., FUEYO, A., MESSINA, N. L., LI, M., CHAN, C. J., SIGL, V., POURCHER, G., RUCKENSTUHL, C., CARMONA-GUTIERREZ, D., LAZAR, V., PENNINGER, J. M., MADEO, F., LOPEZ-OTIN, C., SMYTH, M. J., ZITVOGEL, L., CASTEDO, M. & KROEMER, G. 2012. An Immunosurveillance Mechanism Controls Cancer Cell Ploidy. *Science*, 337, 1678-1684.
- SHACKEL, N. A., MCGUINNESS, P. H., ABBOTT, C. A., GORRELL, M. D. & MCCAUGHAN, G. W. 2002. Insights into the pathobiology of hepatitis C virus-associated cirrhosis - Analysis of intrahepatic differential gene expression. *American Journal of Pathology*, 160, 641-654.
- SHAFFER, A. L., III, YOUNG, R. M. & STAUDT, L. M. 2012. Pathogenesis of Human B Cell Lymphomas. In: PAUL, W. E. (ed.) *Annual Review of Immunology, Vol 30*.
- SHAFFER, A. L., SHAPIRO-SHELEF, M., IWAKOSHI, N. N., LEE, A. H., QIAN, S. B., ZHAO, H., YU, X., YANG, L. M., TAN, B. K., ROSENWALD, A., HURT, E. M., PETROULAKIS, E., SONENBERG, N., YEWDELL, J. W., CALAME, K., GLIMCHER, L. H. & STAUDT, L. M. 2004. XBP1, downstream of Blimp-1, expands the secretory apparatus and other organelles, and increases protein synthesis in plasma cell differentiation. *Immunity*, 21, 81-93.
- SHAFFER, A. L., YU, X., HE, Y. S., BOLDRICK, J., CHAN, E. P. & STAUDT, L. M. 2000. BCL-6 represses genes that function in lymphocyte differentiation, inflammation, and cell cycle control. *Immunity*, 13, 199-212.
- SHAH, J. V., BOTVINICK, E., BONDAY, Z., FURNARI, F., BERNS, M. & CLEVELAND, D. W. 2004. Dynamics of centromere and kinetochore proteins: Implications for checkpoint signaling and silencing. *Current Biology*, 14, 942-952.
- SHELTZER, J. M. 2013. A Transcriptional and Metabolic Signature of Primary Aneuploidy Is Present in Chromosomally Unstable Cancer Cells and Informs Clinical Prognosis. *Cancer Research*, 73, 6401-6412.
- SHEN, Q., CICINNATI, V. R., ZHANG, X., IACOB, S., WEBER, F., SOTIROPOULOS, G. C., RADTKE, A., LU, M., PAUL, A., GERKEN, G. & BECKEBAUM, S. 2010. Role of microRNA-199a-5p and discoidin domain receptor 1 in human hepatocellular carcinoma invasion. *Mol Cancer*, 9, 227.

- SHIMADA, K., NAKAMURA, M., ISHIDA, E., HIGUCHI, T., YAMAMOTO, H., TSUJIKAWA, K. & KONISHI, N. 2008. Prostate cancer antigen-1 contributes to cell survival and invasion through discoidin receptor 1 in human prostate cancer. *Cancer Sci*, 99, 39-45.
- SHIN, H. J., BAEK, K. H., JEON, A. H., PARK, M. T., LEE, S. J., KANG, C. M., LEE, H. S., YOO, S. H., CHUNG, D. H., SUNG, Y. C., MCKEON, F. & LEE, C. W. 2003. Dual roles of human BubR1, a mitotic checkpoint kinase, in the monitoring of chromosomal instability. *Cancer Cell*, 4, 483-497.
- SHINTANI, Y., FUKUMOTO, Y., CHAIKA, N., SVOBODA, R., WHEELLOCK, M. J. & JOHNSON, K. R. 2008. Collagen I-mediated up-regulation of N-cadherin requires cooperative signals from integrins and discoidin domain receptor 1. *J Cell Biol*, 180, 1277-89.
- SHIPP, M. A., HARRINGTON, D. P., ANDERSON, J. R., ARMITAGE, J. O., BONADONNA, G., BRITTINGER, G., CABANILLAS, F., CANELLOS, G. P., COIFFIER, B., CONNORS, J. M., COWAN, R. A., CROWTHER, D., DAHLBERG, S., ENGELHARD, M., FISHER, R. I., GISSELBRECHT, C., HORNING, S. J., LEPAGE, E., LISTER, T. A., MEERWALDT, J. H., MONTSERRAT, E., NISSEN, N. I., OKEN, M. M., PETERSON, B. A., TONDINI, C., VELASQUEZ, W. A. & YEAP, B. Y. 1993. A PREDICTIVE MODEL FOR AGGRESSIVE NON-HODGKINS-LYMPHOMA. *New England Journal of Medicine*, 329, 987-994.
- SHIPP, M. A., ROSS, K. N., TAMAYO, P., WENG, A. P., KUTOK, J. L., AGUIAR, R. C. T., GAASENBEEK, M., ANGELO, M., REICH, M., PINKUS, G. S., RAY, T. S., KOVAL, M. A., LAST, K. W., NORTON, A., LISTER, T. A., MESIROV, J., NEUBERG, D. S., LANDER, E. S., ASTER, J. C. & GOLUB, T. R. 2002. Diffuse large B-cell lymphoma outcome prediction by gene-expression profiling and supervised machine learning. *Nature Medicine*, 8, 68-74.
- SHRIVASTAVA, A., RADZIEJEWSKI, C., CAMPBELL, E., KOVAC, L., MCGLYNN, M., RYAN, T. E., DAVIS, S., GOLDFARB, M. P., GLASS, D. J., LEMKE, G. & YANCOPOULOS, G. D. 1997. An orphan receptor tyrosine kinase family whose members serve as nonintegrin collagen receptors. *Mol Cell*, 1, 25-34.
- SLAMON, D. J., GODOLPHIN, W., JONES, L. A., HOLT, J. A., WONG, S. G., KEITH, D. E., LEVIN, W. J., STUART, S. G., UDOVE, J., ULLRICH, A. & PRESS, M. F. 1989. STUDIES OF THE HER-2/NEU PROTO-ONCOGENE IN HUMAN-BREAST AND OVARIAN-CANCER. *Science*, 244, 707-712.
- SMITH, A., CROUCH, S., LAX, S., LI, J., PAINTER, D., HOWELL, D., PATMORE, R., JACK, A. & ROMAN, E. 2015. Lymphoma incidence, survival and prevalence 2004-2014: subtype analyses from the UK's Haematological Malignancy Research Network. *British Journal of Cancer*, 112, 1575-1584.
- SMITH, N., TIERNEY, R., WEI, W., VOCKERODT, M., MURRAY, P. G., WOODMAN, C. B. & ROWE, M. 2013. Induction of interferon-stimulated genes on the IL-4 response axis by Epstein-Barr virus infected human b cells; relevance to cellular transformation. *PLoS One*, 8, e64868.
- SMYTH, G. K. 2004. Linear models and empirical bayes methods for assessing differential expression in microarray experiments. *Statistical applications in genetics and molecular biology*, 3, Article3-Article3.
- SNEERINGER, C. J., SCOTT, M. P., KUNTZ, K. W., KNUTSON, S. K., POLLOCK, R. M., RICHON, V. M. & COPELAND, R. A. 2010. Coordinated activities of wild-type plus mutant

- EZH2 drive tumor-associated hypertrimethylation of lysine 27 on histone H3 (H3K27) in human B-cell lymphomas. *Proceedings of the National Academy of Sciences of the United States of America*, 107, 20980-20985.
- SONG, G., OUYANG, G. L. & BAO, S. D. 2005. The activation of Akt/PKB signaling pathway and cell survival. *Journal of Cellular and Molecular Medicine*, 9, 59-71.
- SONG, M. S., SONG, S. J., AYAD, N. G., CHANG, J. S., LEE, J. H., HONG, H. K., LEE, H., CHOI, N., KIM, J., KIM, H., KIM, J. W., CHOI, E. J., KIRSCHNER, M. W. & LIM, D. S. 2004. The tumour suppressor RASSF1A regulates mitosis by inhibiting the APC-Cdc20 complex. *Nature Cell Biology*, 6, 129-+.
- SOUERS, A. J., LEVERSON, J. D., BOGHAERT, E. R., ACKLER, S. L., CATRON, N. D., CHEN, J., DAYTON, B. D., DING, H., ENSCHEDE, S. H., FAIRBROTHER, W. J., HUANG, D. C. S., HYMOWITZ, S. G., JIN, S., KHAW, S. L., KOVAR, P. J., LAM, L. T., LEE, J., MAECKER, H. L., MARSH, K. C., MASON, K. D., MITTEN, M. J., NIMMER, P. M., OLEKSIJEW, A., PARK, C. H., PARK, C.-M., PHILLIPS, D. C., ROBERTS, A. W., SAMPATH, D., SEYMOUR, J. F., SMITH, M. L., SULLIVAN, G. M., TAHIR, S. K., TSE, C., WENDT, M. D., XIAO, Y., XUE, J. C., ZHANG, H., HUMERICKHOUSE, R. A., ROSENBERG, S. H. & ELMORE, S. W. 2013. ABT-199, a potent and selective BCL-2 inhibitor, achieves antitumor activity while sparing platelets. *Nature Medicine*, 19, 202-208.
- SPAGNOLO, D. V., ELLIS, D. W., JUNEJA, S., LEONG, A. S. Y., MILIAUSKAS, J., NORRIS, D. L. & TURNER, J. 2004. The role of molecular studies in lymphoma diagnosis: a review. *Pathology*, 36, 19-44.
- SPICUGLIA, S., FRANCHINI, D. M. & FERRIER, P. 2006. Regulation of V(D)J recombination. *Current Opinion in Immunology*, 18, 158-163.
- SQUIRE, J. A., BAYANI, J., LUK, C., UNWIN, L., TOKUNAGA, J., MACMILLAN, C., IRISH, J., BROWN, D., GULLANE, P. & KAMEL-REID, S. 2002. Molecular cytogenetic analysis of head and neck squamous cell carcinoma: By comparative genomic hybridization, spectral karyotyping, and expression array analysis. *Head and Neck-Journal for the Sciences and Specialties of the Head and Neck*, 24, 874-886.
- STORCHOVA, Z. & PELLMAN, D. 2004. From polyploidy to aneuploidy, genome instability and cancer. *Nature Reviews Molecular Cell Biology*, 5, 45-54.
- SUDAKIN, V., CHAN, G. K. T. & YEN, T. J. 2001. Checkpoint inhibition of the APC/C in HeLa cells is mediated by a complex of BUBR1, BUB3, CDC20, and MAD2. *Journal of Cell Biology*, 154, 925-936.
- SUH, H. N. & HAN, H. J. 2011. Collagen I Regulates the Self-Renewal of Mouse Embryonic Stem Cells Through alpha 2 beta 1 Integrin- and DDR1-Dependent Bmi-1. *Journal of Cellular Physiology*, 226, 3422-3432.
- SUN, X., PHAN, T. N., JUNG, S. H., KIM, S. Y., CHO, J. U., LEE, H., WOO, S. H., PARK, T. K. & YANG, B. S. 2012. LCB 03-0110, a novel pan-discoidin domain receptor/c-Src family tyrosine kinase inhibitor, suppresses scar formation by inhibiting fibroblast and macrophage activation. *J Pharmacol Exp Ther*, 340, 510-9.
- SWERDLOW, S., CAMPO, E., HARRIS, N., JAFFE, E., PILERI, S. A., STEIN, H., THIELE, J. & VARDIMAN, J. 2008. Large B-cell lymphoma arising in HHV8-associated multicentric Castleman disease. . *WHO Classification of Tumours of Haematopoietic and Lymphoid Tissues*, Fourth Edition.

- SWERDLOW, S. H., CAMPO, E., PILERI, S. A., HARRIS, N. L., STEIN, H., SIEBERT, R., ADVANI, R., GHIELMINI, M., SALLES, G. A., ZELENETZ, A. D. & JAFFE, E. S. 2016. The 2016 revision of the World Health Organization classification of lymphoid neoplasms. *Blood*, 127, 2375-2390.
- TAM, W., GOMEZ, M., CHADBURN, A., LEE, J. W., CHAN, W. C. & KNOWLES, D. M. 2006. Mutational analysis of PRDM1 indicates a tumor-suppressor role in diffuse large B-cell lymphomas. *Blood*, 107, 4090-4100.
- TANG, Y.-C., WILLIAMS, B. R., SIEGEL, J. J. & AMON, A. 2011. Identification of Aneuploidy-Selective Antiproliferation Compounds. *Cell*, 144, 499-512.
- TAO, Q., SWINNEN, L. J., YANG, J., SRIVASTAVA, G., ROBERTSON, K. D. & AMBINDER, R. F. 1999. Methylation status of the Epstein-Barr virus major latent promoter C in iatrogenic B cell lymphoproliferative disease. Application of PCR-based analysis. *Am J Pathol*, 155, 619-25.
- TAYLOR, S. S., HA, E. & MCKEON, F. 1998. The human homologue of Bub3 is required for kinetochore localization of Bub1 and a Mad3/Bub1-related protein kinase. *Journal of Cell Biology*, 142, 1-11.
- TAYLOR, S. S. & KORNEV, A. P. 2011. Protein kinases: evolution of dynamic regulatory proteins. *Trends in Biochemical Sciences*, 36, 65-77.
- TEAM, R. C. 1997. R: A language and environment for statistical computing. *R Foundation for Statistical Computing, Vienna, Austria*.
- THIEBLEMONT, C., BRIERE, J., MOUNIER, N., VOELKER, H.-U., CUCCUINI, W., HIRCHAUD, E., ROSENWALD, A., JACK, A., SUNDSTROM, C., COGLIATTI, S., TROUGOUBOFF, P., BOUDOVA, L., YSEBAERT, L., SOULIER, J., CHEVALIER, C., BRON, D., SCHMITZ, N., GAULARD, P., HOULGATTE, R. & GISSELBRECHT, C. 2011. The Germinal Center/Activated B-Cell Subclassification Has a Prognostic Impact for Response to Salvage Therapy in Relapsed/Refractory Diffuse Large B-Cell Lymphoma: A BIOCORAL Study. *Journal of Clinical Oncology*, 29, 4079-4087.
- THIEBLEMONT, C., DELFAU-LARUE, M. H. & COIFFIER, B. 2012. Lenalidomide in diffuse large B-cell lymphoma. *Adv Hematol*, 2012, 861060.
- THIERY, J. P., ACLOQUE, H., HUANG, R. Y. J. & NIETO, M. A. 2009. Epithelial-Mesenchymal Transitions in Development and Disease. *Cell*, 139, 871-890.
- TIBILETTI, M. G., MILANI, K., MARTIN, V., ZUCCA, E., MOTTA, T., CORTELAZZO, S., PINOTTI, G., MAZZUCHELLI, L., PRUNERI, G., MARTINELLI, G., BARBAZZA, R., CAPELLA, C., BERTONI, F. & IELSG 2007. Chromosome instability and translocation t(11;18) in primary gastric marginal zone B-cell lymphoma of MALT-type. *Hematological Oncology*, 25, 184-188.
- TILL, J. H., BECERRA, M., WATTY, A., LU, Y., MA, Y. L., NEUBERT, T. A., BURDEN, S. J. & HUBBARD, S. R. 2002. Crystal structure of the MuSK tyrosine kinase: Insights into receptor autoregulation. *Structure*, 10, 1187-1196.
- TOKARSKI, J. S., NEWITT, J. A., CHANG, C. Y. J., CHENG, J. D., WITTEKIND, M., KIEFER, S. E., KISH, K., LEE, F. Y. F., BORZILLERRI, R., LOMBARDO, L. J., XIE, D. L., ZHANG, Y. Q. & KLEI, H. E. 2006. The structure of dasatinib (BMS-354825) bound to activated ABL kinase domain elucidates its inhibitory activity against imatinib-resistant ABL mutants. *Cancer Research*, 66, 5790-5797.

- TOMASSON, M. H., XIANG, Z., WALGREN, R., ZHAO, Y., KASAI, Y., MINER, T., RIES, R. E., LUBMAN, O., FREMONT, D. H., MCLELLAN, M. D., PAYTON, J. E., WESTERVELT, P., DIPERSIO, J. F., LINK, D. C., WALTER, M. J., GRAUBERT, T. A., WATSON, M., BATY, J., HEATH, S., SHANNON, W. D., NAGARAJAN, R., BLOOMFIELD, C. D., MARDIS, E. R., WILSON, R. K. & LEY, T. J. 2008. Somatic mutations and germline sequence variants in the expressed tyrosine kinase genes of patients with de novo acute myeloid leukemia. *Blood*, 111, 4797-4808.
- TORBAN, E. & GOODYER, P. 2009. The Kidney and Ear: Emerging Parallel Functions. *Annual Review of Medicine*.
- TORRES, E. M., WILLIAMS, B. R. & AMON, A. 2008. Aneuploidy: Cells losing their balance. *Genetics*, 179, 737-746.
- TSUKASAKI, K., MILLER, C. W., GREENSPUN, E., ESHAGHIAN, S., KAWABATA, H., FUJIMOTO, T., TOMONAGA, M., SAWYERS, C., SAID, J. W. & KOEFFLER, H. P. 2001. Mutations in the mitotic check point gene, MAD1L1, in human cancers. *Oncogene*, 20, 3301-3305.
- TWEEDDALE, M. E., LIM, B., JAMAL, N., ROBINSON, J., ZALCBERG, J., LOCKWOOD, G., MINDEN, M. D. & MESSNER, H. A. 1987 The presence of clonogenic cells in high-grade malignant lymphoma: a prognostic factor. *Blood*, 69, 1307-14.
- TZANKOV, A., GSCHWENDTNER, A., AUGUSTIN, F., FIEGL, M., OBERMANN, E. C., DIRNHOFER, S. & WENT, P. 2006. Diffuse large B-cell lymphoma with overexpression of cyclin E substantiates poor standard treatment response and inferior outcome. *Clinical Cancer Research*, 12, 2125-2132.
- ULLRICH, A. & SCHLESSINGER, J. 1990. SIGNAL TRANSDUCTION BY RECEPTORS WITH TYROSINE KINASE-ACTIVITY. *Cell*, 61, 203-212.
- UNDERWOOD, D. C., OSBORN, R. R., BOCHNOWICZ, S., WEBB, E. F., RIEMAN, D. J., LEE, J. C., ROMANIC, A. M., ADAMS, J. L., HAY, D. W. P. & GRISWOLD, D. E. 2000. SB 239063, a p38 MAPK inhibitor, reduces neutrophilia, inflammatory cytokines, MMP-9, and fibrosis in lung. *American Journal of Physiology-Lung Cellular and Molecular Physiology*, 279, L895-L902.
- VALENCIA, K., ORMAZABAL, C., ZANDUETA, C., LUIS-RAVELO, D., ANTON, I., PAJARES, M. J., AGORRETA, J., MONTUENGA, L. M., MARTINEZ-CANARIAS, S., LEITINGER, B. & LECANDA, F. 2012. Inhibition of collagen receptor discoidin domain receptor-1 (DDR1) reduces cell survival, homing, and colonization in lung cancer bone metastasis. *Clin Cancer Res*, 18, 969-80.
- VALIATHAN, R. R., MARCO, M., LEITINGER, B., KLEER, C. G. & FRIDMAN, R. 2012. Discoidin domain receptor tyrosine kinases: new players in cancer progression. *Cancer Metastasis Rev*, 31, 295-321.
- VANDER KOOI, C. W., JUSINO, M. A., PERMAN, B., NEAU, D. B., BELLAMY, H. D. & LEAHY, D. J. 2007. Structural basis for ligand and heparin binding to neuropilin B domains. *Proc Natl Acad Sci U S A*, 104, 6152-6157.
- VELASQUEZ, W. S., FULLER, L. M., JAGANNATH, S., TUCKER, S. L., NORTH, L. B., HAGEMEISTER, F. B., MCLAUGHLIN, P., SWAN, F., REDMAN, J. R., RODRIGUEZ, M. A. & CABANILLAS, F. 1991. STAGE-I AND STAGE-II DIFFUSE LARGE CELL LYMPHOMAS - PROGNOSTIC FACTORS AND LONG-TERM RESULTS WITH CHOP-BLEO AND RADIOTHERAPY. *Blood*, 77, 942-947.

- VICTORA, G. D. & NUSSENZWEIG, M. C. 2012. Germinal Centers. *In: PAUL, W. E. (ed.) Annual Review of Immunology, Vol 30.*
- VITOLO, U., CHIAPPELLA, A., FRANCESCHETTI, S., CARELLA, A. M., BALDI, I., INGHIRAMI, G., SPINA, M., PAVONE, V., LADETTO, M., LIBERATI, A. M., MOLINARI, A. L., ZINZANI, P., SALVI, F., FATTORI, P. P., ZACCARIA, A., DREYLING, M., BOTTO, B., CASTELLINO, A., CONGIU, A., GAUDIANO, M., ZANNI, M., CICCONE, G., GAIDANO, G., ROSSI, G. & FDN ITALIANA, L. 2014. Lenalidomide plus R-CHOP21 in elderly patients with untreated diffuse large B-cell lymphoma: results of the REAL07 open-label, multicentre, phase 2 trial. *Lancet Oncology*, 15, 730-737.
- VOCKERODT, M., MORGAN, S. L., KUO, M., WEI, W., CHUKWUMA, M. B., ARRAND, J. R., KUBE, D., GORDON, J., YOUNG, L. S., WOODMAN, C. B. & MURRAY, P. G. 2008. The Epstein-Barr virus oncoprotein, latent membrane protein-1, reprograms germinal centre B cells towards a Hodgkin's Reed-Sternberg-like phenotype. *The Journal of Pathology*, 216, 83-92.
- VOCKERODT, M., YAP, L. F., SHANNON-LOWE, C., CURLEY, H., WEI, W., VRZALIKOVA, K. & MURRAY, P. G. 2015. The Epstein-Barr virus and the pathogenesis of lymphoma. *J Pathol*, 235, 312-22.
- VOGEL, W., BRAKEBUSCH, C., FASSLER, R., ALVES, F., RUGGIERO, F. & PAWSON, T. 2000. Discoidin domain receptor 1 is activated independently of beta(1) integrin. *J Biol Chem*, 275, 5779-84.
- VOGEL, W., GISH, G. D., ALVES, F. & PAWSON, T. 1997. The discoidin domain receptor tyrosine kinases are activated by collagen. *Mol Cell*, 1, 13-23.
- VOGEL, W. F., ABDULHUSSEIN, R. & FORD, C. E. 2006. Sensing extracellular matrix: an update on discoidin domain receptor function. *Cell Signal*, 18, 1108-16.
- VOGEL, W. F., ASZODI, A., ALVES, F. & PAWSON, T. 2001. Discoidin domain receptor 1 tyrosine kinase has an essential role in mammary gland development. *Mol Cell Biol*, 21, 2906-17.
- WADSWORTH, P., SHELDEN, E., RUPP, J. & RIEDER, C. 1988. MICROTUBULE DYNAMICS IN ANAPHASE CELLS. *Journal of Cell Biology*, 107, 241A-241A.
- WANG, C. Z., HSU, Y. M. & TANG, M. J. 2005. Function of discoidin domain receptor I in HGF-induced branching tubulogenesis of MDCK cells in collagen gel. *J Cell Physiol*, 203, 295-304.
- WANG, C. Z., SU, H. W., HSU, Y. C., SHEN, M. R. & TANG, M. J. 2006. A discoidin domain receptor 1/SHP-2 signaling complex inhibits alpha2beta1-integrin-mediated signal transducers and activators of transcription 1/3 activation and cell migration. *Mol Biol Cell*, 17, 2839-52.
- WANG, R. H., YU, H. T. & DENG, C. X. 2004a. A requirement for breast-cancer-associated gene 1 (BRCA1) in the spindle checkpoint. *Proc Natl Acad Sci U S A*, 101, 17108-17113.
- WANG, T. L., DIAZ, L. A., ROMANS, K., BARDELLI, A., SAHA, S., GALIZIA, G., CHOTI, M., DONEHOWER, R., PARMIGIANI, G., SHIH, L. M., IACOBUZIO-DONAHUE, C., KINZLER, K. W., VOGELSTEIN, B., LENGAUER, C. & VELCULESCU, V. E. 2004b. Digital karyotyping identifies thymidylate synthase amplification as a mechanism of resistance to 5-fluorouracil in metastatic colorectal cancer patients. *Proc Natl Acad Sci U S A*, 101, 3089-3094.

- WANG, W., HU, S., LU, X., YOUNG, K. H. & MEDEIROS, L. J. 2015. Triple-hit B-cell Lymphoma With MYC, BCL2, and BCL6 Translocations/Rearrangements Clinicopathologic Features of 11 Cases. *American Journal of Surgical Pathology*, 39, 1132-1139.
- WATANABE, T., WU, T., CATALANO, P. J., UEKI, T., SATRIANO, R., BENSON, A. B. & HAMILTON, S. R. 2001. Molecular predictors of survival after adjuvant chemotherapy for colon cancer. *New England Journal of Medicine*, 344, 1196-1206.
- WEAVER, B. A. A., BONDAY, Z. Q., PUTKEY, F. R., KOPS, G., SILK, A. D. & CLEVELAND, D. W. 2003. Centromere-associated protein-E is essential for the mammalian mitotic checkpoint to prevent aneuploidy due to single chromosome loss. *Journal of Cell Biology*, 162, 551-563.
- WEAVER, B. A. A., SILK, A. D., MONTAGNA, C., VERDIER-PINARD, P. & CLEVELAND, D. W. 2007. Aneuploidy acts both oncogenically and as a tumor suppressor. *Cancer Cell*, 11, 25-36.
- WEINER, H. L., HUANG, H., ZAGZAG, D., BOYCE, H., LICHTENBAUM, R. & ZIFF, E. B. 2000. Consistent and selective expression of the discoidin domain receptor-1 tyrosine kinase in human brain tumors. *Neurosurgery*, 47, 1400-9.
- WEISBERG, E., MANLEY, P. W., BREITENSTEIN, W., BRUGGEN, J., COWAN-JACOB, S. W., RAY, A., HUNTLY, B., FABBRO, D., FENDRICH, G., HALL-MEYERS, E., KUNG, A. L., MESTAN, J., DALEY, G. Q., CALLAHAN, L., CATLEY, L., CAVAZZA, C., MOHAMMED, A., NEUBERG, D., WRIGHT, R. D., GILLILAND, D. G. & GRIFFIN, J. D. 2005. Characterization of AMN107, a selective inhibitor of native and mutant Bcr-Abl. *Cancer Cell*, 7, 129-141.
- WEISBERG, E., MANLEY, P. W., COWAN-JACOB, S. W., HOCHHAUS, A. & GRIFFIN, J. D. 2007. Second generation inhibitors of BCR-ABL for the treatment of imatinib-resistant chronic myeloid leukaemia. *Nature Reviews Cancer*, 7, 345-U5.
- WEISENBURGER, D. D. 1985. Lymphoid malignancies in Nebraska: a hypothesis. *The Nebraska medical journal*, 70, 300-5.
- WELS, J., KAPLAN, R. N., RAFII, S. & LYDEN, D. 2008. Migratory neighbors and distant invaders: tumor-associated niche cells. *Genes & Development*, 22, 559-574.
- WENNBORG, A., AMAN, P., SARANATH, D., PEAR, W., SUMEGI, J. & KLEIN, G. 1987. Conversion of the lymphoma line "BJAB" by Epstein-Barr virus into phenotypically altered sublines is accompanied by increased c-myc mRNA levels. *Int J Cancer*, 40, 202-6.
- WHITTLE, H. C., BROWN, J., MARSH, K., GREENWOOD, B. M., SEIDELIN, P., TIGHE, H. & WEDDERBURN, L. 1984. T-cell control of Epstein-Barr virus-infected B cells is lost during *P. falciparum* malaria. *Nature*, 312, 449-450.
- WIERNIK, P. H., LOSSOS, I. S., TUSCANO, J. M., JUSTICE, G., VOSE, J. M., COLE, C. E., LAM, W., MCBRIDE, K., WRIDE, K., PIETRONIGRO, D., TAKESHITA, K., ERVIN-HAYNES, A., ZELDIS, J. B. & HABERMANN, T. M. 2008. Lenalidomide Monotherapy in Relapsed or Refractory Aggressive Non-Hodgkin's Lymphoma. *Journal of Clinical Oncology*, 26, 4952-4957.
- WILLENBROCK, K., KUPPERS, R., RENNE, C., BRUNE, V., ECKERLE, S., WEIDMANN, E., BRAUNINGER, A. & HANSMANN, M. L. 2006. Common features and differences in

- the transcriptome of large cell anaplastic lymphoma and classical Hodgkin's lymphoma. *Haematologica*, 91, 596-604.
- WILSON, W., GERECITANO, J., GOY, A., DE VOS, D., VAISHALEE, P., BARR, P., BLUM, K., SHUSTOV, A., ADVANI, R., LIH, J., WILLIAMS, M., SCHMITZ, R., YANG, Y., PITTALUGA, S., WRIGHT, G., KUNKEL, L., MCGREIVY, J., BALASUBRAMANIAN, S., CHENG, M. & 2012. The bruton's tyrosine kinase (BTK) inhibitor, ibrutinib (PCI-32765), has preferential activity in the ABC subtype of relapsed/refractory de novo diffuse large B-cell lymphoma (DLBCL): interim results of a multicenter, open-label, phase 2 study. *Blood*, 120.
- WITZIG, T. E., REEDER, C. B., LAPLANT, B. R., GUPTA, M., JOHNSTON, P. B., MICALLEF, I. N., PORRATA, L. F., ANSELL, S. M., COLGAN, J. P., JACOBSEN, E. D., GHOBRIAL, I. M. & HABERMANN, T. M. 2011. A phase II trial of the oral mTOR inhibitor everolimus in relapsed aggressive lymphoma. *Leukemia*, 25, 341-347.
- WOOD, K. W., CORNWELL, W. D. & JACKSON, J. R. 2001. Past and future of the mitotic spindle as an oncology target. *Current Opinion in Pharmacology*, 1, 370-377.
- WRIGHT, G., TAN, B., ROSENWALD, A., HURT, E. H., WIESTNER, A. & STAUDT, L. M. 2003. A gene expression-based method to diagnose clinically distinct subgroups of diffuse large B cell lymphoma. *Proceedings of the National Academy of Sciences of the United States of America*, 100, 9991-9996.
- XIAO, C., SRINIVASAN, L., CALADO, D. P., PATTERSON, H. C., ZHANG, B., WANG, J., HENDERSON, J. M., KUTOK, J. L. & RAJEWSKY, K. 2008. Lymphoproliferative disease and autoimmunity in mice with increased miR-17-92 expression in lymphocytes. *Nature Immunology*, 9, 405-414.
- XIAO, Q., JIANG, Y., LIU, Q., YUE, J., LIU, C., ZHAO, X., QIAO, Y., JI, H., CHEN, J. & GE, G. 2015. Minor Type IV Collagen alpha5 Chain Promotes Cancer Progression through Discoidin Domain Receptor-1. *PLoS Genet*, 11, e1005249.
- XU, H., BIHAN, D., CHANG, F., HUANG, P. H., FARNDAL, R. W. & LEITINGER, B. 2012. Discoidin domain receptors promote alpha1beta1- and alpha2beta1-integrin mediated cell adhesion to collagen by enhancing integrin activation. *PLoS One*, 7, e52209.
- XU, H., RAYNAL, N., STATHOPOULOS, S., MYLLYHARJU, J., FARNDAL, R. W. & LEITINGER, B. 2011. Collagen binding specificity of the discoidin domain receptors: binding sites on collagens II and III and molecular determinants for collagen IV recognition by DDR1. *Matrix Biol*, 30, 16-26.
- YAMANAKA, R., ARAO, T., YAJIMA, N., TSUCHIYA, N., HOMMA, J., TANAKA, R., SANO, M., OIDE, A., SEKIJIMA, M. & NISHIO, K. 2006. Identification of expressed genes characterizing long-term survival in malignant glioma patients. *Oncogene*, 25, 5994-6002.
- YANG, S. H., BAEK, H. A., LEE, H. J., PARK, H. S., JANG, K. Y., KANG, M. J., LEE, D. G., LEE, Y. C., MOON, W. S. & CHUNG, M. J. 2010. Discoidin domain receptor 1 is associated with poor prognosis of non-small cell lung carcinomas. *Oncol Rep*, 24, 311-9.
- YAO, X. B., ANDERSON, K. L. & CLEVELAND, D. W. 1997. The microtubule-dependent motor centromere-associated protein E (CENP-E) is an integral component of kinetochore corona fibers that link centromeres to spindle microtubules. *Journal of Cell Biology*, 139, 435-447.

- YAP, D. B., CHU, J., BERG, T., SCHAPIRA, M., CHENG, S. W. G., MORADIAN, A., MORIN, R. D., MUNGALL, A. J., MEISSNER, B., BOYLE, M., MARQUEZ, V. E., MARRA, M. A., GASCOYNE, R. D., HUMPHRIES, R. K., ARROWSMITH, C. H., MORIN, G. B. & APARICIO, S. A. J. R. 2011. Somatic mutations at EZH2 Y641 act dominantly through a mechanism of selectively altered PRC2 catalytic activity, to increase H3K27 trimethylation. *Blood*, 117, 2451-2459.
- ZERLIN, M., JULIUS, M. A. & GOLDFARB, M. 1993. NEP - A NOVEL RECEPTOR-LIKE TYROSINE KINASE EXPRESSED IN PROLIFERATING NEUROEPITHELIA. *Oncogene*, 8, 2731-2739.
- ZHANG, X., HORWITZ, G. A., HEANEY, A. P., NAKASHIMA, M., PREZANT, T. R., BRONSTEIN, M. D. & MELMED, S. 1999. Pituitary tumor transforming gene (PTTG) expression in pituitary adenomas. *Journal of Clinical Endocrinology & Metabolism*, 84, 761-767.
- ZHANG, Y., SU, J., YU, J., BU, X., REN, T., LIU, X. & YAO, L. 2011. An essential role of discoidin domain receptor 2 (DDR2) in osteoblast differentiation and chondrocyte maturation via modulation of Runx2 activation. *J Bone Miner Res*, 26, 604-17.
- ZHOU, H. Y., KUANG, J., ZHONG, L., KUO, W. L., GRAY, J. W., SAHIN, A., BRINKLEY, B. R. & SEN, S. 1998. Tumour amplified kinase STK15/BTAK induces centrosome amplification, aneuploidy and transformation. *Nature Genetics*, 20, 189-193.
- ZHOU, W., GOODMAN, S. N., GALIZIA, G., LIETO, E., FERRARACCIO, F., PIGNATELLI, C., PURDIE, C. A., PIRIS, J., MORRIS, R., HARRISON, D. J., PATY, P. B., CULLIFORD, A., ROMANS, K. E., MONTGOMERY, E. A., CHOTI, M. A., KINZLER, K. W. & VOGELSTEIN, B. 2002. Counting alleles to predict recurrence of early-stage colorectal cancers. *Lancet*, 359, 219-225.
- ZHOU, Z., SEHN, L. H., RADEMAKER, A. W., GORDON, L. I., LACASCE, A. S., CROSBY-THOMPSON, A., VANDERPLAS, A., ZELENETZ, A. D., ABEL, G. A., RODRIGUEZ, M. A., NADEMANEE, A., KAMINSKI, M. S., CZUCZMAN, M. S., MILLENSON, M., NILAND, J., GASCOYNE, R. D., CONNORS, J. M., FRIEDBERG, J. W. & WINTER, J. N. 2014. An enhanced International Prognostic Index (NCCN-IPI) for patients with diffuse large B-cell lymphoma treated in the rituximab era. *Blood*, 123, 837-42.